Regulation of the Metabolic Phenotype of Human Hepatocytes by Glucocorticoids and Androgens

By

Maryam Nasiri

A thesis submitted to the University of Birmingham

For the degree of

DOCTOR OF PHILOSOPHY

School of Clinical and Experimental Medicine
College of Medical and Dental Sciences
University of Birmingham
September 2015

Abstract

Glucocorticoids and androgens have both been implicated in the pathogenesis of non-alcoholic fatty liver disease (NAFLD); androgen deficiency in males, androgen excess in females and glucocorticoid excess in both sexes are associated with NAFLD. Glucocorticoid and androgen action are regulated at a pre-receptor level by the enzyme 5αR2 (SRD5A2) that inactivates glucocorticoids to their dihydrometabolites and converts testosterone to dihydrotestosterone (DHT). We have therefore explored the role of androgens and glucocorticoids and their metabolism by SRD5A2 upon lipid homeostasis in human hepatocytes.

In both primary human hepatocytes and human hepatoma cell lines, glucocorticoids decreased *de novo* lipogenesis in a dose-dependent manner. Whilst androgen treatment (testosterone and DHT) increased lipogenesis in cell lines and in primary cultures of human hepatocytes from female donors, it was without effect in primary hepatocyte cultures from men. SRD5A2 overexpression reduced the effects of cortisol to suppress lipogenesis and this effect was lost following transfection with an inactive mutant construct. Conversely, pharmacological inhibition using the 5αR inhibitors finasteride and dutasteride, augmented cortisol action.

We have demonstrated that manipulation of 5αR2 activity can regulate lipogenesis in human hepatocytes *in vitro*. This may have significant clinical implications for those patients prescribed 5αR inhibitors, in particular augmenting the actions of glucocorticoids to modulate hepatic lipid flux.

Acknowledgments

I would like to thank my supervisors Prof. Jeremy Tomlinson and Dr Laura Gathercole for their consistent guidance and help. I would also like to express my appreciations to all my colleagues on the 2nd floor IBR, in particular Nikolaos Nikolaou.

To my mum who was my first teacher, thank you for teaching me how to live and love, to be ambitious, independent and patient but upon all a human. To my dad, I thank you for always being there for me and support me whenever I needed you, I would have not made it without your help.

To my brothers, you give me love and love does the rest.

To Iwona and Aga, thank you for making me feel at home, being my friend and family.

I want to finish and start with a poem from Omar Kayyam, who was a Persian philosopher, astronomer, mathematician and poet;

Good and evil, our moral prison
Joy and sorrow passing like season
Fate in the way of logic and reason
Is the victim of far worse treason

This work was supported by the Medical Research Council and the School of Clinical and Experimental Medicine, University of Birmingham.

Table of contents

Chapter 1 General Introduction 1
1.1. Obesity epidemic 2
1.1.1. Genetics of obesity 2
1.1.2. Obesity and metabolic syndrome 3
1.2. Liver 4
1.2.1. Liver histology and physiology 5
1.2.2. Hepatocyte embryology and proliferation 11
1.2.3. Metabolic functions of the liver 13
1.2.3.1. Carbohydrate metabolism and in liver 13
1.2.3.1.1. Glycogenesis 14
1.2.3.1.2. Gluconeogenesis 14
1.2.3.1.3. Glycolysis 15
1.2.3.1.4. Glycogenolysis 15
1.2.3.2. Lipid metabolism in the liver 17
1.2.3.2.1. Lipogenesis 17
1.2.3.2.2. Fatty acid Uptake 20
1.2.3.2.3. Lipolysis 21
1.2.3.2.4. β-oxidation 22
1.2.4. Fatty liver disease 24
1.3. Insulin 28
1.3.1. Insulin structure and synthesis 28
1.3.2. Insulin secretion 29
1.3.3. Metabolic actions of insulin 31
1.3.4. Insulin signalling 33
1.3.4.1. Insulin receptor 33
1.3.4.2. Insulin receptor substrates 34
1.3.4.3. Phosphoinositide 3-Kinase 35
1.3.4.4. Protein Kinase B (PKB/akt) 36
1.3.4.4.1. Protein Kinase B and glucose uptake 36
1.3.4.4.2. Protein Kinase B and enzymatic activation 37
1.3.4.4.3. Protein Kinase B and secondary messengers 37
1.3.4.4.4. Protein Kinase B and transcriptional regulation 38
1.4. Steroid hormones; glucocorticoids and androgens 39
1.4.1. Adrenal glands 39
1.4.2. Structure of adrenal steroids 41
1.4.3. Steroidogenesis 42
1.4.4. Glucocorticoids 44
1.4.4.1. Basic HPA axis 44
1.4.4.2. Glucocorticoid action 46
1.4.4.3. Metabolic actions of glucocorticoids 48
1.4.4.4. Pre-receptor glucocorticoid metabolism 49
1.4.4.4.1. 11β-hydroxysteroid dehydrogenase type one 50
1.4.4.4.2. 11β-hydroxysteroid dehydrogenase type two 51
1.4.5. Androgen 52
1.4.5.1. Regulation of testosterone synthesis and secretion 52

1.4.5.2. Androgen action 53
1.4.5.3. Metabolic actions of androgens 54
1.4.5.4. Pre-receptor androgen metabolism 56
1.4.5.4.1. 5αRs 56
1.4.5.4.1.1. 5αR1 57
1.4.5.4.1.2. 5αR2 58
1.4.5.4.1.3. 5αR3 61
1.4.5.4.2. 5βR 61
1.5. Regulation of hepatic lipid metabolism by insulin, glucocorticoids and androgens 62
1.5.1. Insulin and hepatic lipid metabolism 63
1.5.2. The effect of glucocorticoids on hepatic lipid metabolism and NAFLD 64
1.5.3. The effect of androgens on hepatic lipid metabolism and NAFLD 65
1.6. 5αR and NAFLD 67
1.6.1. 5αR knockout 67
1.6.2. 5αR as a therapeutic target 68
1.7. Unanswered questions 69
1.8. Aims 70
Chapter 2 General Methods 71
2.1. Cell culture 72
2.1.1. C3A 72
2.1.1.1. Cell line 72
2.1.1.2. Proliferation 72
2.1.1.3. Freezing down 74
2.1.2. Huh7.5 74
2.1.2.1. Cell line 74
2.1.2.2. Proliferation 74
2.2. Primary human hepatocytes 75
2.2.1. Thawing procedures 75
2.2.2. Cell maintenance 76
2.3. Protein extraction 76
2.3.1. Principle 76
2.3.2. Methods 77
2.4. Measuring protein concentration 77
2.4.1. Principle 77
2.4.2. Methods 77
2.5. Western blotting 78
2.5.1. Principle 78
2.5.2. Methods 78
2.6. RNA extraction 80
2.6.1. Principle 80
2.6.2. Methods 80
2.7. Reverse Transcription (RT) 82
2.7.1. Principle 82
2.7.2. Methods 82
2.8. Polymerase Chain Reaction 83
2.8.1. Principle 83
2.8.2. Methods 83
2.9. Quantitative Polymerase Chain Reaction 84

2.9.1. Principle 84
2.9.2. Methods 84
2.10. *De novo* lipogenesis assay 86
2.10.1. Principle 86
2.10.2. Methods 87
2.11. 5αR2 overexpression 87
2.11.1. C3A cell Transfection 88
2.12. Site Directed Mutagenesis (SDM) 89
2.12.1. Principle 89
2.12.2. Methods 90
2.13. Gas/Liquid Chromatography-Mass Spectrometry (GC/LC-MS) 91
2.13.1. Chromatography 91
2.13.2. Mass Spectrometry 92
2.14. Statistical analysis 93
Chapter 3 Impact of Glucocorticoids upon insulin signalling cascade and lipid metabolism 94
3.1. Aims 95
3.2. Background 95
3.3. Method 98
3.3.1. C3A and Huh7.5 cell cultures and treatments 98
3.3.2. Primary human hepatocytes cell culture and treatments 99
3.3.3. RNA and Protein extraction 100
3.3.4. Real-Time PCR 100
3.3.5. Western blotting 101
3.3.6. Western blotting-separating ACC1/2 isoforms 101
3.3.7. *De novo* lipogenesis assay 103
3.4. Results 106
3.4.1. GC regulation of insulin signalling in C3As and primary hepatocytes 106
3.4.1.1. Gene expression 106
3.4.1.2. Protein expression 107
3.4.1.2.1. Insulin signalling 107
3.4.1.2.2. GCs and insulin signalling 109
3.4.2. GC regulation of lipid homeostasis in C3As and primary hepatocytes 110
3.4.2.1. Gene expression 110
3.4.2.2. Protein expression 112
3.4.2.3. *De novo* lipogenesis in C3As, Huh7.5s and primary human hepatocyte cultures 113
3.4.2.4. *De novo* lipogenesis in primary cultures 116
3.5. Discussion 119
Chapter 4 Impact of androgens on hepatic insulin sensitivity and lipid metabolism comparing male and female hepatocytes 124
4.1. Aims 125
4.2. Background 125
4.3. Method 127
4.3.1. C3A cell culture and treatments 127
4.3.2. Primary human hepatocytes cell culture and treatments 127
4.3.3. RNA extraction 128
4.3.4. Real-Time PCR 128

4.3.5. AR overexpression 128
4.3.6. *De novo* lipogenesis assay 129
4.4. Results 130
4.4.1. Optimising the *in vitro* model by comparing the gene profiles 130
4.4.2. Androgen regulation of insulin signalling in C3As 131
4.4.2.1. Gene expression 131
4.4.3. Androgen regulation of lipid homeostasis in C3As and primary hepatocytes 132
4.4.3.1. Gene expression in C3As 132
4.4.4. *De novo* lipogenesis assay in C3As 132
4.4.5. *De novo* lipogenesis assay in primary hepatocytes 133
4.5. Discussion 136
Chapter 5 Pre-receptor metabolism of GCs as a regulator of metabolic phenotype in human liver 139
5.1. Aims 140
5.2. Background 140
5.3. Method 142
5.3.1. C3A cell culture and treatments 142
5.3.2. Primary human hepatocytes cell culture and treatments 142
5.3.3. RNA extraction 143
5.3.4. Real-Time PCR 143
5.3.5. SRD5A2 overexpression 143
5.3.6. Site directed mutagenesis (SDM) 144
5.3.7. Gas and Liquid chromatography/Mass spectrometry (GC/MS and LC/MS) 144
5.3.8. *De novo* lipogenesis assay 146
5.4. Results 147
5.4.1. Pre-receptor enzyme expression in primary human hepatocytes and liver cell lines 147
5.4.1.1. mRNA expression 147
5.4.2. Regulation of pre-receptor modifying enzymes by GCs, androgens in C3A cells 148
5.4.2.1. mRNA expression 148
5.4.3. Modulation of SRD5A2 expression and activity 149
5.4.3.1. Transfection 149
5.4.3.1.1. mRNA expression 150
5.4.3.1.2. Enzymatic activity 151
5.4.3.1.3. Functional impact of modulation of pre-receptor GC metabolism upon *de novo* lipogenesis in human hepatocytes 152
5.4.3.1.3.1. Genetic manipulation in C3A cells 152
5.4.3.2. Pharmacological manipulation of 5αR activity in primary human hepatocytes 154
5.4.3.2.1. *De novo* lipogenesis assay 154
5.5. Discussion 155
Chapter 6 Molecular characterisation of patients with abnormal A-ring reductase activity 158
6.1. Aims 159
6.2. Background 159
6.3. Method 161
6.3.1. GC/MS 161

6.3.2. DNA extraction from patients' blood samples 161
6.3.3. Designing primers for A-ring reductases 161
6.3.4. Optimising the primers by PCR 162
6.3.5. Sequencing 163
6.4. Results 165
6.4.1. Patient identification 165
6.4.1.1. Urine analysis 165
6.4.1.2. Sequencing analysis 166
6.4.1.2.1. 5αR2 166
6.4.1.2.2. 5αR1 169
6.4.1.3. Splice variants in 5αR1 170
6.5. Discussion 173
Chapter 7 Final discussion 177
Chapter 8 Future studies 184
Conference proceedings 188
Appendix 191
References 200
Publications 234

List of Figures

Figure 1-1 Simplified diagram of blood flow through the liver. The liver receives blood from hepatic artery carrying oxygenated blood (red box), and also from the portal vein providing high nutrition blood (blue box). The blood in these two vessels passes through sinusoids within the liver where oxygen and nutrients can be exchanged. Blood leaves the liver and drains in to the hepatic vein where eventually joins the inferior vena cava to enter the right atrium of heart. 5
Figure 1-2 The structure of the hepatocyte cell. The hepatocytes contain a nucleus and many cellular organelles associated with secretary functions including ER and Golgi, and metabolic functions including mitochondria. Some of the hepatocytes form the sinusoids wall by lying adjacent to endothelial cells. Hepatocytes and endothelial cells are separated by small spaces called the space of Disse..... 7
Figure 1-3 The liver lobes are made up of hexagonal lobules which comprise of rows of hepatocytes. The hepatocytes are in close contact with sinusoids and canaliculi. The structure of the liver lobules, representing three different models for the arrangements of bile duct, hepatic artery and portal vein; classic hepatic lobule (a), portal lobule (b) and portal acinus (c)..... 9
Figure 1-4 The Liver growth and repopulation occurs in two different ways; by proliferation and differentiation of oval cells or replication of mature hepatocytes. 11
Figure 1-5 Oval cells derive from the portal area of the lobule and have the ability to differentiate to either biliary epithelial cells or hepatocytes. The oval cells response to cytokines and growth factors for hepatocytes regeneration is divided into four stages; activation, proliferation, migration and differentiation. 13
Figure 1-6 Anabolic and catabolic pathways in fasted (a) and fed state (b) in liver. In fasting state; glycogenolysis (glycogen breakdown to glucose monomers) (a-1), gluconeogenesis (synthesis of glucose from amino acids, glycerol, and lactate)(a-2) and fatty acid uptake(a-3) are increased while VLDL production is decreased, in order to provide energy. In fed state; glycogenesis (glycogen synthesis from glucose) (b-1) and glycolysis (glucose conversion to pyruvate and subsequently to acetyl CoA) (b-2) as well as *de novo* lipogenesis (acetyl CoA conversion to fatty acids) (b-4), esterification (combination of fatty acids with glycerol to produce triglyceride) (b-5) and VLDL packaging (b-5) pathways are enhanced while gluconeogenesis is blocked, in order to store energy. Abbreviations: Glucose 6-P=glucose 6-phosphate, VLDL= very low density lipoprotein..... 16
Figure 1-7 *De novo* lipogenesis and subsequent triglyceride (TAG) synthesis. *De novo* lipogenesis is including rate limiting carboxylation of acetyl CoA to malonyl-CoA by acetyl CoA carboxylase (ACC) and the conversion of malonyl-CoA to palmitate by fatty acid synthase (FAS), Esterification results from combination of free fatty acids (FFA) with glycerol which can produce monoglyceride(MAG), dilyceride(DAG), and triglyceride(TAG). 18
Figure 1-8 Lipid metabolism within the liver. The FFAs, provided by either *de novo* lipogenesis or fatty acid uptake, undergo esterification to produce TAG. TAG can be packaged in VLDL particles and be secreted into circulation. However, during fasting, TAG undergoes lipolysis and subsequently β-oxidation to generate ATP (ACC= acetyl CoA carboxylase, ATGL= adipose triglyceride lipase, CPT= Carnitine palmitoyl-CoA transferase, DAG= diacylglyceride, FAS= fatty acid synthase, FFA= free fatty acid, HL= hepatic Lipase, HSL= hormone sensitive lipase, LDL= low density lipoprotein, MAG=

monoacylglyceride,MAGL= monoacylglyceride lipase, TAG= triglyceride, VLDL= very low density lipoprotein).....24
Figure 1-9 Stages of liver damage in NAFLD. NAFLD demonstrates a spectrum of liver disease ranging from simple hepatic steatosis. Inflammation can convert steatosis to non-alcoholic steato-hepatitis (NASH) which can end up in cirrhosis with liver failure.....25
Figure 1-10 The amount of intracellular TAG is a balance between accumulation, by *de novo* lipogenesis or FA uptake and by loss from the breakdown of fatty acids by β-oxidation or it can be packaged into VLDL and released into circulation.....26
Figure 1-11 The principles of insulin synthesis in pancreatic β-cells. Insulin is synthesised as preproinsulin and enters the ER to form proinsulin. Proinsulin is then transported to the golgi and converted to insulin.....29
Figure 1-12 The processes leading to insulin secretion in pancreatic β-cells. Glucose is transported into β-cells through GLUT2 glucose transporters and metabolised to ATP. Elevated ATP/ADP ratio closes the ATP-sensitive potassium channels, leading to cell membrane depolarisation. Cell-surface calcium channels are opened and promoting calcium influx into the β-cells. An increase in calcium triggers the exocytosis of insulin.....31
Figure 1-13 Energy balance by anabolism and catabolism and the co-factors involved. 32
Figure 1-14 The insulin signalling pathways involved in the metabolic actions of insulin. In summary, when insulin binds its receptor the receptor auto phosphorylates. This then binds and phosphorylates insulin receptor substrate, which activates PI3K which leads via a secondary messenger to AKT phosphorylation. This activation of AKT increases glucose uptake (through GLUT4 translocation to the plasma membrane), glycogen synthesis (through GSK phosphorylation), and lipogenesis (through AMPK activation) whilst inhibiting gluconeogenesis (through FOXO1 and PEPCK supression) and β-oxidation (through AMPK activation). Abbreviations: IRS1/2= Insulin receptor substrate1/2, SH2= Src-homology 2, PI3K= Phospho-inositide 3 Kinase , PIP2/3= Phosphatidylinositol-3, 4-diphosphate 2/3, AKT/PKB= Protein Kinase B, mTOR= Mammalian target of rapamycin, PDK1= Phosphoinositide- dependent protein kinase 1, cAMP= Cyclic adenosine monophosphate, PKA= Protein kinase A, LKB1= Liver kinase B1, AMPK= AMP-kinase, GSK= Glycogen synthase kinase, FOXO1= Forkhead box-containing protein, PEPCK= Phosphoenolpyruvate carboxykinase. 39
Figure 1-15 The adrenal glands are positioned above the kidneys and are divided into adrenal medulla and the cortex which itself is divided into three zones; the glomerulosa, fasciculata and reticularis. 40
Figure 1-16 Standard structure of adrenal steroids, the numbers represent the carbon atoms and the letters designate the rings.....41
Figure 1-17 The major enzymatic reactions in 3 zones of adrenal cortex; allowing the specific steroid biosynthesis in each zone. These three zones are named glomerulosa, fasculata and reticularis which are responsible for synthesis of mineralocorticoids, glucocorticoids, and androgens respectively. 44
Figure 1-18 The hypothalamo-pituitary-adrenal (HPA) axis; a negative feedback mechanism presents whereby GC inhibits its own release. When cortisol is adequate, a negative feedback operates on pituitary gland and hypothalamus to reduce the output of corticotropin-releasing hormone (CRH) and adrenocorticotropic hormone (ACTH) which leads to a reduction in cortisol secretion.....45
Figure 1-19 The glucocorticoid receptor. (NTD= N-terminal domain, DBD= DNA binding domain, LBD= ligand binding domain and hinge region). 47

Figure 1-20 The mechanism of glucocorticoid action; upon GC binding, GR disassociates, translocates into nucleus and regulates gene transcription. 48
Figure 1-21 Pre-receptor glucocorticoid metabolism; In liver, 11β-HSD1 acts predominately as an oxoreductase due to the presence of co-factor NADPH which is generated by H6PDH enzyme. However, 11β-HSD2 works as a dehydrogenase and requires NAD^+ as a co-factor. 51
Figure 1-22 The androgen receptor. (NTD= N-terminal domain, DBD= DNA binding domain, LBD= ligand binding domain and hinge region). 53
Figure 1-23 The mechanism of androgen action; upon DHT binding, AR disassociates, translocates into nucleus and regulates gene transcription. 54
Figure 1-24 5αRs convert GCs to their less active dihydrometabolites with subsequent conversion to tetrahydrometabolites. In addition, they catalyse the conversion of testosterone to the more potent androgen, DHT. Therefore, 5αRs activity make less cortisol and more DHT available to attach their nuclear receptor, translocate to the nucleus and activate the transcription of the gene. 57
Figure 1-25 Mutations identified in SRD5A2; because of consanguinity the prevalence of variant mutations would cluster differently in variant ethnic population (Maimoun et al. 2011). 60
Figure 1-26 The major metabolites of cortisone and cortisol and the enzymes involved catalysing the conversions. 5αR metabolises cortisol to 5α-dihyrocortisol with a following conversion to 5α-tetrahydrocortisol (5αTHF) by 3α-HSD. However, 5βR is able to metabolise both cortisol and cortisone and following 3α-HSD activity generates 5β-tetrahydrocortisol (5βTHF) and 5β-tetrahydrocortisone (5βTHE). 62
Figure 2-1 C3As morphology after day 2 (a) and 3 (b) of proliferation. 73
Figure 2-2 Primary human hepatocytes morphology after day 2. 76
Figure 2-3 The impact of cortisol treatment (100, 250 and 1000nM) on 18s abundance in four different experimental replicates in C3As. The PCR data demonstrate that cortisol treatment has no impact on 18s values, validating its use as an internal housekeeping gene. 86
Figure 2-4 pcDNA3.1 vector (Picture is taken from Invitrogen-Thermo Fisher Scientific website;https://www.thermofisher.com/order/catalog/product/V79020)(a), schematic diagram of 5αR2 coding sequence (presented in red) cloned into the vector(presented in black)(b). ... 88
Figure 2-5 Site directed mutagenesis (SDM) technique which has three major steps; mutant strand synthesis, DpnI designation of template, and transformation. Picture is taken from Quikchange (Agilent Technologies) website. 90
Figure 3-1 Cells were split into three 24 well plates, and fasted overnight before treatment. Cells were then treated with cortisol for 24h and finally harvested for RNA and protein extraction, and *de novo* lipogenesis assay. 98
Figure 3-2 Primary hepatocytes were split into two 12 and one 24 well plates. Cells were fasted in William's E medium for 3h and then treated with cortisol in presence and absence of insulin for 24 hours. Finally, cells were harvested for RNA and protein extraction, and *de novo* lipogenesis assay. 100
Figure 3-3 Separation of ACC1/2 isoforms in human hepatocytes using anti phospho and total ACC antibodies but this was not sufficient for quantification. 102
Figure 3-4 Time dependent (1, 3, 6, 24, and 48h) preliminary *de novo* lipogenesis assays in C3A cells; it was identified that the optimal acetate incubation time to achieve the largest impact of insulin stimulation on *de novo* lipogenesis to be at the final 6h of the treatment. Insulin concentration=50nM, data are presented as ^{14}C-acetate incorporation into lipid (%from control without insulin, mean ± s.e) of n=4 experiments and one way ANOVA with

Tukey's post-hoc analysis was applied using Sigmastat 3.1 to compare insulin stimulated treatments to no insulin treatments (*p<0.05 vs. no insulin). 104
Figure 3-5 Time dependent (1, 3, 6, 24 and 48h) preliminary *de novo* lipogenesis assays in primary hepatocytes; it was identified that the optimal acetate incubation time to achieve the largest impact of insulin stimulation on *de novo* lipogenesis to be at the final 6h of the treatment. Insulin concentration=5nM, data are presented as ^{14}C-acetate incorporation into lipid (% from control without insulin, mean ± s.e) of n=7 experiments and one way ANOVA with Tukey's post-hoc analysis was applied using Sigmastat 3.1 to compare insulin stimulated treatments to no insulin treatments (*p<0.05 vs. no insulin). 104
Figure 3-6 No insulin stimulation was detected in C3As using anti phospho-AKT T308 and S473. Total AKT protein expression remained unchanged. These are representative western blots of n=4 experiments and insulin dose range was 1, 10, 20, 50, and 100nM for 15min. . 108
Figure 3-7 Insulin (dose range 10 and 100 nM for 15mins) pre-treatment increases insulin stimulated PKB/akt (S473) phosphorylation in a dose dependent manner in Huh 7.5 cells without changing total PKB/akt. These are representative western blots of n=4 experiments. 108
Figure 3-8 Cortisol does not affect insulin-stimulated PKB/akt (S473) phosphorylation or total PKB/akt protein expression in Huh 7.5 cells. These are representative western blots of n=3 experiments. Abbreviations: Ins, insulin (50nM for 15mins); F, cortisol (dose range 100, 250, 1000nM for 24h). 109
Figure 3-9 Cortisol induces a dose-dependent increase in insulin stimulated PKB/akt phosphorylation without alternation in total PKB/akt in primary cultures. Data presented are the mean ± s.e of n=4 experiments with representative western blots inserted above. Bands are quantified relative to β-actin as internal loading control and one way ANOVA with Dunnett's post-hoc analysis was applied using Sigmastat3.1 to compare multiple cortisol treatments to control (*p<0.05 vs. control). Abbreviations: Ins, insulin (50nM for 15mins); F, cortisol (dose range 100, 250, 1000nM for 24h). 110
Figure 3-10 Cortisol (250nM for 24h) increases mRNA expression of ACC2 and FAS in C3A cells. Data are the mean values from n=7 experiments and expressed as mean arbitrary unit values ± s.e. Student's t-tests were applied using Sigmastat 3.1 to compare cortisol treatment to control (*p<0.05 vs. control). 111
Figure 3-11 There is no convincing effect of cortisol (F, dose range 100, 250, 1000nM for 24h) but insulin (5nM for 15mins) decreased the inhibitory phosphorylation in primary cultures of human hepatocytes and this would be predicted to increase lipogenesis. No effect was observed with total ACC levels. These are representative western blots of n=4 experiments. 113
Figure 3-12 Cortisol decreases *de novo* lipogenesis in a dose dependent manner in C3As. Data are presented as ^{14}C-acetate incorporation into lipid (% from control, mean ± s.e) of n=7 experiments. One way ANOVA test with Dunnett's post-hoc analysis was applied using Sigmastat 3.1 to compare multiple cortisol treatments to control (*p<0.05 vs. control), and ANOVA test with Tukey's post-hoc analysis was used to compare multiple cortisol treatment (†p<0.05 vs. cortisol 100nM and §p<0.05 vs. cortisol 250nM). Cortisol dose range= 100, 250, 1000nM for 24h 114
Figure 3-13 No significant insulin stimulation lipogenesis was observed in C3A cells. Data are presented as ^{14}C-acetate incorporation into lipid (% from control, mean ± s.e) of n=4 experiments and one way ANOVA with Dunnett's post-hoc analysis was applied using Sigmastat 3.1 to compare multiple insulin treatments to control. Insulin concentrations= 20, 40, 60 and 80nM for 24h. 114

Figure 3-14 In C3As insulin (50nM for 24h) alone increases lipogenesis modestly but not significantly. However, in presence of cortisol (250nM for24h) this reaches statistical significance. Data are presented as ^{14}C-acetate incorporation into lipid (% from control, mean ± s.e) of n=7 experiments and Student's t-tests were applied using Sigmastat 3.1 to compare cortisol treatment in presence of insulin to cortisol alone (*p<0.05 vs. cortisol). 115
Figure 3-15 *De novo* lipogenesis remained unchanged after cortisol (dose range 100, 250, 1000nM for 24h) pre-treatment in Huh7.5 cells. Data are presented as ^{14}C-acetate incorporation into lipid (% from control, mean ± s.e) of n=4 experiments and one way ANOVA with Dunnett's post-hoc analysis was applied using Sigmastat 3.1 to compare multiple cortisol treatments to control. 116
Figure 3-16 Insulin (5nM, 24h) stimulates lipogenesis significantly in primary cultures compared to C3A cell line. Data are presented as percentage, however, the actual counts differ between primary and C3A cells. Therefore, the purpose of this graph is solely to compare the insulin sensitivity. Data are presented as ^{14}C-acetate incorporation into lipid (% from control, mean ± s.e) of n=4 experiments and Student's t-tests were applied using Sigmastat 3.1 to compare insulin treatment to control (*p<0.05 vs. control). 116
Figure 3-17 Cortisol decreases *de novo* lipogenesis in a dose dependent manner in primary hepatocyte. However, co-incubation with insulin (5nM for24h) was able to reverse the cortisol effects. Data are presented as ^{14}C-acetate incorporation into lipid (% from control, mean ± s.e) of n=4 experiments.one way ANOVA with Dunnett's post-hoc analysis was applied using Sigmastat 3.1 to compare multiple cortisol treatments to control (*p<0.05vs. control), and ANOVA with Tukey's post-hoc analysis was used to compare cortisol in presence of insulin treatments to cortisol alone († p<0.05vs. cortisol). Cortisol dose range= 100, 250, 1000nM for 24h 118
Figure 3-18 GC decreases *de novo* lipogenesis in the absence of insulin (fasted state) in all three insulin target tissues. However in the presence of insulin (fed state) GC decreases lipogenesis in muscle with an increase in liver and adipose tissue. 122
Figure 4-1 Testosterone (50nM, 24h) increases mRNA expression of GR in C3As. Data are the mean values from n=7 experiments and expressed as mean arbitrary unit values ± s.e). Student's t-test was applied using Sigmastat 3.1 to compare testosterone treatment to control (*p<0.05 vs. control). 131
Figure 4-2 Androgen receptor (AR) overexpression alone, and in the presence of T=testosterone (50nM, 24h) or DHT (10nM, 24h) increases *de novo* lipogenesis in C3As. However, neither T (50nM, 24h) nor DHT (10nM, 24h) further enhanced *de novo* lipogenesis on AR overexpressed C3A cells. Data are presented as ^{14}C-acetate incorporation into lipid (dpm, mean ± s.e) of n=4 experiment and one way ANOVA with Dunnett's post-hoc analysis was applied using Sigmastat 3.1 to compare testosterone and DHT treatments to control (*p<0.05 vs. control). 133
Figure 4-3 In primary cultures of male donors, testosterone (5 and 50nM, 24h) nor DHT (10nM, 24h) have any effect on *de novo* lipogenesis. However, insulin sensitivity is confirmed again in primary hepatocytes. Insulin concentration=5nM, data are presented as ^{14}C-acetate incorporation into lipid (% from control, mean ± s.e) of n=4 experiment and one way ANOVA with Tukey's post-hoc analysis was applied using Sigmastat 3.1 to compare insulin stimulated treatments to no insulin treatments (*p<0.05 vs. no insulin). 134
Figure 4-4 In primary cultures of female donors, testosterone at 5nM (for 24h) increased *de novo* lipogenesis and this stimulatory effect was augmented in presence of insulin (5nM for 24h). However, DHT (10nM) decreased *de novo* lipogenesis compared to control. Data are presented as ^{14}C-acetate incorporation into lipid (% from control, mean ± s.e) of n=4

experiment and one way ANOVA with Dunnett's post-hoc analysis was applied using Sigmastat 3.1 to compare multiple treatments with control (*p<0.05 vs. control no insulin). 135
Figure 5-1 Testosterone (50nM, 24h) increases mRNA expression of GR in C3As. Data are the mean values from n=7 experiments and expressed as mean arbitrary unit values ± s.e. Student's t-test was applied using Sigmastat 3.1 to compare testosterone treatment to control (*p<0.05 vs. control). 149
Figure 5-2 70% SRD5A2 transfection efficiency in C3As was observed using a plasmid containing green fluorescence protein (GFP). 149
Figure 5-3 5αR2 overexpression was confirmed by Real-time PCR (a). Increased 5αR2 expression was observed following transfection into C3A cells compared to vector. There is a very low endogenous level of 5αR2 expression in vector only cells but it is not absent, and therefore, it is not a true negative control (b). Data presented are mean ± s.e of n=3 experiments and Student's t-test was applied using Sigmastat 3.1 to compare 5αR2 overexpression to vector (*p<0.05 vs. vector). 150
Figure 5-4 Transfection of wild-type 5αR2 (in contrast to the mutant R246Q construct) in C3As is associated with increased dihydrotestosterone [DHT] generation from testosterone (100nM). Data presented are mean ± s.e of n=3 experiments and pcDNA3.1is the vector. One way ANOVA with Dunnett's post-hoc analysis was applied using Sigmastat 3.1 to compare the wild-type 5αR2 and the mutant R246Q construct to vector (*p<0.05 vs. vector). 151
Figure 5-5 Transfection of wild-type 5αR2 (in contrast to the mutant R246Q construct) in C3As is associated with increased cortisol (200nM) clearance. Data presented are mean ± s.e of n=3 experiments and pcDNA3.1is the vector. Student's t-test was applied using Sigmastat 3.1 to compare the cortisol clearance between 5αR2 overexpression and vector (*p<0.05 vs. vector). 152
Figure 5-6 In C3A cells, the decrease in lipogenesis associated with increasing doses of cortisol was abolished in cells transfected with wild-type 5αR2. Data are presented as ^{14}C-acetate incorporation into lipid (% from control, mean ± s.e) of n=5 experiment. One way ANOVA with Dunnett's post-hoc analysiswas applied using Sigmastat 3.1 to compare multiple cortisol treatments to control (*p<0.05 vs. control), and ANOVA with Tukey's post-hoc analysis was used to compare cortisol in presence of insulin treatments to cortisol alone († p<0.05 vs. cortisol). Cortisol dose range= 100, 250, 1000nM for 24h 153
Figure 5-7 Transfection of mutant R246Q 5αR2 did not affect the ability of cortisol to supress lipogenesis. Data are presented as ^{14}C-acetate incorporation into lipid (% from control, mean ± s.e) of n=3 experiment and one way ANOVA with Dunnett's post-hoc analysis was applied using Sigmastat 3.1 to compare multiple treatments with control (*p<0.05 vs. control). Cortisol dose range= 100, 250, 1000nM for 24h. 153
Figure 5-8 In primary cultures of human hepatocytes, pharmacological inhibition of 5αRs with either the selective (finasteride, 500nM) or nonselective inhibitor (dutasteride, 500nM), augments the action of cortisol (250nM) to suppress lipogenesis. Data are presented as ^{14}C-acetate incorporation into lipid (% from control, mean ± s.e) of n=4 experiment and one way ANOVA with Dunnett's post-hoc analysis was applied using Sigmastat 3.1 to compare multiple treatments to control (*p<0.05, **p<0.01 vs. control) and ANOVA with Tukey's post-hoc analysis was used to compare multiple treatments to cortisol(§ P<0 .05, §§ P<0 .01 vs. cortisol). 154
Figure 6-1 Genomic locations of designed primers. Primers were designed using NCBI, Primer3 online websites (http://bioinfo.ut.ee/primer3-0.4.0/), and Oligo calc software. These

primers were synthesised by Alta bioscience (University of Birmingham, Birmingham, UK). 162
Figure 6-2 Optimising of exon 1 of each SRD5As in a range of 8 different temperatures (53.4 to 65^{o}C) using electrophoresis on 1% agarose gel, best annealing temperatures are shown by arrows. 163
Figure 6-3 The 5αTHF/THF ratio is a marker of 5αR activity. The 5aTHF/THF ratio in men and women of these patients (shown in red) are almost two fold lower than normal mean 5aTHF/THF ratio in men (blue) and in women (purple).....166
Figure 6-4 DNA sequence chromatograph from patient E indicating; a) C to G transversion resulting in a leucine (L) for valine (V) amino acid substitution at codon 89 (L89V) polymorphism, b) G to A transversion resulting in a threonine for alanine amino acid substitution at codon 49 (A49T) polymorphism. Data were analysed using CLC DNA workbench software.....168
Figure 6-5 DNA sequence chromatograph from patient G indicating an A to C nucleotide substitution in rs186093099 polymorphism. Data were analysed using CLC DNA workbench software. 170
Figure 6-6 SRD5A1 gene has 2 splice variants (longer splice variant with 5 exons shown by black arrow and a shorter one with 4 exons indicated with blue arrow). The polymorphism in our patient makes the longer splice (5 exons) more potent and this may explain the metabolic phenotype. 171
Figure 6-7 Conventional PCR analysis demonstrates a reduced amount of the short splice variant in patient with the rs186093099 SNP (red arrow) in comparison with controls (green arrow).cDNA from muscle was used for both patients and controls.....172
Figure 7-1 Tissue specific GC action to regulate lipid metabolism and insulin action. GCs induce insulin resistance in skeletal muscle and insulin sensitivity in adipose tissue. We have described insulin sensitisation by GCs in human hepatocytes and this may lead to increased lipid accumulation (as in adipose tissue) in the fed state. This may represent an important mechanism in the development of the Cushing's phenotype and its associated adverse metabolic features.....179
Figure 7-2 GCs acting in isolation decrease lipogenesis but enhance insulin-stimulated lipogenesis. We discovered that 5αR overexpression ameliorates the effects of cortisol upon lipid metabolism but chemical inhibition of 5αR augments the actions of cortisol. This may suggests that in presence of insulin, 5αR inhibitors enhance cortisol action to act synergistically with insulin to drive lipid accumulation. This finding has potentially significant implications for patients taking finasteride and dutasteride. 182

List of Tables

Table 1-1 The metabolic processes are zoned in hepatocytes. The metabolic activity compared between zoneI and zoneIII in hepatocytes is presented in this table. 10
Table 1-2 Five major groups of adrenal steroid: oestrogen, androgen, progestogen, mineralocorticoid and glucocorticoid 42
Table 1-3 Comparison of human 5αR1 and 2 isoforms. 60
Table 2-1 Detailed nutrient contents of MEM media, it is a low glucose media with glucose concentration of 1g/l. 73
Table 2-2 List of antibodies used for western blot analysis. 80
Table 2-3 List of primers which are provided by Applied Biosystems. The information in this table is gathered from: http://www.appliedbiosystems.com/absite/us/en/home/applications-technologies/real-time-pcr.html. 85
Table 3-1 mRNA expression of insulin signalling genes in C3As in response to cortisol (F, 250nM for 24h) treatment. Data are expressed as mean ΔCt values ± s.e of n=7 experiments and Student's t-tests were applied using Sigmastat 3.1 to compare cortisol treatment to control. 106
Table 3-2 mRNA expression of insulin signalling genes in primary hepatocytes in response to cortisol (F, dose range 100, 250, 1000nM for 24h) treatment alone (a) and co-incubation with insulin (5nM for 24h) (b). INS=Insulin, IRS=Insulin receptor, data are expressed as mean ΔCt values ± s.e of n=4 experiments and one way ANOVA with Dunnett's post-hoc analysis was applied using Sigmastat 3.1 to compare multiple cortisol treatments to control (a) and multiple cortisol with insulin treatments to insulin alone (b). 107
Table 3-3 mRNA expression of lipid metabolism genes in C3As in response to cortisol (F, 250nM for 24h) treatment. Data are expressed as mean ΔCt values ± s.e of n=7 experiments and Student's t-tests were applied using Sigmastat 3.1 to compare cortisol treatment to control. 111
Table 3-4 mRNA expression of lipid metabolism genes in primary cultures of human hepatocytes in response to cortisol (F, dose range 100, 250, 1000nM for 24h) treatment alone (a) and co-incubation with insulin (5nM, 24h) (b). Data are expressed as mean ΔCt values ± s.e of n=4 experiments and one way ANOVA with Dunnett's post-hoc analysis was applied using Sigmastat 3.1 to compare multiple cortisol treatments to control (a) and multiple cortisol with insulin treatments to insulin alone (b). 112
Table 4-1 Gene expression profiles were compared between Primary Hepatocytes, HepG2, Huh7.5 and C3A cell lines. Primary hepatocytes are the only model that expresses mRNA encoding AR. Data are expressed as ΔCt values. 130
Table 4-2 mRNA expression of pre-receptor regulation and insulin signalling genes in C3As in response to testosterone (50nM, 24h) treatment. Data are expressed as mean ΔCt values ± s.e of n=5 experiments and Student's t-tests were applied using Sigmastat 3.1 to compare testosterone treatment to control. 131
Table 4-3 mRNA expression of lipid metabolism genes in C3As in response to testosterone (50nM, 24h) treatment. Data are expressed as mean ΔCt values ± s.e of n=5 experiments and Student's t-test were applied using Sigmastat 3.1 to compare testosterone treatment to control. 132
Table 5-1 Gene expression profiles were compared between Hepatcytes, HepG2, Huh7.5 and C3A cell lines. SRD5A2 expressed the least and the most in C3As and primary hepatocytes

respectively. Therefore, C3As and primary hepatocytes were used for overexpression and chemical inhibition of SRD5A2 respectively. Data are expressed as ΔCt values. 147
Table 5-2 mRNA expression of pre-receptor regulation genes in C3As in response to cortisol (250nM, 24h) (a) and testosterone (50nM, 24h) treatment (b). Only testosterone (50nM, 24h) increases mRNA expression of GR. Data are expressed as mean ΔCt values ± s.e of n=5 experiments and Student's t-tests were applied using Sigmastat 3.1 to compare cortisol and testosterone treatments to their controls. 148
Table 6-1 Urinary steroid metabolite analysis from all the 9 individual patients (A to I). The 5αTHF/THF ratio is a marker of 5αR activity. Data are presented in nM, F=Female, M=Male. 165
Table 6-2 Polymorphisms identified in SRD5A2 in UTR3 and coding regions of patients D, E, G and I. No polymorphisms were identified in patients A, B, C, F or H. The sequencing of DNA was performed by the Functional Genomic Laboratory at the University of Birmingham, Plasmid to Profile sequencing (Birmingham, UK) and data were analysed using CLC DNA workbench software. 167
Table 6-3 Polymorphisms identified in SRD5A1. There are three coding sequence changes but they do not cause amino acid changes. In patient G and A (highlighted rows), SNPs with low allele frequencies were identified. In patient G and A the SNP is located in intron1/exon2 boundary, and intron 3 respectively. Data were generated by Beckman Coulter Genomics Inc. (Danvers, MA, US). 169

Abbreviations

11β-HSD1	11β-hydroxysteroid dehydrogenase type one
11β-HSD2	11β-hydroxysteroid dehydrogenase type two
5αR1	5α-reductase 1
5αR2	5α-reductase 2
5αR3	5α-reductase 3
5βTHE	5β-tetrahydrocortisone
5βTHF	5β-tetrahydrocortisol
ACC	Acetyl CoA carboxylase
ACTH	Adrenocorticotropic hormone
AGTL	Adipose triglyceride lipase
ALIOS	American lifestyle induced obesity syndrome
AMPK	AMP-kinase
AR	Androgen receptor
ARE	Androgen response elements
ATP	Adenosine triphosphate
AU	Arbitrary units
BAT	Brown adipose tissue
BMI	Body mass index
BSA	Bovine serum albumin
cAMP	Cyclic adenosine monophosphate
CDG	Congenital disorder of glycosylation
cDNA	Complementary DNA
CPT1	Carnitine palmitoyl-CoA transferase I
CPTII	Carnitine palmitoyl-CoA transferase II
CRH	Corticotropin-releasing hormone
Ct	Cycle threshold
CVD	Cardiovascular disease
CYP2E1	Cytochrome P450 2E1
DAG	Diglyceride
DHEA	Dehydroepiandrosterone
DHT	Dihydrotestosterone
DGAT	Diacyly glycerol acyl transferase
DMSO	Dimethyl sulfoxide

DSD	Disorder of Sex Development
EGF	Epidermal growth factor
eIF2B	Eukaryotic initiation factor 2B
ER	Endoplasmic reticulum
F	Cortisol
FFA	Free fatty acids
FAS	Fatty acid synthase
FOXO	Forkhead box-containing protein
FTO	Fat mass and obesity-associated
G6Pase	Glucose-6- phosphatase
GC-MS	Gas chromatography-mass spectrometry
GDB	Global disease burdon
GFP	Green fluorescence protein
GIP	Gastric inhibitory polypeptide
GLP-I	Glucagon-like intestinal peptide I
GnRH	Gonadotropin releasing hormone
GPAT	Glycerol phosphate acyl transferase
GR	Glucocorticoid receptor
GRE	Glucocorticoid response elements
GS	Glycogen synthase
GSK	Glycogen synthase kinase
GWA	Genome wide association
H6PDH	Hexose-6 phosphate dehydrogenase
HDL	High-density lipoprotein
HGF	Hepatocyte growth factor
HL	Hepatic lipase
HMP	Hexose monophosphate pathway
HPA	Hypothalamus-pituitary-adrenal
HRP	Horseradish peroxidase
HSD	Hydroxysteroid dehydrogenases
HSL	Hormone sensitive lipase
HSP	Heat shock proteins
HTN	Hypertension
IDL	Intermediate density lipoprotein
IFN_{γ}	Interferon gamma
IGF	Insulin-like growth factor

IL-6	Interleukin 6
INSIG2	Insulin induced gene 2
IR	Insulin receptor
IRS	Insulin receptor substrate
LBD	Ligand binding domain
LC-MS	Liquid chromatography-mass spectrometry
LDL	Low-density lipoprotein
LH	Luteinizing hormone
LIF	Leukaemia inhibitory factors
LKB1	Liver kinase B1
LPL	Lipoprotein lipase
LXR	Liver X receptor
MAGL	Monoglyceride lipase
MAPK	Mitogen-activated protein kinase
MC2R	Melanocortin 2 receptor
MC4R	Melanocortin 4 receptor
MOTMS	Methyloxamine-trimethylsilylethers
MR	Mineralocorticoid receptor
MRAP	Melanocortin 2 receptor associated protein
MTBE	Methyl tert butyl ether
mTOR	Mammalian target of rapamycin
NAFLD	Non-alcoholic fatty liver disease
NASH	Non-alcoholic steatohepatitis
NHS	National Health Service
OM	Omental
OSM	Oncostatin M
PCOS	Polycystic ovarian syndrome
PDE3B	Phosphodiesterase 3B
PDK1	Phosphoinositide- dependent protein kinase 1
PEPCK	Phosphoenolpyruvate carboxykinase
PH	Pleckstrin-homology domain
PI3K	Phospho-inositide 3 Kinase
PIP2	Phosphatidylinositol-3, 4-diphosphate 2
PIP3	Phosphatidylinositol-3, 4-triphosphate 3
PKA	Protein kinase A
PKB	Protein kinase B

PKC	Protein kinase C
PNPLA3	Papatin-like phospholipase domain-containing 3
PTB	Phosphotyrosine binding domain
PVDF	Polyvinylidene difluoride
RT	Reverse Transcription
SC	Subcutaneous
SCD1	Stearoyl-CoA desaturase1
SH2	Src-homology 2
SHBG	Sex hormone binding globulin
SNP	Single nucleotide polymorphism
SNS	Sympathetic nervous system
SREBP-1c	Sterol regulatory element binding protein 1c
StAR	Steroidogenic acute regulatory protein
SDM	Site directed mutagenesis
SNP	Single nucleotide polymorphism
STK11	Serine/thereonine kinase 11
T2D	Type 2 diabetes
TAG	Triglyceride
TCA	Tricarboxylic acid cycle
TGF	Transforming growth factor
TNF	Tumour necrosis factor
tPA	Tissue-type plasminogen activator
TWEAK	TNF-like weak inducer of apoptosis
uPA	Urokinase-type plasminogen activator
VLDL	Very low density lipoproteins
WAT	White adipose tissue
WGA	Whole genome amplification
WHO	World health organization
ZF	Zona fasciculata
ZG	Zona glomerulosa
ZR	Zona reticularis

Chapter 1 General Introduction

1.1.Obesity epidemic

Obesity has become a global epidemic, with more than 1.3 billion overweight or obese patients worldwide (Chiang et al. 2011); 60% of adults are considered as obese or overweight (Hurt et al. 2010). The increase in numbers of overweight children is also alarming, having increased from 6% to 19% in the past 25 years (Ogden et al. 2007). Obesity and extreme obesity are characterised as a body mass index (BMI) greater than 30 and 40kg/m^2, respectively. A BMI of more than 25kg/m^2 is considered overweight (Hurt et al. 2010).

According to the World Health Organisation (WHO), in the global disease burdon (GDB) study analysing the leading causes of global mortality and disease burden, obesity and overweight were ranked within the top ten (Lopez et al. 2006). Obesity is associated with a number of diseases including diabetes mellitus, hypertension, hyperlipidemia, and some cancers (Field et al. 2001;Renehan et al. 2008). Moreover, obesity conveys a significant economic burden to society; in 2006–07, overweight and obesity-related ill health cost the National Health Service (NHS) in excess of £5 billion (Scarborough et al. 2011). The magnitute of obesity epidemic has highlighted the need to study the consequences and, in particular, to understand the regulation of fat metabolism.

1.1.1.Genetics of obesity

Genetics play a key role in the regulation of adiposity affecting human body weight (Barsh et al. 2000) and several genes have been implicated in predisposing the human body to weight gain. Genome wide association (GWA) scans have identified multiple gene loci that are associated with and contribute to the development of obesity. Single nucleotide polymorphisms (SNPs) in the fat mass and obesity-associated (FTO) gene have been shown

to be associated with obesity in many GWAs (Dina et al. 2007) , as well as insulin induced gene 2 (INSIG2) (Herbert et al. 2006). The mutations in FTO were associated with declined satiety (Wardle et al. 2008) and increased food intake. INSIG2 is involved in fatty synthesis within the liver and overexpression in rats was able to decrease hepatic lipogenesis (Takaishi et al. 2004). Mutations in this gene were shown to be associated with abnormal lipid metabolism in obese children (Wang et al. 2010).

1.1.2.Obesity and metabolic syndrome

The metabolic syndrome is a cluster of risk factors that increase cardiovascular morbidity and mortality. Although there are different definitions, the World Health Organisation (WHO) criteria are insulin resistance combined with any two of the following: central obesity, hypertriglyceridaemia, low high-density lipoprotein (HDL), cholesterol, hypertension, fasting hyperglycaemia, microalbuminuria (Alberti et al. 2006).

Insulin resistance has a central role in the development of the metabolic syndrome. As insulin resistance develops, the pancreatic β-cells produce more insulin in order to maintain glucose levels within the normal range. However, if the β-cells fail to produce enough insulin to prevent hyperglycaemia, glucose intolerance develops and this may eventually lead to type 2 diabetes (T2D) (Kahn 2003). Diabetes is associated with cardiovascular disease with macrovascular consequences including atherosclerosis and microvascular manifestations including retinopathy and nephropathy, causing blindness and renal failure (Creager et al. 2003). In addition, there is a strong association between obesity and non-alcoholic fatty liver disease (NAFLD), the heaptic manifestation of the metabolic syndrome , and also a variety of cancers, including hepatocellular carcinoma (Dowman et al. 2014).

1.2.Liver

The liver is the largest organ (second only to the skin) and the heaviest gland in the human body, weighing between 1200g to 1500g in an average adult. It is located under the diaphragm and occupies the upper right region of the abdominal cavity. This organ has two main lobes, a large right and a smaller left lobe, divided by the falciform ligament which extends from the diaphragm to the surface of the liver (Tortora and Derrickson 2011; Boron and Boulpaep 2009).

The hepatic artery is the main blood vessel feeding the liver with oxygenated blood from the aorta (Stevens and Lowe 2005). The liver also receives blood from the portal vein draining the splanchnic circulation including the small and large intestines, stomach, pancreas and spleen (Young and Heath 2000; Boron and Boulpaep 2009). The blood in these two vessels passes through sinusoids within the liver where oxygen and nutrients can be exchanged. Blood then leaves the liver through the hepatic vein and eventually joins the inferior vena cava to enter the right atrium of heart (Young and Heath 2000; Stevens and Lowe 2005) (Figure 1-1).

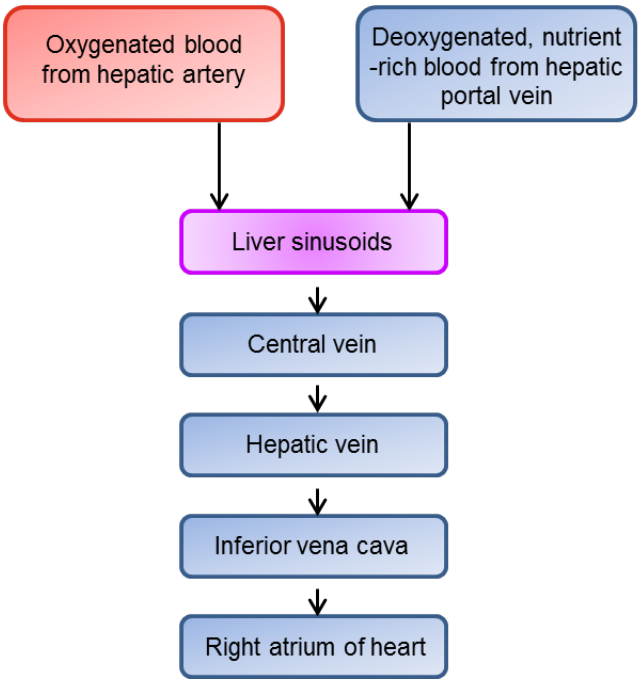

Figure 1-1 Simplified diagram of blood flow through the liver. The liver receives blood from hepatic artery carrying oxygenated blood (red box), and also from the portal vein providing high nutrition blood (blue box). The blood in these two vessels passes through sinusoids within the liver where oxygen and nutrients can be exchanged. Blood leaves the liver and drains in to the hepatic vein where eventually joins the inferior vena cava to enter the right atrium of heart.

1.2.1.Liver histology and physiology

Hepatocytes are the main functional cells in the liver, occupying 80% of liver parenchymal volume. Hepatocytes are polyhedral cells with large round nuclei, containing two to eight times the normal complement of chromosomes. These cells can store glycogen and lipid in large quantities. The cytoplasm has an eosinophilic granular appearance due to the large number of free ribosomes, rough endoplasmic reticulum (ER), and mitochondria which are crucial for providing energy for the multiple metabolic functions of the liver.

Endothelial cells, Kupffer cells and Stellate cells are the other key types of cells within the liver. Kupffer cells are a part of monocyte-macrophage defence which remove particulate matter from blood by their phagocytic action. Stellate cells store vitamin A in lipid droplets

and also produce extracellular matrix and collagen. During liver injury these cells are activated and can participate in fibrogenesis through collagen deposition (Boron and Boulpaep 2009; Young and Heath 2000) (Figure 1-2).

Cultures of isolated primary hepatocytes are the best *in vitro* model compared to cell lines which are being used in liver studies, as they resemble the human genes profile and human model the most. However, primary hepatocytes are expensive, and as donors with a BMI over 30, diabetes, viral infection, high alcohol consumption, or are on GC and related medications often need to be excluded, samples can be rare. Furthermore, they represent a monolayer culture where there is no interaction between hepatocytes and other liver cells. In order to reproduce *in vitro* the functional cell to cell connections observed *in vivo*, it is important to consider cell to cell interaction and proximity. As an example, the importance of the cell interaction in fibrogenesis induced by fat accumulation observed in NAFLD has been studied. Giraudi et al. designed an experiment in which mono culture hepatocytes and co-culture model of hepatocyte with stellate cells were both exposed to free fatty acids for 24h up to 144h. Increased steatosis by free fatty acids was observed in both simultaneous co-culture and monoculture. However, the activation of stellate cells and collagen biosynthesis was greater when cells were in close contact (Giraudi et al. 2015). In the current work we used cultures of isolated primary hepatocytes to simplify the system. However, animal and human models were used with other colleagues in the group in order to compare different models and to have a more comprehensive understanding.

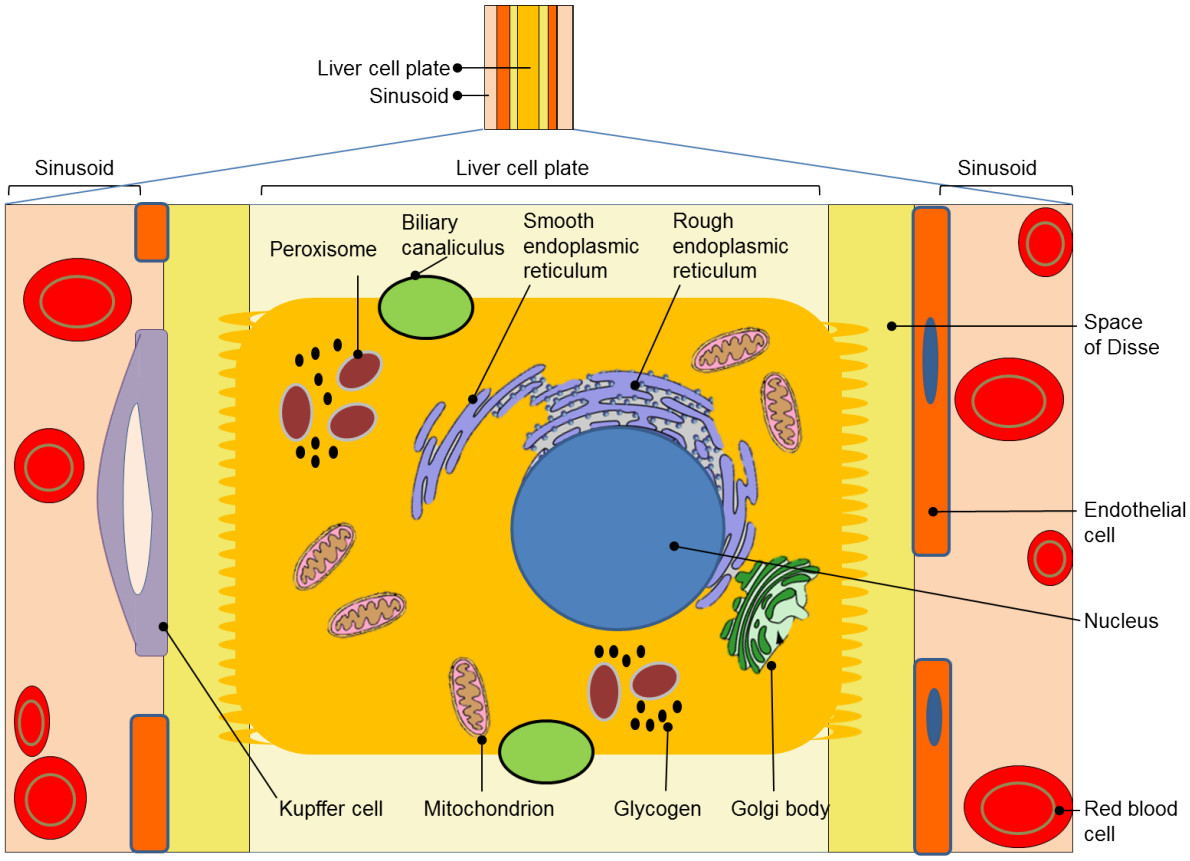

Figure 1-2 The structure of the hepatocyte cell. The hepatocytes contain a nucleus and many cellular organelles associated with secretary functions including ER and Golgi, and metabolic functions including mitochondria. Some of the hepatocytes form the sinusoids wall by lying adjacent to endothelial cells. Hepatocytes and endothelial cells are separated by small spaces called the space of Disse.

Liver cells are arranged and aligned to form lobules, and rows of these hexagonal shape lobules create defined liver lobes. Other than hepatocytes, the liver comprises bile cannaliculi and hepatic sinusoids containing bile and blood, respectively (Figure 1-3). Therefore, hepatocytes have three critical surfaces based on their transporting role; intercellular, canalicular and sinusoidal. The major part of the hepatocyte surface is sinusoidal (~70%), where material is transferred between hepatocytes and sinusoids through the space of Disse (an extracellular gap between sinusoids and hepatocytes (Figure 1-2). The hepatocyte membrane is covered with microvilli that extend into this gap increasing the surface area for

blood solute transport. Intercellular (transfers substances from cell to cell) and canalicular (drains bile from hepatocytes into canaliculi) both account for approximately 15% of the hepatocyte surface area (Young and Heath 2000; Stevens and Lowe 2005).

Anatomically and functionally, the arrangement of the hepatocytes, bile duct and hepatic sinusoids has been described in three different models; 1.classic hepatic lobule and 2.portal lobule, with the emphasis on the lobule hexagonal shape and bile acid secretion respectively. These were thought to be the correct anatomical arrangement for many years (Tortora and Derrickson 2011), however, the hepatic (or portal) acinus has been proposed as the third model and describes a zonal relationship between hepatocytes and blood vessels (Rappaport 1980) (Figure 1-3). This model emphasizes the importance of the oxygenated arterial blood supply and proposes an oxygenation gradient from the portal triad (a unit consisting of a bile duct, one branch of the hepatic artery and one of the hepatic vein) towards the central hepatic vein (Tortora and Derrickson 2011). Only the third model is discussed further below.

Although the exact boundaries are hard to define, cells in hepatic acinus are organised in three zones;

- Zone I (periportal): cells in this zone receive the highest oxygen and nutrient concentrations as a consequence of their location adjacent to the portal triad. These cells are the last to die and the first to regenerate following liver injury. However, they have the highest response to toxin exposure and bile obstruction.

- Zone III (pericentral): is the furthest from portal triad and located close to the central vein. Zone III cells receive the least oxygen and nutrients and rarely regenerate. However, these cells considered to be crucial for detoxication and biotransformation of drugs.

- Zone II hepatocytes are located between zone I and III with intermediate functional characteristics (Boron and Boulpaep 2009; Tortora and Derrickson 2011).

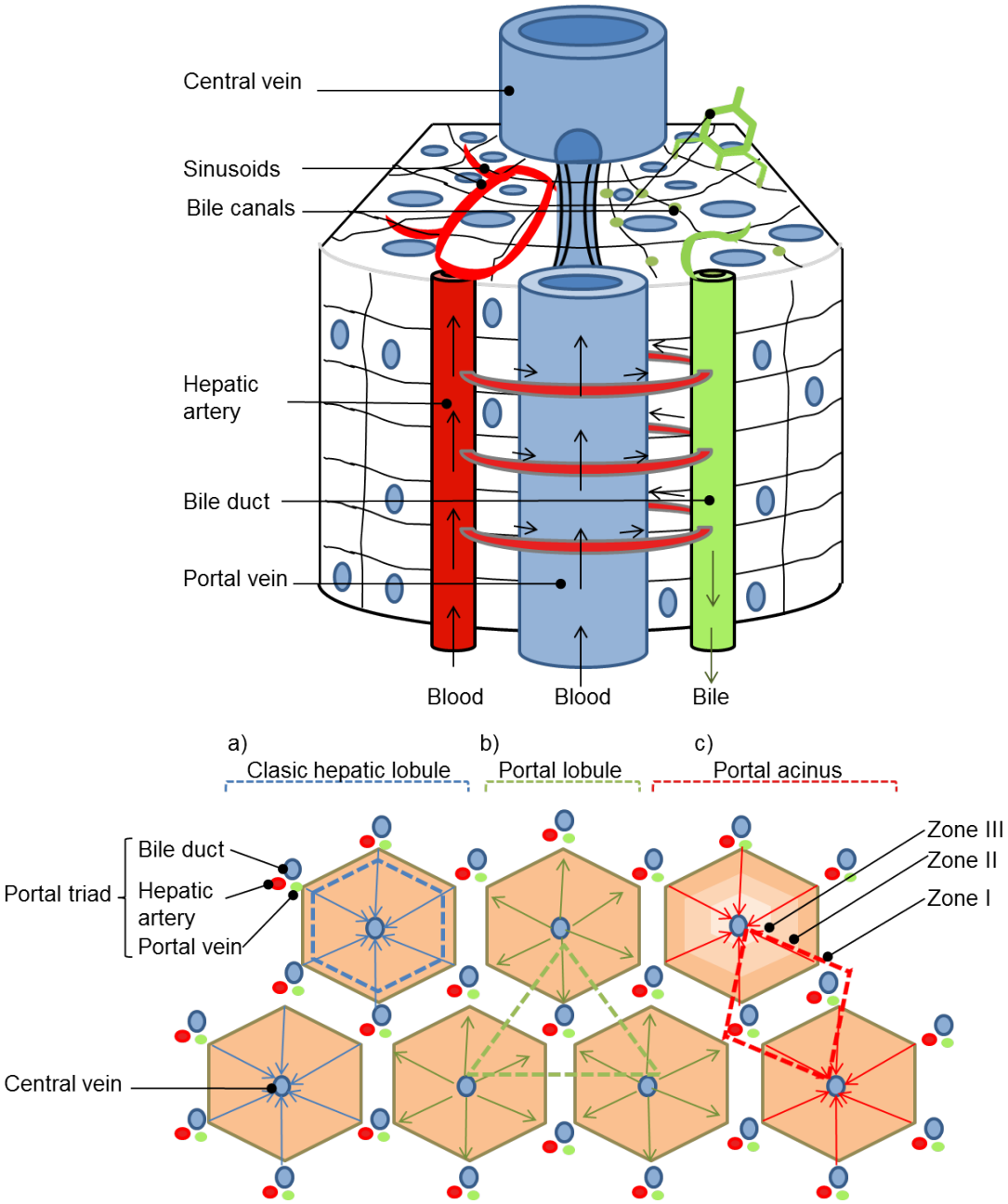

Figure 1-3 The liver lobes are made up of hexagonal lobules which comprise of rows of hepatocytes. The hepatocytes are in close contact with sinusoids and canaliculi. The structure of the liver lobules, representing three different models for the arrangements of bile duct, hepatic artery and portal vein; classic hepatic lobule (a), portal lobule (b) and portal acinus (c).

The metabolic processes (metabolism of amino acids, carbohydrate and lipid) are also zoned as a consequence of this heterogeneity in distribution of metabolic enzymes across the acinus. Periportal hepatocytes are shown to be mostly gluconeogenic while pericentral cells are predominantly glycolytic (Jungermann and Katz 1982). With regard to lipid metabolism, the main focus in this thesis, pericentral hepatocytes in zone III are thought to have greater levels of lipogenesis while periportal hepatocytes have higher levels of the β-oxidation (Guzman and Castro 1989). The predominant metabolic activity is compared between zone I and III in Table 1-1 (the named pathways in this table are only briefly introduced but will be discussed in detail in section 1.2.3). This zonation has an important effect on lipid metabolism and the development of hepatic steatosis. In obese leptin deficient ob/ob mice, the hepatic steatosis observed in these mice was distributed in pericentral hepatocytes (Wiegman et al. 2003). In humans, simple steatosis starts in the pericentral area extending towards the intermediate and periportal zones as the disease develops (Chalasani et al. 2008).

Zone I	Zone III
Gluconeogenesis (from lactate, amino acids, glycerol)	**Glycogen synthesis** (from glucose)
Glycogen degradation (conversion of glycogen to glucose)	**Glycolysis** (conversion of glucose to pyruvate)
Oxidative energy metabolism (oxygen utilization, β-oxidation - converting fatty acids to acyl CoA to generate ATP)	***De Novo* Lipogenesis** (fatty acid synthesis from acetyl CoA)
Cholesterol synthesis	**Bile acid biosynthesis**
Amino acid catabolism	**Ketogenesis** (conversion of fatty acids to ketone bodies)
Ureagenesis (from ammonia, amino acid nitrogen)	**Glutamine synthesis** (from ammonia, glutamate)

Table 1-1 The metabolic processes are zoned in hepatocytes. The metabolic activity compared between zoneI and zoneIII in hepatocytes is presented in this table.

1.2.2.Hepatocyte embryology and proliferation

The liver is embryologically derived from the anterior part of the foregut endoderm at about the middle of the third week or early fourth week of pregnancy (Sherwood et al. 2009). Although hepatocytes and biliary epithelial cells arise from endoderm, blood vessels, stellate and kupffer cells arise from mesodermal progenitor cells (Zorn 2008).

Hepatocytes have little proliferative activity. However, they have a rapid proliferative response following liver injury where hepatocytes can be generated by replication of existing mature hepatocytes. When mature hepatocytes replication is delayed or inhibited, repopulation occurs by proliferation and differentiation of progenitor liver cells known as oval cells (Duncan et al. 2009) (Figure 1-4).

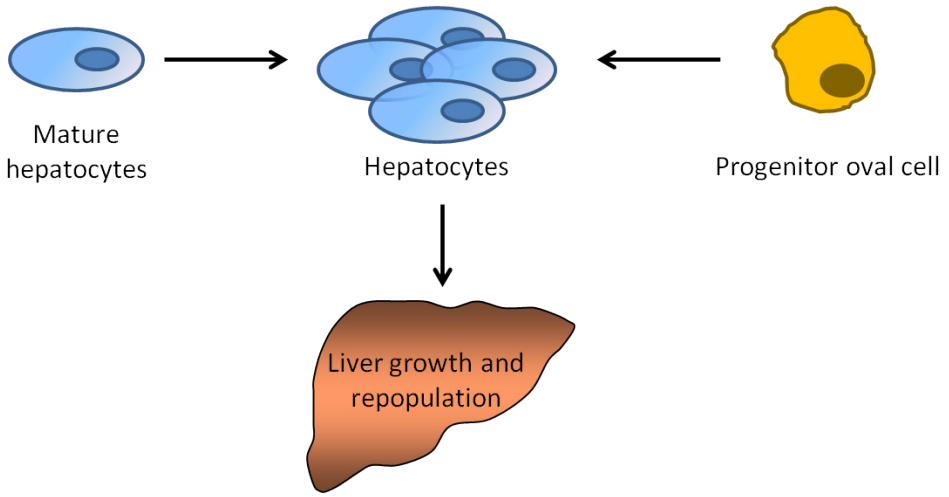

Figure 1-4 The Liver growth and repopulation occurs in two different ways; by proliferation and differentiation of oval cells or replication of mature hepatocytes.

Oval cells derive from the portal area of the lobule where the putative hepatic stem cell is located. Oval cells have the ability to differentiate to either biliary epithelial cells or hepatocytes, and therefore these cells are termed liver progenitor cells.

Hepatocyte regeneration is a multistep process including various cytokines and growth factors. The oval cells response to these factors can be divided into four stages; activation, proliferation, migration and differentiation. The first signalling event that initiates oval cell activation occurs through interferon gamma (IFN_{γ}), interleukin 6 (IL-6) and tumour necrosis factor (TNF) receptor type 1. IFN_{γ} deficient mice have an impaired oval cell response but elevated hepatocyte regeneration after partial hepatectomy. There is also evidence to suggest contributions of other members of TNF family in activation of oval cells. TNF-like weak inducer of apoptosis (TWEAK) ligand and its receptor, Fn14 are members of the TNF family. Transgenic mice overexpressing TWEAK in hepatocytes have increased oval cell numbers but no effect on hepatocytes suggesting that TWEAK is selective in its ability to regulate the oval cell response (Jakubowski et al. 2005).

There are other growth factors that can act as primary stimuli for the proliferation step including hepatocyte growth factor (HGF), epidermal growth factor (EGF) and transforming growth factor (TGF) (Jakubowski et al. 2005). Plasminogen activators are involved in a proteolytic cascade that appears to play a crucial role in tissue regeneration. Urokinase-type plasminogen activator (uPA) and tissue-type plasminogen activator (tPA) are specifically involved in oval cell expansion and migration during liver regeneration by conferring a proliferative advantage to oval cells in an extracellular matrix containing both latin and fibrin growth factors (Bisgaard et al. 1998). Oncostatin M (OSM) and its receptor, from the IL-6 cytokine family, are also important in the differentiation of oval cells to hepatocytes (Okaya et al. 2005). In addition, leukaemia inhibitory factors (LIF) are also known to induce this differentiation (Omori et al. 1996) (Figure 1-5).

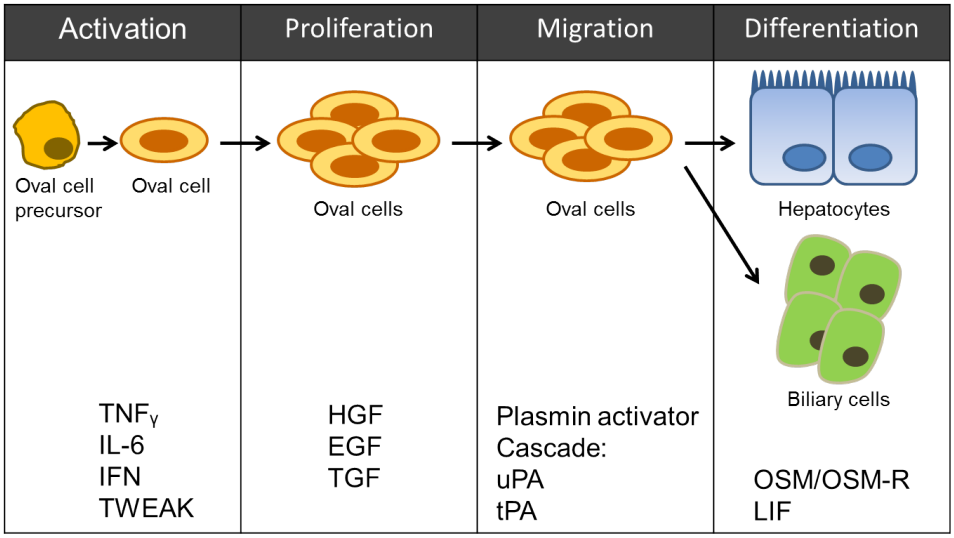

Figure 1-5 Oval cells derive from the portal area of the lobule and have the ability to differentiate to either biliary epithelial cells or hepatocytes. The oval cells response to cytokines and growth factors for hepatocytes regeneration is divided into four stages; activation, proliferation, migration and differentiation.

1.2.3.Metabolic functions of the liver

The liver has many metabolic functions including bile acid synthesis and secretion, bilirubin excretion, detoxification and elimination of metabolites and storage of fat soluble vitamins (Stevens and Lowe 2005). It produces urea, non-essential amino acids and most of the circulating plasma proteins from amino acids. However, its major role is in protein, carbohydrate and lipid metabolism (Boron and Boulpaep 2009). The principle focus of this thesis is lipid metabolism, but a brief over view of carbohydrate metabolism will also be presented.

1.2.3.1.Carbohydrate metabolism and in liver

Liver plays a significant role in regulation of carbohydrate metabolism by maintaining glucose levels in a normal range. This happens through metabolic processes that either

regulate glucose synthesis or break down which in turn are highly controlled by insulin (Raddatz and Ramadori 2007).

1.2.3.1.1.Glycogenesis

The process of glycogen synthesis from glucose is called glycogenesis. This includes phosphorylation of glucose to glucose 6-phosphate by glucokinase and then conversion to glycogen by glycogen synthase (Harvey and Champe 2005) (Figure 1-6, b-1). In the liver, insulin increases glycogenesis and so promotes glucose storage in the fed state (Sutherland et al. 1993).

1.2.3.1.2.Gluconeogenesis

Gluconeogenesis is the synthesis of glucose from amino acids, glycerol, and lactate (Figure 1-6, a-2) Release of glucose from liver into the circulation during fasting is of fundamental importance to maintain circulatory glucose levels. Therefore, gluconeogenesis increases overnight and during prolonged fasting, to maintain blood glucose. However, in the fed state in the liver, the elevated insulin to glucagon ratio inactivates the essential enzymes for gluconeogenesis including glucose-6- phosphatase (G6Pase), phosphoenolpyruvate carboxykinase (PEPCK) (discussed in 1.3.4.4.4) and fructose 1,6-bisphosphatase. Fructose 1,6-bisphosphatase is inactivated through cyclic adenosine monophosphate (cAMP) and its phosphorylation (see section 1.3.4.4.3) (Harvey & Champe 2005).

1.2.3.1.3.Glycolysis

Glycolysis is a series of reactions whereby glucose is converted to pyruvate and subsequently to acetyl CoA. The acetyl CoA produced in this pathway can be used in fatty acid synthesis or can be oxidised through the tricarboxylic acid cycle (TCA) and to generate adenosine triphosphate (ATP) (Figure 1-6, b-2). In the liver, insulin drives glycolysis in the fed state (Gomez-Lechon et al. 1990) through activation of the rate-limiting enzymes of glycolysis including phosphofructokinase (Harvey & Champe 2005).

1.2.3.1.4.Glycogenolysis

The process of glycogen breakdown, by sequential removal of glucose monomers, catalysed by glycogen phosphorylase, is termed glycogenolysis (Figure 1-6, a-1). In the liver, glycogenolysis is increased during fasting, in order to release of glucose to the circulation (Sutherland, Leighton, & Cohen 1993).

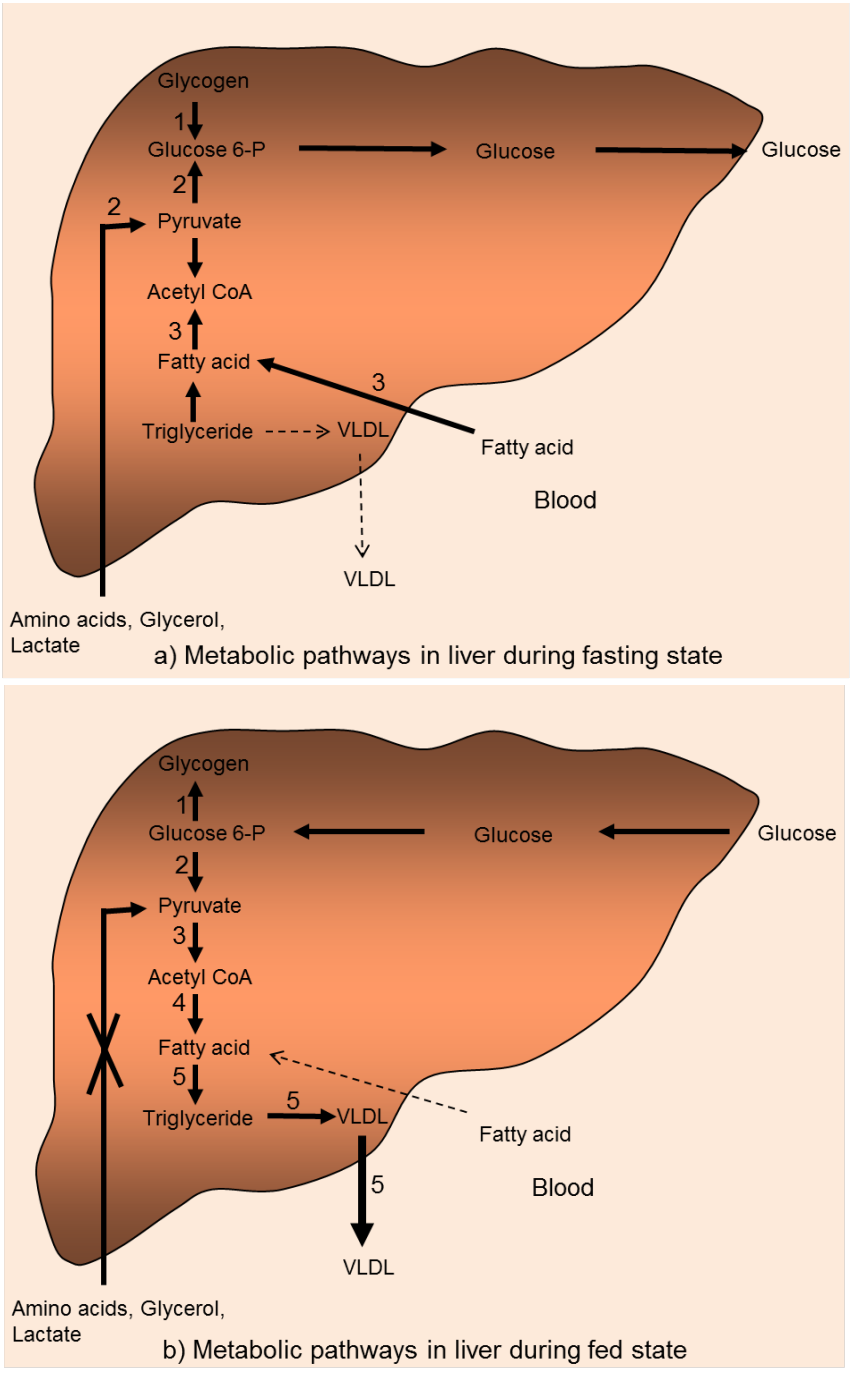

Figure 1-6 Anabolic and catabolic pathways in fasted (a) and fed state (b) in liver. In fasting state; glycogenolysis (glycogen breakdown to glucose monomers) (a-1), gluconeogenesis (synthesis of glucose from amino acids, glycerol, and lactate)(a-2) and fatty acid uptake(a-3) are increased while VLDL production is decreased, in order to provide energy. In fed state; glycogenesis (glycogen synthesis from glucose) (b-1) and glycolysis (glucose conversion to pyruvate and subsequently to acetyl CoA) (b-2) as well as de novo lipogenesis (acetyl CoA conversion to fatty acids) (b-4), esterification (combination of fatty acids with glycerol to produce triglyceride) (b-5) and VLDL packaging (b-5) pathways are enhanced while gluconeogenesis is blocked, in order to store energy. Abbreviations: Glucose 6-P=glucose 6-phosphate, VLDL= very low density lipoprotein.

1.2.3.2.Lipid metabolism in the liver

The amount of intracellular triglyceride (TAG) is a balance between fat accumulation and fat loss. In the liver, this is regulated by fat accumulation through *de novo* lipogenesis and fatty acid uptake or by the breakdown of fatty acid via β-oxidation or TAG can be packaged into very low density lipoprotein (VLDL) and released into circulation.

1.2.3.2.1.Lipogenesis

Lipogenesis includes both *de novo* lipogenesis, where fatty acids are synthesised from simple sugars in particular glucose, and their subsequent esterification to glycerol to form TAG (Figure 1-6, b-3,4,5). During *de novo* lipogenesis or fatty acid synthesis, carbons from acetyl CoA are incorporated into a growing fatty acid chain. The first and rate limiting step in *de novo* lipogenesis is the ATP-dependent carboxylation of acetyl CoA to malonyl-CoA by acetyl CoA carboxylase (ACC). The fatty acid synthase (FAS) enzyme then condenses the malonyl-CoA produced with acetyl CoA and the subsequent reactions between the growing acetyl CoA chain and newly synthesised malonyl-CoA eventually result in the formation of a 16 carbons fatty acid palmitate (Ruderman et al. 2003) (Figure 1-7). There are two isoforms of ACC, ACC1 in cytosol and ACC2 on the outer mitochondrial membrane (Zhao et al. 2010). In lipogenic tissues, including the liver, ACC1 is the rate-limiting step in lipogenesis. Indeed, liver-specific ACC1 knockout mice have decreased hepatic lipid accumulation (Mao et al. 2006). Although both isoforms mediate the conversion of acetyl CoA to malonyl-CoA, the malonyl-CoA produced by ACC2 inhibits carnitine palmitoyl-CoA transferase I (CPTI) and as a consequence results in inhibition of mitochondrial β-oxidation (Zhao et al. 2010).

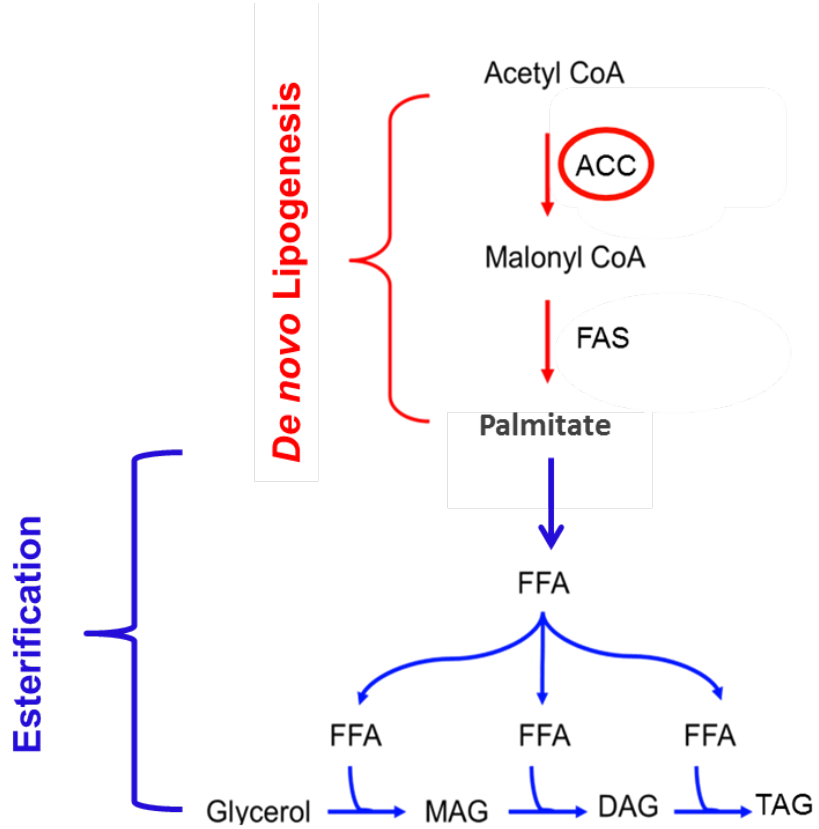

Figure 1-7 De novo lipogenesis and subsequent triglyceride (TAG) synthesis. De novo lipogenesis is including rate limiting carboxylation of acetyl CoA to malonyl-CoA by acetyl CoA carboxylase (ACC) and the conversion of malonyl-CoA to palmitate by fatty acid synthase (FAS), Esterification results from combination of free fatty acids (FFA) with glycerol which can produce monoglyceride(MAG), dilyceride(DAG), and triglyceride(TAG).

Free fatty acids (FFA) for TAG synthesis are available from fatty acid uptake and *de novo* lipogenesis within the liver (Postic and Girard 2008). Esterification of FFAs to a glycerol backbone to form TAG is the next step in lipogenesis. Esterification of glycerol to TAG is mediated by two enzymes: diacyly glycerol acyl transferase (DGAT) and glycerol phosphate acyl transferase (GPAT). DGAT has two isoforms namely DGAT1 and DGAT2; DGAT1 is primarily expressed in white adipose tissue and small intestine while DGAT2 is highly expressed in white adipose tissue and liver. There is evidence in literature showing these two enzymes play different roles in TAG synthesis. DGAT1 knockout mice have approximately

50% less TAG in tissues and are protected from insulin resistance and diet-induced obesity through increased energy expenditure pathways (Chen et al. 2002; Smith et al. 2000). However, in a study using antisense oligonucleotides (ASO) in rats with diet-induced NAFLD, DGAT2 ASO (but not DGAT1 ASO) rat improved hepatic steatosis and insulin sensitivity (Choi et al. 2007). Finally, the liver packages TAG into VLDL particles and secretes them into the blood to be used by other tissues (Harvey & Champe 2005). TAG is nonpolar, and therefore it needs to be packaged into lipoproteins to be transported in the plasma. Plasma lipoproteins are separated to five groups according to their size, mobility, electrophoretic, hydrated density, and also their relative content of TAG, cholesterol and protein. These five major classes are; chylomicron, very low-density lipoprotein (VLDL), high-density lipoprotein (HDL), low-density lipoprotein (LDL),and intermediate lipoprotein (IDL) (Cox and Garcia-Palmieri 1990).

Nascent VLDLs are produced in the lumen of the ER in hepatocytes. VLDLs are composed of a TAG core covering with phospholipids, cholesterol and apoproteins. Among several apoproteins, apoprotein B provides structural ability to the VLDL particle, and therefore is the most important one. VLDL size is ranged between 35 to 100nM diameters. After biogenesis, they transport from the ER lumen into the golgi in hepatocytes and this transportation is facilitated by the VLDL transport vesicles. In golgi they are processed and finally post-golgi mature VLDL particles are transported to the plasma membrane and secreted to the circulatory system (Tiwari and Siddiqi 2012).

ACC1 activity is highly regulated through post-transcriptional phosphorylation. ACC1 can be phosphorylated at different residues leading to activation or inhibition of ACC1 activity (Hardie 1992). For example: phosphorylation at ser-29 induces ACC1 activity (Haystead et al.

1988) but phosphorylation at ser-79, 1200, and 1215 negatively regulates its activity (Hardie 1992). On the other hand, insulin increases lipogenesis via activating AMP-kinase (AMPK) which then negatively phosphorylates ACC1 (Witters and Kemp 1992) (see section 1.3.4.4.3).

1.2.3.2.2.Fatty acid Uptake

The liver takes up two forms of fatty acids from dietary lipid; 1.directly from long chain fatty acids and 2.in the form of large proteolipids called chylomicrons. Chylomicrons are absorbed into enterocytes (intestinal mucosal cells) and are composed predominantly of TAGs which are packaged with phospholipids, cholesterol and apoproteins. TAG in chylomicrons is hydrolysed by lipoprotein lipase (LPL) on the capillary endothelium walls in muscle and adipose tissue. The products of this digestion are glycerol, fatty acids and remnant chylomicrons. The first two products of LPL, fatty acids and glycerol, enter the muscle and adipose tissue and remnant chylomicrons remain in circulation and move towards liver. Remnant chylomicrons are smaller chylomicrons which are mainly TAG, rich in cholesterol, and therefore they can enter hepatocytes by endocytosis through a specific low-density lipoprotein (LDL) receptor called the LDL related receptor. Long chain fatty acids can enter the hepatocytes directly by simple 'flip–flop' diffusion across the lipid bilayer or through fatty acid transporter FAT/CD36. The importance of FAT/CD36 in fatty acid uptake in muscle and adipose tissue is well described (Bonen et al. 2007;Silverstein and Febbraio 2009) but the expression of hepatic FAT/CD36 is reported to be low (Berk 2008;Luiken et al. 2002). However, there is evidence that FAT/CD36 protein expression is increased with the TAG content presenting in different models of hepatic steatosis (Buque et al. 2012).

As described in section 1.2.3.3.1, the liver synthesises TAG by *de novo* lipogenesis which is also packaged with phospholipids, cholesterol and apoproteins into VLDL. VLDL enters circulation to reach muscle and adipose tissue where it is hydrolysed by LPL to fatty acids, glycerol, VLDL remnant and intermediate density lipoprotein (IDL). The fatty acids and glycerol are used as fuel in muscle and as storage in adipose tissue. IDL is taken up by liver, to a lesser extend compared to LDL, through the LDL receptor.

Hepatic lipase (HL) is expressed on the basolateral surface of the hepatocytes and on endothelial cells (Sanan et al. 1997) as well as in circulation. This is a multifunctional protein that works as a lypolytic enzyme as well as a ligand binding function that facilitates lipid uptake depending on site of expression. HL directly binds to IDL, LDL, VLDL remnant and HDL and enhances their uptake into hepatocytes through cell surface receptors including LDL receptor (Krapp et al. 1996;Marques-Vidal et al. 1994) (Figure 1-8).

1.2.3.2.3.Lipolysis

TAG represents the body's main source of energy and through lipases activity in adipose tissue it is hydrolysed to produce FFA which is subsequently get into circulation and can be used by other distant tissues such as muscle and liver in the process of β-oxidation to generate ATP (see section 1.2.3.3.4).

As mentioned in section 1.2.3.3.2, HL has a classical function as a lipolytic enzyme hydrolysing TAG to diglyceride (DAG) and FFA as well as phospholipid to lysophospholipid and FFA, in liver and also in circulation. Patients with HL deficiency accumulate plasma VLDL, IDL, LDL, HDL and chylomicron remnants presenting with hypertriglyceridemia and hypercholesterolemia (Breckenridge et al. 1982;Hegele et al. 1993).

Two other main lipolytic enzymes are hormone sensitive lipase (HSL) and monoglyceride lipase (MAGL) which work together to hydrolyse TAG completely. HSL can use both TAG and DAG as substrates, removing the first and second fatty acids from TAG. MAGL removes the last fatty acid releasing glycerol (Figure 1-8). These enzymes as well as other lipases such as adipose triglyceride lipase (ATGL) are highly expressed in adipose tissue where the majority of lipolysis within the body occurs. However, HSL and ATGL have been shown to directly affect hepatic lipid metabolism as hepatic overexpression of HSL and ATGL promote release of fatty acids and β-oxidation (Reid et al. 2008).

Perilipin is a lipid droplet associated protein family which consists of five members named Plin1 to 5 and Plin5 is highly expressed in liver. Plin5 binds directly to ATGL inhibiting the ATGL- lipid droplet aggregation (Dalen et al. 2007).

1.2.3.2.4.β-oxidation

Breaking down fatty acids to generate acyl CoA occurs through the process of β-oxidation within mitochondria. In the liver, acetyl CoA produced from this pathway can either be used to form ketone bodies or can enter the Krebs cycle and generate ATP (Sprecher et al. 1995).

This oxidation is the main source of energy for the liver, notably during fasting. CPT is the rate-limiting enzymatic step in β-oxidation, transferring acyl CoA into the mitochondria. CPTI is positioned in the outer mitochondrial membrane and facilitates this transport by conjugating the fatty acid chain with carnitine. The free CoA is then released into the cytosol, and the Acyl carnitine is transported to the inner membrane (Harvey & Champe 2005;Zammit 1999). Acyl carnitine is transported across the inner membrane by carnitine acylcarnitine translocase (CAT) (Murthy and Pande 1984). Carnitine palmitoyl-CoA transferase II (CPTII)

is bound to the matrix side of the inner mitochondria by which Acyl carnitine is converted back to fatty acyl CoA releasing the molecule of carnitine (Johnson et al. 1995). In the mitochondria matrix, the fatty acids enter a cycle of multiple reactions, producing NADH, FADH2 and acetyl CoA. NADH and FADH2 produce ATP when oxidized by the electron transport chain. Finally, the acetyl CoA can then enter the tricarboxylic acid (TCA) cycle to generate more ATPs.

As discussed previously CPTI activity is inhibited by malonyl CoA produced by ACC2. In addition, ACC2 is negatively regulated by AMPK (see section 1.3.4.4.3) and therefore co-ordinately decreasing lipogenesis and increasing β-oxidation (Figure 1-8).

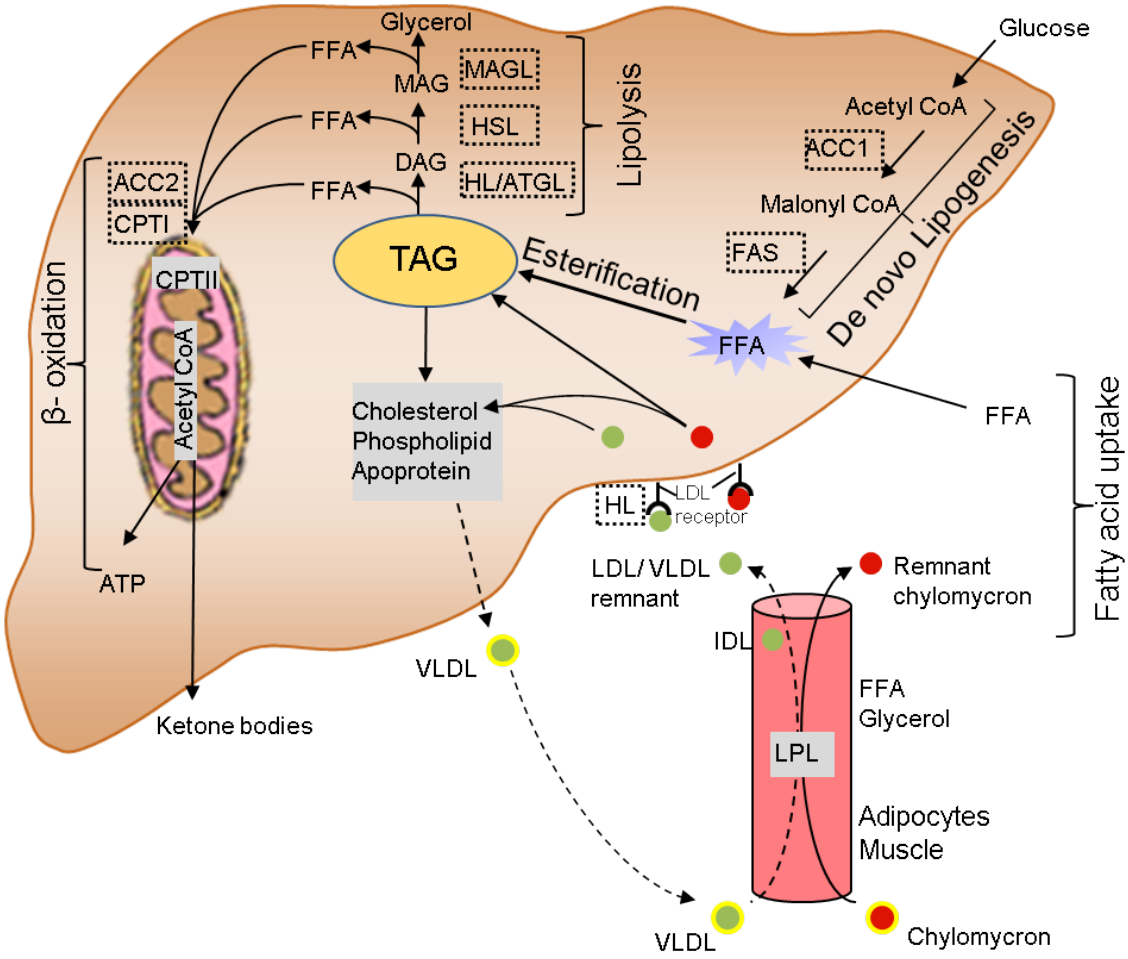

Figure 1-8 Lipid metabolism within the liver. The FFAs, provided by either de novo lipogenesis or fatty acid uptake, undergo esterification to produce TAG. TAG can be packaged in VLDL particles and be secreted into circulation. However, during fasting, TAG undergoes lipolysis and subsequently β-oxidation to generate ATP (ACC= acetyl CoA carboxylase, ATGL= adipose triglyceride lipase, CPT= Carnitine palmitoyl-CoA transferase, DAG= diacylglyceride, FAS= fatty acid synthase, FFA= free fatty acid, HL= hepatic Lipase, HSL= hormone sensitive lipase, LDL= low density lipoprotein, MAG= monoacylglyceride,MAGL= monoacylglyceride lipase, TAG= triglyceride, VLDL= very low density lipoprotein).

1.2.4.Fatty liver disease

Non-alcoholic fatty liver disease (NAFLD) is considered to be the hepatic manifestation of the metabolic syndrome (Lim et al. 2010;Pascale et al. 2010). It is associated with the development of obesity and insulin resistance, and it may be present in up to 90% of obese

individuals (Nugent and Younossi 2007). NAFLD is not only prevalent among adults but its incidence is rapidly increasing in children (Franzese et al. 1997;Tominaga et al. 1995). NAFLD is characterised by accumulation of fat in the liver and refers to a progressive spectrum of disease ranging from simple hepatic steatosis to inflammatory non-alcoholic steatohepatitis (NASH), fibrosis, and liver cirrhosis (Trauner et al. 2010) (Figure 1-9).

.

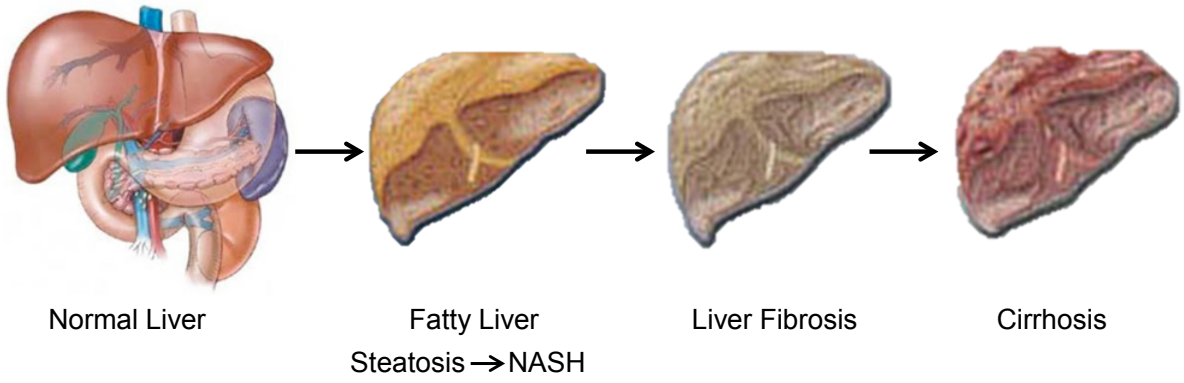

Figure 1-9 Stages of liver damage in NAFLD. NAFLD demonstrates a spectrum of liver disease ranging from simple hepatic steatosis. Inflammation can convert steatosis to non-alcoholic steato-hepatitis (NASH) which can end up in cirrhosis with liver failure.

The earliest stage of NAFLD is reversible hepatic steatosis, where excess TAG accumulates in lipid droplets within the cytoplasm of hepatocytes. True hepatic steatosis is defined when lipid is present in more than 5% of hepatocytes. Studying biopsy-proven NAFLD patients, a simple steatosis has a benign clinical course without excess mortality (Ekstedt et al. 2006). However, the disease can progress to inflammation, termed non-alcoholic steatohepatitis (NASH). NASH may eventually cause scarring and fibrosis (Jou et al. 2008) and whilst the liver may function normally initially, progressive fibrosis and scarring liver cirrhosis is associated with cardiovascular and liver mortality (Ekstedt et al. 2015).

NAFLD occurs when lipid deposition is excessive reflecting an imbalance between lipid accumulation by *de novo* lipogenesis or fatty acid uptake and lipid clearance via fatty acid β-oxidation or TAG-rich lipoprotein secretion (Barrows et al. 2005;Lou-Bonafonte et al. 2011) (Figure 1-10).

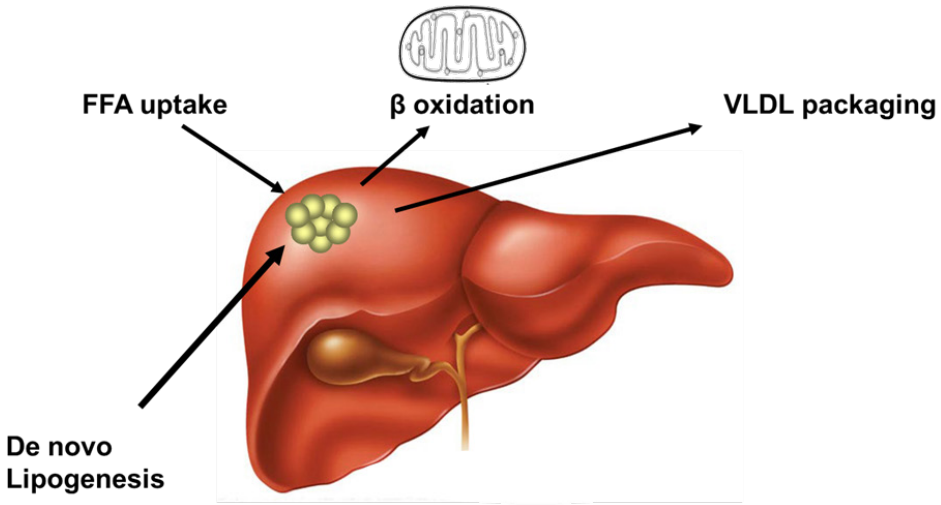

Figure 1-10 The amount of intracellular TAG is a balance between accumulation, by de novo lipogenesis or FA uptake and by loss from the breakdown of fatty acids by β-oxidation or it can be packaged into VLDL and released into circulation.

Liver biopsy remains the 'gold-standard' for the diagnosis and staging of NAFLD (Chalasani et al. 2012). In a clinical study patients with NAFLD who underwent a liver biopsy also received intravenous infusion and oral administration of multiple stable isotopes; [$^{13}C_1$] sodium acetate, [1,2,3,4 $^{13}C_4$] potassium palmitate and [$^{2}H_{31}$] glycerol-tripalmitin, which were used to track the rate of fatty acids. This study defined the metabolic pathways that contribute to hepatic lipid accumulation, with the greatest proportion (59%) of TAG re-esterified from circulating FFAs 26.1% from *de novo* lipogenesis and 14.9 % from dietary fatty acids (Donnelly et al. 2005). A separate study compared the contribution of *de novo* lipogenesis to VLDL-TAG in the fasted and fed states. During fasting, 77.2% of VLDL-TAG was derived from serum FFAs with only 4% from *de novo* lipogenesis. However, after feeding, the

proportion derived from circulating FFAs decreased to 43.6% and that from *de novo* lipogenesis increased to 8.6%, with 15.2% from chylomicron remnant-TAG and 10.3% from dietary fatty acids (Barrows and Parks 2006).

Despite the high prevalence of steatosis only a minority (7 out of 127 NAFLD patients or 5.4%) (Ekstedt et al. 2006) progress to steatohepatitis and therefore poorly defined triggering factors are needed in order to develop NASH (Anstee et al. 2013). Both dietary or environmental factors and genetics can influence the progression of NAFLD. The best genetic predictor of NAFLD is well recognised to be a loss of function mutation (I148M) in papatin-like phospholipase domain-containing 3 (PNPLA3, also known as adiponutrin) (Romeo et al. 2008). PNPLA3 is from the papatin family that has nonspecific lipid acyl hydrolase activity with the preference for TAG (Galliard 1971). The I148M mutation enhances TAG accumulation by inhibiting lipid breakdown (He et al. 2010) and also has been associated with progression or complications of NAFLD including NASH, cirrhosis and hepatocellular carcinoma (Zimmer and Lammert 2011) . In addition, genetic variation in cytochrome P450 2E1 (CYP2E1, an endoplasmic monooxygenase oxidising alcohols and FAs) is also reported to be related to NASH (Piao et al. 2003).

There are additional factors that are associated with NAFLD progression. These include, elevated levels of tumour necrosis factor α (TNF-α), interleukin 6 (IL-6) (Feldstein 2010), and lipotoxicity- induced endoplasmic reticulum (ER) stress resulting from improperly folded proteins aggregating in the ER (Yang et al. 2010).

1.3.Insulin

Insulin is the principal hormone controlling glucose metabolism. It is secreted from the β-cells of the pancreatic islet in response to elevated blood glucose levels although different stimuli such as amino acids and gastrointestinal hormones are also able to modulate its secretion (Rasmussen et al. 1990). In addition to its metabolic actions, insulin has strong mitogenic and anti-apoptotic effects which are regulated via the MAPK (mitogen-activated protein kinase) pathway (Chen et al. 2012).

1.3.1.Insulin structure and synthesis

Insulin gene transcription occurs only in pancreatic β-cells resulting in a full length mRNA production which is then translated to a single polypeptide precursor called pre-proinsulin. This polypeptide is attached to the ER membrane and consists of four domains; two chains (A and B), a connecting region known as C-peptide and an N-terminal signal peptide (Sanger 1960). Once the signal peptide is cleaved, proinsulin is formed and enters the ER lumen. The sulphide bridges between A and B chains are formed as a consequence of the oxidising ER environment. Proinsulin is transported to the golgi complex where a subsequent removal of the C-peptide results in insulin formation. The mature hormone with two peptide chains (A and B) is then packaged from the golgi by exocytosis and accumulates within the secretory granules in cytoplasm (Boron and Boulpaep 2009) (Figure 1-11).

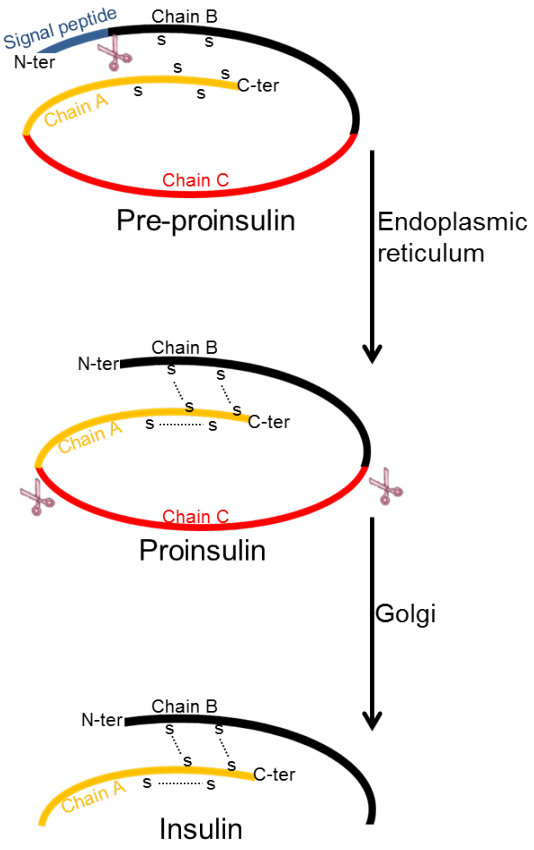

Figure 1-11 The principles of insulin synthesis in pancreatic β-cells. Insulin is synthesised as preproinsulin and enters the ER to form proinsulin. Proinsulin is then transported to the golgi and converted to insulin.

1.3.2.Insulin secretion

Insulin secretion is regulated by a variety of positive and negative stimuli. Nutrients such as glucose and amino acids-especially arginine (Tang et al. 2013) and leucine (Yang et al. 2010) as well as gastric hormones including glucagon-like intestinal peptide I (GLP-I), gastric inhibitory polypeptide (GIP) and cholecystokinin, are known to enhance insulin secretion. However due to insulin's primary role in glucose metabolism, glucose is the major regulator of secretion.

Elevated blood glucose triggers insulin secretion by the following mechanism. High circulating glucose is transported into β-cells through GLUT2 glucose transporters. This intracellular glucose is metabolised via glycolysis, producing pyruvate which then enters the mitochondria and generates adenosine triphosphate (ATP). The elevation in ATP/ADP ratio closes ATP-sensitive potassium channels, results in increased intracellular potassium which leads to cell membrane depolarisation (Smith et al. 1989). This activates voltage gated calcium channels promoting calcium influx into the cytosol (Bergsten et al. 1994) which also triggers intercellular calcium release. A rise in calcium concentration evokes the exocytosis of the secondary granules containing insulin (Figure 1-12).

There are also inhibitory mechanisms controlling insulin secretion especially during stress and also when energy mobilization is required for example during physical exercise (Peterson 2007). Adrenaline, somatostatin and leptin are known to be negative stimuli for insulin release. Adrenaline is the most potent of these inhibitors and simultaneously activates potassium channels whilst inactivating calcium channels within the β-cells (Debuyser et al. 1991).

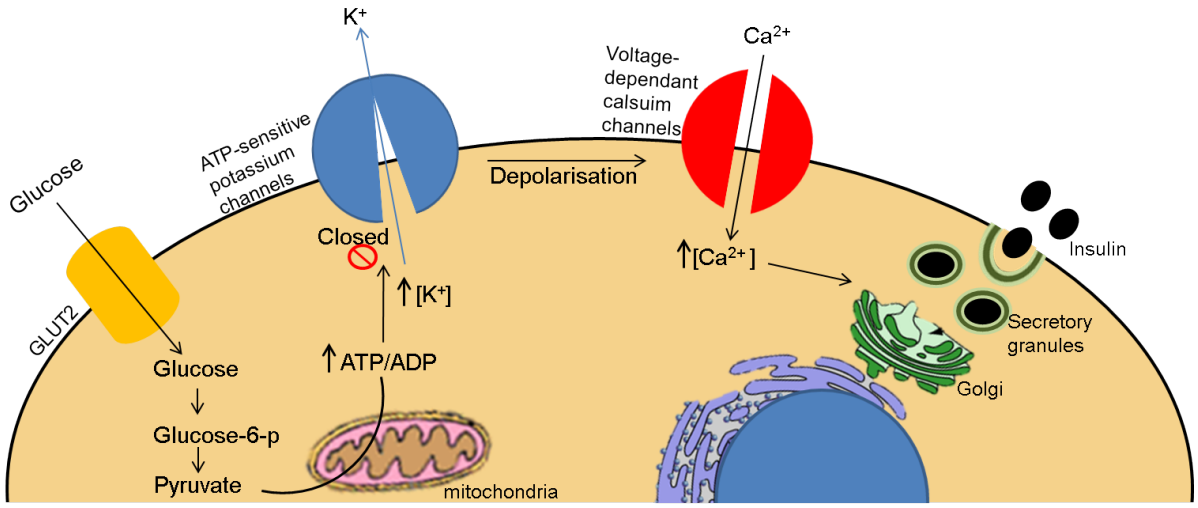

Figure 1-12 The processes leading to insulin secretion in pancreatic β-cells. Glucose is transported into β-cells through GLUT2 glucose transporters and metabolised to ATP. Elevated ATP/ADP ratio closes the ATP-sensitive potassium channels, leading to cell membrane depolarisation. Cell-surface calcium channels are opened and promoting calcium influx into the β-cells. An increase in calcium triggers the exocytosis of insulin.

1.3.3.Metabolic actions of insulin

Insulin plays the key role in the switching of metabolism from the fed to the fasted state.

In the fed state, anabolic metabolism predominates and nutrients are stored as glycogen, TAG, and proteins. Levels of glucose, amino acids, and triglycerides are temporarily raised 2-4 hours after ingestion of food in the post-absorptive phase. The secretion of insulin is increased in response to elevated levels of glucose and amino acid, while, the release of glucagon is decreased by the alpha cells of the pancreas. This elevated insulin to glucagon ratio and the availability of other substrates are the two key factors which make the absorptive phase an anabolic period (Figure 1-13).

During this period, glucose is the main energy source for all tissues, and the liver takes up glucose, lipids, and amino acids which can then be metabolised, stored or routed to other

tissues (Harvey & Champe 2005). Acetyl CoA as a glycolytic product is used to synthesise fatty acids through *de novo* lipogenesis. Long-chain fatty acids are taken up into triglycerides, cholesterol and phospholipids. These lipids are stored in lipid droplets or secreted into the circulation as VLDL particles (Figure 1-13).

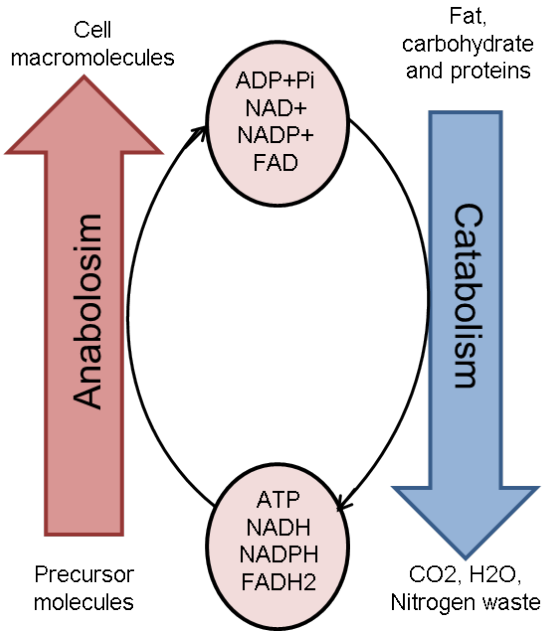

Figure 1-13 Energy balance by anabolism and catabolism and the co-factors involved.

The fasted state is a catabolic period where insulin secretion is decreased in response to reduced levels of glucose and amino acids, while, the release of glucagon and adrenaline is increased. This reduced insulin to glucagon ratio and lower substrate availability drive catabolic metabolism (Figure 1-13).

Insulin target tissues (adipose tissue, muscle, and liver) function in a way to achieve two priorities: first, to maintain adequate plasma glucose level, and second, to metabolise fatty acids and ketone bodies to provide energy for all tissues (Harvey & Champe 2005). During fasting, the liver secretes glucose through both glycogenolysis and gluconeogenesis. Fasting

induces lipolysis in adipose tissue to release FFAs which are converted into ATP and ketone bodies in the liver by mitochondrial β-oxidation and ketogenesis. Ketone bodies can then be used as metabolic fuel for extra-hepatic tissues, mainly the brain (Figure 1-13).

Detailed liver metabolic processes are regulated by hormonal systems which will be discussed in detail in section 1.5.

1.3.4. Insulin signalling

Insulin actions are mediated via the insulin receptor (IR) initiating a cascade of cell-signalling responses involving phosphorylation of insulin receptor substrate (IRS) proteins. These proteins have a large number of tyrosine and serine phosphorylation sites on their C-terminal domains. Tyrosine phosphorylation is required for activation of phospho-inositide 3 Kinase (PI3K). PI3K predominantly mediates insulin metabolic actions via activating protein kinase B (PKB/Akt) (Alessi et al. 1997a). Finally, activated PKB/Akt can then modulating many metabolic actions of insulin within the body (Figure 1-14).

1.3.4.1.Insulin receptor

Insulin mediates its signalling actions through cell surface receptors, tyrosine kinases, in particular the insulin receptor (IR) and also the insulin-like growth factor (IGF) receptor. However, the IGF receptor has an approximately 100-fold less affinity for insulin compared to its cognate ligand, IGF1 (Andersen et al. 1992). IR is composed of two extracellular α-subunits and two transmembrane β-subunits which are linked by a disulphide bond. The α-subunits are known as hormone binding domains while the β-subunits confer tyrosine kinase activity. When insulin binds to the α-subunits, the receptor undergoes conformational changes

leading to the auto-phosphorylation of specific tyrosine residues on the cytosolic β-subunits (Ballotti et al. 1989) (Figure 1-14)

1.3.4.2.Insulin receptor substrates

Upon activation by insulin, the auto-phosphorylated insulin receptor then leads the phosphorylation of numerous cellular proteins including the insulin receptor substrate (IRS) proteins (Figure 1-14).

Six isoforms of IRS have been identified to date (IRS1-6) (Cai et al. 2003) from which IRS1 and IRS2 are shown to be more important in mediating metabolic signal transduction (Araki et al. 1994;Patti et al. 1995). In liver, IRS2 is the dominant IRS and its downregulation appeared to be mainly responsible for insulin resistance, studying the ob/ob mice (Kerouz et al. 1997).

Sharing a high degree of homology, all IRS proteins have both pleckstrin-homology domain (PH) and phosphotyrosine binding domain (PTB) close to the N-terminal which is responsible for the high affinity of these substrates for IR. The C-terminal is more variable, containing a large number of tyrosine and serine phosphorylation sites, and confer IRS activity. Tyrosine phosphorylation of IRS, in particular IRS1/2, causes a linkage between IRS and various effector proteins containing src-homology 2 (SH2) domains resulting in multi-subunit signalling complexes. One of the best known SH2 domain proteins is phosphoinositide-3 kinase (PI3K). As an example, phosphorylation at tyr612 and tyr632 are required for activation of PI3K (Esposito et al. 2001). However, phosphatase SH2 can negatively regulate the IRS tyrosine phosphorylation thereby reducing the metabolic actions of insulin.

In addition, IRS has serine phosphorylation sites which, for the most part, are inhibitory to IRS function. Approximately 124 and 129 serine phosphorylation sites have been identified for IRS1 and IRS2, respectively (Park et al. 2013). For example, the serine phosphorylation at residue 307 of IRS1, situated on the PTB-domain of insulin receptor (IR), is shown to inhibit the IRS1/IR interaction using yeast-tri-hybrid assay (Aguirre et al. 2000).

Studies carried out in ob/ob mouse model of obesity demonstrate decreased insulin signalling, with lower receptor kinase activity, insulin binding, IRS1 protein expression, IRS1 associated PI3K activity, in liver, muscle and fat tissue (Anai et al. 1998;Goodyear et al. 1995;Kerouz et al. 1997). Furthermore, IRS serine phosphorylation is a key regulator of IRS function and is considered a major contributor to insulin resistance and diabetes (Bouzakri et al. 2006).

Although IRS proteins have a high degree of homology, their role in insulin/IGF1signaling is shown to be complementary rather than identical. IRS1 knockout mice have a growth defect due to the IGF resistance, mainly in skeletal muscle (Araki et al. 1994). However, the IRS2 knockout mice are disruptive to insulin signalling, primarily in liver (Kubota et al. 2000).

1.3.4.3.Phosphoinositide 3-Kinase

Insulin mediates its metabolic actions via IRS activation of PI3K. PI3K is an heterodimer consisting of a catalytic subunit (p110), and a regulatory subunit (p85) (Yu et al. 1998). Following binding with IRS, PI3K converts the lipid membrane phosphatidylinositol-3, 4-diphosphate (PIP2) to phosphatidylinositol-3, 4-triphosphate (PIP3). PIP3 is known to be the most biologically active 3' phosphor-inositide, and acts as a second messenger activating the PH-domains containing proteins including PKB/akt (Alessi et al. 1997) (Figure 1-14).

1.3.4.4.Protein Kinase B (PKB/akt)

There are four members of the PKB family; PKBα, PKBβ1&2 and PKBγ (akt1, 2 and 3 respectively). All isoforms consist of an N-terminal PH-domain, a central kinase (serine/threonine) domain, and a C-terminal regulatory domain. The PIP3, generated by PI3K, binds with PH-domain of PKB/akt (Downward 1998). This causes the translocation of PKB/akt from the cytosol to the plasma membrane, where it is phosphorylated at residue Thr308 by phosphoinositide-dependent protein kinase 1 (PDK1) (Stephens et al. 1998). In addition, within its regulatory domain, Ser473 phosphorylation by the mammalian target of rapamycin (mTOR) results in full PKB/akt activation (Sarbassov et al. 2005) (Figure 1-14).

1.3.4.4.1.Protein Kinase B and glucose uptake

One of the principal roles of activated PKB/akt is to increase glucose transport into the cells by inducing the translocation of the glucose transporter, GLUT4, to the plasma membrane. GLUT4 is located in cytosolic vesicles containing GTP-activating proteins (Rab GTPase) which are required for the movement of these vesicles to the plasma membrane. An AKT substrate, AS160, is also present in GLUT4 vesicles, and inhibits the Rab GTPase. Activated PKB/akt can directly phosphorylate AS160 which leads to AS160 binding the cytosolic scaffold protein, 14-3-3. Upon this association, AS160 is removed from the vesicle, relieving its inhibition on Rab GTPase. This allows GLUT4 translocation to the plasma membrane and thereby increasing glucose uptake (Ramm et al. 2006;Sano et al. 2003) (Figure 1-14).

1.3.4.4.2.Protein Kinase B and enzymatic activation

PKB/akt regulates many metabolic enzymes including glycogen synthase kinase (GSK). Glycogen synthase (GS) is a key enzyme in glycogen synthesis which is inhibited by GSK when GSK is in the non-phosphorylated state. Activated PKB/akt causes GSK phosphorylation, relieving the inhibition on GS and increasing glycogen synthesis (Sutherland et al. 1993). In addition, PKB/akt has an important role in the regulation of transcription and protein synthesis via inactivation of GSK. Phosphorylated GSK can increase protein synthesis by removing a negative phosphorylation on the transcription factor, eukaryotic initiation factor 2B (eIF2B) (Welsh and Proud 1993) (Figure 1-14).

1.3.4.4.3.Protein Kinase B and secondary messengers

PKB/akt also modulates insulin signalling through regulation of second messengers levels within the cell, particularly cyclic adenosine monophosphate (cAMP). High levels of cAMP activate protein kinase A (PKA) that phosphorylates serine/thereonine kinase 11 (STK11), also known as liver kinase B1 (LKB1). Subsequently, phosphorylated LKB1 activates 5'AMP activated protein kinase (AMPK) which negatively phosphorylates acetyl CoA carboxylase (ACC). ACC is a rate limiting enzyme in lipogenesis as well as inhibiting β-oxidation through malonyl CoA production (discussed in detail in section 1.2.3.3.1). In the presence of insulin, PKB/akt activates phosphodiesterase 3B (PDE3B) by phosphorylation. Activated PDE3B hydrolyses the cAMP to inactive 5'AMP, alleviating the AMPK inhibition on ACC which results in a shift from fatty acid oxidation to fatty acid storage or lipogenesis (Kitamura et al. 1999). In addition, PKA activates glycogen synthase and inhibits the conversion of glycogen to glucose (Mehrani and Storey 1993) (Figure 1-14).

1.3.4.4.4.Protein Kinase B and transcriptional regulation

PKB/akt can modulate the expression of multiple metabolic enzymes by regulating the activity of transcription factors. The forkhead box-containing protein (FOXO) family are key transcription factors in metabolic regulation, for example, in the liver, FOXO1 modulates the expression of the genes involved both in lipid and glucose metabolism (Altomonte et al. 2003;Matsumoto et al. 2007).

FOXO1 drives expression of rate-limiting gluconeogenic enzymes, glucose-6- phosphatase (G6Pase) and phosphoenolpyruvate carboxykinase (PEPCK). In addition, The FOXO family is negatively activated by PKB/akt. This means in response to insulin, FOXO1 is inhibited by PKB/akt and therefore, gluconeogenesis is blocked through down regulation of G6Pase and PEPCK. In fed state, liver-specific FOXO1 overexpressed mice shown an increase in expression of genes involved in lipid transport and a decrease in expression of rate-limiting genes in glycolysis and lipid synthesis (Zhang et al. 2006). In contrast, using the same model, enhanced lipogenesis and liver steatosis has been reported (Qu et al. 2006) (Figure 1-14).

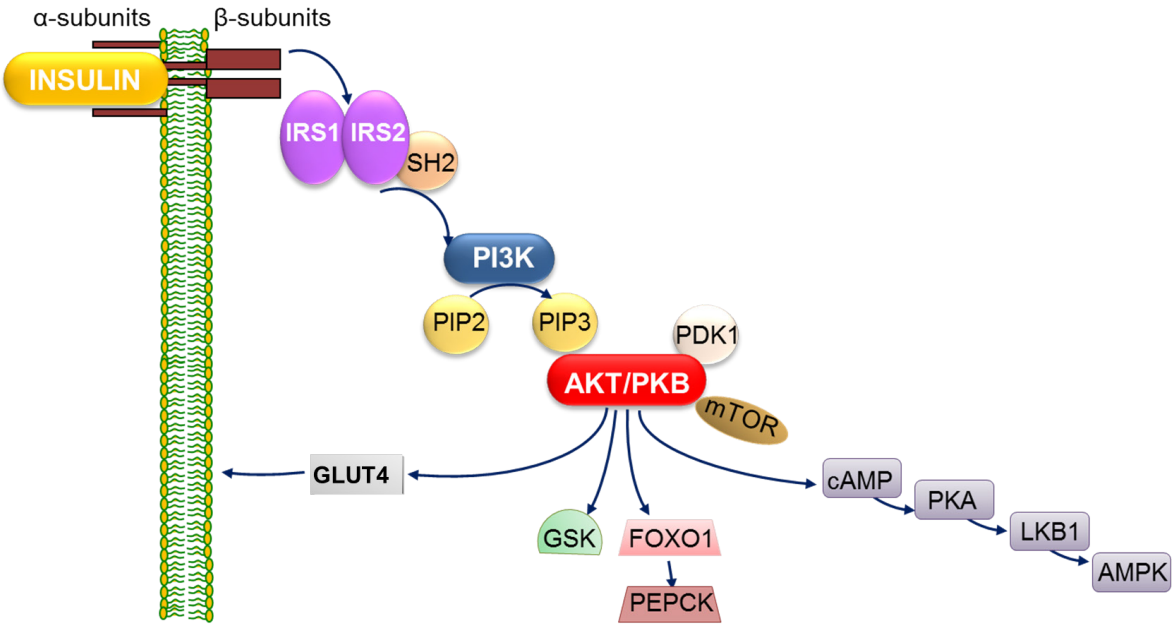

Figure 1-14 The insulin signalling pathways involved in the metabolic actions of insulin. In summary, when insulin binds its receptor the receptor auto phosphorylates. This then binds and phosphorylates insulin receptor substrate, which activates PI3K which leads via a secondary messenger to AKT phosphorylation. This activation of AKT increases glucose uptake (through GLUT4 translocation to the plasma membrane), glycogen synthesis (through GSK phosphorylation), and lipogenesis (through AMPK activation) whilst inhibiting gluconeogenesis (through FOXO1 and PEPCK suppression) and β-oxidation (through AMPK activation). Abbreviations: IRS1/2= Insulin receptor substrate1/2, SH2= Src-homology 2, PI3K= Phospho-inositide 3 Kinase , PIP2/3= Phosphatidylinositol-3, 4-diphosphate 2/3, AKT/PKB= Protein Kinase B, mTOR= Mammalian target of rapamycin, PDK1= Phosphoinositide- dependent protein kinase 1, cAMP= Cyclic adenosine monophosphate, PKA= Protein kinase A, LKB1= Liver kinase B1, AMPK= AMP-kinase, GSK= Glycogen synthase kinase, FOXO1= Forkhead box-containing protein, PEPCK= Phosphoenolpyruvate carboxykinase.

1.4.Steroid hormones; glucocorticoids and androgens

1.4.1.Adrenal glands

There are two adrenal glands in total, each weighing approximately 4g. One adrenal gland is situated on top of each kidney. Each gland is wrapped in a fibrous capsule and comprises two distinct structures; an outer structure called the adrenal cortex and an inner structure named the adrenal medulla. These two structures have different origins; the cortex is derived from

mesoderm whilst the medulla is derived from neural crest cells. They are functionally and anatomically distinct. The cortex can be further subdivided into three layers: an outer layer located close to the capsule called, the zona glomerulosa (ZG); a middle layer called, zona fasciculata (ZF); and an inner layer close to the medulla called, zona reticularis (ZR). ZG is the thinnest layer in adrenal cortex and it is responsible for mineralocorticoid production, principally aldosterone. ZF is the thickest layer in the centre of the cortex and secrets GCs predominantly. Finally the ZR, which occupies less cortical space than ZF and more than ZG and synthesises mainly androgens. The adrenal medulla is a part of neuroendocrine system, producing adrenaline and noradrenaline (Arlt and Stewart 2005) (Figure 1-15).

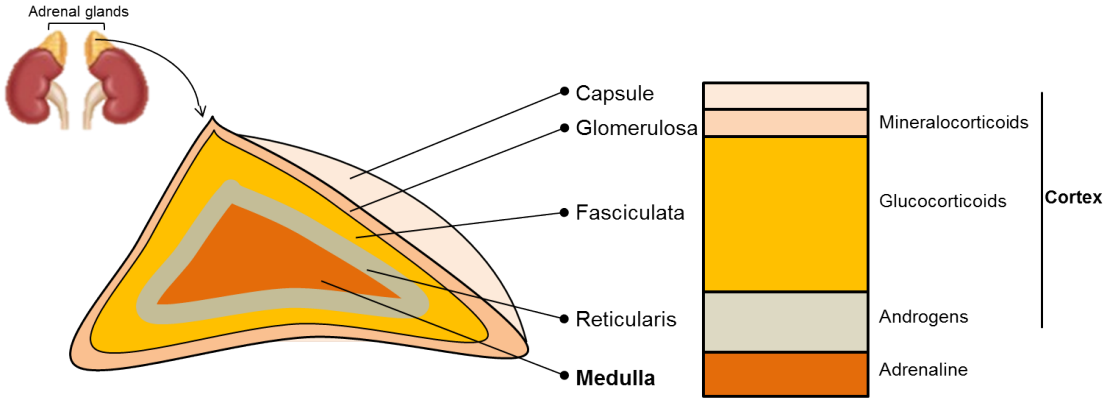

Figure 1-15 The adrenal glands are positioned above the kidneys and are divided into adrenal medulla and the cortex which itself is divided into three zones; the glomerulosa, fasciculata and reticularis.

The blood supply to the adrenal glands are the branches of the inferior phrenic artery, renal artery and the aorta which penetrates the cortex and medulla. The right adrenal gland is drained into the inferior vena cava via a short vein. However the left gland has a longer vein which drains into the renal vein (Rieder et al. 2010).

1.4.2.Structure of adrenal steroids

Testicular and ovarian cells, specific neuronal cells of the brain, trophoblast cells of the placenta and adrenal cortex are the only cells able to synthesise steroids from a cholesterol precursor. All steroids share a basic structure of a three cyclohexane rings and one cyclopentane ring (Figure 1-16).

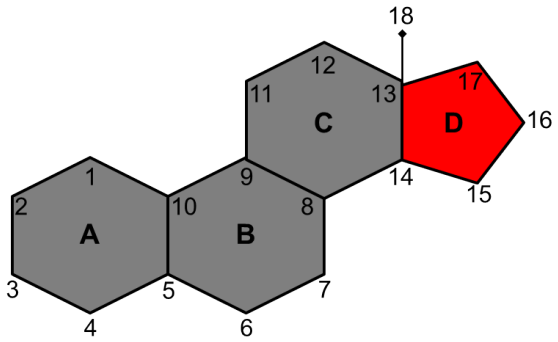

Figure 1-16 Standard structure of adrenal steroids, the numbers represent the carbon atoms and the letters designate the rings.

Differences in biological activity are due to differing number of carbon atoms and the side groups on the basic ring structure. Based on this, steroids are categorised into five major groups which are summarised in Table 1-2.

Group	Number of carbon atoms	Structure	Tissue of origin
Oestrogen	C18	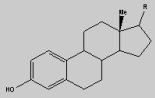	Placenta Gonads Adrenal cortex Adipose tissue Breast Endometrium
Androgen	C19	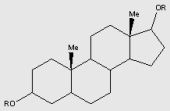	Gonads Adrenal glands
Progestogen	C21	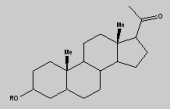	Gonads
Mineralocorticoid	C21	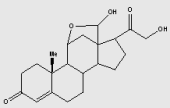	Adrenal cortex
Glucocorticoid	C21	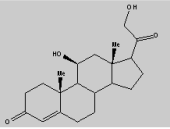	Adrenal cortex

Table 1-2 Five major groups of adrenal steroid: oestrogen, androgen, progestogen, mineralocorticoid and glucocorticoid

1.4.3.Steroidogenesis

All the steroids defined in Table 1-2 are synthesised from the precursor cholesterol in the adrenal cortex. As discussed in section 1.4.1, each zone of the adrenal cortex is responsible for synthesis of a particular steroid subclass as a result of distinct enzymatic profiles.

The initial step of steroidogenesis is the transportation of cholesterol from the outer to the inner mitochondrial membrane by steroidogenic acute regulatory protein (StAR) (Miller 2007).

Within mitochondria, cholesterol is converted to pregnenolone in all zones through the rate-limiting enzyme, cytochrome P450scc (Thiboutot et al. 2003). This enzyme is a member of the cytochrome P450 superfamily, which has a diverse array of functions including reduction,

oxidation and hydroxylation. P450scc enzyme cleaves between C20 and C22 of the cholesterol side group and its action is NADPH dependent. After this step, the bio-pathways branch to synthesise mineralocorticoids, glucocorticoids or androgens. The ZG synthesises mineralocorticoids as it is the only zone which expresses aldosterone synthase (P450c18). Although the ZF and ZR lack P450c18, they both contain P450c17. This enzyme has 17α-hydrolylase and 17,20-lyase activity in ZF and ZR, respectively. Its 17α-hydrolylase activity results in 17-OH-pregnenolone synthesis and produces GCs as its final products. However, its 17,20-lyase activity, which itself is dependent upon flavoprotein cytochrome b5 availability, predominates in ZR and generates adrenal androgen precursors, androstendione and dehydroepiandrosterone (DHEA) (Arlt & Stewart 2005).

There are also a number of enzymes involved in the androgenic and oestrogenic metabolism including hydroxysteroid dehydrogenases (HSD), aromatase and 5α-reductases (5αR) (discussed in detail in section 1.4.4.4 and 1.4.5.4). Different isoforms of each enzyme have been identified and these enzymes act on multiple substrates, represented in Figure 1-17.

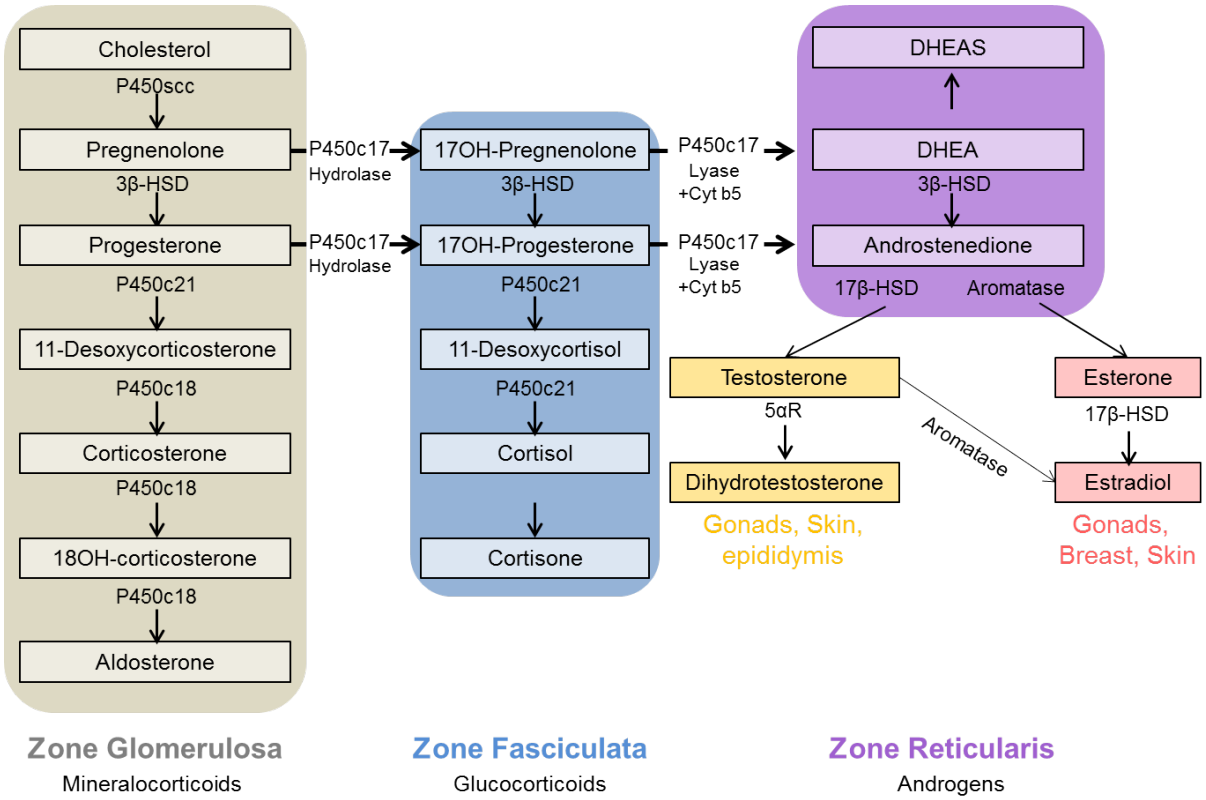

Figure 1-17 The major enzymatic reactions in 3 zones of adrenal cortex; allowing the specific steroid biosynthesis in each zone. These three zones are named glomerulosa, fasculata and reticularis which are responsible for synthesis of mineralocorticoids, glucocorticoids, and androgens respectively.

1.4.4.Glucocorticoids

1.4.4.1.Basic HPA axis

The secretion of glucocorticoids by the adrenal glands is under the control of the hypothalamo-pituitary-adrenal (HPA) axis. Following neural stimuli from the brain, corticotropin-releasing hormone (CRH) is released by hypothalamic neurons and stimulates the release of adrenocorticotropic hormone (ACTH) from the anterior pituitary into the circulation which can finally lead to cortisol production by acting on the adrenal cortex (Taves et al. 2011).

Circulating ACTH binds the G protein-coupled melanocortin 2 receptor (MC2R) and melanocortin 2 receptor associated protein (MRAP) which are expressed on adrenal gland leading to the formation of the cAMP (Hofland et al. 2012). This induces activation of cAMP-dependent protein kinase A (PKA) (see section 1.3.4.4.3) enhancing cholesterol uptake into the mitochondria by increasing StAR phosphorylation (Clark et al. 2000), mRNA expression and translation (Clark et al. 1995).

The whole process drives steroidogenesis and cortisol production. However, this loop is completed by the negative feedback of cortisol on hypothalamus and pituitary gland inhibiting CRH and ACTH synthesis and release (Figure 1-18).

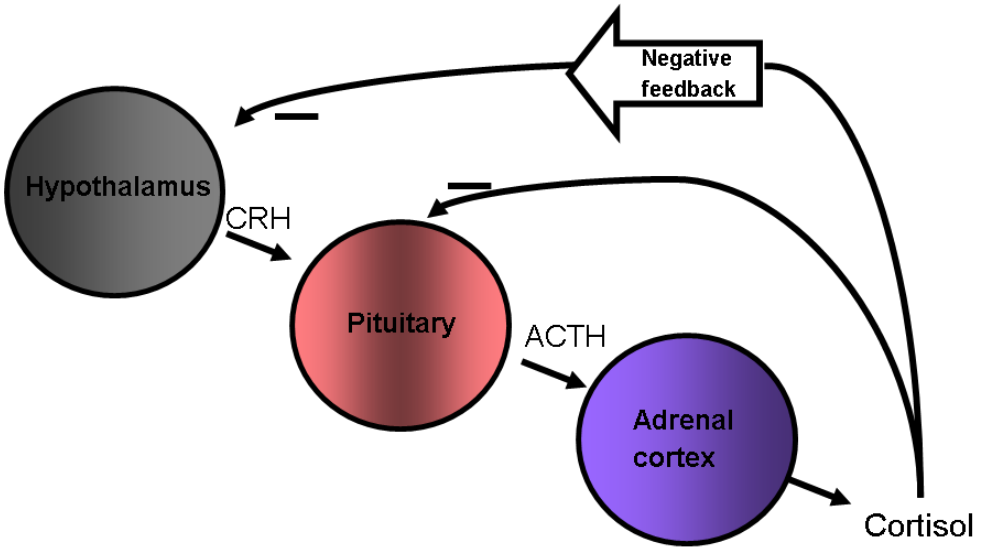

Figure 1-18 The hypothalamo-pituitary-adrenal (HPA) axis; a negative feedback mechanism presents whereby GC inhibits its own release. When cortisol is adequate, a negative feedback operates on pituitary gland and hypothalamus to reduce the output of corticotropin-releasing hormone (CRH) and adrenocorticotropic hormone (ACTH) which leads to a reduction in cortisol secretion.

ACTH levels change in a 24 hours cycle in a circadian rhythm and as a consequence cortisol secretion follows the same pattern. The circadian rhythm in cortisol secretion peaks just

before waking, with a decline through the day and reaches its lowest level in the first few hours of the sleep. However, cortisol levels increase in response to stress independently of the circadian rhythm (Becker et al., 2001; Larsen et al., 2003).

In addition to circadian rhythm, the HPA axis exhibits a rapid ultradian rhythm where glucocorticoids are released from the adrenal glands in hourly pulses. This causes rapid changes of hormone levels in the blood and also within the target tissues such as brain (Droste et al., 2008). Ultradian glucocorticoids pulses activates the glucocorticoid receptor and induce pulsatile glucocorticoid receptor (GR)-glucocorticoid response elements (GRE) interactions (GR and GRE are explained in section 1.4.4.2) which results in pulsatile gene transcription (Spiga et al., 2014).

1.4.4.2. Glucocorticoid action

The cellular effects of GCs are classically mediated via the glucocorticoid receptor (GR). The importance of the GR is highlighted by studies from global GR-deficient mice which show severe abnormalities and die after birth because of lung failure (Cole et al. 1995). GR is a ligand dependent nuclear receptor and has four main functional domains: N-terminal, DNA binding, and ligand binding domains, and a short amino acid sequence called the hinge region (Beato et al. 1996;Giguere et al. 1986) (Figure 1-19).

In its inactive form, GR is part of a multi-protein complex within the cytoplasm. This complex consists of several proteins including two heat shock proteins (HSP90, HSP60), p59, calreticulin, (Beato, Truss, & Chavez 1996), immunophilin (Pratt and Toft 1997) and many other proteins all with differing function.

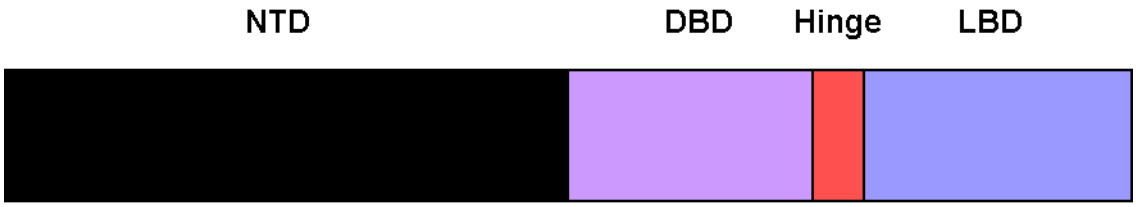

Figure 1-19 The glucocorticoid receptor. (NTD= N-terminal domain, DBD= DNA binding domain, LBD= ligand binding domain and hinge region).

The GR- HSP90 association allows access by the steroid ligand through opening the GR hydrophobic steroid binding cleft. When the steroid hormone binds, the HSP-immunophilin complex dissociates and the GC bound receptor translocates into the nucleus. In the nucleus, GR interacts with glucocorticoid response elements (GRE) and activates the transcription of the target gene (Beato 1989;Beato, Truss, & Chavez 1996;Jantzen et al. 1987). GRE is formed of a palindromic sequence separated by a 3 bp hinge. GR binds to this symmetric structure as a dimer, which is known to be the active regulatory form. GR dimerises via its DNA binding domain to bind to GRE and induces gene expression (Drouin et al. 1993) (Figure 1-20). In contrast, GR activation can also down regulate gene transcription by binding with negative GRE sites with promoter regions and have a negative influence on HPA axis subsequently (Drouin et al. 1993).

The GR has two alternative splice variants encoding GRα and GRβ, with different affinities for GC. In human, GRα mRNA expression is higher than the β isoform (Rivers et al. 1999). GRα has a high affinity for GCs, whereas GRβ has a low affinity for GCs and can also act as a negative regulator of GRα and inhibit its activity (Hollenberg et al. 1985;Oakley et al. 1999).

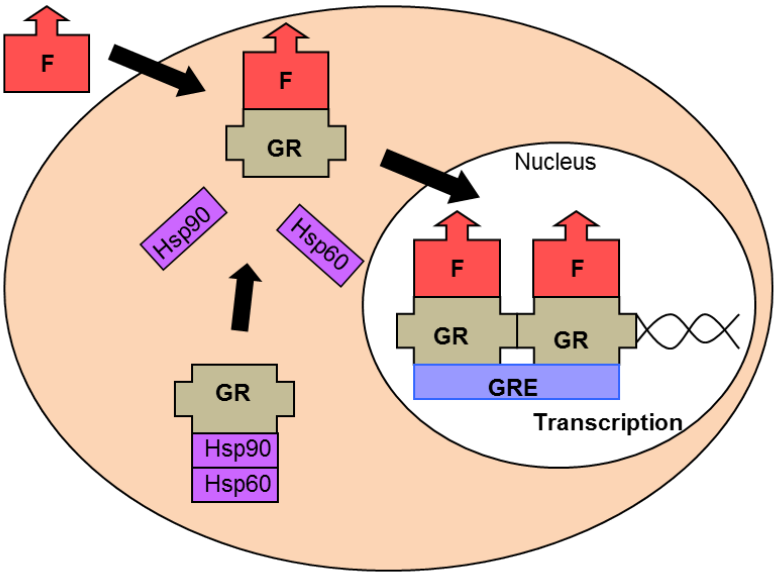

Figure 1-20 The mechanism of glucocorticoid action; upon GC binding, GR disassociates, translocates into nucleus and regulates gene transcription.

In addition to the classic genomic effects of GCs, there are also rapid nongenomic effects that can occur within minutes and without transcription. This can be mediated via alternative signalling pathways including G-protein, MAPK, cAMP and protein kinase C (PKC) (Losel et al. 2003). Such functions are initiated at the cell membrane through membrane-bound or cytoplasmic receptors (Stahn and Buttgereit 2008) and not affected GR or MR (Haller et al. 2008).

1.4.4.3.Metabolic actions of glucocorticoids

GCs have a potent role in the regulation of growth and development including maturation of the lung and CNS, as well as the control of postnatal growth (Buckingham 2006). In addition, GCs have anti-inflammatory actions and play a critical role in regulation of carbohydrate and energy balance (Arlt and Stewart 2005).

With regard to carbohydrate metabolism, GCs promote glycogenolysis and gluconeogenesis (Mueller et al. 2012). The role of GCs in lipid metabolism is less clear and it is reported to have a tissue specific response (Djurhuus et al. 2002). GCs alone decrease lipogenesis but can act synergistically with insulin to augment lipid accumulation (Hazlehurst et al. 2013;Wang et al. 2012).

GCs increase hepatic *de novo* lipogenesis, and have an opposite actions to insulin they stimulate lipolysis in adipose tissue (Baxter and Forsham 1972) resulting in increased circulating FFAs (Divertie et al. 1991;Xu et al. 2009). Regarding fat metabolism with liver, they also increase VLDL production (Taskinen et al. 1983) as well as TAG synthesis (Dolinsky et al. 2004).

1.4.4.4.Pre-receptor glucocorticoid metabolism

Endogenous GCs are metabolised through a series of enzymes that include the 11β-hydroxysteroid dehydrogenases and the A-ring reductases, which act as pre-receptor signalling mechanism controlling the access of active GCs to both GR and MR (Eyre et al. 2001).

The two isozymes of 11β-hydroxysteroid dehydrogenase (11β-HSD1/2) exist in both human and rodents. In human, they are responsible for interconversion of inactive cortisone and active cortisol while facilitates the conversion between inactive 11dehydrocorticosterone and active corticosterone in rodents. They play a key role in controlling the availability of cortisol to activate the GR. In contrast, endogenous glucocorticoids (cortisol and cortisone) are primarily inactivated via a series of enzymes, termed A-ring reductases. These enzymes, 5α-reductases (5αRs) and 5β-reductase (5βR) (will be only referred as 5αR and 5βR in the

current study), convert cortisol and cortisone to dihydrometabolites which are then metabolised to tetrahydrometabolites by 3α-hydroxysteriod dehydrogenase (Nixon et al. 2012). This results in reduced cortisol availability to bind and activate GR. A-ring reductases will be discussed in detail in section 1.4.5.4.

1.4.4.4.1.11β-hydroxysteroid dehydrogenase type one

11β-hydroxysteroid dehydrogenase type one (11β-HSD1) converts inactive cortisone to active cortisol and is highly expressed in metabolic target tissues including liver, adipose tissue, and muscle. Its role is therefore to enhance local GC action through regeneration of active steroid. 11β-HSD1 possesses both oxoreductase (cortisone to cortisol) and dehydrogenase (cortisol to cortisone) activity that is dependent upon tissue and physical or developmental status of a cell type. The oxoreductase direction of 11β-HSD1 is due to the presence of abundant co-factor, NADPH which is generated by the enzyme, hexose-6 phosphate dehydrogenase (H6PDH) (Bujalska et al. 2008;Lavery et al. 2006). *In vivo*, 11β-HSD1 has predominantly (although not exclusively) oxoreductase role (Tomlinson et al. 2004)(Figure 1-21).

Selective 11β-HSD1 inhibitors decrease GCs generation, improve glucose tolerance and insulin sensitivity, and cause weight loss in rodents and primates (Alberts et al. 2002;Barf et al. 2002). In clinical studies in patients with type 2 diabetes, selective 11β-HSD1 inhibitors decrease hepatic glucose production rate (without any changes in glucose disposal). In addition, studying the plasma, total and LDL cholesterol decreased without any alteration in HDL cholesterol or TAG level (Morgan and Tomlinson 2010).

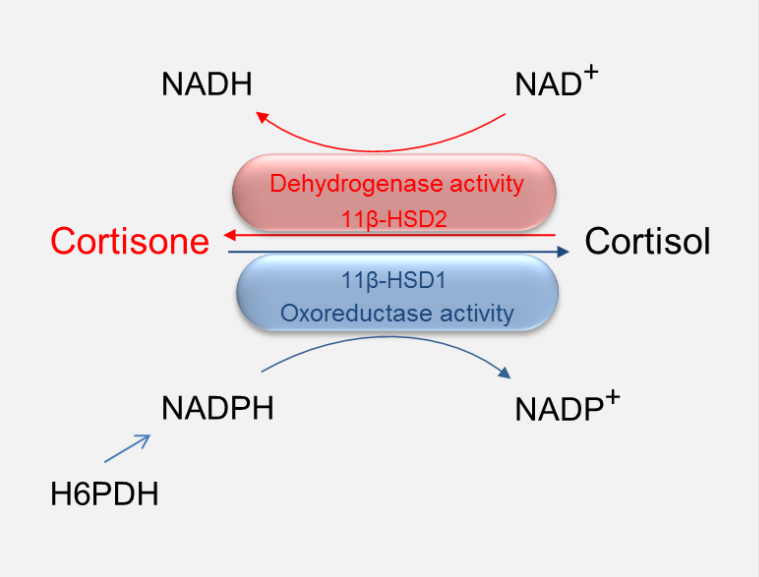

Figure 1-21 Pre-receptor glucocorticoid metabolism; In liver, 11β-HSD1 acts predominately as an oxoreductase due to the presence of co-factor NADPH which is generated by H6PDH enzyme. However, 11β-HSD2 works as a dehydrogenase and requires NAD^+ as a co-factor.

1.4.4.4.2.11β-hydroxysteroid dehydrogenase type two

11β-HSD2 is mainly expressed in mineralocorticoid target tissues including the kidney, colon, and malignant tissue including breast tumours (Yakirevich et al. 2008). In contrast with 11β-HSD1, 11β-HSD2 is involved in inactivating cortisol to cortisone. 11β-HSD2 requires NAD^+ as a co-factor to act in the dehydrogenase direction which results in inactivation of glucocorticoids (Kim and Cho 2010) (Figure 1-21). In plasma, cortisol is bound to corticosteroid-binding globulin (CBG), and to a lesser extend to albumin. Although CBG concentration is much lower than albumin in human plasma, it has much higher affinity for cortisol (Sandberg and Slaunwhite 1959). Therefore, over 80% of the plasma cortisol is bound to CBG (Brien 1981). Cortisol is able to bind and activate the MR with the same efficacy as its endogenous ligand, aldosterone and therefore defects in 11β-HSD2 (genetic or pharmacological) allow GC- activation of the MR leading to hypertension and renal sodium

retention, termed apparent mineralocorticoid excess (Palermo et al. 1996;Stewart et al. 1996). The role of 11β-HSD2 is, therefore, to prevent GC activation of MR (Edwards et al. 1988).

1.4.5.Androgen

1.4.5.1.Regulation of testosterone synthesis and secretion

Testosterone is a steroid hormone belonging to the androgen group and is the predominant sex hormone in males. DHEA and its sulphate ester, DHEAS, are known as the most abundant steroid hormones in the body produced primarily in adrenal glands. Testosterone is derived from cholesterol and synthesised from the precursors dehydroepiandrosterone (DHEA) and androstenedione, primarily in the Leydig cells of the testes in males, and secondarily by the adrenal cortex in the outer portion of adrenal glands. In addition, a small amount is produced in the thecal cells of the ovary in females. Synthesis and secretion are regulated by the HP-gonadal axis, where gonadotropin releasing hormone (GnRH) stimulates the pituitary to release luteinizing hormone (LH). Subsequently, LH stimulates the synthesis and release of testosterone from the testes (Rang et al. 1999).

Testosterone is transported to target tissues via the circulation either as free testosterone or bound to specific plasma proteins. Circulating testosterone is bound to sex hormone binding globulin (SHBG) (68%) or weakly bound to albumin (30%) and only 1-2% remains unbound (Vermeulen and Verdonck 1968). The primary role of androgens is in the development of primary and secondary sexual characteristics, driving sexual differentiation, development and maintenance of the male phenotype (Silverthorn 1998).

1.4.5.2.Androgen action

Testosterone is converted to Dihydrotestosterone (DHT) by 5αRs (see section 1.4.5.4). DHT binds the androgen receptor with higher affinity than testosterone and is believed to be the most potent circulating androgen (Janne et al. 1993). The androgen receptor (AR) is a ligand dependent nuclear receptor with four main structural and functional domains: N-terminal, DNA binding, ligand binding domain (LBD), and a short amino acid sequence called the hinge region (Figure 1-22).

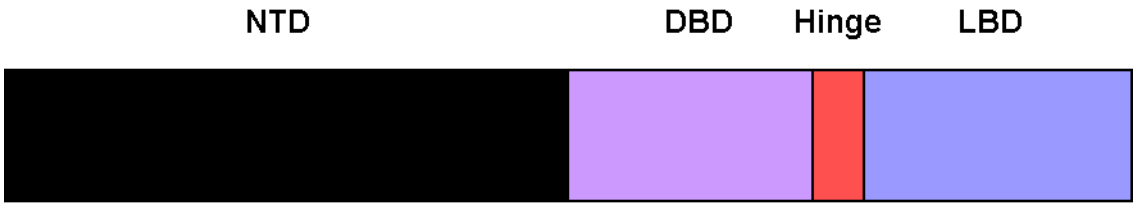

Figure 1-22 The androgen receptor. (NTD= N-terminal domain, DBD= DNA binding domain, LBD= ligand binding domain and hinge region).

In its inactive form, AR is a part of a multi-protein complex within the cytoplasm. This complex consists of several proteins including HSP molecules (HSP90, 70 and 56) cytoskeletal proteins and other chaperones (Lonergan and Tindall 2011).

90% of free testosterone is converted to DHT on entering cells of the prostate and genital tissues. Conformational changes in the AR occur once DHT binds to the LBD. Upon binding, the complex disassociates and then translocates to the nucleus. In the nucleus and upon binding to DNA, AR dimerises via its DNA binding domain (Truss and Beato 1993). The AR dimer binds to androgen response elements (ARE) and activates gene transcription (Brinkmann et al. 1999)(Figure 1-23).

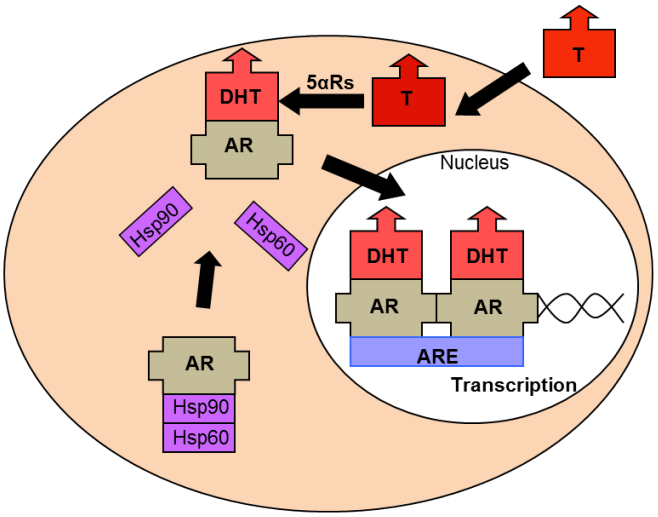

Figure 1-23 The mechanism of androgen action; upon DHT binding, AR disassociates, translocates into nucleus and regulates gene transcription.

Testosterone can also directly bind to the AR, with the similar mechanism to DHT, resulting in gene transcription. However, Testosterone can be metabolised via alternative pathways for example, conversion to 17β-estradiol, through the enzymatic activity of aromatase, and subsequent activation of the oestrogen receptor (Rommerts 2004). In addition, testosterone may also act via non-genomic mechanisms binding a G-protein coupled receptor which initiates a cAMP-mediated pathway. This regulates intracellular calcium concentrations which can further activate intracellular signalling, influencing specific proteins and cellular responses (Benten et al. 1999).

1.4.5.3.Metabolic actions of androgens

Testosterone plays a key role in lipid, carbohydrate and protein metabolism. In liver, testosterone deficiency is associated with elevated TAG and cholesterol, decreased insulin sensitivity and impaired glucose tolerance (Kelly and Jones 2013). In an *in vitro* study using

human liver cell line, testosterone increased insulin receptor mRNA expression (Parthasarathy et al. 2009). Similarly, studying the orchidectomised rats, insulin receptor mRNA and protein expressions were significantly increased following testosterone administration (Muthusamy et al. 2011). In addition, reduced GLUT4 mRNA expression was observed in liver, adipose and muscle tissue by testosterone depreciation via castration of male rats (Muthusamy et al. 2009).

The role of androgens on hepatic lipid metabolism remains controversial. Vozke et al. (2010) reported that low testosterone was associated with hepatic steatosis. Interestingly, DHT has been predicted to have an opposing action with increased hepatic Stearoyl-CoA desaturase1 (SCD1) (Moverare-Skrtic et al. 2006). SCD1 is predominantly expressed in liver, and specifically converts *de novo* lipogenesis-derived saturated fatty acids to monounsaturated fatty acids (Li et al. 2009). SCD1 activity, under a high sugar diet, demonstrates a strong negative correlation with liver fat content which suggests that SCD1 activity protects from fat accumulation (Silbernagel et al. 2012).

Treating the human prostate cancer cell line LNCaP with synthetic androgen, R1881, increased the expression of *de novo* lipogenesis rate limiting enzymes such as ACC and FASN through stimulating expression of sterol regulatory element binding proteins (SREBPs). SREBPs are transcription factors that control and coordinate lipogenic enzymes (Swinnen et al. 1997). Studies in animal and human adipose cell lines show that both testosterone and DHT inhibit AMPK by down regulating LKB1 expression (McInnes et al. 2012a).

In addition, testosterone effects differ in insulin target tissues and the molecular mechanisms underpinning the testosterone action on regulating metabolic pathways are not clear. Plus, testosterone metabolic effects may be different in the presence / absence of insulin (Kelly and

Jones 2013). Therefore, detailed characterisation of testosterone effects in different insulin target tissues in presence/absence of insulin is warranted.

1.4.5.4.Pre-receptor androgen metabolism

1.4.5.4.1.5αRs

In addition to their role in GC clearance by converting cortisol to its dihydrometabolites, 5αRs can reduce testosterone to the more potent androgen, DHT, altering the steroid availability (less cortisol, more DHT) to bind their nuclear receptors and thereby regulating gene transcription (Figure 1-24). However, 5αRs have higher affinity for androgens compared to GCs (Andersson and Russell 1990). Apart from GC and androgens, 5αRs also accept many other steroid substrates including progesterone and mineralocorticoids (Purdy et al. 1990).

5αRs are microsomal enzymes and are NADPH dependent (Frederiksen and Wilson 1971). Three isoforms of 5αRs have been identified to date, with different biochemical properties and sensitivity to substrates, which will be discussed in detail.

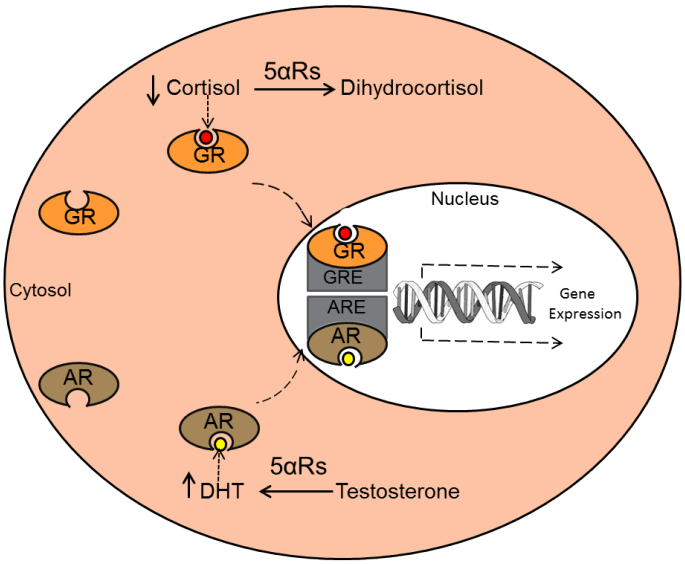

Figure 1-24 5αRs convert GCs to their less active dihydrometabolites with subsequent conversion to tetrahydrometabolites. In addition, they catalyse the conversion of testosterone to the more potent androgen, DHT. Therefore, 5αRs activity make less cortisol and more DHT available to attach their nuclear receptor, translocate to the nucleus and activate the transcription of the gene.

1.4.5.4.1.1.5αR1

The gene encoding 5αR1 (SRD5A1) was identified on chromosomes 5 and has 5 exons and 4 introns. 5αR1 is a hydrophobic protein with a PH optimum of 6-8.5 (Andersson et al. 1991). It consists of 259 amino acids with a molecular weight of 29kDa (Labrie et al. 1992;Russell and Wilson 1994). It is expressed in both human and mouse liver and also in skin (nongenital) and adipose tissue (Russell and Wilson 1994).

Although testosterone is the most widely recognized substrate of this enzyme, progesterone has a lower K_m and therefore enzymatically may be the preferred substrate (Andersson and Russell 1990;Normington and Russell 1992).

Dutasteride is a dual inhibitor of both isoforms, 5αR1 and 5αR2, reducing circulating DHT by nearly 95% compared to the baseline (Schwartz et al. 1997). MK-386 was reported to be the

selective inhibitor of 5αR1 with 90% efficiency (Schwartz et al. 1996) but this compound is neither commercially available nor used in clinical practice.

The biological diagnosis of 5αR deficiency is normally defined by an increase in the T/DHT ratio. To date, no mutation but several polymorphisms have been identified in SRD5A1. For example at exon 1, single nucleotide polymorphism (SNP); rs248793 (G>C), has been associated with an increase in DHT/T ratio suggesting an elevated 5αR1 activity (Ellis et al. 2005). DHT is the most potent hormone considered to be important in prostate cancer and therefore 5αR activity is important in determining the prostate cancer risk. In 426 individuals (205 controls vs. 221 with prostate cancer), several SNPs in different 5αR isoforms were chosen to be studied. They measured the serum DHT and when they correlated this data with the patients' genotype, they found out that in rs1691053 (SRD5A1) SNP the patients with GG genotype has the highest serum DHT while the AA genotype has the lowest. They showed that GG genotype is the potent genotype in the prostate cancer patients compared to controls and therefore suggested that this SNP in SRD5A1 is associated with increased prostate cancer risk through increasing 5αR activity (Setlur et al. 2010).

1.4.5.4.1.2.5αR2

The gene encoding 5αR2 (SRD5A2) lies on chromosomes 2 and has 5 exons and 4 introns. 5αR2 is also a hydrophobic protein with a PH optimum around 5 (Andersson et al. 1991). It has 254 amino acids with a molecular weight of 28 kDa, and shares less than 50% homology with 5αR1 (Labrie et al. 1992;Russell and Wilson 1994).

5αR2 is expressed in human liver but not in mouse liver. 5αR2 is predominantly expressed in androgen-target organs such as prostate, epididymis and seminal vesicles (Russell and Wilson 1994).

Finasteride is a highly specific enzyme for inhibition of 5αR2. In comparison with 5αR1, 5αR2 has much higher affinity for androgen substrates such as testosterone. Several mutations (Figure 1-25) and polymorphisms have been identified throughout the coding and non-coding regions of SRD5A2 (Maimoun et al. 2011). Since 5αR2 converts testosterone to a more potent androgen (DHT), mutations in this enzyme lead to 46XY DSD (Disorder of Sex Development) where external genitalia fail to develop normally. However, excessive androgen generation through the activity of 5αR2 has been implicated in the following conditions: polycystic ovary syndrome, breast cancer, prostate cancer and male pattern baldness (Ellis et al. 1998;Jakimiuk et al. 1999;Ji et al. 2004;Labrie et al. 1993).

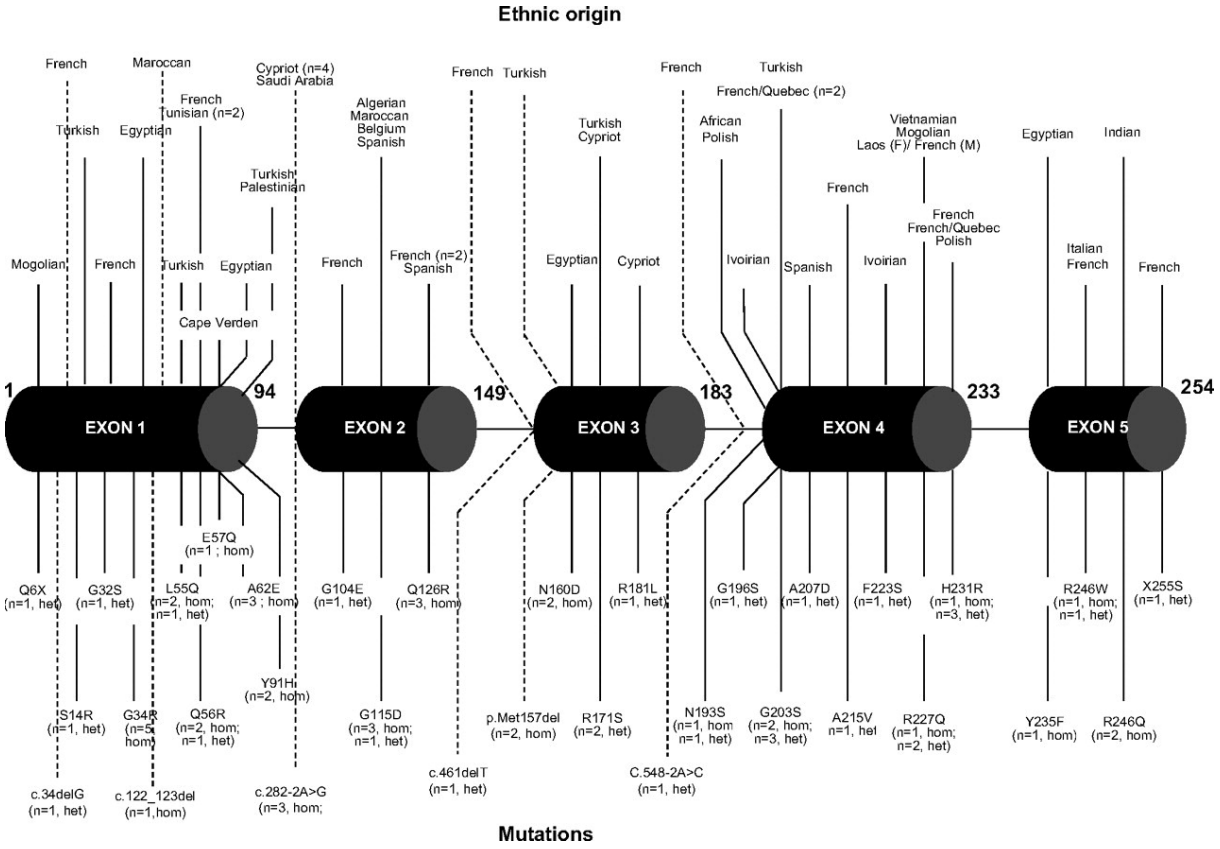

Figure 1-25 Mutations identified in SRD5A2; because of consanguinity the prevalence of variant mutations would cluster differently in variant ethnic population (Maimoun et al. 2011).

A comparison of human 5αR1 and 2 is summarised in Table 1-3.

	5αR1	5α2
Gene Structure	5 exons, 4 introns	5 exons, 4 introns
Gene	SRD5A1	SRD5A2
Chromosome Location	5p15	2p23
Size	259 amino acids, 29 kDa	254 amino acids, 28 kDa
Tissue Distribution	Liver, nongenital skin, prostate, brain, adipose tissue	Prostate, epididymis, seminal vesicle, genital skin, uterus, Liver, breast, hair follicle, placenta, brain
pH optima	Neutral to basic	Acidic or neutral
Prostate Level	Low	High
Substrate (T) affinity	Low	High

Table 1-3 Comparison of human 5αR1 and 2 isoforms.

1.4.5.4.1.3.5αR3

5αR3, encoded by SRD5A3, was identified recently (Uemura et al. 2008) and its role is less clear, but thought to be more important in reducing non-steroidal substrates (Cantagrel et al. 2010a). However, using an SRD5A3 construct, it is able to convert testosterone (Uemura et al. 2008) and androstenedione (Yamana et al. 2010) to their 5α-dihydro-metabolites. Its major role however is likely to be for N-linked glycosylation in post-transcription modification of proteins which presents with mutations in 5αR3 gene that result in a congenital disorder of glycosylation (CDG) (Kahrizi et al. 2011).

1.4.5.4.2.5βR

5βR gene (AKR1D1) is located on chromosome 7. AKR1D1 is also highly expressed in hepatocytes and its crystal structure has been determined (Faucher et al. 2008). AKR1D1 is able to metabolise both cortisol and cortisone and following 3α-HSD activity generates 5β-tetrahydrocortisol (5βTHF) and 5β-tetrahydrocortisone (5βTHE). While 5αRs reduced testosterone to 5α-dihydrotestosterone, 5βR converts progesterone to 5β-pregnane-3,20-diol (Figure 1-26).

Moreover, 5βR has a role in bile acid production and mutations in AKR1D1 gene lead to cholestatic liver disease in infants which can progress to liver failure (Lemonde et al. 2003). AKR1D1 knockout mice showed altered hepatic steroid with a 30±4% decrease in cortisone clearance and a 3.9±0.5-fold increase in the ratio of 5α-cortisone/cortisol metabolite generation, when compared to wildtype. In addition, bile acid concentrations were lower in AKR1D1 knockout male and female mice, with a dramatic change in male in comparison with wildtype (females: 310±67 pmol/mg (WT), 113±23 pmol/mg (knockout); male:

1164±626 pmol/mg (WT), 122±42 pmol/mg (knockout) p< 0.01, mean ± s.e). AKR1D1 knockout mice have a sexually dimorphic metabolic phenotype, where female knockouts are protected from the metabolic consequences of a high fat diet with increased insulin sensitivity and improved glucose tolerance (Gathercole et al. 2015). These findings suggest that AKR1D1 inhibition could be beneficial in female patients with metabolic disease, although further work is needed to establish the mechanisms by which AKR1D1 regulates metabolism, and whether it has potential as a therapeutic target.

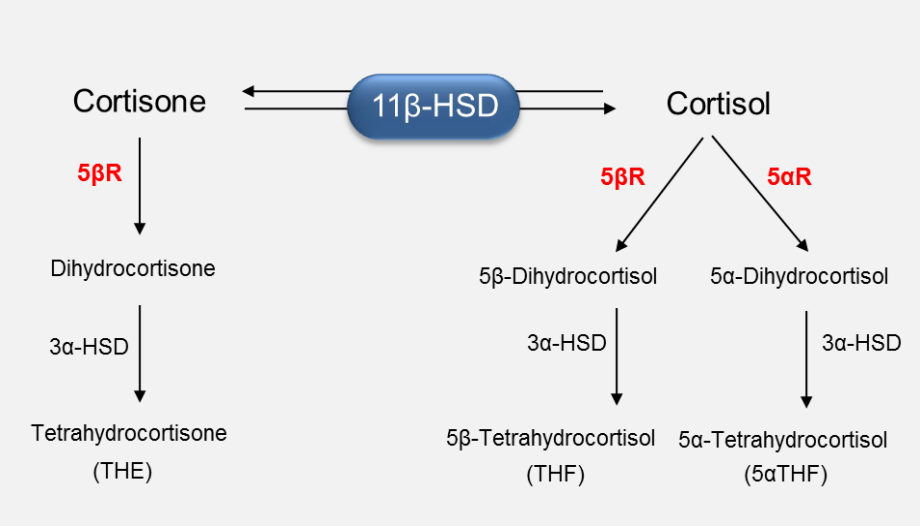

Figure 1-26 The major metabolites of cortisone and cortisol and the enzymes involved catalysing the conversions. 5αR metabolises cortisol to 5α-dihyrocortisol with a following conversion to 5α-tetrahydrocortisol (5αTHF) by 3α-HSD. However, 5βR is able to metabolise both cortisol and cortisone and following 3α-HSD activity generates 5β-tetrahydrocortisol (5βTHF) and 5β-tetrahydrocortisone (5βTHE).

1.5.Regulation of hepatic lipid metabolism by insulin, glucocorticoids and androgens

Circulating lipids are important in cardiovascular disease (CVD); there is a strong association between elevated serum triglyceride and CVD (Sarwar et al. 2007). In addition, increased

level of total and LDL cholesterol is observed in the development of CVD. However, there is a strong inverse association between HDL cholesterol levels and CVD, and elevated total cholesterol/HDL cholesterol ratio has been used as a marker of severity of CVD (Platt et al. 2015). Most of these lipids are produced and regulated within the liver. There are various transcriptional and post transcriptional factors, as well as hormones contributing to the regulation of hepatic lipogenesis. The liver X receptor (LXR) is an important transcriptional regulator by controlling the expression of lipogenic genes such as ACC, FAS and sterol regulatory element binding protein 1c (SREBP-1c) (Repa et al. 2000). SREBP-1c itself is a transcription factor which drives the expression of lipogenic genes involved in TAG synthesis and *de novo* lipogenesis (Kim et al. 1998).

Post transcriptional regulation is also crucial, since phosphorylation of key lipogenic enzymes regulates their activity. In this thesis, I have focused on hormonal regulation of hepatic lipogenesis, in particular the role insulin, GCs and androgens and therefore the effect of these hormones upon lipogenesis is discussed in detail.

1.5.1. Insulin and hepatic lipid metabolism

Insulin increases *de novo* lipogenesis via several distinct pathways, in particular through the PI3K-dependent pathway, (PI3K/AKT/mTOR), which regulates lipogenic gene expression (ACC1 and FAS) by increasing SREBP-1c expression (Azzout-Marniche et al. 2000), and VLDL production (Savage and Semple 2010). In addition, insulin represses autophagy, which is a response to starvation, and leads to hepatic lipid degradation (Rautou et al. 2010). Overall therefore, insulin increases lipogenesis and decreases lipid degradation in hepatocytes.

Although the precise mechanisms are not clear, there is an association between hepatic steatosis and insulin resistance. This may be due to increased fatty acid concentrations available for esterification to TAG as a consequence of inadequate suppression of lipolysis of adipose tissue. Interestingly however, even in the insulin resistant state, the effect of insulin to augment lipogenesis is unexpectedly maintained and even enhanced by hyperinsulinemia whilst the fatty acid oxidation is decreased (Nagle et al. 2009).

1.5.2.The effect of glucocorticoids on hepatic lipid metabolism and NAFLD

GCs are important regulators of hepatic lipid metabolism genes including FASN and ACC1/2 (Wang et al. 2012), promoting *de novo* lipogenesis and FFA usage and stimulating hepatic steatosis (Dolinsky et al. 2004;Norrheim et al. 1990). GCs also regulate fatty acid and cholesterol synthesis (Giudetti and Gnoni 1998) and HDL processing in hepatocytes (Bocharov et al. 1995), contributing to the lipid accumulation whilst reducing VLDL secretion. However, this decreased TAG secretion has not been consistent across all studies (Dolinsky et al. 2004).

In human foetal hepatocytes, GCs cause a dose-dependent increase in cholesterol synthesis (Carr and Simpson 1984). Some studies suggest that GCs alone can increase lipid accumulation in hepatocytes (Dich et al. 1983;Mangiapane and Brindley 1986) while others have shown a synergistic relationship with insulin to augment lipid storage, by increasing synthesis and decreasing secretion (Amatruda et al. 1983;Mendoza-Figueroa et al. 1988).

Rodent models have enhanced our understanding of the role of GCs in the pathogenesis of NAFLD. Rodents develop hepatic steatosis after being treated with corticosterone (D'Souza et

al. 2012;Morgan et al. 2014). The suggested mechanisms underpinning this were reduced TAG secretion, increased DGAT expression and FFA delivery to the circulation. In addition, GC excess in combination with a high fat diet was associated with fibrosis (D'Souza et al. 2012). Increased CD36 expression has been reported following GC treatment, suggesting a potential magnitude to lipid accumulation within the liver (Morgan et al. 2014). Selective hepatic GR knockdown in mice ameliorates hepatic steatosis. These mice show reduced fat accumulation within the liver, decreasing fatty acid uptake and increasing ACC2 and CPT1 expression (Lemke et al. 2008).

In humans, the relationship between GCs and the pathogenesis of NAFLD has not been explored in detail. Patients with GCs excess (Cushing's syndrome) develop NAFLD in up to 20% of the cases, as measured using computerised tomography (Rockall et al. 2003). Furthermore, there is some evidence to suggest that patients with type 2 diabetes and NAFLD, may display sub-clinical hypercortisolism (Targher et al. 2005). Whilst activation of HPA axis has been reported in patients with NAFLD (Zoppini et al. 2004), larger epidemiological studies have shown no association between circulation cortisol levels and NAFLD (Hubel et al. 2015). These inconsistencies in these data may point towards a more tissue specific role of GCs in the pathogenesis of the NAFLD.

1.5.3.The effect of androgens on hepatic lipid metabolism and NAFLD

The role of androgens in the pathogenesis of metabolic disease remains controversial. There is evidence documenting an association between hypogonadism and NAFLD (Kim et al. 2012;Volzke et al. 2010) with some evidence for improvement following androgen treatment (Haider et al. 2010;Hoyos et al. 2012). Assessing with CT imaging, obese men taking

testosterone for 18 weeks have demonstrated a significant decrease in hepatic fat (Hoyos et al. 2012). However, a recent study using MRI has reported no effect of testosterone therapy on liver fat in older men with mobility limitation (Huang et al. 2013).

Studying animal models, orchidectomised mice on a high fat diet increased hepatic fat when compared to controls. However, testosterone administration to these mice was able to ameliorate the hepatic steatosis (Senmaru et al. 2013). In addition, hepatic AR knockout mice on a high fat diet developed insulin resistance and hepatic steatosis. This observation was made in male but interestingly not in female mice (Lin et al. 2008). Adipose-specific AR knockout mice on high fat diet resemble human type 2 diabetes, with early insulin resistance and evolving insulin deficiency, and unlike liver-specific knockout mice there was no evidence of hepatic steatosis. In addition, compared to the liver-specific AR knockout mice, the nonesterified fatty acids (NEFA) levels were normal in Adipose-specific AR knockout mice; suggesting the observed insulin resistance is unlikely to be related to the spillover of the fatty acids to extra adipose organs and possibly via the dysregulation of insulin sensitising adipokines (McInnes et al. 2012b).

Interestingly, women with hyperandrogenic polycystic ovary syndrome (PCOS) are predisposed to developing NAFLD (Jones et al. 2012). However, the prevalence of NAFLD is higher in white men compared to white women (Browning et al. 2004). This sex dimorphism in hepatic steatosis was shown to be due to the combination of the prolonged increase in *de novo* lipogenesis and lower dietary fatty acid oxidation in men compared to women which may induce fatty acid esterification and storage pathways, leading to a greater VLDL production or increased liver fat accumulation (Pramfalk et al. 2015).

Overall although androgens have been implicated in the pathogenesis of NAFLD, the exact role of testosterone in the molecular mechanism of steatosis remains controversial with conflicting data in the published literature.

1.6.5αR and NAFLD

1.6.1.5αR knockout

Recently, the role of 5αRs in GC and androgen metabolism in the context of NAFLD and metabolic phenotype has been highlighted in studies using 5αR1 and 5αR2 knockout mice. Mice were fed normal chow or American lifestyle induced obesity syndrome (ALIOS) diet, a high fat high fructose diet generated hepatic steatosis and inflammation (Tetri et al. 2008), for 6 or 12 months. Mice, lacking 5αR1 (but not 5αR2), developed greater hepatic steatosis compared to WT animals. In addition, at 12 months, 60% of mice fed on ALIOS diet developed hepatocellular carcinoma. However, only 20% of 5αR2 knockout mice and none of 5αR1 knockout mice developed hepatocellular carcinoma, at 12 months. This suggests that mice lacking 5αR1 are prone to hepatic steatosis but protected from hepatocellular carcinoma. Mice do not express hepatic 5αR2 which might explain the conflicting data where 5αR1 knockout mice develop hepatic steatosis but not 5αR2 knockout mice (Dowman et al. 2013).

Additional studies on 5αR1 knockout mice indicate an approximate 80% reduction in glucocorticoid clearance compared to wildtype (Livingstone et al. 2014). Furthermore, on high fat diet feeding they develop greater weight gain, hyperinsulinaemia, hepatic steatosis and are more prone to hepatic fibrosis (Livingstone et al. 2015).

1.6.2.5αR as a therapeutic target

There is a relationship between 5αR activity and metabolic phenotype, as measured by urinary steroid metabolites. 5αR activity increases with BMI and also with NAFLD but decreases with weight loss (Crowley et al. 2014;Konopelska et al. 2009;Tomlinson et al. 2008). In addition, increased 5αR activity has been reported in NASH but not in simple steatosis, suggesting differences in activity according to the stage of the disease (Ahmed et al. 2012). Liver biopsy studies have demonstrated conflicting data; 5αR2 mRNA expression level was reported to be increased in patients with NASH, but in other studies no changes were observed in hepatic 5αR1 and 2 expression levels across the spectrum of NAFLD. However, immunohistochemical staining demonstrated increased protein levels of 5αR1 but not 5αR2 as NAFLD develops (Dowman et al. 2013).

Very recently, in a clinical study, dual inhibition of 5αR1 and 2 with dutasteride has been shown to be associated with decreased peripheral insulin sensitivity. However, specific effects on the liver were not examined (Upreti et al. 2014). In a recent study, healthy male volunteers were treated with finasteride or dutasteride for a period of three weeks, dutasteride treatment increased hepatic insulin resistance and the rate of hepatic *de novo* lipogenesis. However, finasteride was without effect; suggesting that either 5αR1, or dual 5αR1 and 2, inhibition is required for the observed increase in hepatic lipid accumulation (Hazlehurst et al. 2016).

1.7.Unanswered questions

The rational of this work is based upon the phenotype of NAFLD. Glucocorticoids and androgens have both been implicated in the pathogenesis of NAFLD; androgen deficiency in males, androgen excess in females and glucocorticoid excess in both sexes are associated with NAFLD. However, the precise molecular mechanism underpinning hepatic lipid accumulation regulated by these steroid hormones, is not clear. Insulin enhances fat mass and it is clear that GCs induce insulin resistance. Thus, GC action upon global insulin sensitivity is likely to be the combination of metabolic events in different target organs. Previously within our group, the effect of GCs and insulin upon fat metabolism have been studied in adipose tissue and skeletal muscle. The metabolic effects of GCs on liver insulin sensitivity and lipid metabolism are complex but it is widely believed that GCs induce insulin resistance, studying mainly rodents (Guillaume-Gentil et al. 1993). However, studies in human liver models have not been performed.

In addition, GCs and androgens are regulated at the pre-receptor level by A-ring reductases. There is an emerging role for overexpression of A-ring reductases as a therapeutic target in the treatment of metabolic diseases, in particular NAFLD. However, the effect of these enzymes upon hepatic lipid metabolism in human liver has not been stablished in detail and most studies used rodents. Therefore, there is a need to characterise A-ring reductases using liver human models and also to see if manipulation of these enzymes can alter the metabolic phenotype.

1.8.Aims

- Define the impact of GCs upon lipid homeostasis and insulin sensitivity in human hepatocytes (Chapter '3').

- Characterise the impact of androgens upon lipid homeostasis and insulin sensitivity in human hepatocytes (Chapter '4').

- Determine the contribution of pre-receptor GC metabolism in the development of an unfavourable metabolic phenotype in human liver cultures of hepatocytes (Chapter '5').

- Study if manipulation of pre-receptor GC metabolism can alter the metabolic phenotype (Chapter '5').

- Define putative mutations or polymorphisms through genetic sequencing of SRD5A1 and 2 in patients with abnormal steroid metabolite ratios suggesting an altered 5αR activity (Chapter '6').

Chapter 2 General Methods

Methods specific to individual chapters are found in the methods sections of those chapters. Unless otherwise stated methods were carried out using Sigma -Aldrich Chemical Company (Pool, Dorset, UK) reagents and cell culture plastic ware from Corning (Artington, Surrey, UK).

2.1.Cell culture

2.1.1.C3A

2.1.1.1.Cell line

C3A cells are a subclone of the hepatoma-derived HepG2 cell line (Parvez et al. 2011) which express the GC receptor but unlike HepG2 cells they lack 5αR2 expression and that is the reason they are the preferable model in this study. However, they lack IRS2 expression which was confirmed in this study, and therefore the Huh 7.5 cells were used as a more insulin sensitive cell line. In addition, Huh 7.5 and HepG2s carry a loss of function mutation, I148M, in PNPLA3 gene which is the best genetic predictor for NAFLD and increases TAG accumulation (Dutta 2015). C3As have not been checked for this gene but they are a subclone of HepG2s and most probably they represent the same mutation. The origin of C3A cells is the liver of a 15 year old Caucasian male, with hepatocellular carcinoma. Liver cells were first extracted and then immortalized by transfection host. One of the important characteristics of C3As is the ability to grow in low glucose media. This cell line was purchased from ATCC (Middlesex, UK) and cells were delivered frozen.

2.1.1.2.Proliferation

Cells were maintained in cell bind 25cm^2 TC flasks in 5mL of MEM (PAA, Somerset, UK) supplemented with 1% L-Glutamine, 1% Penicillin/Streptomycin, 1% Mem non- essential amino acid and 10% Foetal Calf Serum (FCS) at 37ºC in a humidified atmosphere of air with 5% CO_2. At 70% confluence cells were trypsinised and split 1 in 3 into fresh flasks. Prior to experiments, cells were trypsinised and subcultured into 24 well CellBind TC plates. Medium was replaced every two days and cells were cultured until 70% confluent (Figure2-1).

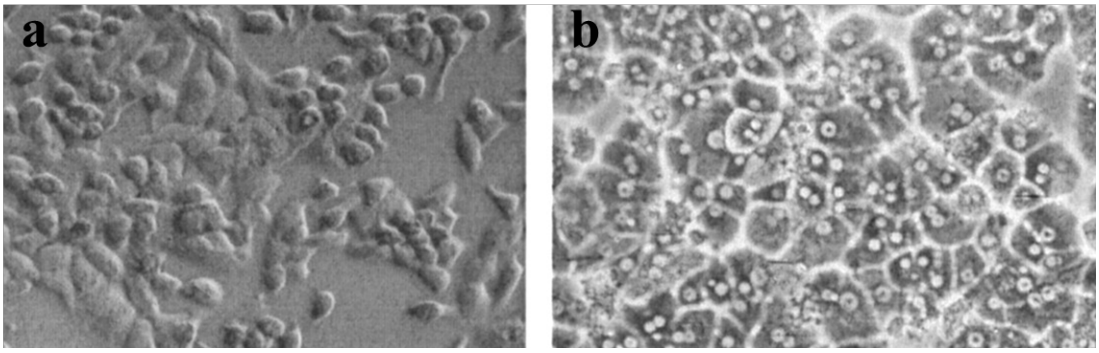

Figure 2-1 C3As morphology after day 2 (a) and 3 (b) of proliferation.

The nutrient contests of MEM media is shown in table 2-1. The reason this media was chosen is the low glucose contents (1g/L) as higher glucose concentration can drive *de novo* lipogenesis (Table 2-1).

Component	g/L	Component	g/L
Amino Acids		Inorganic Salts	
L-Arginine • HCl	0.126	Calcium Chloride	0.2
L-Cystine • 2HCl	0.0313	Magnesium Sulfate (anhydrous)	0.09767
L-Glutamine	0.292	Potassium Chloride	0.4
L-Histidine • HCl • H2O	0.042	Sodium Chloride	6.8
L-Isoleucine	0.052	Sodium Phosphate Monobasic (anhydrous)	0.122
L-Leucine	0.052		
L-Lysine • HCl	0.0725		
L-Methionine	0.015	Other	
L-Phenylalanine	0.032	Glucose	1
L-Threonine	0.048	Phenol Red • Na	0.011
L-Tryptophan	0.01		
L-Tyrosine • 2Na • 2H2O	0.0519		
L-Valine	0.046		
Choline Chloride	0.001		
Folic Acid	0.001		
myo-Inositol	0.002		
Niacinamide	0.001		
D-Pantothenic Acid (hemicalcium)	0.001		
Pyridoxal • HCl	0.001		
Riboflavin	0.0001		
Thiamine • HCl	0.001		

Table 2-1 Detailed nutrient contents of MEM media, it is a low glucose media with glucose concentration of 1g/l.

2.1.1.3.Freezing down

At 70% confluence, cells were trypsinised and centrifuged at 1500 g for 5 min. The pellet was resuspended in 1mL of freezing serum, FCS with 10% dimethyl sulfoxide (DMSO). Cell mixture was aliquotted into 1.5mL cyrovials and slowly frozen at the rate of 1^{o}C/ min in a cryofreezing chamber (Nalgene, Hereford, UK) at -80^{o}C overnight. Cells were transferred to liquid nitrogen for long-term storage afterwards.

2.1.2.Huh7.5

2.1.2.1.Cell line

Huh7.5 cells are well differentiated hepatoma-derived cell line that was taken from a male donor. These cells were a gift from the liver laboratories (IBR 5th floor, Clinical and experimental medicine department, University of Birmingham) and all experiments on Huh7.5 cells were carried out with the help of Dr. Reina Lim Teegan. Cells were cultured in MEM with 10% FCS and split into 24 well plates.

2.1.2.2.Proliferation

Cells were maintained in cell bind 25cm2 TC flasks in 5mL of MEM (PAA, Somerset, UK) supplemented with 1% L-Glutamine, 1% Penicillin/Streptomycin, 1% Mem non- essential amino acid and 10% Foetal Calf Serum FCS at 37^{o}C in a humidified atmosphere of air with 5% CO_2. At 70% confluence cells were trypsinised and split 1 in 3 into fresh flasks. Prior to experiments, cells were trypsinised and subcultured into 24 well CellBind TC plates. Medium was replaced every two days and cells were cultured until 70% confluent.

2.2.Primary human hepatocytes

Cryoplatable human hepatocytes were purchased from BioreclamationIVT Technologies (Baltimore, USA). Cryoplatable hepatocytes were isolated from whole livers not resections and the tissue was cryopreserved the same day to receive the highest quality hepatocytes. Each order was made considering the donor serology and phenotype provided by the company. Cells were delivered in a liquid nitrogen shipping container and transferred to liquid nitrogen on arrival.

2.2.1.Thawing procedures

Prior to thawing, *InVitroGRO* CP medium (BioreclamationIVT Technologies, Baltimore, USA) was pre-warmed to 37ºC and supplemented with *Torpedo* Antibiotic mix (1mL per 45mL CP medium). Primary hepatocyte vials were brought up on ice from liquid nitrogen storage. The vials were then placed in a 37ºC water bath and shaken gently until the cells pulled away from the vial wall. Cells were then transferred to the pre-made CP medium and remaining cells in the vial were washed with 1mL of hepatocyte suspension. The thawing step was done in 90-120 seconds in order to get the best viability (approximately 70% healthy cells) and then this viability and also the cell count were measured using Trypan blue. The hepatocyte containing tube was inverted 3 times to resuspend the cells and the homogeneous suspension was gently plated by placing the pipet on the side of the wells. For seeding, the acceptable concentration for 24 and 12 well plates is 350,000 and 700,000 cells per well respectively, in order to reach 70% viability. BD BioCoat collagen I cell culture plates (BD Biosciences, New Jersey, USA) were only applied as advised by BioreclamationIVT.

2.2.2.Cell maintenance

Cells were plated on collagen using *InVitroGRO* CP medium (BioreclamationIVT Technologies, Baltimore, USA) and after four hours this was replaced by *InVitroGRO* HI medium supplemented with *Torpedo* Antibiotic mix (1mL per 45mL HI medium). Cells were incubated at 37ºC in a humidified atmosphere of air with 5% CO_2 overnight. Having found many unattached cells in some primary cultures and following consultation with BioreclamationIVT, cells were kept in *InVitroGRO* CP medium for 18 hours and only were replaced with fresh CP medium if required (Figure 2-2). All the media were aspirated and replaced carefully to avoid disrupting cell monolayer.

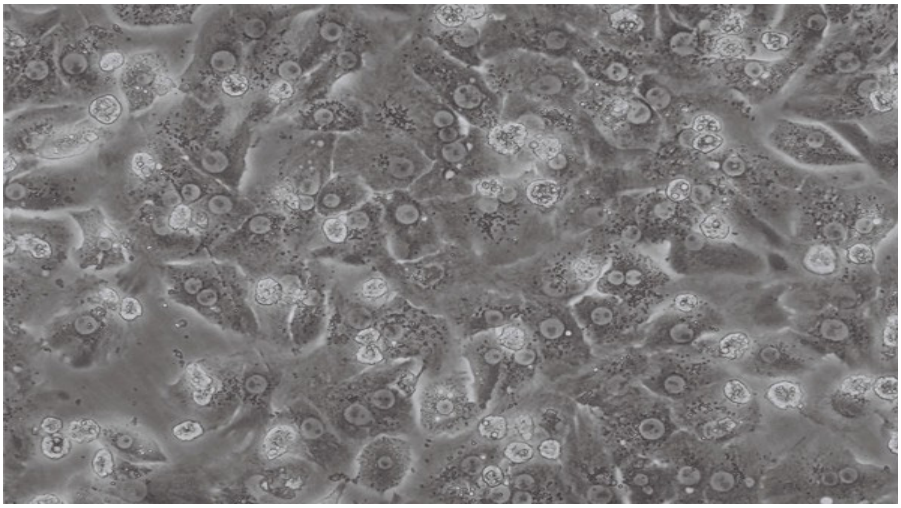

Figure 2-2 Primary human hepatocytes morphology after day 2.

2.3.Protein extraction

2.3.1.Principle

In order to extract proteins, monolayer cells were lysed in buffer containing protease and phosphatase inhibitors, and detergent. This lysate was used to break the cell membranes and insoluble cell debris removed by centrifugation subsequently.

2.3.2.Methods

Cells were washed on ice with PBS and 100µl of RIPA buffer (1mM EDTA, 150mM NaCl, 0.25% SDS, 1% NP40, 50mM Tris pH 7.4, supplemented with protease inhibitor (Roche, Sussex, UK) and phosphatase inhibitor (Thermofisher, Surrey, UK) was added per well of a 24 well plate. Cells were scraped with a 1mL syringe plunger and lysate transferred into Eppendorf tubes and then incubated at -80ºC for 10 to 20 min. The lysates were thawed on ice and centrifuged at 12000 g for 15 min at 4ºC. Finally the supernatants, containing soluble proteins, were transferred to new Eppendorf tubes and stored at -80ºC.

2.4.Measuring protein concentration

2.4.1.Principle

Total protein concentrations were measured using the BioRad RC DC protein assay (BioRad, Herts, UK). This colourmetric assay is based on the reaction of protein with an alkaline copper tartrate solution and then reduction of Folin reagent. This generates a reduced Folin species with a characteristic blue colour, with a maximum absorbance at 750nm and a minimum absorbance at 405nm.

2.4.2.Methods

Protein assays were carried out according to the manufacturer protocol (BioRad, Herts, UK) in a 96 well plate. To make protein standards, bovine serum albumin (BSA) was dissolved in RIPA buffer and then serially diluted to obtain the following concentrations: 0, 0.5, 1, 2, 4 and 6 mg/mL. 5 µl of either sample or protein standards was added per well in duplicate. Subsequently, 20µl of solution A (alkaline copper tartrate solution) and 200µl of solution B

(Folin solution) were added per well. After incubation for 10min at room temperature the absorbance was read at 690nM on a vector3 1420 multilabel counter (PerkinElmer, Bucks, UK).

2.5.Western blotting

2.5.1.Principle

This method is performed to measure the relative amounts of specific protein in a mixed protein sample. Prior to western blotting, protein samples are boiled to remove all proteins' secondary and tertiary structures. Then proteins are separated by size using SDS-Page electrophoresis.

After protein separation, they are transferred to a polyvinylidene difluoride (PVDF) or nitrocellulose membrane. This membrane is blocked using a solution containing a generic protein such as milk or BSA to prevent non-specific binding to the membrane and subsequently incubated with a primary antibody that binds specifically to the protein of interest. The membrane is then incubated with the secondary antibody which is conjugated to horseradish peroxidise (HRP) and directed against the primary antibody. HRP catalyses the oxidation of a luminal substrate producing blue light. This reaction is captured on a photographic film.

2.5.2.Methods

SDS-PAGE and protein transfer were performed in BioRad mini protein 3 apparatus (BioRad, Herts, UK). 10 to 40µg of protein was mixed with 5x loading buffer and boiled at 95ºC for 5 min. Samples were run on a 8-12% gradient SDS-PAGE gel (BioRad, Herts, UK) at 200 V

for 1 h to 90 min. Precision Plus Protein Standard (BioRad, Herts, UK) was used as a marker. Protein samples were then transferred at 100v for 1h to a nitrocellulose membrane (GE Healthcare, Bucks, UK). To check the efficiency of transfer, the membrane was incubated in Ponceau stain for 1min and rinsed with water until the protein bands observed.

Membranes were blocked in 7mL of blocking buffer (PBS 0.1% Tween 5% Milk Powder) for 1hr at room temperature and rinsed with washing buffer afterwards. Primary antibody (Table 2-2) was added to the membrane and incubated overnight at 4^{o}C.After three washes with washing buffer (1 x PBS 0.1% Tween), membrane was incubated with secondary antibody (discussed in detail in section 3.3.5) for 1h at room temperature. Before the developing step, the membrane was washed 3X with washing buffer. Enhanced Chemiluminescence (ECL, GE Healthcare, Bucks, UK) was used for antibody detection. 0.5mL from both substrate A and B was mixed to reach a 1mL reaction mixture per membrane and applied on membrane for 2 min.

Finally, the membrane was exposed to photographic film (Perkin Elmer, Surrey, UK) in a dark room for 30sec to 1h. Films were developed on Compact X4 automatic film processor (Xograph Imaging Systems, Gloustershire, UK).

Peptide/protein Target	Antibody	Manufacturer	Species raised in; monoclonal or Polyclonal	Dilution used
PKB/akt	Anti-PKB/akt	Millipore, Hertfordshire, UK	Rabbit monoclonal	1/1000
Phospho-PKB/akt (ser473)	Anti-phospho PKB/ akt (ser473)	R&D Systems, Abingdon, UK	Rabbit polyclonal	1/1000
Phospho-PKB/akt (Thr308)	Anti-phospho PKB/ akt (Thr308)	Cell Signalling Technology, Danvers, MA, USA	Rabbit polyclonal	1/1000
Phospho-Acetyl CoA Carboxylase (Ser79)	Anti-phospho Acetyl CoA Carboxylase (Ser79)	Millipore, Watford, UK	Rabbit polyclonal	1/1000
Acetyl CoA Carboxylase	Anti Acetyl CoA Carboxylase (Avidin-HRP)	Sigma -Aldrich Chemical Company, Pool, Dorset, UK)	Rabbit polyclonal	1/1000
β-Actin	Anti-β- Actin (HRP)	Abcam plc, Cambridge, UK	Rabbit monoclonal	1/5000

Table 2-2 List of antibodies used for western blot analysis.

2.6.RNA extraction

2.6.1.Principle

To extract total RNA from a monolayer of cells or from tissue explants, Tri-Reagent was applied. Tri-Reagent contains phenol and guanidine thiocyanate which together can inhibit RNase activity.

2.6.2.Methods

After washing the cells on ice with PBS, 1 mL of Tri-Reagent was added per well of a 24 well plate and incubated at room temperature for 5 min. Cell lysates in Tri-Reagent were then transferred to Eppendorf tubes. 200 µl of chloroform was added per 1mL of reagent for each tube. Tubes were vigorously shaken for 10sec and incubated at room temperature for 15 min.

The mixture was centrifuged at 16000 g for 15 min at 4ºC to separate the RNA in the aqueous phase from the DNA and protein at the interface. The aqueous phase was transferred to a new Eppendorf tube and 500 µL of isopropanol was added. The tubes were inverted 4 times and then incubated at room temperature for 15 min, and subsequently centrifuged at 16000 g for 15 min.

The supernatant was aspirated and the RNA pellet was washed with 75% ethanol, centrifuged, and aspirated again to remove the ethanol wash. The RNA pellet was air dried for 5 min, resuspended in 20 to 50µl of RNase free water and stored at -80oC.

The quality of the RNA then assessed by electrophoresis on 1% agarose gel with 0.15 µg/mL GelRed (Cambridge biosciences LTD, Cambridge, UK). The intact RNA run on a gel will have two sharp, clear 18s and 28s rRNA bands which are visualised under UV light. The 28s rRNA band is approximately twice as intense as the 18s rRNA band in an intact RNA, and therefore, this 2/1 ratio (28s/18s) is a good indication of the high quality RNA. Degraded RNA will not present the 2/1 (28s/18s) ratio or will not have a sharp rRNA band and will have a smeared appearance. A very low molecular weight smear is a completely degraded RNA. All the samples were run beside Ambion's RNA millennium markers (Thermofisher, Surrey, UK) to allow the size of any bands to be determined and also to check if the gel was run properly.

The RNA concentration and purity is measured by NanoDrop ND-1000 UV-Vis Spectrophotometer (Thermofisher, Surrey, UK). All measurements were made using 1 µl of RNA with respect to a blank (nuclease free water). RNA has a maximum absorption at 260nm and its concentration is determined by the OD reading at 260nm. In addition to OD260, measurements should be taken at 280nm and 230nm. The OD260/OD280 ratio is an

indication of the protein contamination in the sample. Pure RNA has an OD260/OD280 ratio of 2.1. However, the RNA with the ratios in the range of 1.8 - 2.0 is considered acceptable. OD230 is an indicator of other contamination (such as ethanol used in RNA isolation method) and the ideal OD260/OD230 is greater than 1.5.

2.7.Reverse Transcription (RT)

2.7.1.Principle

Reverse transcription (RT) is used to convert single stranded RNA into complementary DNA (cDNA). The extracted RNA is heated to denatured secondary structure and cooled subsequently to facilitate annealing of random hexomers to the RNA template. After annealing step, the RNA-bound primer is extended with the help of reverse transcriptase and RNase inhibitor to generate a complementary DNA copy of the RNA template. Finally, it is heated to a high temperature to inactivate reverse transcriptase which is also an end point for the reaction. This cDNA can then be used in a PCR reaction.

2.7.2.Methods

RT reactions were performed using Applied Biosystems Reverse Transcription Kit (Applied Biosystems, Warrington, UK). 1µg of RNA was diluted in nuclease free water to a final volume of 10µl, and 10µl of 2x RT master mix was added to this RNA dilution. To generate a 2x RT master mix, components were added in the following order: 2 µl of 10x RT buffer, 0.8µl of 25x dNTPs mix (100mM), 2µl of 10x RT Random primers, 1µl of Multiscribe reverse transcriptase, 1µl of RNase Inhibitor, and 3.2 µl of Nuclease free water. Samples were incubated at 25ºC for 10min followed by 37ºC for 120min, and then 85ºC for 5min to

denature the reverse transcriptase, using a thermal cycler (Applied Biosystems, Warrington, UK).

2.8.Polymerase Chain Reaction

2.8.1.Principle

PCR is performed in order to amplify the specific region of DNA or cDNA using oligonucleotide primers which are complementary to the 3' and 5' ends of this region of interest. Double stranded DNA is heated with high temperature to denature and cooled subsequently to facilitate the primers annealing process. At the end, the temperature is increased so that Taq DNA polymerase can extend the oligonucleotides and produce the complementary DNA strands.

2.8.2.Methods

In a 10µl reaction the following components were added: MasterMix (final concentration 1x), forward and reverse primers (1 µM final concentration), and 100nM of DNA. In a thermal cycler (Biometra, Goettingen, Germany) samples were incubated at 94°C for 2min and then cycled 35 times at 94°C for 20 sec, 53.4 to 65°C for 20 sec, and 72°C for 30 sec. Samples were then incubated for 72°C for 5min.

2.9.Quantitative Polymerase Chain Reaction

2.9.1.Principle

Real-time PCR is used for detection of a PCR product while it accumulates during the PCR reaction using a fluorogenic probe. This probe is synthesised with a fluorescent reporter dye on its 5'and a quencher dye on its 3'end. Primers are complementary to the 5' and 3' ends of a region of interest and the oligonucleotide probe binds to the DNA template, downstream from one of the primer sites. Once the primer is extended, the probe is cleaved by the Taq DNA polymerase activity. The probe cleavage separates the reporter and the quencher dye which leads to an increase in the reporter dye signal. The removal of the probe from the template DNA is crucial for PCR process which allows primer extension until it reaches the end of the DNA. As the amount of reporter dye signal is increased in each cycle, the fluorescence intensity proportional to the amount of PCR product produced is augmented.

The value at which the target sequence is detected called cycle threshold (Ct). As this technique is used for relative quantification, the ΔCt (Ct of the target gene – Ct of the18s) values are calculated. There is an inverse relationship between ΔCt values and mRNA expression.

2.9.2.Methods

All real-time PCR experiments were carried out using Applied Biosystems reagents and gene expression assays (Warrington, UK) (list of primers used in the current study is shown in Table 2-3). The 18s rRNA was used as control and all reactions were carried out in duplicate in 96-well plates (Applied Biosystems, Warrington, UK). The 18s rRNA contains forward

and reverse primers plus a labelled probe and has been used at a final concentration of 25mM each.

Gene symbol	Exon boundary (Ref seq)	Assay location (Ref Seq)	Amplicon length	Product order number	Gene symbol	Exon boundary (Ref seq)	Assay location (Ref Seq)	Amplicon length	Product order number
AKT1	4-5 5-6 4-5	627 711 841	66	Hs00178289	SRD5A1 (5αR1)	2-3	654	120	Hs00602694
AKT2	9-10 8-9 9-10	1098 1005 1135	62	Hs01086102	SRD5A2 (5αR2)	1-2	353	83	Hs00165843
INS	2-3	245	69	Hs00914338	SRD5A3 (5αR3)	3-4	678	99	Hs00430681
IRS1	1-2	3799	69	Hs00178563	AKR1D1 (5βR)	1-2	170	103	Hs00818881
IRS2	1-1	3991	70	Hs00275843	H6PDH	2-3	899	57	Hs00188728
ACC1	31-32 31-32 29-30 30-31 35-36	4364 3931 4001 4112 5038	65	Hs01046047	GR	4-5 4-5 4-5 4-5 4-5	1959 1789 1692 1585 2461	73	Hs00353740
ACC2	1-2	667	88	Hs00153715	AR	4-5 4-5	3289 740	72	Hs00171172
Cpt1A	11-12	1516	75	Hs00912671	11β-HSD1	3-4 2-3 3-4	378 376 350	67	Hs01547870
FAS	3-4	399	62	Hs01005622	11β-HSD2	1-2	384	50	Hs00388669
DGAT2	6-7 7-8	1146 1275	69	Hs01045913					

Table 2-3 List of primers which are provided by Applied Biosystems. The information in this table is gathered from: http://www.appliedbiosystems.com/absite/us/en/home/applications-technologies/real-time-pcr.html.

In all experiments, the following components were added per single reaction: 10 µl of 2x Master Mix, 1 µl of either 20x expression assay or 18s mixture, 100ng of cDNA and nuclease free water up to 20µl per well. Nuclease free water was added instead of cDNA to negative control wells. Plates were run on 7500 real-time PCR system (Applied Biosystems, Warrington, UK). All data were corrected to 18s. The validity of 18s as an internal control was confirmed by comparing 18s abundance in 4 experimental replicates after cortisol

treatment (cortisol 100, 250 and 1000nM vs. control) (Figure 2-3). Ct values were used to determine ΔCt (Ct of the target gene – Ct of the 18s), with a higher ΔCt meaning lower gene expression. Where significant changes were found PCR data were also presented either as a fold change ($2^{-\text{difference in }\Delta CT}$) or arbitrary units (AU) ($10^5 * (2^{\Delta ct})$).

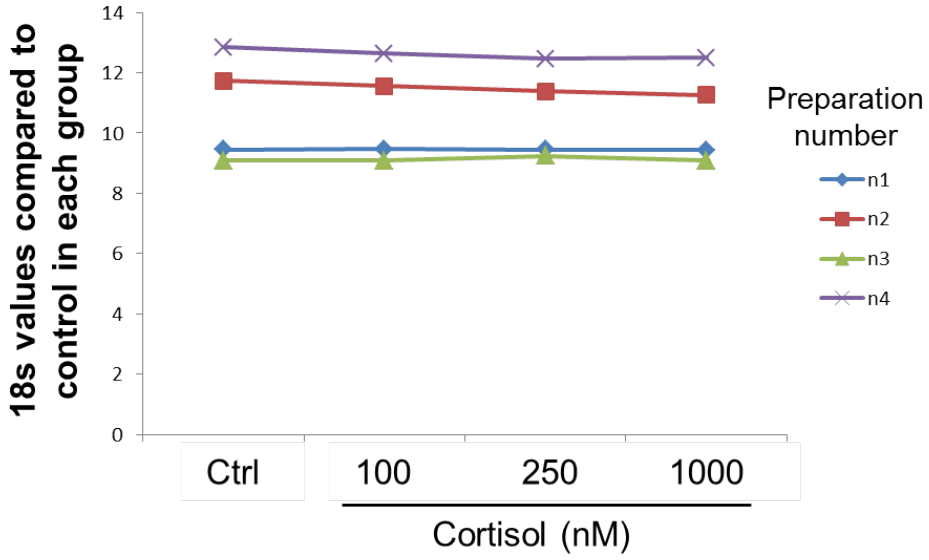

Figure 2-3 The impact of cortisol treatment (100, 250 and 1000nM) on 18s abundance in four different experimental replicates in C3As. The PCR data demonstrate that cortisol treatment has no impact on 18s values, validating its use as an internal housekeeping gene.

2.10.*De novo* lipogenesis assay

2.10.1.Principle

De novo lipogenesis assay, also called Acetyl-CoA Carboxylase assay (ACC), is a multi-step assay. ACC is the rate-limiting enzyme in *de novo* lipogenesis with the role in carboxylation of acetyl-CoA to malonyl-CoA. The assay measures 1-[^{14}C]-acetic acid incorporation into lipid, so any change in acetate incorporation is likely to reflect a change in ACC activity. Lipids are extracted from the cells and their radioactivity measured using scintillation counting. We actually measured the acetate incorporation to total lipid fraction which was used as a reflection of *de novo* lipogenesis.

2.10.2.Methods

Prior to *de novo* lipogenesis assay, cells were incubated in a 24 well plate with 1mL of serum free medium. 0.12µCi/L 1-[^{14}C]-acetic acid with cold sodium acetate to a final concentration of 10uM acetate was added to each well and the plate was incubated at 37ºC for 6h. Cells were then washed twice with 1mL of PBS and scraped in 250µl of PBS subsequently. Finally, the scraped cells were transferred into glass tubes.

To extract the lipid fraction, 5mL of chloroform: methanol (2:1 by vol/vol) was added to each glass tube (Folch et al. 1957). The tubes were vortexed for 1min and 1mL of water was added. The glass tubes were vortexed again for 1 min and centrifuged at 3000 g for 10min until two phases were separated. The upper phase was aspirated and the lower faction transferred to a 5mL scintillation tube and evaporated until completely dry using a sample dryer in a fume cupboard. 5mL of scintillation cocktail was then added to each scintillation tube and samples were counted on the Liquid Scintillation Analyzer 2500 RT/AB (Packard, A Canberra Company, Oxfordshire, UK). No cells tube was used as a negative control.

2.11.5αR2 overexpression

In contrast to primary human hepatocytes, C3A 5αR2 expression is very low, and as a result they represent a good model to study the impact of 5αR2 transfection into the cell. The coding sequence of 5αR2 was cloned into the pcDNA3.1 vector (Invitrogen) by Dr Laura Gathercole in our lab and transiently transfected into C3A cells (Figure 2-4).

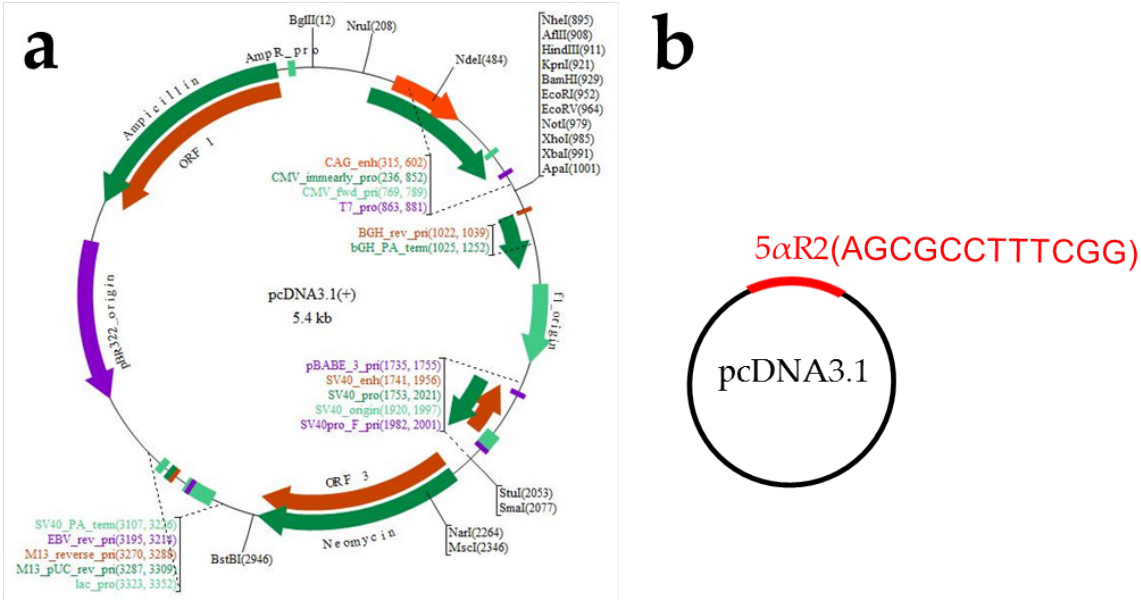

Figure 2-4 pcDNA3.1 vector (Picture is taken from Invitrogen-Thermo Fisher Scientific website;https://www.thermofisher.com/order/catalog/product/V79020)(a), schematic diagram of 5αR2 coding sequence (presented in red) cloned into the vector(presented in black)(b).

2.11.1.C3A cell Transfection

Prior to transfection, cells were seeded into a 24-well plate. Cells were ~60-70% confluent in order to obtain the most efficient transfection result. Transfection mixture was made up using 1.5 µg of DNA diluted in 50 µL of OptiMEM serum free media (Invitrogen, Paisley, UK) and 2 µL of Lipofectamine 2000 (Invitrogen, Paisley, UK) diluted in 50 µL of Optimem serum free media. The mixtures were then incubated at room temperature for 5 mins. Subsequently, diluted DNA was combined with diluted Lipofectamine 2000, and finally after incubation at room temperature for 25 mins, 100 µL of complexes was added drop-wise to each well. The plates were rocked gently and left for incubation at 37ºC.

Transfection duration was 48h and its efficiency was determined using a plasmid containing green fluorescence protein (GFP). Cells expressing GFP can be visualised under a fluorescence microscope and a representative image is shown in figure 5-2 (section 5.4.3.1).

Fluorescent and total cells were counted using an haemocytometer. The efficiency was presented as the % of fluorescent cells/total cells. Changes in 5αR2 mRNA expression level were confirmed by real-time PCR subsequently.

2.12.Site Directed Mutagenesis (SDM)

2.12.1.Principle

Known mutations in SRD5A2 were made using Quikchange II site-directed mutagenesis kit (Agilent Technologies UK Limited, Cheshire, UK). This kit utilizes a double-strand DNA vector (containing the gene of interest) and a set of forward and reverse primers containing the desired mutation. These primers are designed to be complementary to opposite strands of the vector and are extended during temperature cycling using a high fidelity DNA polymerase. This generates a mutated plasmid from the parental DNA template. The parental DNA template is digested by DpnI, which specifically digests methylated and hemimethylated DNA. Finally the vector containing the desired mutation is transformed to competent cells (Figure 2-5).

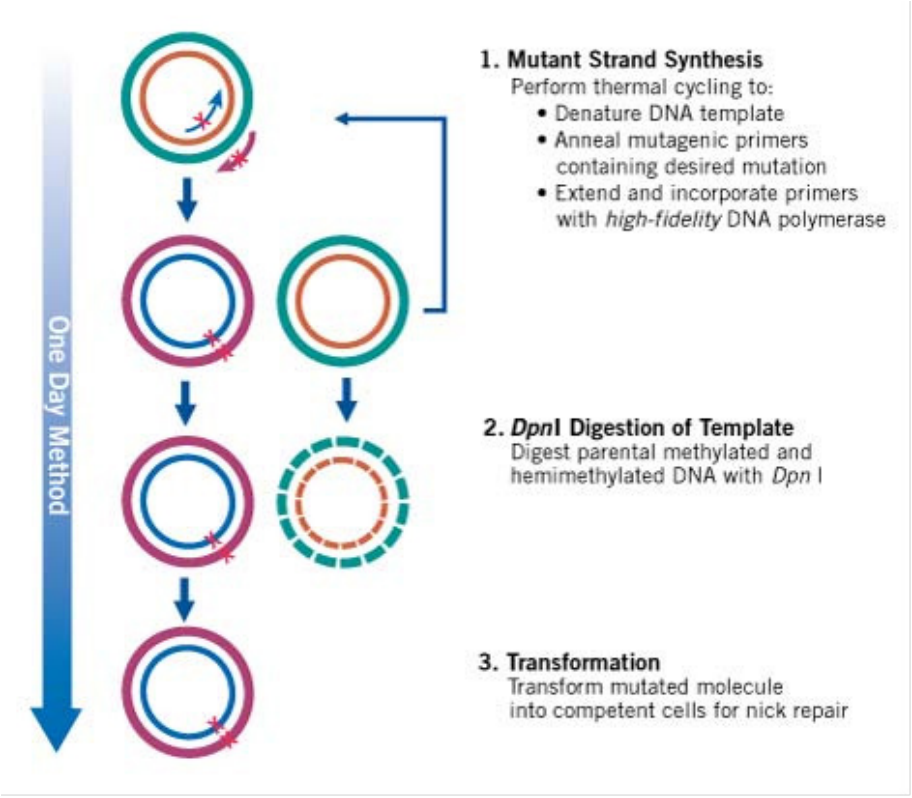

Figure 2-5 Site directed mutagenesis (SDM) technique which has three major steps; mutant strand synthesis, DpnI designation of template, and transformation. Picture is taken from Quikchange (Agilent Technologies) website.

2.12.2.Methods

In a 50µl reaction the following components were added: 5µl of 10× reaction buffer, forward and reverse primers (125ng) 10ng of double-strand DNA template, 1µl of dNTP mix, 3µl of QuikSolution and ddH2O to a final volume of 50µl. In a thermal cycler (Biometra, Goettingen, Germany) samples were incubated at 95°C for 1min and then cycled 18 times at 95°C for 50 sec, 53.4 to 60°C for 50 sec, and 68°C for 60 sec. Samples were then incubated for 68°C for 7min.

1µl of DpnI was added to PCR Eppendorf, vortexed and incubated for 1 hour at 37°C. 1mL of ethanol (100%) was then added to each tube and incubated for 1hour at -80 °C. The mixture

was centrifuged at 16000 g for 20 min at 4ºC and the supernatant aspirated. The DNA pellet was washed with 75% ethanol, centrifuged, and aspirated again to remove the ethanol wash. The DNA pellet was air dried for 10 min, resuspended in 10µl of RNase free water and stored at -80ºC. Finally the DNA vector containing the desired mutation was transformed to XL10-Gold ultracompetent cells.

2.13.Gas/Liquid Chromatography-Mass Spectrometry (GC/LC-MS)

As free steroids are polar compounds they should readily move from an aqueous to an organic environment. This property allows for simple liquid-liquid extractions, this was historically done with dicholoromethane, However MTBE (methyl tert butyl ether) is now the solvent of choice. For conjugated steroids (steroid-sulphates or steroid-glucuronides) which are hydrophilic solid phase extraction is required to extract these from cell media or urine.

After effective, efficient extraction of steroids positive identification is required using a sensitive, reproducible, accurate technique such as mass spectrometry (Krone et al. 2010).

2.13.1.Chromatography

There are two chromatographic techniques which can be linked to mass spectrometers to separate a steroid mixture into specific steroids; these are liquid chromatography and gas chromatography.

Liquid chromatography (LC) permits separation of a mixture of liquid analytes into separate fractions. This is achieved with the use of a column packed with a stationary phase (typically C_{18} and phenyl-hexyl) which retains the analytes. Steroids are retained on the column

stationary phase at differing degrees based on their polarity, increasing the polarity of the mobile phase elutes the steroids sequentially. Typical mobile phases used in steroid analysis via LC/MS have one aqueous and one organic mobile phase such as water/methanol or water/acetonitrile.

Gas chromatography (GC) permits separation of liquid analytes which are vaporised in the GC injector. These gaseous steroids travel through the heated column and arrive at the mass spectrometer at different times due to differences in column liquid phase interaction. GC is used after chemical derivatisation of the steroids to increase the volatility and stability of the steroid. The derivatisation procedures involve addition of a trimethyl-silyl group which adds to any hydroxy group present on the steroid skeleton. Steroid specific gas chromatography columns have been produced; (5%-phenyl)-methylpolysiloxane columns such as the DB5 and the more specialised dimethylpolysiloxane stationary phase columns are widely used.

2.13.2.Mass Spectrometry

Mass Spectrometry in combination with either of these chromatographic separation procedures can be used to stablish a qualitative and quantitative profile of steroids within a sample. After chromatographic separation the steroids sequentially enter the ionisation source of the mass spectrometer.

The general operating principles of mass spectrometry are similar including four steps; ionisation, fragmentation, separation, and detection. The ionisation source vaporises and ionises the sample to produce gaseous ions. There are many types of ionisation source including; electron ionisation (EI), chemical ionisation (CI), atmospheric pressure chemical ionisation (APCI), and electrospray ionisation (ESI). Fragmentation occurs where there is

excess internal energy more than is required to ionise the molecule. This energy can break the molecular bonds. Controlled fragmentation such as collision induced dissociation (CID) in an ion trap, allows structural information about a given molecule to be obtained. In addition, a mass analyser separates ions accurately using magnetic or an electrical field or a combination of both. Finally, a signal proportional to the ion signal (or count) is passed to a data system which processes this raw data into mass spectra and ion chromatograms.

The specific methodology including the use of GC/LC-MS is detailed in related chapter '5' (see section 5.3.7).

2.14.Statistical analysis

Data are presented as mean ± s.e. Normality tests were performed on all data. The tests were passed in all cases and therefore throughout the thesis, parametric statistical tests were used. One way ANOVA on ranks, was used to compare multiple treatments, doses or times. Tukey's and Dunnett's post-hoc analysis were used as follow-up tests to ANOVA. The Tukey's test compares every mean with every other mean while the Dunnett's test compares every mean to a control mean. Statistical analysis on real-time PCR data was performed on mean ΔCT values ± s.e, unless otherwise stated. All analysis was performed using the Sigmastat 3.1 software (System Softwares, CA, USA).

Chapter 3 Impact of Glucocorticoids upon insulin signalling cascade and lipid metabolism

3.1.Aims

- To optimise the *in vitro* model for metabolic assessments in human hepatocytes
- To define the impact of Glucocorticoids upon insulin sensitivity in human hepatocytes
- To study the impact of Glucocorticoids on lipid metabolism in human hepatocytes

3.2.Background

The effects of GCs within the body, especially on the development of obesity and insulin resistance, are well described. These effects are exemplified in patients with circulating GC excess, Cushing's syndrome. The most common observations in these patients are central obesity, hypertension, insulin resistance, type 2 diabetes and in 20% of cases, NAFLD (Shibli-Rahhal et al. 2006). Importantly, 1-2% of the population in United Kingdom and United States are taking prescribed GCs and their side effects create a significant health burden (Overman et al. 2013;Van Staa et al. 2000).

Studies in both human and animal models have demonstrated that GCs induce whole body insulin resistance (Larsson and Ahren 1996;Zarkovic et al. 2008). However, the molecular mechanisms behind this have not been studied in detail. GC action upon global insulin sensitivity is likely to be the combination of metabolic events in different target organs. In adipose tissue, it has been suggested that GCs decrease insulin-stimulated glucose uptake (Sakoda et al. 2000). In contrast, there are some studies that have shown dose and time dependent increases in insulin sensitivity following GC treatment (Gathercole et al. 2007;Tomlinson et al. 2010). These effects also persist after a long-term (7 days) GC administration (Gathercole et al. 2011a). Skeletal muscle is responsible for 80% of glucose

disposal in insulin-stimulated conditions (DeFronzo et al. 1981). This suggests that GCs in this tissue might play a role contributing to global insulin resistance. There are a number of studies that are in agreement with this; direct inhibition of insulin-stimulated glucose uptake by GCs in skeletal muscle has been demonstrated (Dimitriadis et al. 1997;Ruzzin et al. 2005).

The metabolic effects of GCs on liver insulin sensitivity and lipid metabolism are complex but it is widely believed that GCs induce insulin resistance. It has been shown that GCs decrease glucose usage and increase glucose output contributing to insulin resistance in rodents (Guillaume-Gentil, Assimacopoulos-Jeannet, & Jeanrenaud 1993). However, studies in human models have not been performed.

As discussed in detail in section 1.3.4, insulin binding its receptor initiates a complex intra-cellular cascade. In summary, the metabolic actions of insulin occur via the IRS, PI3Kinase axis (Giorgetti et al. 1993) which can result in activation of PKB/akt through S473 and T308 phosphorylation (Hanada et al. 2004). This subsequently allows GLUT4 to translocate to the cell membrane and increase glucose uptake (Larance et al. 2005).

There is a close link between intra-cellular lipid metabolism and the insulin signalling cascade. High plasma FFAs cause insulin resistance (Boden et al. 1991) and this is thought to be mediated by phosphorylation of Ser307 on IRS1 which is responsible for inhibition of IRS-1 function (Yu et al. 2002). In addition, this insulin resistance impairs the interaction with the IR and also targets IRS1 for proteasomal degradation (Sun et al. 1999).

The interaction between GCs and the insulin signalling cascade and their effects on lipid metabolism have been studied in skeletal muscle and adipocytes. GCs enhance insulin action to drive lipid accumulation in human subcutaneous (sc) but not omental (om) adipose primary cultures (Gathercole et al. 2011b). However, in skeletal muscle, GCs induce insulin resistance

with an increase in lipogenesis in both murine and human cell lines and primary cultures (Morgan et al. 2013).

There is evidence that GCs augment insulin action to promote lipid accumulation in rodent hepatocytes. Although dexamethasone alone did not have any effects on lipogenesis in rats, co-incubation with insulin increased lipogenesis (Amatruda et al. 1983).

Defining the interaction between GCs, IR and lipid metabolism will contribute significantly to our understanding of the pathogenesis of NAFLD and hepatic insulin resistance and may lead to the identification of novel treatment targets. Clinical studies have demonstrated a strong link between IR and NAFLD (Targher et al. 2006), but there is also evidence to implicate GC action. Liver specific GC receptor knockdown ameliorates hepatic steatosis in rodent models (Lemke et al. 2008) and liver-selective GR antagonism can improve carbohydrate signalling by reducing hepatic glucose production (Edgerton et al. 2006).

We have therefore characterised the impact of cortisol upon the insulin signalling cascade and intra-cellular lipid metabolism using human tissues. We have used hepatocyte cell lines (C3A and Huh7.5) and also endorsed our findings in primary cultures of human hepatocytes.

3.3.Method

3.3.1.C3A and Huh7.5 cell cultures and treatments

C3A cells were cultured in MEM with 10% FCS and split into 24 well plates, as described in section 2.1.1.2. Before treatment, cells were fasted overnight in MEM without any supplements. Huh7.5 cells are well differentiated hepatoma-derived cell line that was derived from a male donor. These cells were a gift from the liver laboratories (IBR 5th floor, Clinical and experimental medicine department, University of Birmingham) and all experiments on Huh7.5 cells were carried out with the help of Dr. Reina Lim Teegan. Cells were cultured in MEM with 10% FCS and split into 24 well plates, as described in section 2.1.2.2. Before treatment, cells were fasted overnight in MEM without any supplements.

Both C3As and Huh7.5s were treated with cortisol (dose range 100, 250, 1000nM) in order to accurately determine the response to GCs. In experiments investigating protein phosphorylation of the insulin signalling cascade, media was spiked with human insulin (dose range 1, 10, 20, 50 and 100nM) for the final 15 min of treatment (Figure 3-1).

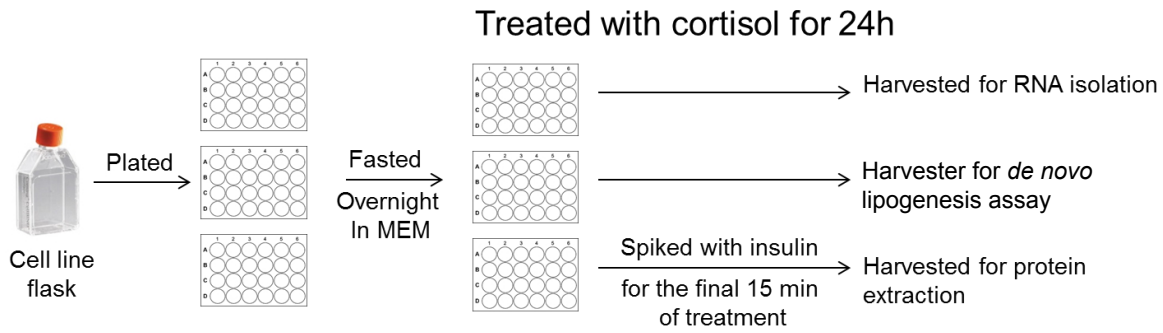

Figure 3-1 Cells were split into three 24 well plates, and fasted overnight before treatment. Cells were then treated with cortisol for 24h and finally harvested for RNA and protein extraction, and de novo lipogenesis assay.

3.3.2.Primary human hepatocytes cell culture and treatments

Primary human hepatocytes were purchased from BioreclamationIVT Technologies (Baltimore, Maryland, United States). Access to the donors' medical history was provided and the four most healthy donors (male n=4, age 54±14years, BMI 28.4±3 kg/m^2, data are expressed as mean ± s.e) were chosen. Diabetic patients or those who had taken GC therapy, or any other related medications were excluded as were those with viral infection and high alcohol consumption (Appendix). Cells were cultured in *InVitroGRO* CP medium (BioreclamationIVT Technologies, Baltimore, USA) and seeded into 12 and 24 collagen coated well plates, as described in section 2.2.2.

Before treatment, cells were fasted for 3 hours in Williams' Medium E (detailed nutrient contents of media can be found at http://www.sigmaaldrich.com/life-science/cell-culture/learning-center/media-formulations/williams.html) without any supplements. The glucose concentration is 2g/L in Williams' Medium E compared to 1g/L in MEM, and therefore, media were corrected for glucose concentration. To define the impact of insulin and GCs, cells were treated with cortisol (dose range 100, 250, 1000nM) in the presence or absence of insulin (5nM, 24h). In all experiments investigating protein phosphorylation of insulin signalling cascade, media was spiked with human insulin (50nM) for the final 15 min of the treatment (Figure 3-2).

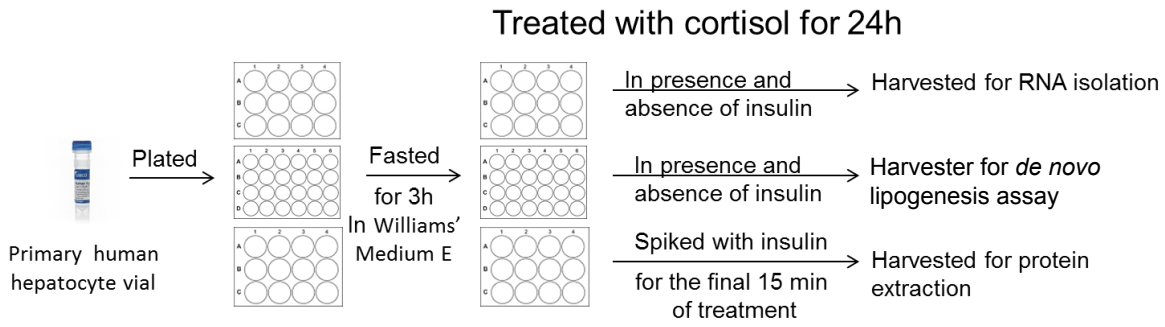

Figure 3-2 Primary hepatocytes were split into two 12 and one 24 well plates. Cells were fasted in William's E medium for 3h and then treated with cortisol in presence and absence of insulin for 24 hours. Finally, cells were harvested for RNA and protein extraction, and de novo lipogenesis assay.

3.3.3.RNA and Protein extraction

After 24 hours of treatment, RNA was extracted (as described in section 2.6.2), from both C3As and primary hepatocytes, using Tri-Reagent. Protein was extracted (as described in section 2.3.2) from C3As, Huh7.5s and primary hepatocytes applying RIPA buffer. The extracted RNA and proteins were then used for Real-Time PCR and Western Blotting.

3.3.4.Real-Time PCR

The mRNA expression levels of insulin signalling (IRS1/2, AKT1/2) and lipid metabolism (ACC1/2, CPT1, DGAT2, GPAT, FAS) genes were determined using ABI-7500 PCR machine (Perkin-Elmer Applied Biosystems, Warrington, UK) as described in section 2.8.2.

18s rRNA gene was used as a control in all reactions and all probes and primers were supplied by Applied Biosystem.

3.3.5.Western blotting

In order to define insulin stimulation, the media from the cells (both in cell lines and primary hepatocytes) were spiked with insulin (explained in section 3.3.1, 3.3.2 and 3.3.3) and proteins were extracted.

Western blot was performed on protein samples, as previously described in section 2.5.2. Anti PKB/AKT (anti total AKT) (Millipore, Hertfordshire, UK), anti phospho-AKT (Thr308) (Cell signalling technology, Danvers, MA, USA) and anti phospho-AKT (serine 473) (R&D Systems, Abingdon, UK) were used as primary antibodies. Polyclonal Goat Anti-Rabbit Immunoglobulins (Dako, Glostrop, Denmark) were used as the secondary antibody and both primary and secondary antibodies were diluted 1/1000. All membranes were re-probed for β-actin antibody (Abcam plc, Cambridge, UK) where the antibodies used at a dilution of 1/5000. Bands were quantified by ImageJ software and expressed relative to β-actin to normalise for gel loading.

3.3.6.Western blotting-separating ACC1/2 isoforms

ACC is the rate-limiting enzyme in lipogenesis, converting acetyl CoA to malonyl-CoA. Although two isoforms of ACC (ACC1 and ACC2) contribute to this conversion, the malonyl-CoA produced by them impacts upon different metabolic pathways. The malonyl-CoA generated by ACC1 is utilised for FFA synthesis whilst ACC2 is located on mitochondria surface and the malonyl-CoA formed by this isoform inhibits CPTI function inhibiting β-oxidation. Thus, separating these isoforms and studying them individually is informative (Ruderman et al. 1999).

These isoforms are encoded by different genes in man (Widmer et al. 1996) but share almost 75% homology in amino acid sequence, and as a result are technically difficult to separate by western blotting. Therefore, specific changes were made to general method of western blotting described in section 2.5.2. Nupage Novex 3-8% Tris-acetate gel and Nupage Tris-acetate SDS running buffer (Invitrogen, Paisley, UK), were used instead of 8-12% gradient SDS-PAGE gel running buffer (BioRad, Herts, UK). The blocking buffer was replaced with the Starting Block Blocking buffer (Pierce, Thermo Fisher Scientific, West Sussex, UK). Anti-phospho-AcCoA (Millipore, Watford, UK) and anti ACC (Avidin-HRP) (Sigma - Aldrich Chemical Company, Pool, Dorset, UK) were used as primary antibodies at the dilution of 1/1000. No secondary antibody was used for anti ACC (Avidin-HRP). Protein samples used for this western blot were isolated from primary human hepatocytes.

Two isoforms of ACC were separated on the gel in both phospho and total ACC. (Figure 3-3). However, this was not sufficient for quantification, and therefore as with many reports in the published literature (Liu et al. 2014;Maslak et al. 2015), both isoforms combined in total were quantified.

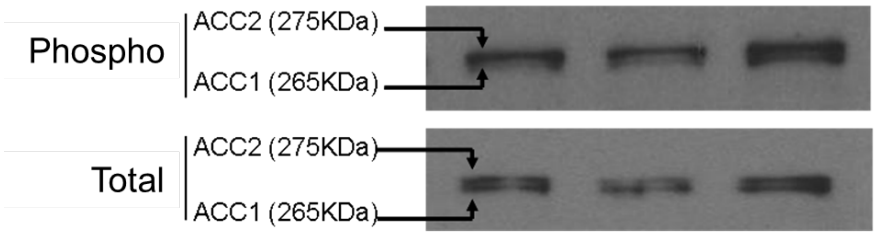

Figure 3-3 Separation of ACC1/2 isoforms in human hepatocytes using anti phospho and total ACC antibodies but this was not sufficient for quantification.

3.3.7.*De novo* lipogenesis assay

In order to investigate the effect of GCs and insulin on lipid accumulation within liver at the functional level, *de novo* lipogenesis was determined by measuring ^{14}C-acetate incorporation into cellular lipid (as described in 2.10.2). This assay was optimised in both C3As (50nM of insulin) (Figure 3-4) and primary cells (5nM of insulin) (Figure 3-5) to identify the optimal incubation time to achieve maximal insulin stimulated *de novo* lipogenesis. At baseline there were significant differences in *de novo* lipogenesis between preparations, in both the C3As and primary human hepatocyte models, however, the responses to treatment were consistent. Therefore, data are calculated as percentage change from untreated control.

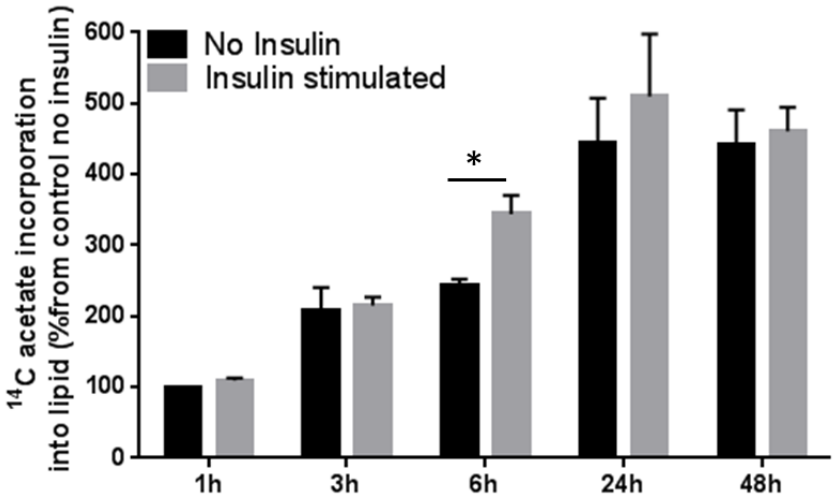

*Figure 3-4 Time dependent (1, 3, 6, 24, and 48h) preliminary de novo lipogenesis assays in C3A cells; it was identified that the optimal acetate incubation time to achieve the largest impact of insulin stimulation on de novo lipogenesis to be at the final 6h of the treatment. Insulin concentration=50nM, data are presented as ^{14}C-acetate incorporation into lipid (%from control without insulin, mean ± s.e) of n=4 experiments and one way ANOVA with Tukey's post-hoc analysis was applied using Sigmastat 3.1 to compare insulin stimulated treatments to no insulin treatments (*p<0.05 vs. no insulin).*

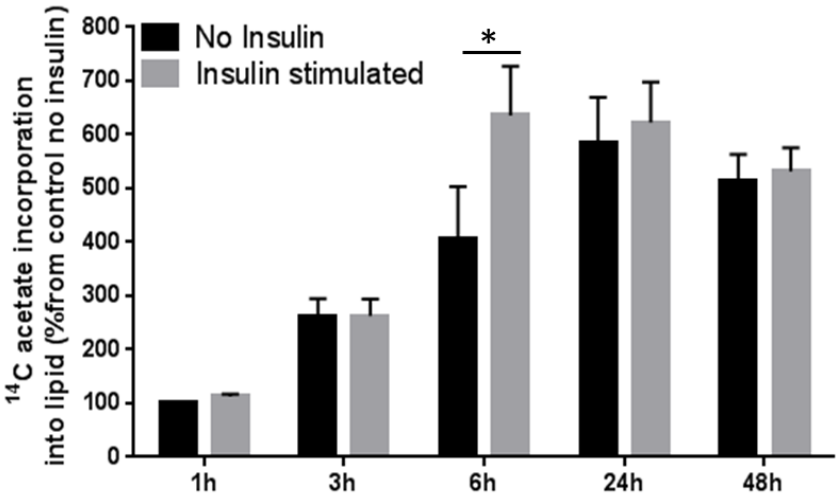

*Figure 3-5 Time dependent (1, 3, 6, 24 and 48h) preliminary de novo lipogenesis assays in primary hepatocytes; it was identified that the optimal acetate incubation time to achieve the largest impact of insulin stimulation on de novo lipogenesis to be at the final 6h of the treatment. Insulin concentration=5nM, data are presented as ^{14}C-acetate incorporation into lipid (% from control without insulin, mean ± s.e) of n=7 experiments and one way ANOVA with Tukey's post-hoc analysis was applied using Sigmastat 3.1 to compare insulin stimulated treatments to no insulin treatments (*p<0.05 vs. no insulin).*

In both C3As and primary cultures, insulin had its most marked effect at 6h. Therefore, we opted that for the final 6h of treatment with steroid hormones, 0.12μCi/L 1-[^{14}C]-acetic acid with cold sodium acetate to a final concentration of 10uM acetate would be added to each well to quantify the relative contribution of *de novo* lipogenesis to total lipid synthesis within the cells. The lipid content of the cells was recovered in chloroform: methanol (2:1 by vol/vol) (Folch et al. 1957) and radioactivity was measured by scintillation counting as described in section 2.10.2.

3.4.Results

3.4.1.GC regulation of insulin signalling in C3As and primary hepatocytes

3.4.1.1.Gene expression

IRS1 and AKT1/2 were all expressed in C3A cells but IRS2 was not expressed. Cortisol pre-treatment did not alter the expression of insulin signalling genes significantly (Table 3-1). Since these cells do not express IRS2, performing the same experiment on an alternative cell line or/and primary cultures of human hepatocytes was justified.

Gene	Control	Cortisol (250 nM)	P Value
AKT1	15.20 ± 0.60	15.14 ± 0.50	NS
AKT2	16.30 ± 0.35	16.14 ± 0.42	NS
IRS1	17.98 ± 1.09	17.60 ± 1.05	NS
IRS2	Not detected		

Table 3-1 mRNA expression of insulin signalling genes in C3As in response to cortisol (F, 250nM for 24h) treatment. Data are expressed as mean ΔCt values ± s.e of n=7 experiments and Student's t-tests were applied using Sigmastat 3.1 to compare cortisol treatment to control.

IRS1/2, INS, and AKT1/2 were all expressed in primary cultures. However, neither cortisol nor insulin pre-treatment altered the expression of insulin signalling genes significantly (Table 3-2). Although gene transcription was not altered by GCs, this does not represent the major regulatory step in insulin signalling, as most gene products are heavily post transcriptionally modified. Therefore, looking at protein expression and functional activity is warranted.

a)

Gene	Control	F100(nM)	F250(nM)	F1000(nM)	P Value
AKT1	15.67 ± 0.44	16.06 ± 0.57	15.29 ± 0.59	15.48 ± 0.54	NS
AKT2	16.40 ± 0.43	16.27± 0.54	15.24 ± 0.41	15.47± 0.35	NS
INS	15.34 ± 0.58	15.15 ± 0.65	14.98 ± 1.07	14.63 ± 0.56	NS
IRS1	16.45 ± 0.53	16.68 ± 0.74	15.73 ± 1.06	15.32 ± 0.24	NS
IRS2	14.90 ± 0.56	15.03 ± 0.58	14.62 ± 0.84	14.40 ± 0.44	NS

b)

Gene	Ins(5nM)	F100(nM)+Ins	F250(nM)+Ins	F1000(nM)+Ins	P Value
AKT1	15.47 ± 0.51	14.83 ± 0.42	14.65 ± 0.25	15.56 ± 0.21	NS
AKT2	15.32 ± 0.49	15.31± 0.41	14.63 ± 0.25	15.08± 0.37	NS
INS	15.31 ± 0.77	15.02 ± 0.41	14.34 ± 0.42	14.54 ± 0.45	NS
IRS1	16.53 ± 0.60	15.67 ± 0.18	15.01 ± 0.55	15.19 ± 0.52	NS
IRS2	14.92 ± 0.54	14.48 ± 0.19	13.93 ± 0.68	14.51 ± 0.50	NS

Table 3-2 mRNA expression of insulin signalling genes in primary hepatocytes in response to cortisol (F, dose range 100, 250, 1000nM for 24h) treatment alone (a) and co-incubation with insulin (5nM for 24h) (b). INS=Insulin, IRS=Insulin receptor, data are expressed as mean ΔCt values ± s.e of n=4 experiments and one way ANOVA with Dunnett's post-hoc analysis was applied using Sigmastat 3.1 to compare multiple cortisol treatments to control (a) and multiple cortisol with insulin treatments to insulin alone (b).

3.4.1.2.Protein expression

3.4.1.2.1.Insulin signalling

In order to determine whether the C3A cell line is a good model to study the insulin signalling cascade, activating T308 and S473 phosphorylation of AKT, and total AKT protein expression levels were measured in response to brief insulin stimulation (15min). We observed no significant changes in phosphorylation of AKT residues T308 and S473, consistent with a lack of insulin stimulation. Total AKT expression did not change (Figure 3-6). The lack of insulin response was also endorsed from our preliminary model optimisation studies examining ^{14}C-acetate incorporation into lipid (Figure 3-4).

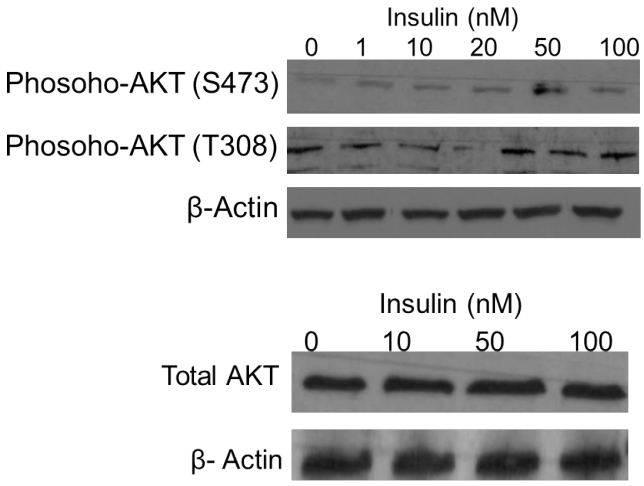

Figure 3-6 No insulin stimulation was detected in C3As using anti phospho-AKT T308 and S473. Total AKT protein expression remained unchanged. These are representative western blots of n=4 experiments and insulin dose range was 1, 10, 20, 50, and 100nM for 15min.

In order to identify a cell line that was more insulin responsive and therefore more representative of the *in vivo* situation, experiments were repeated in Huh7.5 cells. Insulin stimulated PKB/akt phosphorylation (S437) in Huh7.5 cells, in a dose-dependent manner without having any effect on total PKB/akt levels (Figure 3-7).

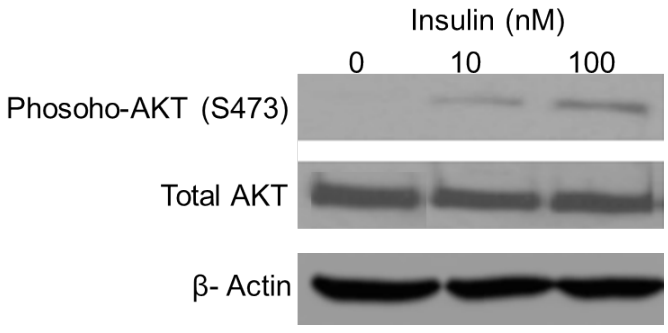

Figure 3-7 Insulin (dose range 10 and 100 nM for 15mins) pre-treatment increases insulin stimulated PKB/akt (S473) phosphorylation in a dose dependent manner in Huh 7.5 cells without changing total PKB/akt. These are representative western blots of n=4 experiments.

3.4.1.2.2. GCs and insulin signalling

To determine the interaction between GC and insulin signalling and to investigate whether cortisol may regulate of insulin sensitivity in human hepatocytes, PKB/akt phosphorylation was measured in Huh7.5 cells. Cortisol did not change insulin stimulated PKB/akt phosphorylation (S473) or total PKB/akt protein expression (Figure 3-8).

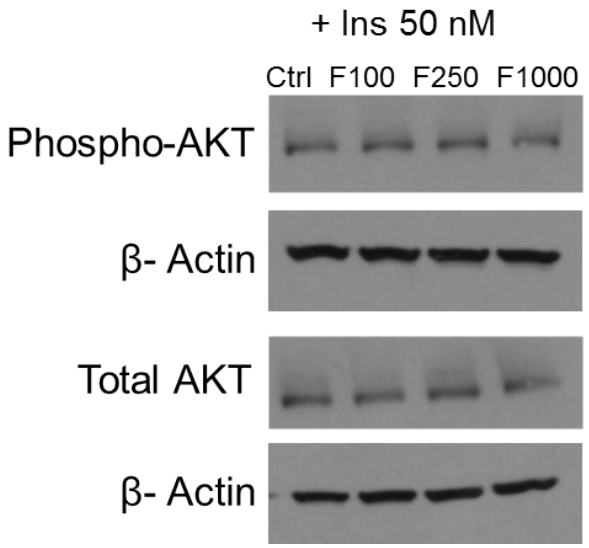

Figure 3-8 Cortisol does not affect insulin-stimulated PKB/akt (S473) phosphorylation or total PKB/akt protein expression in Huh 7.5 cells. These are representative western blots of n=3 experiments. Abbreviations: Ins, insulin (50nM for 15mins); F, cortisol (dose range 100, 250, 1000nM for 24h).

Although Huh7.5s were insulin sensitive, we observed no changes with cortisol pre-treatment and as an hepatoma cell line, they may not be representative of human hepatocyes. Therefore, the same experiment was performed in primary cultures of human hepatocytes.

PKB/akt phosphorylation was measured in human hepatocytes after cortisol pre-treatment with an insulin spike (50nM). In contrast to our observations in cell lines, cortisol increased insulin-stimulated PKB/akt phosphorylation (S473) in a dose-dependent manner as quantified

by ImageJ software and expressed relative to β-actin as an internal control. Total PKB/akt protein expression remained unchanged (Figure 3-9).

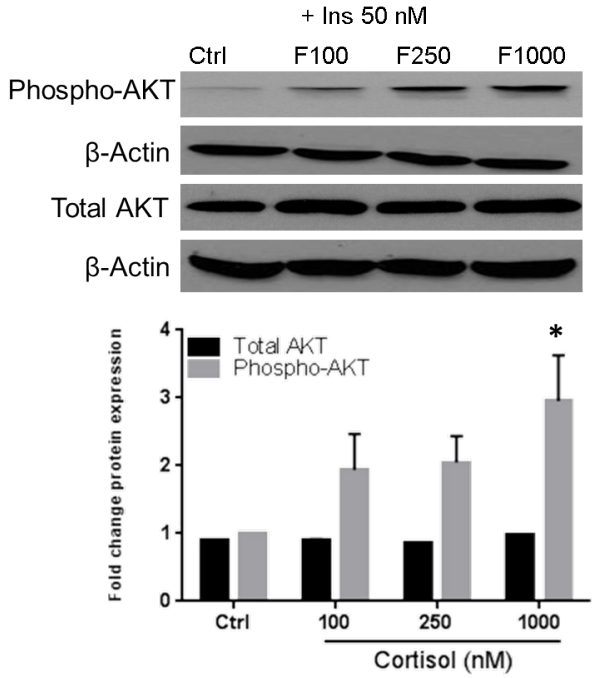

*Figure 3-9 Cortisol induces a dose-dependent increase in insulin stimulated PKB/akt phosphorylation without alternation in total PKB/akt in primary cultures. Data presented are the mean ± s.e of n=4 experiments with representative western blots inserted above. Bands are quantified relative to β-actin as internal loading control and one way ANOVA with Dunnett's post-hoc analysis was applied using Sigmastat3.1 to compare multiple cortisol treatments to control (*p<0.05 vs. control). Abbreviations: Ins, insulin (50nM for 15mins); F, cortisol (dose range 100, 250, 1000nM for 24h).*

3.4.2.GC regulation of lipid homeostasis in C3As and primary hepatocytes

3.4.2.1.Gene expression

ACC1/2, CPT1, DGAT2, GPAT, and FAS were all expressed in C3A cells (Table 3-3). Among the key genes involved in lipid metabolism, cortisol pre-treatment increased mRNA expression of ACC2 (0.005±0.003 (control) vs. 0.008±0.004 (cortisol), mean arbitrary unit

values ± s.e, p<0.05) and FAS (0.071±0.007 (control) vs. 0.110±0.019 (cortisol), mean arbitrary unit values ± s.e, p<0.05), Figure 3-10, but not ACC1, diacyly glycerol acyl transferase 2 (DGAT2) and glycerol phosphate acyl transferase (GPAT).

Gene	Control	Cortisol (250 nM)	P Value
ACC1	16.53 ± 0.63	16.22 ± 0.61	NS
ACC2	21.04 ± 1.78	20.58 ± 1.89	P<0.05
Cpt1A	17.34 ± 0.71	17.16 ± 0.60	NS
FAS	14.20 ± 0.53	13.89 ± 0.59	P<0.05
DGAT2	12.97 ± 0.52	12.88 ± 0.05	NS
GPAT	18.10±0.22	18.01±0.17	NS

Table 3-3 mRNA expression of lipid metabolism genes in C3As in response to cortisol (F, 250nM for 24h) treatment. Data are expressed as mean ΔCt values ± s.e of n=7 experiments and Student's t-tests were applied using Sigmastat 3.1 to compare cortisol treatment to control.

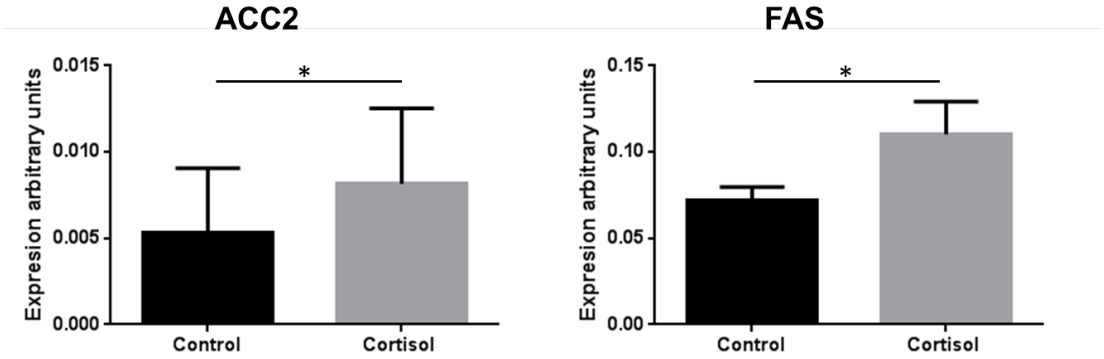

*Figure 3-10 Cortisol (250nM for 24h) increases mRNA expression of ACC2 and FAS in C3A cells. Data are the mean values from n=7 experiments and expressed as mean arbitrary unit values ± s.e. Student's t-tests were applied using Sigmastat 3.1 to compare cortisol treatment to control (*p<0.05 vs. control).*

ACC1/2, CPT1, DGAT2 and FAS were all expressed in primary cultures. However, neither cortisol nor insulin pre-treatment altered the expression of lipid metabolism genes significantly (Table 3-4).

a)

Gene	Control	F100(nM)	F250(nM)	F1000(nM)	P Value
ACC1	16.93 ± 0.48	17.43 ± 0.35	17.01 ± 0.81	16.68 ± 0.21	NS
ACC2	18.23 ± 0.78	18.02 ± 0.73	17.74 ± 0.83	17.57 ± 0.79	NS
Cpt1A	15.06 ± 0.31	15.22 ± 0.36	14.61 ± 0.64	14.77 ± 0.28	NS
FAS	15.99 ± 0.20	16.04 ± 0.33	15.69 ± 0.37	15.37± 0.40	NS
DGAT2	15.50 ± 0.61	15.71 ± 0.58	15.46 ± 0.43	16.27 ± 0.18	NS

b)

Gene	Ins(5nM)	F100(nM)+Ins	F250(nM)+Ins	F1000(nM)+Ins	P Value
ACC1	16.57 ± 0.45	16.05 ± 0.41	15.77 ± 0.29	16.07 ± 0.45	NS
ACC2	18.17 ± 0.90	17.58 ± 0.94	17.21 ± 0.94	17.44 ± 0.83	NS
Cpt1A	15.49 ± 0.44	14.50 ± 0.34	14.09 ± 0.21	14.69 ± 0.47	NS
FAS	15.57 ± 0.32	15.37 ± 0.35	14.97 ± 0.35	15.34± 0.39	NS
DGAT2	15.54 ± 0.62	15.25 ± 0.89	14.92 ± 0.50	15.28 ± 0.85	NS

Table 3-4 mRNA expression of lipid metabolism genes in primary cultures of human hepatocytes in response to cortisol (F, dose range 100, 250, 1000nM for 24h) treatment alone (a) and co-incubation with insulin (5nM, 24h) (b). Data are expressed as mean ΔCt values ± s.e of n=4 experiments and one way ANOVA with Dunnett's post-hoc analysis was applied using Sigmastat 3.1 to compare multiple cortisol treatments to control (a) and multiple cortisol with insulin treatments to insulin alone (b).

3.4.2.2.Protein expression

In order to investigate the mechanisms underpinning the impact of cortisol upon lipogenesis at the protein level, western blotting was performed using anti-phospho and total ACC antibodies. ACC1 and ACC2 activities are regulated by phosphorylation at inhibitory residues serine-79 and serine-218, respectively, mediated through and AMPK-dependent pathway (Morgan et al. 2013). Pre-treatment with cortisol did not result in changes in total ACC protein expression. In addition, cortisol did not regulate phosphorylation at ser-79/218

residue. However, insulin decreased ser-79/218 phosphorylation, which would predict increased functional lipogenic activity (Figure 3-11).

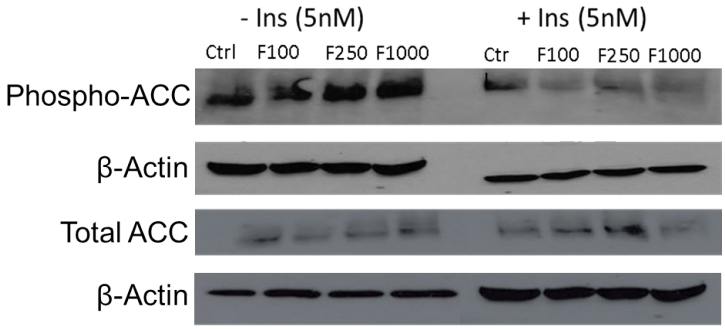

Figure 3-11 There is no convincing effect of cortisol (F, dose range 100, 250, 1000nM for 24h) but insulin (5nM for 15mins) decreased the inhibitory phosphorylation in primary cultures of human hepatocytes and this would be predicted to increase lipogenesis. No effect was observed with total ACC levels. These are representative western blots of n=4 experiments.

3.4.2.3.*De novo* lipogenesis in C3As, Huh7.5s and primary human hepatocyte cultures

Cortisol decreased lipogenesis in a dose dependent manner in C3A cells (85.6±6.6% [100nM], 73.5±7.9% [250nM], 55.04±5.6% [1000nM] vs. control (100%), $p<0.05$, mean ± s.e) (Figure 3-12).

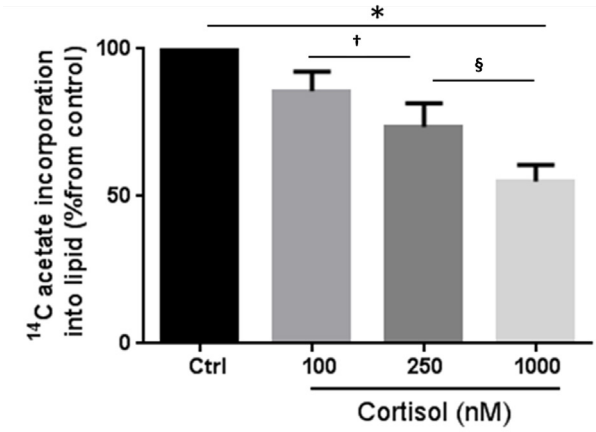

*Figure 3-12 Cortisol decreases de novo lipogenesis in a dose dependent manner in C3As. Data are presented as ^{14}C-acetate incorporation into lipid (% from control, mean ± s.e) of n=7 experiments. One way ANOVA test with Dunnett's post-hoc analysis was applied using Sigmastat 3.1 to compare multiple cortisol treatments to control (*p<0.05 vs. control), and ANOVA test with Tukey's post-hoc analysis was used to compare multiple cortisol treatment (†p<0.05 vs. cortisol 100nM and §p<0.05 vs. cortisol 250nM). Cortisol dose range= 100, 250, 1000nM for 24h*

To study the effect of insulin on lipogenesis and also to identify the optimal insulin concentration to achieve maximal insulin stimulated lipogenesis, C3As were treated with insulin (dose range 20, 40, 60, 80nM). No significant insulin stimulation lipogenesis was identified in C3As (Figure 3-13).

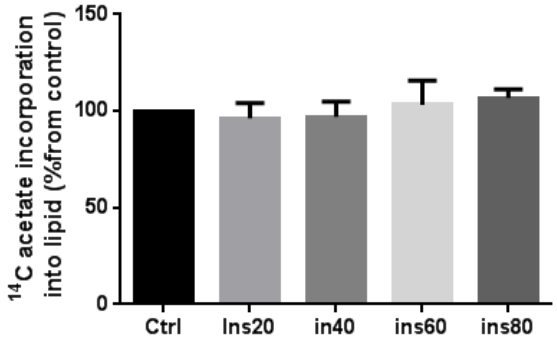

Figure 3-13 No significant insulin stimulation lipogenesis was observed in C3A cells. Data are presented as ^{14}C-acetate incorporation into lipid (% from control, mean ± s.e) of n=4 experiments and one way ANOVA with Dunnett's post-hoc analysis was applied using Sigmastat 3.1 to compare multiple insulin treatments to control. Insulin concentrations= 20, 40, 60 and 80nM for 24h.

In the absence of cortisol, and consistent with the data presented on the insulin signalling cascade protein expression, insulin (50nM) had no effect upon lipogenesis (114.9±12.4% vs. control (100%), p=NS). Interestingly, when C3A cells were pre-treated with cortisol (250nM, 24h), the stimulatory effect of insulin upon lipogenesis was augmented (mean % increase in lipogenesis following insulin, 14.9±12.4% (control) vs. 38.2±12.3% (cortisol), $p<0.05$, mean ± s.e) (Figure 3-14).

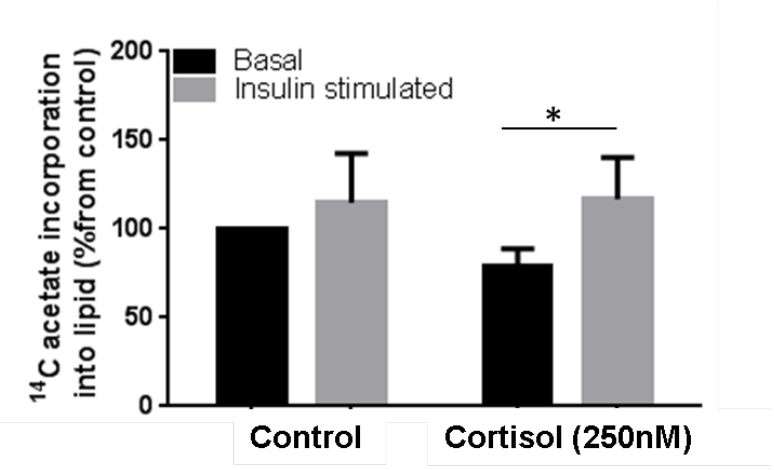

*Figure 3-14 In C3As insulin (50nM for 24h) alone increases lipogenesis modestly but not significantly. However, in presence of cortisol (250nM for24h) this reaches statistical significance. Data are presented as ^{14}C-acetate incorporation into lipid (% from control, mean ± s.e) of n=7 experiments and Student's t-tests were applied using Sigmastat 3.1 to compare cortisol treatment in presence of insulin to cortisol alone (*p<0.05 vs. cortisol).*

Based on gene and protein expression studies, Huh7.5 cells were more insulin sensitive compared to C3As and were used as an alternative cell line to explore the effect of GCs and insulin on liver lipogenesis. However, no significant changes were observed in lipogenesis after pre-treatment with cortisol (Figure 3-15).

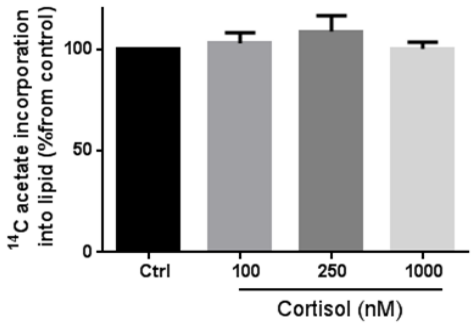

Figure 3-15 De novo lipogenesis remained unchanged after cortisol (dose range 100, 250, 1000nM for 24h) pre-treatment in Huh7.5 cells. Data are presented as ^{14}C-acetate incorporation into lipid (% from control, mean ± s.e) of n=4 experiments and one way ANOVA with Dunnett's post-hoc analysis was applied using Sigmastat 3.1 to compare multiple cortisol treatments to control.

3.4.2.4.*De novo* lipogenesis in primary cultures

Significant insulin stimulation of lipogenesis was observed in primary human heaptocye cultures compared to our observations in C3A cells (Figure 3-16).

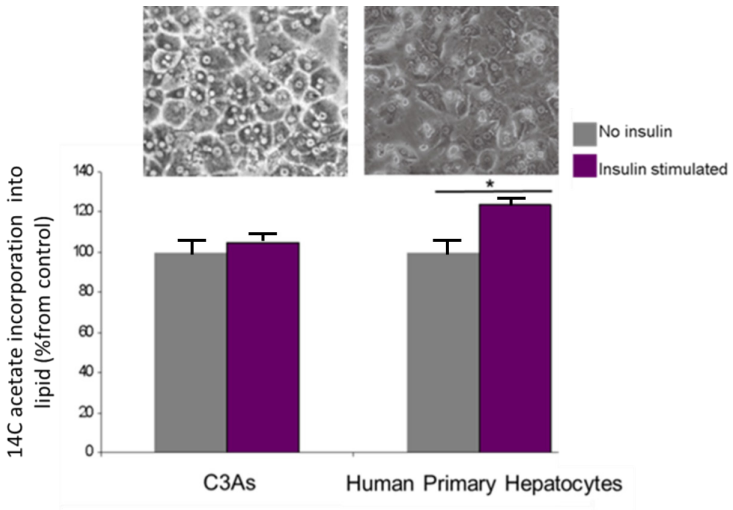

*Figure 3-16 Insulin (5nM, 24h) stimulates lipogenesis significantly in primary cultures compared to C3A cell line. Data are presented as percentage, however, the actual counts differ between primary and C3A cells. Therefore, the purpose of this graph is solely to compare the insulin sensitivity. Data are presented as ^{14}C-acetate incorporation into lipid (% from control, mean ± s.e) of n=4 experiments and Student's t-tests were applied using Sigmastat 3.1 to compare insulin treatment to control (*p<0.05 vs. control).*

Endorsing our findings in C3As, in the absence of insulin, cortisol caused a dose-dependent decrease in lipogenesis in human primary cultures (97.7% [100nM], 85.1% [250nM], 67.08% [1000nM] vs. control (100%), $p<0.05$, mean ± s.e). However, co-incubation with insulin (5nM) was able to reverse the effects of cortisol (130.3% [INS + 100nM cortisol] vs. 97.7% [100nM cortisol]; 139.9% [INS + 250nM cortisol] vs. 85.1% [250nM cortisol]; 152.37% [INS + 1000nM cortisol] vs. 67.08% [1000nM cortisol], $p<0.05$, mean ± s.e). This data from *de novo* lipogenesis assay was in consistent with our observation at ACC protein expression level as inactivating phosphorylation of ACC was decreased following incubation with insulin.

Interestingly, the ability of insulin to stimulate lipogenesis was augmented at the highest doses of cortisol and this stimulatory effect of insulin upon lipogenesis was augmented in a dose dependent manner (130.3% [INS + 100nM cortisol], 139.9% [INS + 250nM cortisol], 152.37% [INS + 1000nM cortisol] vs. Insulin (127.8%), $p<0.05$, mean ± s.e) (Figure 3-17).

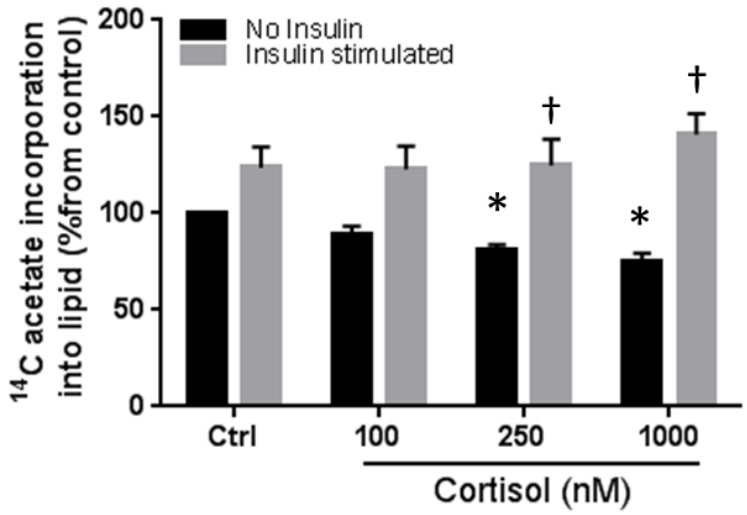

*Figure 3-17 Cortisol decreases de novo lipogenesis in a dose dependent manner in primary hepatocyte. However, co-incubation with insulin (5nM for24h) was able to reverse the cortisol effects. Data are presented as ^{14}C-acetate incorporation into lipid (% from control, mean ± s.e) of n=4 experiments.one way ANOVA with Dunnett's post-hoc analysis was applied using Sigmastat 3.1 to compare multiple cortisol treatments to control (*p<0.05vs. control), and ANOVA with Tukey's post-hoc analysis was used to compare cortisol in presence of insulin treatments to cortisol alone († p<0.05vs. cortisol). Cortisol dose range= 100, 250, 1000nM for 24h*

3.5.Discussion

The specific interaction between GCs and insulin in liver has not been fully examined and studies have mainly been performed in rodent cell lines (Saad et al. 1995;Wang et al. 1995). Few studies used human models and no studies have been performed on primary cultures of isolated human hepatocytes. In our study, experiments have been performed on a novel human cell line, C3A, and findings endorsed in primary cultures of human hepatocytes. C3A cells are a sub clone of the hepatoma-derived HepG2 cell line (Parvez, Purcell, & Emerson 2011) and express the GC receptor.

In rodent hepatocytes (Foa hepatoma cells), GCs alone increased IRS1 expression in liver. However, when cells were treated with GC in combination with insulin, the effect of insulin to decrease IRS1 levels dominated (Saad, Folli, & Kahn 1995). In the C3A cell line, we were unable to detect any significant insulin stimulation as measured by AKT phosphorylation sites (T308 and S473). Subsequently, no changes were observed in expression of insulin signalling pathway genes in GC pre-treated cells. In addition, we have now shown that C3A cells do not express IRS2, underpinning a lack of insulin response. Importantly, IRS2 (compared to IRS1) is thought to be more crucial in determining insulin resistance in mouse liver (Kido et al. 2000;Previs et al. 2000). Therefore, our observations in C3A cells could either be explained by species specificity (human vs. mouse) or simply by a lack of insulin response.

Huh 7.5s were used as an alternative, potentially more insulin sensitive cell line, but again no significant changes were observed after GC treatment. Therefore, we carried out definitive insulin signalling experiments in primary human hepatocytes. Although we were not able to detect any significant effects of GCs on insulin signalling at mRNA expression level, GC exposure increased insulin stimulated PKB/akt phosphorylation at S473 suggesting increased

insulin sensitivity. Whilst this *in vitro* observation may appear to conflict with widely held beliefs about GCs causing global insulin resistance, we and others have previously reported insulin sensitisation of human adipocytes by GCs (Gathercole et al. 2007; Tomlinson et al. 2010). However, the *in vivo* situation is more complex and clinical studies may point towards GCs causing hepatic insulin resistance (Hazlehurst et al. 2013). This highlights the importance of extrapolating with caution *in vitro* observations into the clinical setting.

GCs have been widely reported to drive lipogenesis and limit β-oxidation which may contribute to lipid accumulation (Amatruda et al. 1983;Mangiapane and Brindley 1986). Selective hepatic GR knockdown in mice reduces fat accumulation within the liver, decreasing fatty acid uptake and increasing ACC2 and CPT1 expression (Lemke et al. 2008). *In vitro* studies in cultured rat hepatocytes have also suggested that GCs promote VLDL secretion (Wang, McLeod, Yao, & Brindley 1995).

Our data have examined the effects of GC alone and in combination with insulin using primary and human cell lines. In the C3A cells, cortisol alone increased mRNA expression of ACC2 and FAS but not ACC1, diacyly glycerol acyl transferase 2 (DGAT2) and glycerol phosphate acyl transferase (GPAT). However, cortisol alone decreased *de novo* lipogenesis in a dose dependent manner in C3As probably reflecting rate-limiting, post-transcriptional regulation.

In primary human hepatocyte cultures, no significant changes in lipogenic gene expression were observed with GC pre-treatment. However, GCs in isolation were able to decrease lipogenesis consistent with our C3A cell data in agreement with adipose tissue (Gathercole et al.2011b). Our data therefore suggest that in the fasting state (in the absence of insulin) within

liver, the elevated GC to insulin ratio will result in a net inhibitory effect upon local lipogenesis.

In many situations, GC and insulin have opposing actions, but the specific interaction of GC and insulin signalling in hepatocytes remains controversial with conflicting data in the published literature (Caro and Amatruda 1982;Klein et al. 2002;Kosaki and Webster 1993;Olefsky et al. 1975). However, there is some evidence showing that GC may potentiate the action of insulin to promote lipogenesis within hepatocytes (Amatruda, Danahy, & Chang 1983). In addition, mice treated with corticosterone increased hepatic triglyceride which was confirmed by histology, quantitative TAG assay and serum free fatty acid levels (Morgan et al. 2014).

Interestingly, when C3A cells were treated with GC in combination with insulin, the effect of insulin to induce an increase in lipogenesis was augmented. This stimulatory effect of insulin upon lipogenesis was also enhanced in a dose dependent manner in an identical experiment in primary human hepatocytes in which it was paralleled by a decrease in ser-79/218 phosphorylation of ACC. This raises the possibility that in the physiological fed state, when insulin to GC ratio is elevated, insulin and GC act synergistically promoting lipid storage. Our data on GC impact on insulin action upon increasing hepatic lipogenesis is consistent with the published data (Berthiaume et al. 2007;Hazlehurst et al. 2013;Wang et al. 2004) on subcutaneous adipose tissue. Overall therefore, we propose, that this reflects the function of liver to mobilize lipid during fasting and to store lipid in the fed state (Figure 3-18).

Metabolic target tissue	Fasted High GC/Low insulin	Fed High GC/High insulin
	↓	↓
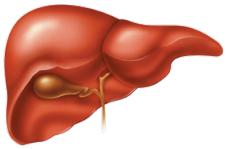	↓	↑
	↓	↑

Figure 3-18 GC decreases de novo lipogenesis in the absence of insulin (fasted state) in all three insulin target tissues. However in the presence of insulin (fed state) GC decreases lipogenesis in muscle with an increase in liver and adipose tissue.

In summary, my data have added to the concept of tissue specific response of metabolic target tissues to glucocorticoids and insulin. We determined that the concept of GCs to induce 'global' insulin resistance might reflect inhibition of insulin action in skeletal muscle, with insulin sensitivity in adipose tissue and potentially the liver. Accordingly, GCs decrease lipogenesis in muscle (Morgan et al. 2013) and increase it in adipose tissue (Gathercole et al. 2011a) and hepatocytes in the fed (high insulin) state (Hazlehurst et al. 2013). This may help explain the increased fat mass, obesity and hepatic steatosis observed in state of GC excess where GCs and insulin can act synergistically to drive lipid accumulation.

However, the *in vitro* data that we have generated in primary cultures and cell lines need to be tested in clinical studies. Such studies that have been performed within the group have begun to suggest that GCs may cause hepatic insulin resistance (alongside skeletal muscle insulin

resistance and adipose insulin sensitisation) (Hazlehurst et al. 2013) and this reflects the relative simplicity of cell culture models as opposed to complex *in vivo* physiology.

One of the challenges of this study was using the right model; C3As were not highly insulin sensitive and Huh7.5 did not respond to GC treatments. However, all the experiments were also carried out in primary cultures which are significantly insulin sensitive. Primary cultures are expensive, and therefore, we were not able to perform further functional assays such as β-oxidation to have a better understanding of GCs effects on hepatic lipid metabolism. The optimisation of western blotting on separation of ACC1 and 2 isoforms was not successful, and therefore, the western blotting was carried out using total ACC. Basal *de novo* lipogenesis were significantly lower in primary hepatocytes compared to C3As. This may represent differences in cell origin, C3As are an hepatocellular carcinoma cell line and cancer cells have higher rates of lipogenesis (Swinnen et al. 2006). Two different media were used for culturing the primary hepatocytes and C3A cells which may contribute to differences in baseline levels of lipogenesis. However, cells were fasted in serum free media and corrected for the glucose levels (initial glucose levels in MEM and Williams' E media are 1 and 2g/L, respectively- these media were glucose only without any fatty acids supplementation). These factors can impact on both basal lipogenesis and the response to stimuli, however the response to treatment was similar in each of the models.

Chapter 4 Impact of androgens on hepatic insulin sensitivity and lipid metabolism comparing male and female hepatocytes

4.1.Aims

- To optimise an *in vitro* model for metabolic assessments in human hepatocytes
- To define the impact of androgens upon insulin sensitivity in human hepatocytes and to compare effects in hepatocytes from male and female donors
- To study the impact of androgens on lipid metabolism in human hepatocytes and to compare effects in hepatocytes from male and female donors

4.2.Background

Low testosterone is reported to be associated with increased body fat, obesity, type 2 diabetes and insulin resistance (Wang et al. 2011). However, the effect of testosterone on hepatic liver metabolism has not been studied in detail. Vozke et al. (2010) reported that low testosterone was associated with hepatic steatosis. Moreover, hepatic AR knockout mice fed a high fat diet have improved insulin resistance and hepatic steatosis. However, testosterone levels were not measured in this study (Lin et al. 2008). Interestingly, DHT has been predicted to have an opposing action with increased hepatic Stearoyl-CoA desaturase1 (SCD1), a rate-limiting step in monounsaturated fatty acid synthesis (Moverare-Skrtic et al. 2006). Conversely, women with hyperandrogenic polycystic ovary syndrome (PCOS) are predisposed to developing NAFLD that appears to be independent of insulin resistance or obesity (Jones et al. 2012).

Moreover, testosterone can have different pathways of action; conversion to DHT or binding directly to AR, conversion to 17β-estradiol via the action of aromatase and subsequent activation of the ER, and through non-genomic mechanisms (discussed in detail in section 1.4.1.2).

Ultimately, the relationship between hepatic steatosis and testosterone concentrations remains controversial with conflicting data in the published literature. Therefore, the interaction between insulin and androgen in hepatic lipid metabolism needs further investigations.

4.3.Method

4.3.1.C3A cell culture and treatments

C3A cells were cultured in MEM with 10% FCS and split into 24 well plates, as described in section 2.1.1.2. Before treatment, cells were fasted overnight in serum free MEM without any supplements. C3As were treated with testosterone (dose range 5, 50nM) and DHT (10nM) in order to accurately determine the response to androgens.

4.3.2.Primary human hepatocytes cell culture and treatments

Primary human hepatocytes were purchased from BioreclamationIVT Technologies (Baltimore, Maryland, United States). Access to the donors' medical history was provided and the 8 most healthy donors (male: n=4, age 54±14years, BMI 28.4±3 kg/m^2; female: n=4, age 56±4.7years, BMI 23.98±3.1 kg/m^2, data are expressed as mean ± s.e) were chosen. Diabetic patients or those who had taken GC therapy, or any other related medications were excluded as were those with viral infection and high alcohol consumption (Appendix). Cells were cultured in *InVitroGRO* CP medium (BioreclamationIVT Technologies, Baltimore, USA) and seeded into 12 and 24 collagen coated well plates, as described in section 2.2.2.

Before treatment, cells were fasted for 3 hours in Williams' Medium E without any supplements. To define the impact of insulin and androgens, cells were treated with testosterone (dose range 5, 50nM) and DHT (10nM) in the presence or absence of insulin (5nM, 24h).

4.3.3.RNA extraction

After 24 hours of treatment, RNA was extracted as described in section 2.6.2, from both C3As and primary hepatocytes, using Tri-Reagent. The extracted RNA was then used for Real-Time PCR.

4.3.4.Real-Time PCR

The mRNA expression levels of insulin signalling (IRS1/2, AKT1/2) and lipid metabolism (ACC1/2, CPT1, DGAT2, GPAT, FAS) genes were determined using ABI-7500 PCR machine (Perkin-Elmer Applied Biosystems, Warrington, UK) as described in section 2.8.2.18s rRNA gene was used as a control in all reactions and all probes and primers were supplied by Applied Biosystem.

4.3.5.AR overexpression

In contrast to primary human hepatocytes, AR expression is very low in C3As, and therefore the coding sequence of AR was cloned into the pcDNA3.1 vector (Invitrogen, Paisley, UK) by Dr Silvia Parajes in our lab and transiently transfected into C3A cells with a help of a master's student, Nikolaos Nikolaou, as described in section 2.11.1. Cells were then treated with and without testosterone (50nM) and DHT (10nM) for the final 6h of transfection. The transfection efficiency was determined using a plasmid containing green fluorescence protein (GFP).

4.3.6.*De novo* lipogenesis assay

In order to investigate the effect of androgens and insulin on lipid accumulation within liver at a functional level, *de novo* lipogenesis was determined by measuring ^{14}C-acetate incorporation into cellular lipid. This assay was optimised in both C3As (50nM of insulin) and primary cells (5nM of insulin) to identify the optimal incubation time to achieve maximal insulin stimulated *de novo* lipogenesis. As described previously (chapter 3 section 3.3.6), in both C3As and primary cultures, insulin had its most marked effect at 6h. Based on this optimization, for the final 6h of treatment with steroid hormones, 0.12μCi/L 1-[^{14}C]-acetic acid with cold sodium acetate to a final concentration of 10uM acetate was added to each well to quantify the relative contribution of *de novo* lipogenesis to total lipid synthesis within the cells. The lipid content of the cells was recovered in chloroform: methanol (2:1 by vol/vol) (Folch et al. 1957) and radioactivity was measured by scintillation counting as described in section 2.10.2.

4.4.Results

4.4.1.Optimising the *in vitro* model by comparing the gene profiles

In order to choose the most appropriate model to study the effect of androgens upon lipid metabolism and insulin sensitivity in liver, gene expression profiles were compared between available liver cell lines and primary hepatocytes. Interestingly, only primary hepatocytes expressed the AR, and therefore, primary hepatocytes represent the best model (Table 4-1). However, C3As represent a good model for AR overexpression study as they do not express AR gene and also are a less expensive model compared to primary cultures. In addition, choosing C3As as the cell line model would give us the ability to compare the effect of GCs and androgens on hepatic lipogenesis as the main cell line used in our GC studies was C3As. Therefore, we started our experiments using C3As and then carried out the experiments in primary cultures.

Gene	Hepatocytes	HepG2	Huh	C3A
11β-HSD1	10.75	19.68	20.50	19.56
11β-HSD2	17.59	15.31	14.51	14.88
5αR1	14.51	14.19	13.26	13.81
5αR2	10.22	15.23	15.44	18.91
AR	11.34	No expression	No expression	No expression
GR	11.81	12.09	11.50	12.08

Table 4-1 Gene expression profiles were compared between Primary Hepatocytes, HepG2, Huh7.5 and C3A cell lines. Primary hepatocytes are the only model that expresses mRNA encoding AR. Data are expressed as ΔCt values.

4.4.2. Androgen regulation of insulin signalling in C3As

4.4.2.1.Gene expression

Testosterone pre-treatment did not alter the expression of insulin signalling genes and among steroid hormone metabolizing and signalling genes, only GR expression level was increased significantly (Table 4-2 and Figure 4-1).

Gene	Control	Testosterone (50 nM)	P Value
GR	16.46 ± 0.40	15.80 ± 0.47	P<0.05
5αR1	17.07 ± 0.79	16.90 ± 0.89	NS
5α33	14.14 ± 0.65	13.76 ± 0.90	NS
5βR	16.40 ± 0.43	15.97± 0.60	NS
H6PDH	15.09 ± 0.47	14.88 ± 0.61	NS
AKT1	15.20 ± 0.60	15.17 ± 0.53	NS
AKT2	16.30 ± 0.35	16.03 ± 0.53	NS
IRS1	17.98 ± 1.09	17.61 ± 0.95	NS

Table 4-2 mRNA expression of pre-receptor regulation and insulin signalling genes in C3As in response to testosterone (50nM, 24h) treatment. Data are expressed as mean ΔCt values ± s.e of n=5 experiments and Student's t-tests were applied using Sigmastat 3.1 to compare testosterone treatment to control.

.

*Figure 4-1 Testosterone (50nM, 24h) increases mRNA expression of GR in C3As. Data are the mean values from n=7 experiments and expressed as mean arbitrary unit values ± s.e). Student's t-test was applied using Sigmastat 3.1 to compare testosterone treatment to control (*p<0.05 vs. control).*

4.4.3.Androgen regulation of lipid homeostasis in C3As and primary hepatocytes

4.4.3.1.Gene expression in C3As

No significant changes were identified in lipid metabolism gene expression after testosterone (50nM) pre-treatment (Table 4-3).

Gene	Control	Testosterone (50 nM)	P Value
ACC1	16.53 ± 0.63	16.28 ± 0.64	NS
ACC2	21.04 ± 1.78	20.70 ± 1.82	NS
Cpt1A	17.34 ± 0.71	17.16 ± 0.65	NS
FAS	14.20 ± 0.53	14.15 ± 0.70	NS

Table 4-3 mRNA expression of lipid metabolism genes in C3As in response to testosterone (50nM, 24h) treatment. Data are expressed as mean ΔCt values ± s.e of n=5 experiments and Student's t-test were applied using Sigmastat 3.1 to compare testosterone treatment to control.

4.4.4.*De novo* lipogenesis assay in C3As

AR overexpression was confirmed by real-time PCR (30.04 ± 0.018AU AR vs. 0.02 ± 0.003AU control, $p<0.05$). Both testosterone and DHT treatment increased basal *de novo* lipogenesis (124.9 ± 6.2% [50nM testosterone], 128.1 ± 4.7% [10nM DHT] vs. 100% control of n=4, $p<0.05$ mean ± s.e). Even in the absence of testosterone or DHT, AR overexpression alone caused a significant increases in 1-[^{14}C]-acetate incorporation into lipid (202.7±10.8% AR vs. 100% control [vector only] of n=4, $p<0.05$, mean ± s.e). Treatment with either testosterone or DHT did not further enhance lipid accumulation (209.6 ±16.5%% [50nM testosterone], 224.6 ± 8.6% [10nM DHT] vs. 202.7±10.8% (control), mean ± s.e, $p<0.05$) (Figure 4-2).

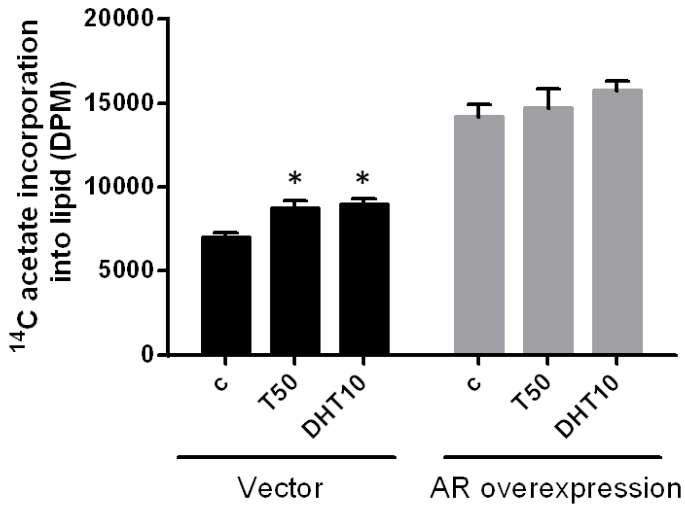

*Figure 4-2 Androgen receptor (AR) overexpression alone, and in the presence of T=testosterone (50nM, 24h) or DHT (10nM, 24h) increases de novo lipogenesis in C3As. However, neither T (50nM, 24h) nor DHT (10nM, 24h) further enhanced de novo lipogenesis on AR overexpressed C3A cells. Data are presented as ^{14}C-acetate incorporation into lipid (dpm, mean ± s.e) of n=4 experiment and one way ANOVA with Dunnett's post-hoc analysis was applied using Sigmastat 3.1 to compare testosterone and DHT treatments to control (*p<0.05 vs. control).*

4.4.5.*De novo* lipogenesis assay in primary hepatocytes

Insulin stimulation of lipogenesis was observed in primary cultures (153.92 ± 18.77 % [INS] vs. control (100%), 133.27 ± 4.4% [INS + 5nM testosterone] vs. 102.08 ± 12.32% [5nM testosterone], 181.31 ± 22.23% [INS + 10nM DHT] vs. 123.76 ± 13.72% [10nM DHT], (5nM insulin) of n=4, $p<0.05$, mean ± s.e). However, there were no significant changes in *de novo* lipogenesis following testosterone or DHT treatment in primary cultures from male donors (Figure 4-3).

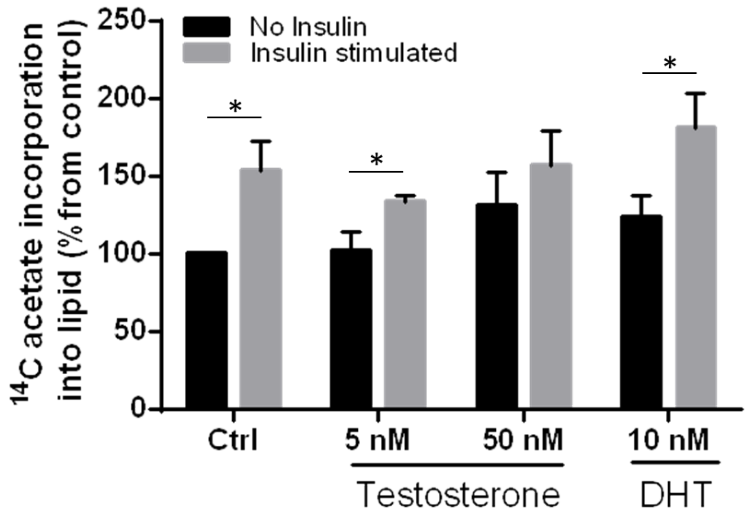

*Figure 4-3 In primary cultures of male donors, testosterone (5 and 50nM, 24h) nor DHT (10nM, 24h) have any effect on de novo lipogenesis. However, insulin sensitivity is confirmed again in primary hepatocytes. Insulin concentration=5nM, data are presented as ^{14}C-acetate incorporation into lipid (% from control, mean ± s.e) of n=4 experiment and one way ANOVA with Tukey's post-hoc analysis was applied using Sigmastat 3.1 to compare insulin stimulated treatments to no insulin treatments (*p<0.05 vs. no insulin).*

In contrast, in samples from female donors, testosterone increased lipogenesis (139.66 ± 17.63% [5nM testosterone] vs. 100% (control) of n=4, p<0.05, mean ± s.e) and this stimulatory effect of testosterone upon *de novo* lipogenesis was augmented in the presence of insulin (153.89 ± 18.74% [INS + 5nM testosterone] vs. 100% (control) of n=4, p<0.05, mean ± s.e). Interestingly, DHT decreased lipogenesis in hepatocytes from female donors only (100% (control) vs. 61.38 ± 10.42% [10nM DHT] of n=4, p<0.05, mean ± s.e) (Figure 4-4).

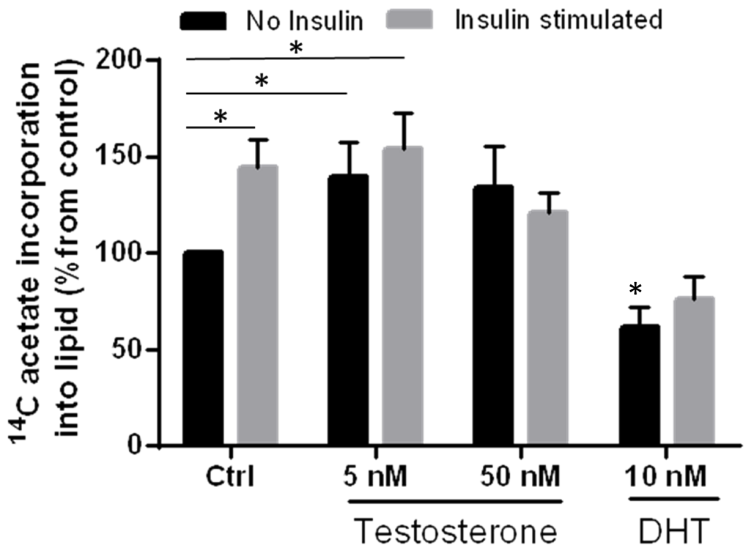

*Figure 4-4 In primary cultures of female donors, testosterone at 5nM (for 24h) increased de novo lipogenesis and this stimulatory effect was augmented in presence of insulin (5nM for 24h). However, DHT (10nM) decreased de novo lipogenesis compared to control. Data are presented as ^{14}C-acetate incorporation into lipid (% from control, mean ± s.e) of n=4 experiment and one way ANOVA with Dunnett's post-hoc analysis was applied using Sigmastat 3.1 to compare multiple treatments with control (*p<0.05 vs. control no insulin).*

4.5.Discussion

In this study, we have shown that androgens are able to increase lipid accumulation within C3A cells and in primary cultures of human hepatocytes from female, but not male donors. Cross-sectional clinical studies have shown that low testosterone concentrations are associated with increased hepatic steatosis in men (Kim et al. 2012;Volzke et al. 2010) and are consistent with findings in rodent models suggesting that DHT treatment can decrease hepatic lipid accumulation. In contrast, women with polycystic ovarian syndrome (PCOS), a condition characterised by androgen excess as well as insulin resistance, are at an increased risk of developing NAFLD although the precise contribution of each of these processes (insulin resistance and androgen excess) to the development of NALFD remains unclear (Jones et al. 2012;Markou et al. 2010).

Although *in vitro* cell models are not able to replicate all the processes that contribute to the development of NAFLD *in vivo*, in C3A cells, high doses of testosterone (50nM), and DHT increased *de novo* lipogenesis. However, lipogenic gene expression changes were not mirrored the *de novo* lipogenesis assay as no significant changes were observed after testosterone (50nM) pre-treatment suggesting that post-transcriptional modification of enzyme activity may be important.

Interestingly, in primary cultures, we observed sexually dimorphic effects. In cells derived from male donors, androgen treatment failed to have a significant impact upon lipogenesis, however in female samples, 5nM testosterone increased *de novo* lipogenesis. It is interesting to note that DHT did not alter lipogenesis in hepatocytes from male donors, but decreased lipogenesis in female hepatocytes. The mechanisms underpinning this observation and the physiological relevance (the concentrations of DHT used far exceed those seen in the female

circulation) are not clear. The discrepancy between the effects of androgens on C3A cells and in primary cultures may reflect origin of C3A cells from human hepatoma (and the well described impact of androgens upon their pathogenesis) (Kalra et al. 2008) and this serves to emphasize the important of endorsing *in vitro* observations in additional models including human primary cultures.

Differential tissue-specific effects are also well described. In prostate cells, androgens also increase *de novo* lipogenesis (Moon et al. 2011;Swinnen et al. 1997) whilst in adipose tissue, they inhibit pre-adipocyte differentiation and adipogenesis (Chazenbalk et al. 2013;Singh et al. 2006).

Enhancing androgen action through androgen receptor overexpression increased *de novo* lipogenesis providing further evidence as to the potent ability of this pathway to regulate lipid accumulation. Interestingly, we observed no additional effects of providing additional AR ligand, perhaps suggesting maximal stimulation with receptor overexpression alone. Furthermore, AR overexpression alone in the absence of ligand was able to increase lipogenesis. While, it is possible that this may reflect existing intracellular androgen availability, ligand-independent activation of the AR remains plausible. This has been identified as a potential mechanism that might be crucial in regulating cell growth in the context of malignancy (Chung et al. 2014) notably in prostate cancer (Kasina and Macoska 2012) although the precise mechanisms that underpin ligand-independent AR activation remain unclear.

Importantly, not all actions of androgens upon the liver may be mediated by classical AR signalling. AR-independent regulation of lipogenesis in the liver has been observed in

testicular feminized mice that lack a functional androgen receptor, with a reduction in lipogenesis following testosterone treatment (Kelly et al. 2014).

One of the limitations of the study was that no hepatic cell line expressed AR. However, C3As were transfected with AR and primary cultures were used as an alternative model. Primary cultures are expensive, and therefore, we were not able to perform further functional assays such as β-oxidation to have a better understanding of androgens effects on hepatic lipid metabolism. In addition, there are other sex hormones such as oestrogen which is involved in lipid metabolism and also the ratio between testosterone and this hormone might also play a role in lipid accumulation. Tamoxifen, which is a selective oestrogen receptor modulator and it is widely used in treatment of oestrogen- responsive breast cancer, induces the development of NAFLD as its frequent side effect (Murata et al. 2000). In a study using orchidectomised rats on high fat diet, they showed that estradiol and DHT can separately decrease lipid accumulation in zone 3 and 1 respectively. However, when these rats were treated with estradiol and DHT together, they observed an additive positive effect on normalising impaired fat accumulation in all three zones of their livers (Zhang et al. 2013). We only studied testosterone and DHT effect on lipid metabolism and did not study the effect of oestrogen which is a limitation of this study and might be one of the reasons for the observed sexually dimorphic responses from primary cultures on androgens and lipid metabolism in female donors compared to males

.

Chapter 5 Pre-receptor metabolism of GCs as a regulator of metabolic phenotype in human liver

5.1.Aims

- To determine the contribution of pre-receptor GC metabolism (through the activity of the A-ring reductases) to control GC availability in liver cell models
- To define the impact of manipulation of pre-receptor GC metabolism to alter metabolic phenotype (lipid homeostasis) in human liver cell models

5.2.Background

The effects of GCs within the body especially on the development of obesity and insulin resistance are well described. This is exemplified by patients with excessive circulating GC, Cushing's syndrome. The most common observations in these patients are central obesity, hypertension, insulin resistance and in some cases type-2-diabetes (T2D) (Van Staa et al. 2000). In patients with simple obesity and insulin resistance, circulating cortisol is not increased (Fraser et al. 1999). However, intracellular GC metabolism, especially in insulin target tissues (including liver, adipose tissue, and muscle) is an important regulatory step.

The 11β-HSD1 isoform predominates in liver and adipose tissue, and therefore amplifying local GC effects (Tomlinson et al. 2004). Non-selective inhibitors of 11β-HSD type 1 and 2 (carbenoxolone), increased insulin sensitivity in T2D and improved hepatic insulin sensitivity in human (Andrews et al. 2003;Walker et al. 1995). Moreover, selective inhibition of 11β-HSD1 decreased local GC and improved insulin sensitivity in muscle (Alberts et al. 2002;Alberts et al. 2003). As 11β-HSD1 has been considered as a therapeutic target, A-ring reductases might be as important with the opposite action of cortisol clearance.

We have shown that increased global 5αR activity is associated with impaired glucose tolerance and may be a future predictor of metabolic disease (Crowley et al. 2014;Tomlinson et al. 2008). The lack of SRD5A2 expression in the mouse liver (contrasting with human liver) has limited the interpretation of data from SRD5A2 knock out mice (Dowman et al. 2013) and has highlighted the importance of the use of human models. There are no *in vitro* data using human cells that have begun to explore the mechanisms that might be responsible for the observations seen in rodent models or in clinical studies. The translational importance of this not only relates to enhancing our understanding of the pathogenesis of NAFLD, but also to the widespread use of SRD5A2 inhibitors including the selective SRD5A2 inhibitor, finasteride, and the non-selective (SRD5A1 and 2) inhibitor, dutasteride.

5.3.Method

5.3.1.C3A cell culture and treatments

C3A cells were cultured in MEM with 10% FCS and split into 24 well plates, as described in section 2.1.1.2. Before treatment, cells were fasted overnight in MEM without any supplements. C3As were treated with testosterone (50nM) and cortisol (dose range 250, 500, 1000nM) in order to accurately determine the pre-receptor GC response.

5.3.2.Primary human hepatocytes cell culture and treatments

Primary human hepatocytes were purchased from BioreclamationIVT Technologies (Baltimore, Maryland, United States). Access to the donors' medical history was provided and the 4 most healthy donors (male: n=4, age 54±14years, BMI 28.4±3 kg/m2, data are expressed as mean ± s.e) were chosen. Diabetic patients or those who had taken GC therapy, or any other related medications were excluded as were those with viral infection and high alcohol consumption (Appendix). Cells were cultured in *InVitroGRO* CP medium (BioreclamationIVT Technologies, Baltimore, USA) and seeded into 12 and 24 collagen coated well plates, as described in section 2.2.2.

Before treatment, cells were fasted for 3 hours in Williams' Medium E without any supplements. To define the impact of 5αR inhibitors, cells were treated with cortisol (250nM), finasteride (500nM) and dutasteride (500nM) alone and in combination with 250nM of cortisol. 250 nM is a physiological concentration of cortisol and the higher does for cortisol was not used as the aim of this experiment was to test if finasteride and dutasteride can enhance the effect of cortisol. In addition, it is not entirely clear if finasteride and dutasteride

are competitive or uncompetitive inhibitors, therefore, 500nM which is twofold excess concentration of these inhibitors (compared to cortisol concentration of 250nM) was used.

5.3.3.RNA extraction

After 24 hours of treatment, RNA was extracted (as described in section 2.6.2), from both C3As and primary hepatocytes, using Tri-Reagent. The extracted RNA was then used for Real-Time PCR.

5.3.4.Real-Time PCR

The mRNA expression levels of pre-receptor regulation (GR, SRD5A1 and 3, H6PDH), insulin signalling (IRS1/2, AKT1/2) and lipid metabolism (ACC1/2, CPT1, DGAT2, GPAT, FAS) genes were determined using ABI-7500 PCR machine (Perkin-Elmer Applied Biosystems, Warrington, UK) as described in section 2.8.2.

18s rRNA gene was used as a control in all reactions and all probes and primers were supplied by Applied Biosystem.

5.3.5.SRD5A2 overexpression

In contrast to primary human hepatocytes, SRD5A2 expression is very low in C3As, and therefore the coding sequence of SRD5A2 was cloned into the pcDNA3.1 vector (Invitrogen, Paisley, UK) by Dr Laura Gathercole in our lab and transiently transfected into C3A cells as described in section 2.11.1. C3As were then treated with and without testosterone (50nM) and

cortisol (dose range 250, 500, 1000nM) for the final 24h of transfection. The transfection efficiency was determined using a plasmid containing green fluorescence protein (GFP).

5.3.6.Site directed mutagenesis (SDM)

The R246Q mutant was inserted by site directed mutagenesis into the SDR5A2 cDNA using the Quikchange II site-directed mutagenesis kit (Agilent Technologies UK Limited, Cheshire, UK) as per the manufactures guidance (described in section 2.12.2). Sequencing was then performed to confirm if the correct mutation had been made. The R246Q mutant was transiently transfected into C3A cells as described in section 2.11.1. C3As were then treated with and without testosterone (50nM) and cortisol (dose range 250, 500, 1000nM) for the final 24h of transfection. The transfection efficiency was determined using a plasmid containing green fluorescence protein (GFP).

5.3.7.Gas and Liquid chromatography/Mass spectrometry (GC/MS and LC/MS)

Cortisol was measured by gas chromatography mass spectrometry (GC-MS). The method was adapted from a historic in house method using for more than 20 years (Arlt et al. 2011). Cortisol was extracted from cell media after addition of the internal standard cortisol-d4 (which is labelled with deuterium residues that allows specific ion detection). Briefly, transfected cells were incubated with 200nM of cortisol for 24 hours. One mL of media was collected, extracted by solid-phase extraction (SPE) and the samples were derivatised overnight to form methyloxime trimethylsilylethers. The final derivative was dissolved in 55 µL cyclohexane, which was transferred to an autosampler vial for gas chromatography/mass

spectrometry (GC/MS) analysis. An Agilent 5973 instrument (www.agilent.com) was used in a selected ion monitoring mode. Cortisol was positively identified by comparison to an authentic reference standard that gave a double peak at approximately 25.7 min, monitored ion was cortisol 605 and cortisol-d4 609 was used as an internal control.

5αR activity was measured using liquid chromatography/mass spectrometry (LC/MS). Briefly, cells were incubated with 100nM T for 30 minutes. Media was removed and transferred into glass tubes. Five milliliters dichloromethane was added to each tube, vortexed for 30 seconds, and then centrifuged for 10 minutes at 1500 g. The aqueous phase was removed and the steroid-containing organic solvent phase evaporated in air to dryness. The steroid extract was analyzed using LC-MS/MS (Xevo TQ mass spectrometer combined with an acquity uPLC system) with an electro-spray ionisation source in positive ion mode. Steroid hormones were eluted from a BEH C_{18} 2.1 × 50 mm 1.7 μm column using a methanol/water gradient system, solvent A was water 0.1% formic acid, and B was methanol 0.1% formic acid. The flow rate was 0.6 mL/min and starting conditions were 45% B increasing linearly to 75% B over 5 minutes. Steroid hormones were positively identified by comparison of retention times and mass transitions to steroid standards. Retention time, mass transitions quantifier ion (qualifier ion) testosterone 2.8min, 289>97 (289>109), testosterone-d3 2.7min, 292>109 (292>97), DHT 3.0min, 291>255, (291>159), DHT-d3 3.0min 294>258, (294>159). Testosterone-d3 and DHT-d3 were used as internal standard.

All the samples for GC, LC/MS were prepared by a master's student, Nikolaos Nikolaou, and the data were analysed by Dr Angela Taylor.

5.3.8.*De novo* lipogenesis assay

In order to investigate the effect of pre-receptor GC metabolism, 5αRs, on lipid accumulation within liver at the functional level, *de novo* lipogenesis rates were determined by measuring ^{14}C-acetate incorporation into cellular lipid. This assay was optimised in both C3As (50nM of insulin) and primary cells (5nM of insulin) to identify the optimal incubation time to achieve maximal insulin stimulated *de novo* lipogenesis. As optimised previously (chapter 3 section 3.3.6), in both C3As and primary cultures, insulin had its most marked effect at 6h. Therefore, we opted that for the final 6h of treatment with steroid hormones, 0.12μCi/L 1-[^{14}C]-acetic acid with cold sodium acetate to a final concentration of 10uM acetate would be added to each well to quantify the relative contribution of *de novo* lipogenesis to total lipid synthesis within the cells. The lipid content of the cells was recovered in chloroform: methanol (2:1 by vol/vol) (Folch et al. 1957) and radioactivity was measured by scintillation counting as described in section 2.10.2.

.

5.4.Results

5.4.1.Pre-receptor enzyme expression in primary human hepatocytes and liver cell lines

5.4.1.1.mRNA expression

In order to choose the most appropriate model to study the effect of pre-receptor GC metabolism upon lipid metabolism and insulin sensitivity in liver, gene expression profiles were compared between available liver cell lines and primary hepatocytes. C3A cells and primary hepatocytes expressed the least and the most SRD5A2 respectively, and therefore, representing good *in vitro* models for this study (Table 5-1).

Gene	Hepatocytes	HepG2	Huh	C3A
11β-HSD1	10.75	19.68	20.50	19.56
11β-HSD2	17.59	15.31	14.51	14.88
5αR1	14.51	14.19	13.26	13.81
5αR2	10.22	15.23	15.44	18.91
AR	11.34	No expression	No expression	No expression
GR	11.81	12.09	11.50	12.08

Table 5-1 Gene expression profiles were compared between Hepatcytes, HepG2, Huh7.5 and C3A cell lines. SRD5A2 expressed the least and the most in C3As and primary hepatocytes respectively. Therefore, C3As and primary hepatocytes were used for overexpression and chemical inhibition of SRD5A2 respectively. Data are expressed as ΔCt values.

5.4.2. Regulation of pre-receptor modifying enzymes by GCs, androgens in C3A cells

5.4.2.1.mRNA expression

To determine the contribution of pre-receptor GC metabolism to GC and androgen metabolism in liver cell line, gene expressions were measured after GC and testosterone treatment. GC was without effect (Table 5-2) and testosterone pre-treatment only increased GR expression level significantly (Table 5-2 and Figure 5-1).

a)

Gene	Control	Cortisol (250 nM)	P Value
GR	16.46 ± 0.40	16.03 ± 0.26	NS
5αR1	17.07 ± 0.79	16.88 ± 0.84	NS
5αR3	14.14 ± 0.65	13.95 ± 0.64	NS
5βR	16.40 ± 0.43	16.27± 0.54	NS
H6PDH	15.09 ± 0.47	14.88 ± 0.51	NS

b)

Gene	Control	Testosterone (50 nM)	P Value
GR	16.46 ± 0.40	15.80 ± 0.47	P<0.05
5αR1	17.07 ± 0.79	16.90 ± 0.89	NS
5αR3	14.14 ± 0.65	13.76 ± 0.90	NS
5βR	16.40 ± 0.43	15.97± 0.60	NS
H6PDH	15.09 ± 0.47	14.88 ± 0.61	NS

Table 5-2 mRNA expression of pre-receptor regulation genes in C3As in response to cortisol (250nM, 24h) (a) and testosterone (50nM, 24h) treatment (b). Only testosterone (50nM, 24h) increases mRNA expression of GR. Data are expressed as mean ΔCt values ± s.e of n=5 experiments and Student's t-tests were applied using Sigmastat 3.1 to compare cortisol and testosterone treatments to their controls.

*Figure 5-1 Testosterone (50nM, 24h) increases mRNA expression of GR in C3As. Data are the mean values from n=7 experiments and expressed as mean arbitrary unit values ± s.e. Student's t-test was applied using Sigmastat 3.1 to compare testosterone treatment to control (*p<0.05 vs. control).*

5.4.3.Modulation of SRD5A2 expression and activity

5.4.3.1.Transfection

An acceptable (approximately 70%) transfection efficiency of SRD5A2 in C3As was observed by using a plasmid containing green fluorescence protein (GFP) (Figure 5-2).

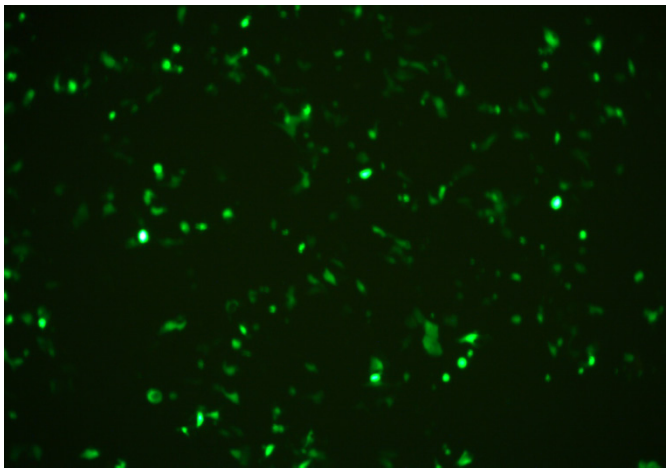

Figure 5-2 70% SRD5A2 transfection efficiency in C3As was observed using a plasmid containing green fluorescence protein (GFP).

5.4.3.1.1.mRNA expression

More than 1000-fold increase was observed in the mRNA expression level of SRD5A2 in C3A transfected cells compared to control (vector only) cells (SRD5A2:1000-Fold 3.8 ± 0.2 [Transfected] vs. 13.8 ± 0.3 [vector only], mean ΔCt values ± s.e) (Figure 5-3).

a)

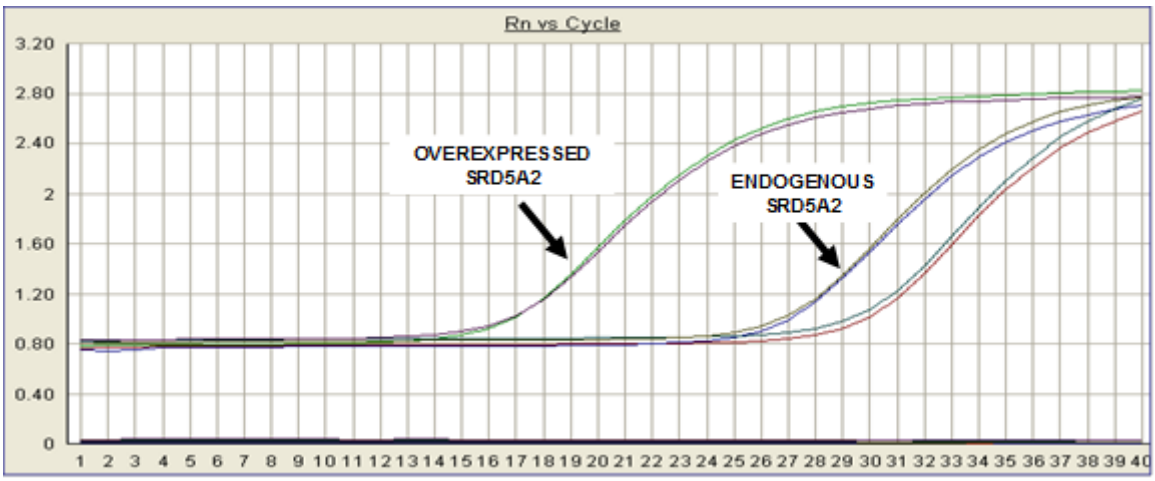

b)

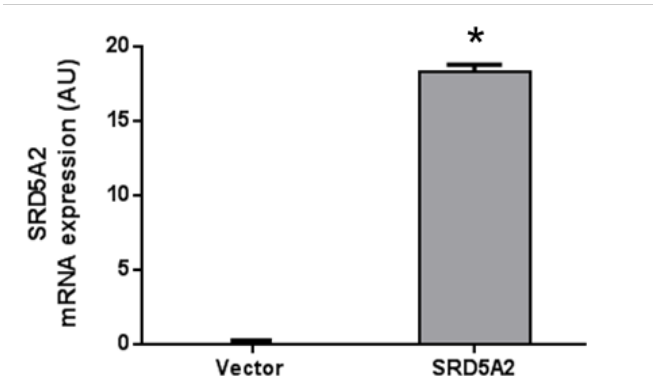

*Figure 5-3 5αR2 overexpression was confirmed by Real-time PCR (a). Increased 5αR2 expression was observed following transfection into C3A cells compared to vector. There is a very low endogenous level of 5αR2 expression in vector only cells but it is not absent, and therefore, it is not a true negative control (b). Data presented are mean ± s.e of n=3 experiments and Student's t-test was applied using Sigmastat 3.1 to compare 5αR2 overexpression to vector (*p<0.05 vs. vector).*

5.4.3.1.2.Enzymatic activity

Functional activity was confirmed through increased DHT generation following incubation with testosterone (DHT: 7.5±0.2 [vector] vs. 126.4±14.7nM [SRD5A2], initial testosterone concentration=100nM, mean ± s.e, $p<0.05$) (Figure 5-4) and clearance of cortisol (77nM [SRD5A2] vs. 130nM [vector], initial cortisol concentration=200nM, $p<0.05$, mean ± s.e) (Figure 5-5) as measured by LC/MS and GC/MS respectively. The mutant SRD5A2 construct, R246Q, was without activity. Conversion of testosterone to DHT was similar to that observed in the vector only transfection control (DHT: 7.5±0.2 [vector] vs. 9.2±0.8 nM [SRD5A2- R246Q], $p<0.05$, mean ± s.e) (Figure 5-4).

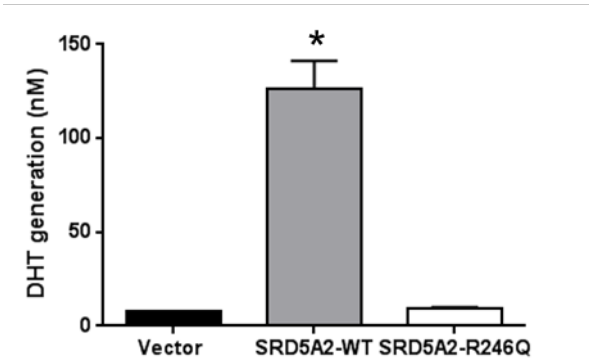

*Figure 5-4 Transfection of wild-type 5αR2 (in contrast to the mutant R246Q construct) in C3As is associated with increased dihydrotestosterone [DHT] generation from testosterone (100nM). Data presented are mean ± s.e of n=3 experiments and pcDNA3.1is the vector. One way ANOVA with Dunnett's post-hoc analysis was applied using Sigmastat 3.1 to compare the wild-type 5αR2 and the mutant R246Q construct to vector (*p<0.05 vs. vector).*

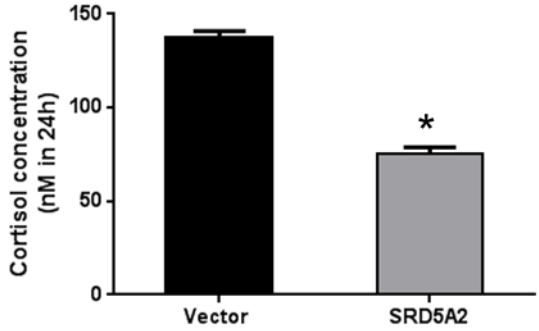

*Figure 5-5 Transfection of wild-type 5αR2 (in contrast to the mutant R246Q construct) in C3As is associated with increased cortisol (200nM) clearance. Data presented are mean ± s.e of n=3 experiments and pcDNA3.1is the vector. Student's t-test was applied using Sigmastat 3.1 to compare the cortisol clearance between 5αR2 overexpression and vector (*p<0.05 vs. vector).*

5.4.3.1.3.Functional impact of modulation of pre-receptor GC metabolism upon *de novo* lipogenesis in human hepatocytes

5.4.3.1.3.1.Genetic manipulation in C3A cells

As observed previously, cortisol decreased *de novo* lipogenesis in a dose dependent manner in C3A cells transfected with the vector construct alone. In the absence of cortisol, SRD5A2 overexpression had no effect. However, in the presence of cortisol, SRD5A2 restored lipogenesis to levels observed in untreated controls (82.5% [100nM cortisol] vs. 103.3% [SRD5A2+100nM cortisol], 71.01% [250nM cortisol] vs. 109.4% [SRD5A2+250nM cortisol], 61.9% [1000nM cortisol] vs. 103.8% [SRD5A2+1000nM cortisol], $p<0.05$, mean ± s.e), control=100%) (Figure 5-6).

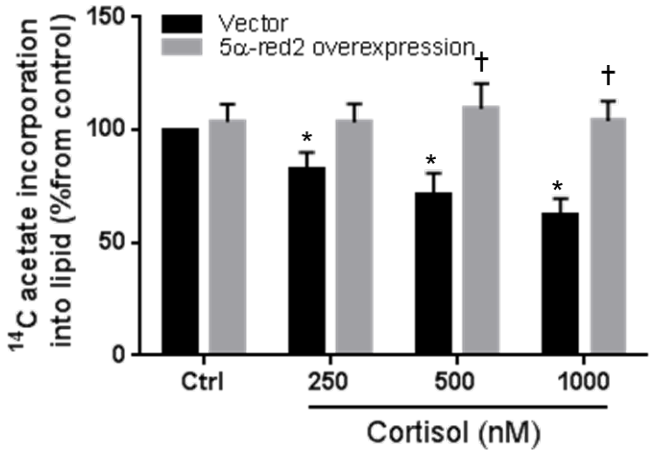

*Figure 5-6 In C3A cells, the decrease in lipogenesis associated with increasing doses of cortisol was abolished in cells transfected with wild-type 5αR2. Data are presented as ^{14}C-acetate incorporation into lipid (% from control, mean ± s.e) of n=5 experiment. One way ANOVA with Dunnett's post-hoc analysiswas applied using Sigmastat 3.1 to compare multiple cortisol treatments to control (*p<0.05 vs. control), and ANOVA with Tukey's post-hoc analysis was used to compare cortisol in presence of insulin treatments to cortisol alone († p<0.05 vs. cortisol). Cortisol dose range= 100, 250, 1000nM for 24h*

Complementary experiments using the R246Q SRD5A2 construct that is devoid of functional activity did not alter cortisol mediated suppression of *de novo* lipogenesis (Figure 5-7)

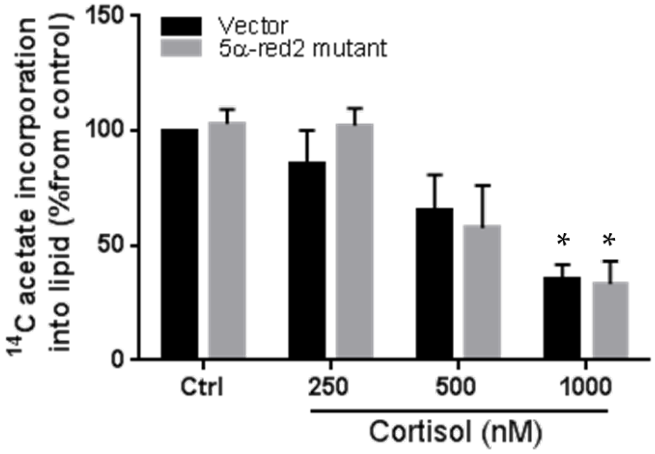

*Figure 5-7 Transfection of mutant R246Q 5αR2 did not affect the ability of cortisol to supress lipogenesis. Data are presented as ^{14}C-acetate incorporation into lipid (% from control, mean ± s.e) of n=3 experiment and one way ANOVA with Dunnett's post-hoc analysis was applied using Sigmastat 3.1 to compare multiple treatments with control (*p<0.05 vs. control). Cortisol dose range= 100, 250, 1000nM for 24h*

5.4.3.2.Pharmacological manipulation of 5αR activity in primary human hepatocytes

5.4.3.2.1.*De novo* lipogenesis assay

To further endorse these findings, experiments were undertaken using pharmacological inhibitors of 5αR isoforms in primary cultures of human hepatocytes. Primary cultures of hepatocytes are a better model to use for inhibitors study as they express high levels of both 5αR1 and 2, and therefore can potentially help to identify which isoform is most important. On their own the inhibitors, finasteride or dutasteride, were without effect. However, consistent with our transfection studies, both finasteride (selective SRD5A2 inhibitor) and dutasteride (nonselective SRD5A1 and 2 inhibitor) augmented the action of cortisol to suppress *de novo* lipogenesis (88.3±5.3% [cortisol 250nM] vs. 76.9±5.2% [cortisol 250nM+finasteride 500nM], $p<0.05$ and 66.3±5.9% [cortisol 250nM+dutasteride 500nM], $p<0.01$, mean ± s.e) (Figure 5-8).

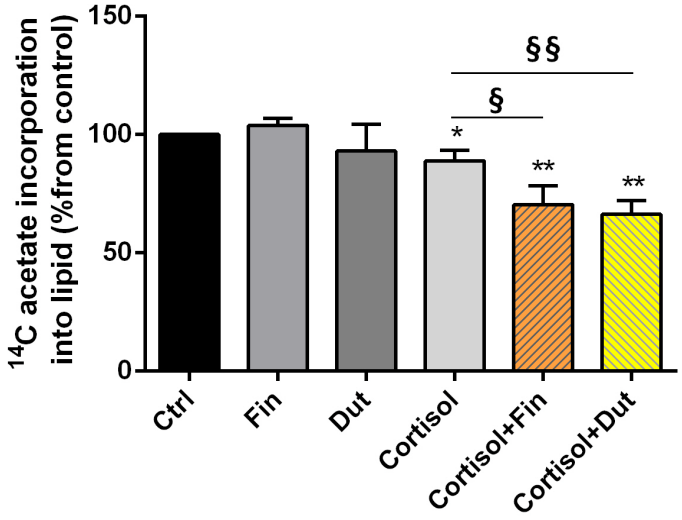

Figure 5-8 In primary cultures of human hepatocytes, pharmacological inhibition of 5αRs with either the selective (finasteride, 500nM) or nonselective inhibitor (dutasteride, 500nM), augments the action of cortisol (250nM) to suppress lipogenesis. Data are presented as ^{14}C-acetate incorporation into lipid (% from control, mean ± s.e*) of n=4 experiment and one way ANOVA with Dunnett's post-hoc analysis was applied using Sigmastat 3.1 to compare multiple treatments to control (*p<0.05, **p<0.01 vs. control) and ANOVA with Tukey's post-hoc analysis was used to compare multiple treatments to cortisol(§ P<0 .05, §§ P<0 .01 vs. cortisol).*

5.5.Discussion

A-ring reductases have a dual action, inactivating cortisol to dihydrocortisol with a subsequent conversion to tetrahydrocortisol, and activating testosterone to DHT. However, the ability of testosterone to regulate lipid metabolism does not appear to be dependent upon the presence of SRD5A2. The C3A cell line expresses SRD5A2 at a low level, and yet both testosterone and DHT were able to stimulate lipogenesis to a similar extent as discussed in chapter 4 (section 4.4.4). Our experiments therefore focused on the role of SRD5A2 to regulate the effects of GCs upon liver metabolism.

We have successfully overexpressed SRD5A2 in C3As. In control cells (vector only) cortisol decreased lipogenesis in a dose dependent manner as we have previously described in chapter 3 (section3.4.2.3). 5αR2 transfected cells were able to overcome and recover the inhibitory action of cortisol upon lipogenesis. Thus, selective (finasteride) and non-selective (dutasteride) inhibition of hepatic 5αR2 decreased lipogenesis in human liver. This was in contrast with the published data using animal models which suggest 5αRs (mainly focused on 5αR1) activity increase susceptibility to development of fatty liver (Livingstone et al. 2009). However, 5αR2 activity has not been studied in human cell line in the published literature.

While genetic ablation of SRD5A1 in rodent models increases lipid accumulation and fibrosis, the precise mechanisms that underpin this are not clear (Dowman et al. 2013;Livingstone et al. 2015). In a recently published clinical study, nonselective 5αRinhibition with dutasteride was associated with peripheral insulin resistance and it has been suggested that this may reflect a specific role for SRD5A1 in skeletal muscle (Upreti et al. 2014). The precise impact upon liver fat accumulation could not be determined as pre and post intervention assessment of hepatic lipid content was not performed.

In the presence of insulin, cortisol and insulin act synergistically to increase lipid accumulation in primary human hepatocytes (as described in chapter 3 section 3.4.2.4). 5αR inhibitors decrease cortisol clearance and therefore enhance cortisol action to act synergistically with insulin (probably in the fed, postprandial state) to drive lipid accumulation. We have clinical evidence to suggest that this might be the case as healthy male volunteers increased liver fat associated with elevated rates of *de novo* lipogenesis after dutasteride treatment (Hazlehurst et al. 2016) and this also seems to be endorsed from findings in the rodent 5αR1 knockout mice who develop increased hepatic lipid accumulation (Dowman et.al 2013).

As obesity, diabetes and the metabolic syndrome are rising within population in western countries, NAFLD becomes an increasingly important cause of morbidity and mortality. Current treatments principally reduce cardiovascular risks and improve metabolic variables. The most effective treatment, for those with NAFLD who have advanced liver fibrosis, is weight-reducing surgery. However, there is not yet a highly effective therapy for these patients and few liver-specific therapies are available (Dowman et al. 2011). Hence, modulation of hepatic 11bHSD1 and the A-ring reductases may represent a novel therapy for patients with NAFLD (Dowman et al. 2010).

Although it is been reported that increased hepatic 5αR activity has been demonstrated in patients with IR and NAFLD (Konopelska et al. 2009), the actual role of each isoform and their contribution to the regulation of hepatic lipogenesis is not clear. However, we have demonstrated a novel role for 5αR2 in human hepatocytes which if overexpressed can be used as an attractive therapeutic target for patients with IR and NAFLD. This has also important

implications to the large numbers of patients with prostate-related disease prescribed 5αR inhibitors.

We have shown that 5αR inhibitors decrease cortisol clearance and we have hypothesised that they might enhance cortisol action, and therefore, enhanced cortisol availability could then act synergistically with insulin to drive lipid accumulation. However, one of the limitations of this study is that we have not tested this hypothesis due to the lack of time. Therefore, experiments including co-incubation of cells treated with 5αR inhibitors with both cortisol and insulin should be planned in future studies. In addition, there is no specific 5αR1 inhibitor available, and therefore, it has not been used in this study.

Chapter 6 Molecular characterisation of patients with abnormal A-ring reductase activity

6.1.Aims

- To define putative mutations or polymorphisms through genetic sequencing of SRD5A1 and 2 in patients with abnormal steroid metabolite ratios suggestive of reduced 5αR activity.

6.2.Background

5α1, 2, and 3 enzymes are encoded by SRD5A1, 2, and 3 genes. Each gene has 5 exons. More than 40 mutations have been reported in all five exons of SRD5A2 (Cheon 2011). However, mutations in 5αR1 have not been described yet. Recently mutations have been identified in SRD5A3 resulting in a new type of congenital disorder of glycosylation (CDG) (Cantagrel et al. 2010). SRD5A3 probably does not have a major role in androgens or GC metabolism. Only recently, SRD5A3 was discovered to metabolise testosterone to DHT (Uemura et al. 2008), however no similar catalytic activities have been found for GCs (Nixon, Upreti, & Andrew 2012).

5αR2 converts testosterone into DHT in the external genitalia. Absent or reduced function of this enzyme causes 46XY DSD (disorder of sexual development). Most affected 46XY individuals with this condition as a result of mutations in 5αR2, have ambiguous external genitalia with a clitoral-like phallus and some have micropenis. They are usually raised as females although they are genetically males (Chan et al. 2009). The main biochemical feature of this syndrome is an elevated testosterone to DHT ratio with elevated plasma testosterone levels with low DHT levels (Zhu and Sun 2005). The DHT/T ratio therefore is an indicator of 5αR activity and interestingly this demonstrates significant heritability and in male twin studies this has been estimated to be around 42% (Meikle et al. 1986). Patients with 5αR2

mutations also have defects in cortisol metabolism consistent with the role of 5αR2 to inactive and clear cortisol. Urinary steroid profile in these patients has shown decreased 5αTHF (Can et al. 1998).

We have identified 9 individuals (referred to them as patient in this report) with abnormal A-ring reductase activity based on urinary GC/MS analysis. Urinary steroid metabolite ratios indicative of 5αR activity were >2 standard deviations lower than the mean from our normative cohort of > 50 individuals. All patients are on no medication that could explain the abnormality and we therefore hypothesised that genetic defects in either SRD5A1 or 2 might underpin these observations. Importantly whilst mutations in 5αR2 are well described, to date, no mutations have been identified in 5αR1 and therefore we questioned whether the urinary steroid metabolite phenotype in these patients might represent the first description of genetic defect in 5αR1.

6.3.Method

6.3.1.GC/MS

Briefly, steroids and their conjugates were extracted from urine samples via solid phase extraction. Samples were deconjugated and then derivatised to form methyloxime-trimethylsilylethers (MOTMS). The final derivative was dissolved in 55ul cyclohexane and analysed by GC/MS as described in detail by (Arlt et al. 2011) and also explained in section 5.3.7. All the samples for GC/MS were prepared by a master's student, Nikolaos Nikolaou, and the data were analysed by Dr Angela Taylor.

6.3.2.DNA extraction from patients' blood samples

After taking the blood from patients with abnormal A-ring reductase activity in clinic, DNA was extracted from all blood samples using the DNA blood maxi kit (50) (Qiagen, Dusseldorf, Germany).

6.3.3.Designing primers for A-ring reductases

The total number of 20 reverse and forward primers for all 10 exons of these 2 genes (SRD5A1 and 2) were designed using NCBI and Primer3 online websites (Figure 6-1). Oligo calc software was also applied to check the melting temperature, potential hairpin formation and self-complementarity of each primer. These primers were synthesised by Alta bioscience (University of Birmingham, Birmingham, UK).

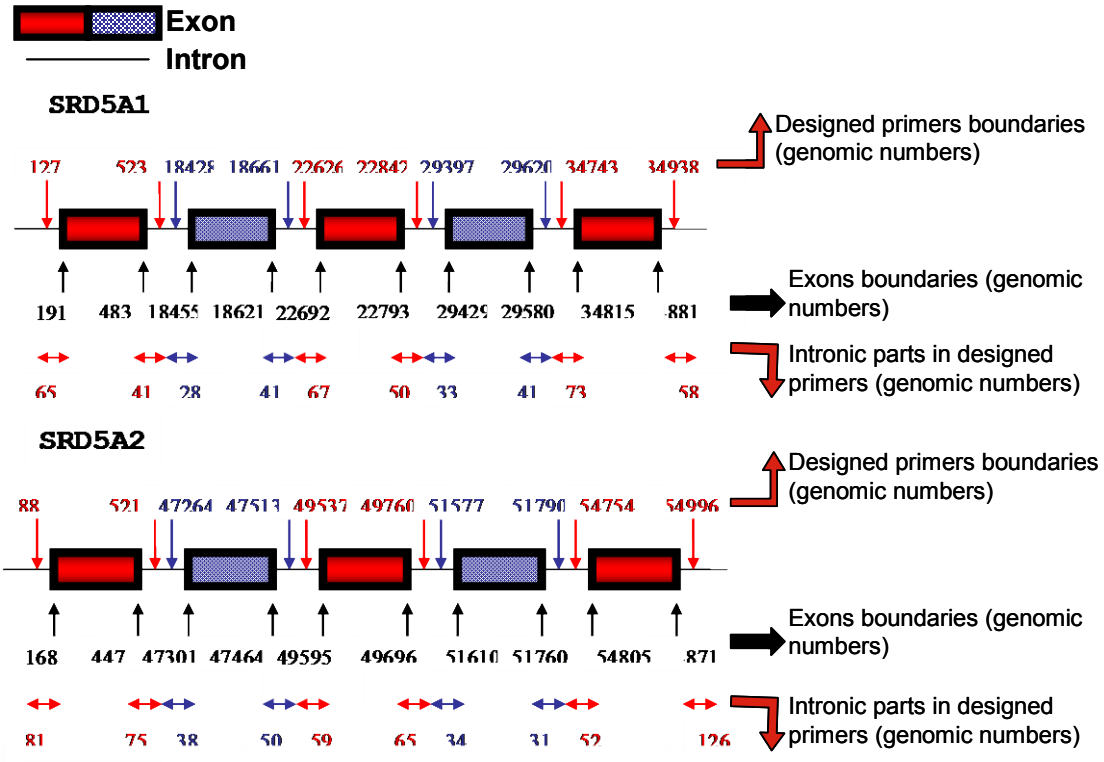

Figure 6-1 Genomic locations of designed primers. Primers were designed using NCBI, Primer3 online websites (http://bioinfo.ut.ee/primer3-0.4.0/), and Oligo calc software. These primers were synthesised by Alta bioscience (University of Birmingham, Birmingham, UK).

6.3.4.Optimising the primers by PCR

In order to define the best annealing temperature, all the primers were optimised in a range of 8 different temperatures (53.4 to 65°C). In a 10µl reaction the following components were added: MasterMix (final concentration 1x), forward and reverse primers (10 µM), and 100nM of DNA (for optimising the primers a control DNA was used trying not to waste the patients' DNA). In a thermal cycler (Biometra, Goettingen, Germany) samples were incubated at 94°C for 2min and then cycled 35 times at 94°C for 20 sec, 53.4 to 65°C for 20 sec and 72°C for 30 sec. Samples were then incubated for 72°C for 5min.

The DNA products were then assessed by electrophoresis on 1% agarose gel with 0.15 µg/mL GelRed (Cambridge biosciences LTD, Cambridge, UK) and visualised by GeneSnap software

subsequently. The annealing temperature which gave the cleanest band was chosen for each exon. Optimising of one exon from each gene is chosen to be shown as an example in Figure 6-2.

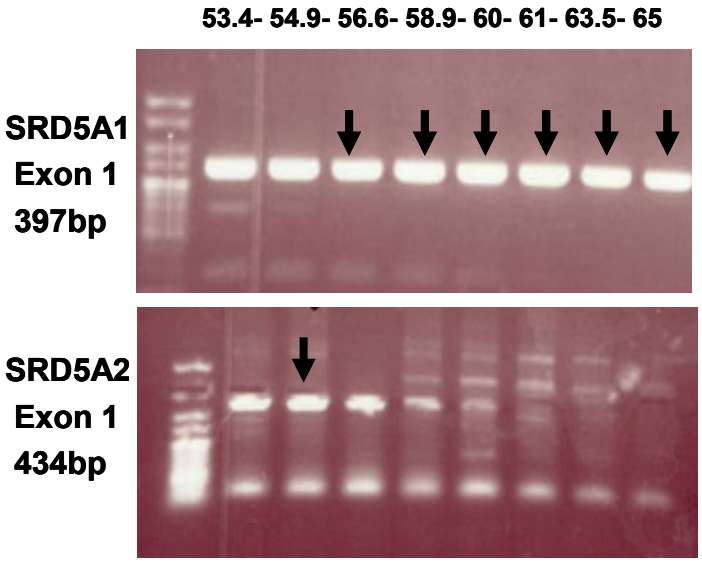

Figure 6-2 Optimising of exon 1 of each SRD5As in a range of 8 different temperatures (53.4 to 65°C) using electrophoresis on 1% agarose gel, best annealing temperatures are shown by arrows.

6.3.5.Sequencing

When the primers were optimised, the actual PCR was carried out on control DNA and later on patients' DNA, using the specific annealing temperature for each exon. The DNA products were then assessed by electrophoresis on 1% agarose gel with 0.15 µg/mL GelRed (Cambridge biosciences LTD, Cambridge, UK) and visualised under UV light. The DNA bands were purified from the gel using DNA mini kit (Qiagen, West Sussex, UK). For preparing a 10µl reaction for each PCR product sample to take for sequencing, each primer (reverse or forward) was added separately to the other components in the following order: Nuclease Free Water (final concentration 1x), forward or reverse primer (3.2pM), and 10nM of DNA.

Finally the samples were sent for sequencing. The sequencing of DNA was performed using an automated ABI 377 sequencer in the Functional Genomic Laboratory at the University of Birmingham, Plasmid to Profile sequencing (Birmingham, UK) and CLC DNA workbench software was used for further analyses of the obtained sequences.

6.4.Results

6.4.1.Patient identification

6.4.1.1. Urine analysis

9 patients (named in alphabetical order; A to I in this report) with abnormal A-ring reductase activity based on urinary GC/MS analysis have been identified (Table 6-1). These patients have altered urinary steroid profiles with low level of 5α-reduced metabolites. The normal mean 5αTHF/THF ratio is 0.89±0.32 in men and 0.67±0.33 in women while the mean 5αTHF/THF ratio in men and women of this research are 0.22±0.11 and 0.13±0.03 respectively (mean ± s.e). This indicates that 5αR activity in patients were approximately >2 standard deviations lower than the mean from our normative cohort of > 50 individuals and it is possible that this may reflect genetic defect in SRD5A1 and/or 2. There is a degree of variability in both 5αTHF and THF, as also seen in a study on 101 obese patients (Tomlinson et al. 2008). This may reflect variability of how complete the 24h urine collection is. In the current study, urine samples were a spot sample, and therefore, it is not possible to quantify 24h production rates for individual metabolites but allows us to compare metabolite ratios. (Figure 6-3).

Patient ID	A	B	C	D	E	F	G	H	I
Gender	F	F	F	M	F	F	F	F	M
5αTHF	389.8	146.11	89.63	305	234	87	160	82	399
THF	2988.71	1293.41	638.74	2579	2326	821	781	541	1183
5αTHF/THF	0.13	0.11	0.14	0.11	0.10	0.10	0.20	0.15	0.33

Table 6-1 Urinary steroid metabolite analysis from all the 9 individual patients (A to I). The 5αTHF/THF ratio is a marker of 5αR activity. Data are presented in nM, F=Female, M=Male.

Mean	Male controls	Male patients	Female controls	Female patients
5αTHF/THF	0.89±0.32	0.22±0.11	0.69±0.33	0.13±0.03

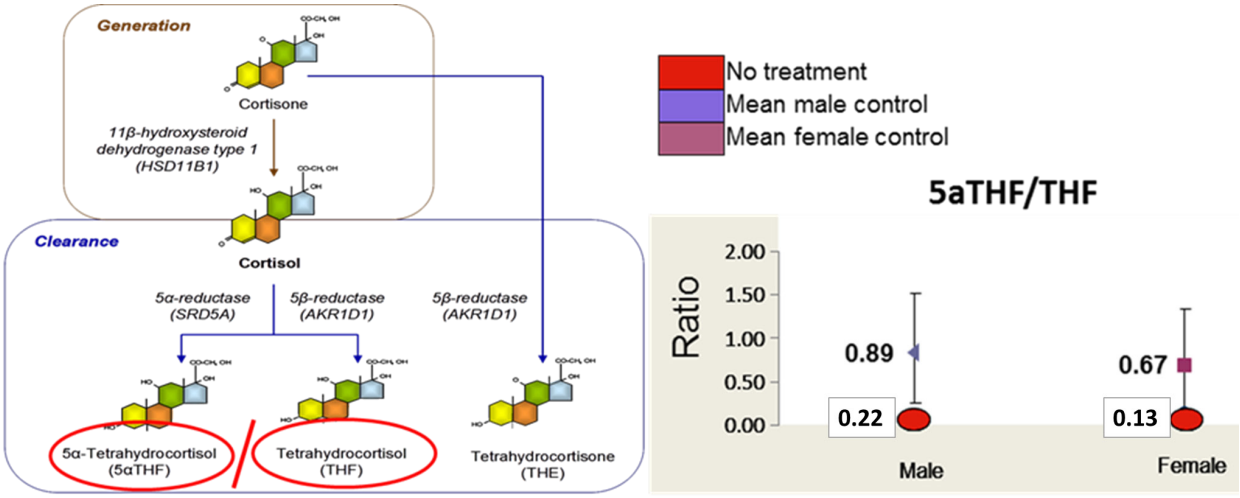

Figure 6-3 The 5αTHF/THF ratio is a marker of 5αR activity. The 5αTHF/THF ratio in men and women of these patients (shown in red) are almost two fold lower than normal mean 5αTHF/THF ratio in men (blue) and in women (purple). Data are presented as mean ± s.e.

6.4.1.2.Sequencing analysis

6.4.1.2.1.5αR2

All 5 exons of SRD5A2 have been sequenced and the results are summarised below

Table 6-2). No polymorphisms were identified in patients A, B, C, F or H.

Patient	ALLELE1	ALLELE2	REGION	DBSNP	AA	AA	AA	AA
COORDINATE					ALLELE	ALLELE2	COORDIN	CODON
D	C	G	coding	rs523349	Leu	Val		CG
E	C	G	coding	rs523349	Leu	Val		CG
E	G	A	coding	rs9282858	Ala	Thr		GA
E	G	A	UTR3	rs28383082				GA
G	C	G	coding	rs523349	Leu	Val		GG
I	C	G	coding	rs523349	Leu	Val		CG
I	G	A	coding	rs9282858	Ala	Thr		GA

Table 6-2 Polymorphisms identified in SRD5A2 in UTR3 and coding regions of patients D, E, G and I. No polymorphisms were identified in patients A, B, C, F or H. The sequencing of DNA was performed by the Functional Genomic Laboratory at the University of Birmingham, Plasmid to Profile sequencing (Birmingham, UK) and data were analysed using CLC DNA workbench software.

In addition, no polymorphisms were found in exon 2, 3 or 4 of SRD5A2 in patients D, E, G or I. However, in exon 1, in four patients (D, G, E and I) a substitution of valine for leucine at codon 89 (Figure 6-4a) was observed (L89V). In addition, in two of these patients (E and I) with L89V, A49T (a substitution of threonine for alanine at codon 49) (Figure 6-4b) polymorphism was identified in the same exon. L89V and A49T variants are not novel and have been identified previously.

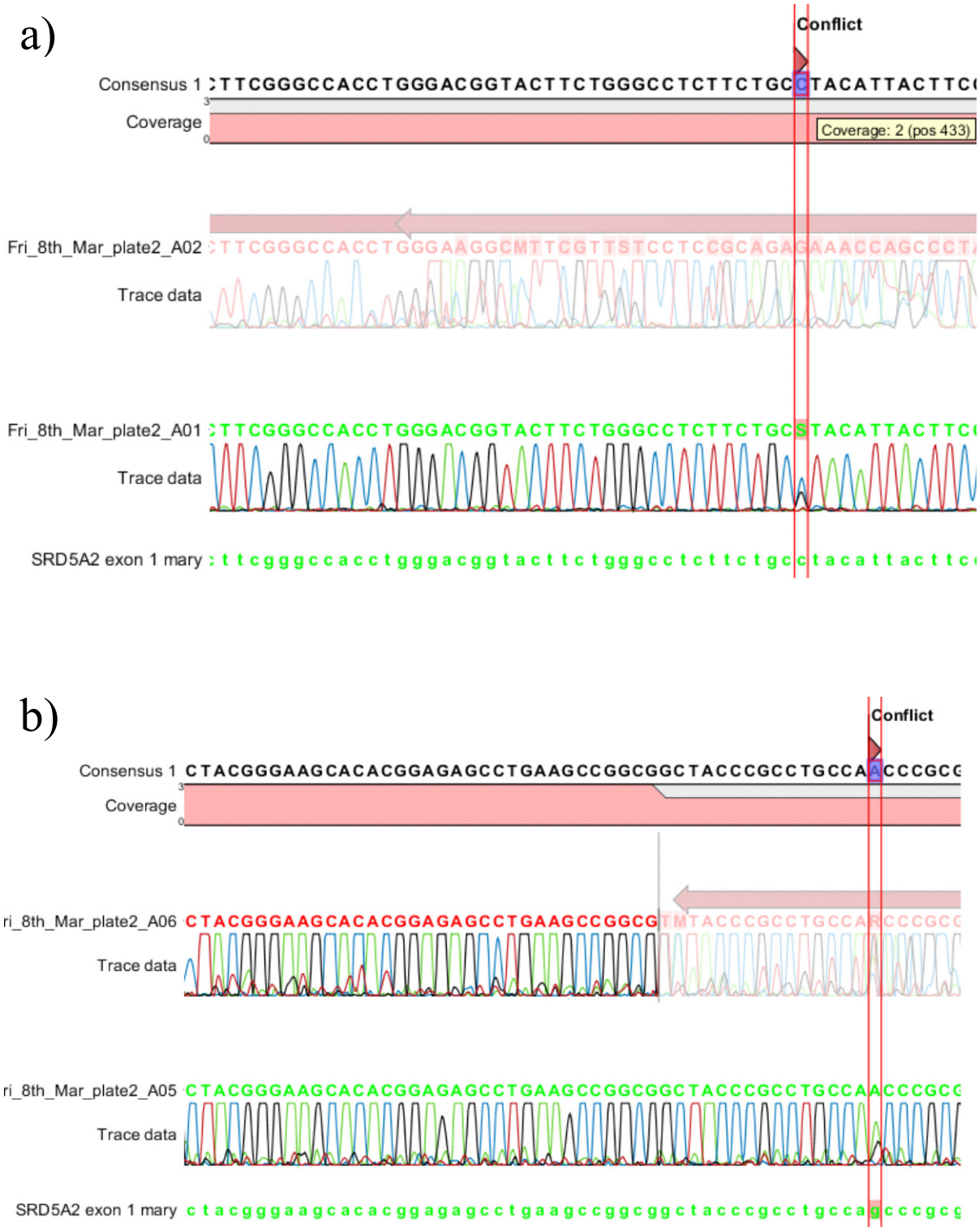

Figure 6-4 DNA sequence chromatograph from patient E indicating; a) C to G transversion resulting in a leucine (L) for valine (V) amino acid substitution at codon 89 (L89V) polymorphism, b) G to A transversion resulting in a threonine for alanine amino acid substitution at codon 49 (A49T) polymorphism. Data were analysed using CLC DNA workbench software.

6.4.1.2.2.5αR1

5αR1 sequencing analysis was performed by Beckman Coulter Genomics Inc. (Danvers, MA, US) and Whole Genome Amplification (WGA) was performed prior to sequencing.

Patient coordinate	Allele 1	Allele 2	Region	DBSNP	AA Alllel1	AA Allel2	AA coordinate	AA codon
D	C	T	intron	8192125			0	
I	C	G	coding	248793	Arg	Arg	30	CG
G	A	C	boundary				0	
E	A	G	coding	3822430	Pro	Pro	103	CC
H	G	A	coding	8192186	Ala	Ala	116	GC
I	G	A	coding	3736316	Thr	Thr	160	AC
A	A	G	intron	168713			0	
F	C	T	UTR3	3297			0	
B	G	A	UTR3	1042150			0	
C	A	G	UTR3	13974			0	
H	T	C	intron	39848			0	

Table 6-3 Polymorphisms identified in SRD5A1. There are three coding sequence changes but they do not cause amino acid changes. In patient G and A (highlighted rows), SNPs with low allele frequencies were identified. In patient G and A the SNP is located in intron1/exon2 boundary, and intron 3 respectively. Data were generated by Beckman Coulter Genomics Inc. (Danvers, MA, US).

Although no exonic mutation was identified in SRD5A1 of these patients, several intronic and 3'UTR single nucleotide polymorphisms (SNPs) were found. The identified SNPs were checked with NCBI SNPs and hapmap databases for their allele frequencies. Two SNPs were identified with low allele frequencies (lower than 0.01) which are highlighted in Table 6-3.

rs186093099 A>C, C= 0.003 AC heterozygote in patient G (Figure 6-5)

rs168713 A>G G= 0.15 GG homozygote= 0.012 in patient A

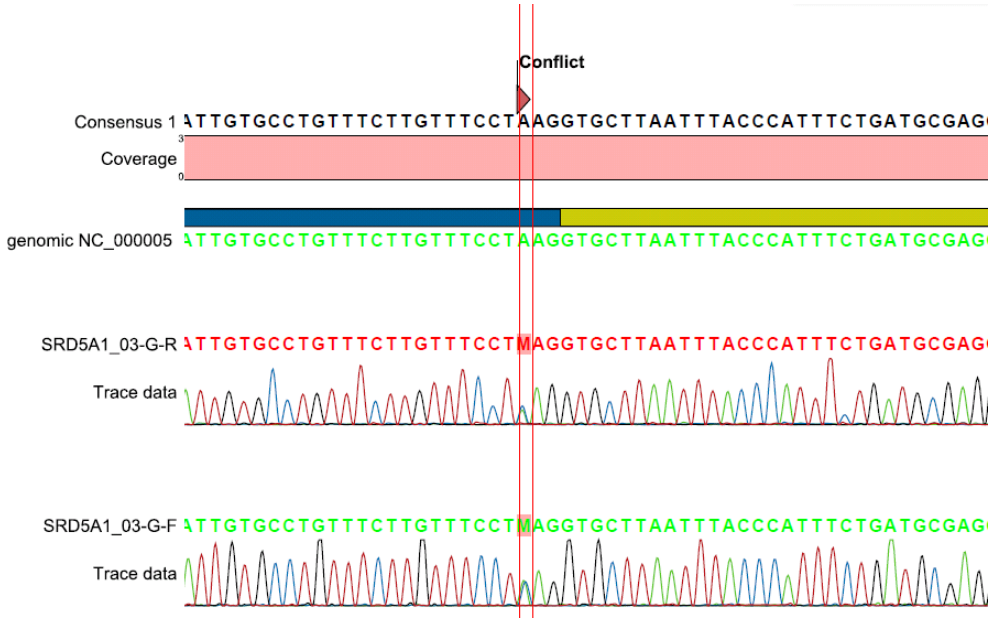

Figure 6-5 DNA sequence chromatograph from patient G indicating an A to C nucleotide substitution in rs186093099 polymorphism. Data were analysed using CLC DNA workbench software.

6.4.1.3.Splice variants in 5αR1

In order to examine whether these SNPs could change the splicing sites, NetGene2 software was used. This program takes the sequence file (only in FASTA) and predicts intronic splice sites in the human genome. No changes in splicing sites were observed comparing rs168713 with the wild type sequence. However, changing nucleotide A to C in (rs186093099) was predicted to increase the potency of a splice site located at intron1/exon2 boundary (0.82 [rs186093099] compared to 0.19 wild-type).

The predicted effect of increased potency at this splice site, is that exon 2 may be retained in the mature mRNA. Studying the NCBI SNPs database, the SRD5A1 gene has different splicing variants, with and without exon 2. Therefore we hypothesised that this SNP predicts a longer splice variant containing exon 2 (Figure 6-6) and that this could potentially impact upon enzyme activity.

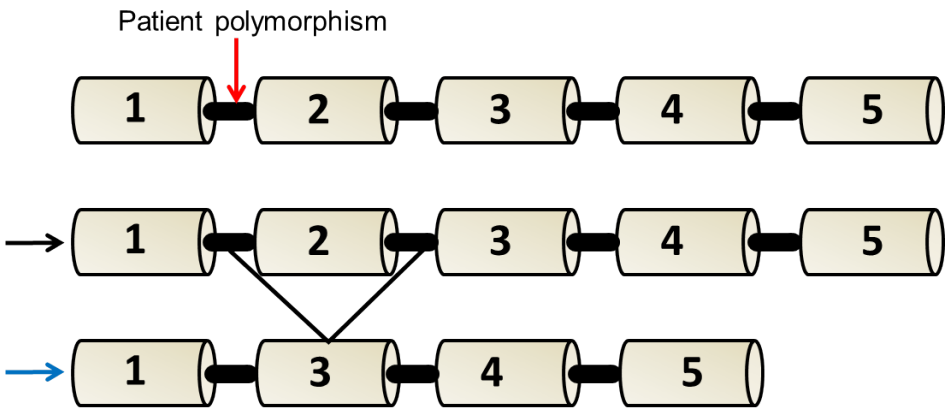

Figure 6-6 SRD5A1 gene has 2 splice variants (longer splice variant with 5 exons shown by black arrow and a shorter one with 4 exons indicated with blue arrow). The polymorphism in our patient makes the longer splice (5 exons) more potent and this may explain the metabolic phenotype.

To test the hypothesis that the presence of this SNP may alter the relative proportion of the long and short splice variants (and that this in turn may translate to an alteration in 5αR1 function), a set of primers were designed to amplify SRD5A1 splice variants comparing patients (with abnormal urinary steroid metabolite ratios) and controls (normal urinary steroid profiles). cDNA from human muscle tissue, obtained following skeletal muscle biopsy performed for a different clinical study (Hassan-Smith et al. 2015), was used for both patients and controls. SRD5A1 is highly expressed in human liver and therefore human primary hepatocyte cDNA was also used as a positive control.

Conventional PCR analysis demonstrated a decreased abundance of the short splice variant in the patients compared to controls, suggesting that the polymorphism may enhance the expression of the long splice variant (Figure 6-7).

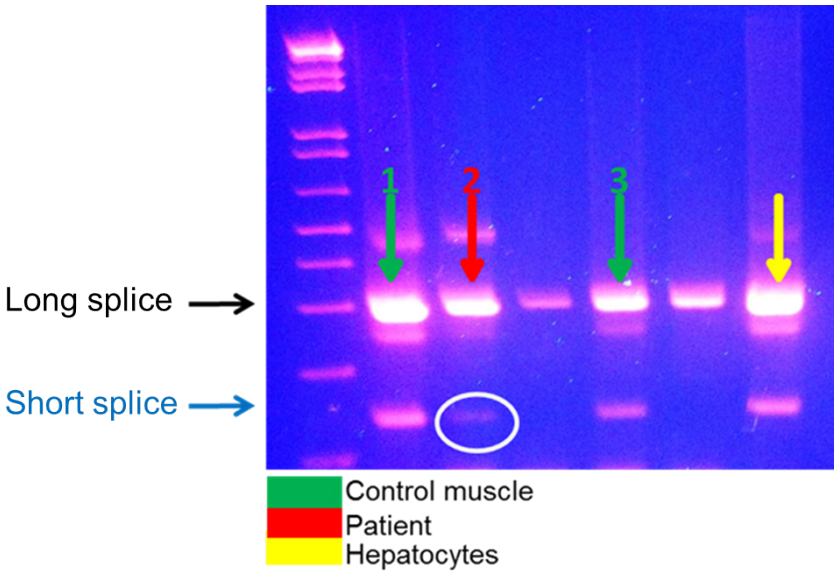

Figure 6-7 Conventional PCR analysis demonstrates a reduced amount of the short splice variant in patient with the rs186093099 SNP (red arrow) in comparison with controls (green arrow).cDNA from muscle was used for both patients and controls.

In order to quantify the preliminary observations made using conventional PCR, semi-quantitative real-time PCR was undertaken using an Applied bio-system assay on demand which amplifies only the long isoform. Despite the results from the conventional PCR, there was no significant difference between expression levels of the long splice variant in patients compared to controls (ΔCT of longer isoform expression; patient 18.18 vs controls; 17.27, 17.81, 19.19, 17.47). Thus, we were unable to confirm our hypothesis that greater incorporation of exon 2 in individuals with rs186093099 polymorphism.

6.5.Discussion

Our results from this chapter have not revealed any exonic mutations in SRD5A1 or SDR5A2 that might explain the abnormal urinary steroid metabolite ratios that we observed in these patients. However, we did observe L89V and A49T polymorphisms in exon 1 of SRD5A2; four patients were identified with L89V from which two were also carrying A49T.

These two polymorphisms have been reported in the published literature and have been widely investigated in association with prostate cancer (Pearce et al. 2002). An increased DHT level is associated with increased prostate cancer risk (Gann et al. 1996;Ross et al. 1992), as it binds to the AR and modulating cell division in the prostate (Coffey 1993) and therefore 5αR activity is important in determining the prostate cancer risk. In an *in vivo* study in 102 Asian individuals, they studied L89V polymorphism. They measured serum DHT concentrations and when they correlated this data with the patients' genotype, they found out that patients with VV genotype had the highest serum DHT while the patients with LL genotype had the lowest. They showed that in in patients with LL genotype the enzyme activity is reduced to 30% suggesting that the VV genotype is associated with higher enzyme activity (Makridakis et al. 1997). This suggests that L89V polymorphism is associated with increased prostate cancer risk through increasing 5αR activity.

In addition, in experiments where the A49T SNP in SRD5A2 has been overexpressed in mammalian COS cells, a 5-fold increase in enzyme activity was observed compared to the wild type (Makridakis et al. 1999). However, studying 449 Finnish patients with prostate cancer; no significant differences were observed in A49T prevalence when compared to controls (Mononen et al. 2001). This is in contrast in what has been reported in African-American, Hispanic (Makridakis et al. 1999) and Caucasians (Jaffe et al. 2000) where the

patients with prostate cancer had higher A49T prevalence when compared to the same ethnic controls. This, together with the *in vitro* data, suggest that A49T might be a race related genetic risk factor for prostate cancer and also SRD5A2 enzyme activity. In our study, L89V and A49T were identified in Caucasian patients with low level of 5α-reduced metabolites and therefore, based on literature, there might be no association between found polymorphisms and the reduced enzyme activity.

Despite being unable to identify any exonic mutations in SRD5A1, we identified a polymorphism within the intron1/exon2 boundary (rs186093099). *In silico*, this polymorphism was predicted to strengthen the intron1/exon2 splice site. A more potent splice site suggests increased incorporation of exon 2, however we were unable to confirm this by PCR. This suggests that SRD5A1 has different splicing variants in population which is not associated with observed reduced enzyme activity and metabolic readouts.

To date, no mutation has been reported in SRD5A1. However several polymorphisms have been associated with progression of prostate cancer; rs518673 and rs166050 in SRD5A1 (Audet-Walsh et al. 2011). SRD5A1 rs248793 was associated with increased DHT/T ratio affecting the circulating androgens level (Ellis et al. 2005). In addition, in a cross-sectional study, an association between SRD5A1 rs248800 and increased risk of hepatitis C related liver disease in male was observed (White et al. 2014). Although we were unable to find an association between SRD5A1 (rs186093099) and the altered urinary steroid profiles, the expanded polymorphism and mutation data base of SRD5A genes has enhanced our understanding of the regulation of 5αR1 expression, in particular the different splicing variants. These different splicing variants, short and long isoforms, might have different activities for which to be proved further studies are needed.

Although we were unable to find a genetic regulation to explain the altered urinary steroid profiles in these patients, this observed 5αR different activity might be regulated post-transcriptionally. We know that obesity and insulin resistance are associated with increased 5αR activity and that this decreases with weight loss and 5αR activity predicts adverse phenotype in the future (Tomlinson et al. 2008), and therefore we hypothesized that these individuals might be protected from this.

In addition, it is known that SNPs can cause structural variation and suggest mRNA structure dependent mechanism by which SNPs can generate allele specific biological consequences. Our data present the contribution of SNPs to structural diversity of mRNA and suggest a significant role for the SNPs by affecting mRNA structure, and eventually biological function (Shen et al. 1999). The known SNPs we found in SRD5A2 (L89V and A49T) are both missense variants as also mentioned on Ensembl website. Using both SIFT and PolyPhen software which predict the effect of SNPs on protein function, L89V variant has a tolerated and benign effect on protein function. However, A49T variant demonstrates a deleterious and possibly damaging effect. Both SNPs had a negative effect on the ability of the enzyme to bind to the testosterone substrate (Russell and Wilson 1994) and L89V decreased the affinity for the NADPH cofactor. The enzyme with A49T has a high Vmax when compared to the normal enzyme due to the change from small size and hydrophobic alanine to medium size and polar threonine (Makridakis et al. 1999). This provides insight into mechanisms of human phenotypic variation and helps studies of disease susceptibility and drug response.

The low number of patients and also amount of samples were the limitations of this study. After sequencing of SRD5A2 in all patients in our lab, due to the low amount of samples left we decided to use the Beckman Coulter Genomics Inc. (Danvers, MA, US) to sequence the

SRD5A1 gene. Using this company, very low amount of cDNA from patients was used as the Whole Genome Amplification (WGA) was performed prior to sequencing. However, sequencing of SRD5A2 in our lab was beneficial to learn new techniques (DNA extraction from blood, designing and optimising primers, and sequencing) and also to use several software such as Oligo calc to design primers and CLC DNA workbench to analyse the sequencing data.

Although we based this study on the 5αTHF/THF ratio obtained from urinary GC/MS analysis, studying the actual 5αTHF and THF levels are also important as increased 5αTHF/THF ratio can be a result of decreased 5αRs activity or increased 5βR activity. However, we have not sequenced the 5βR in these patients due to the lack of cDNA samples available and that is one of the limitations of this study. Moreover, studying the actual values of these metabolites is important. There is a degree of variability in both 5αTHF and THF values. In order to quantify an absolute change in production rate, of either 5α or 5β-reduced metabolites, a 24h urine collection is needed. In the current study we compared relative ratios of 5α or 5β-reduced metabolites in spot urines, therefore, they reflect a measure of A-ring reductase activity which could be due to altered 5α or 5βR activity.

In addition, the different splicing variants (short and long SRD5A1) may have different activities. However, the short and long SRD5A1 constructs has not been generated due to the lack of time and should be planned in future studies.

Chapter 7 Final discussion

Increased *de novo* lipogenesis is associated with metabolic disease and in particular with NAFLD (Kawano and Cohen 2013). Patients with NAFLD have increased levels of FAS, ACC1 and SREBP1c, and the contribution of *de novo* lipogenesis to the accumulated TAG is increased to 26% (Donnelly et al. 2005). Furthermore, *de novo* lipogenesis generates saturated fatty acids, predominantly palmitate, and patients with NAFLD have increased saturated fatty acid levels and in particular palmitate (Kotronen et al. 2009a; Sanders and Griffin, 2016). Saturated fatty acids are also known as 'bad' fat (Alkhouri et al. 2009); studies show an association between increased saturated fatty acids, in particular palmitic acid, and insulin resistance (Kotronen et al. 2009b). Therefore, the focus of the current study was on *de novo* lipogenesis and how steroid hormones can affect this pathway.

The impact of GCs to regulate carbohydrate metabolism in particular gluconeogenesis in the fasting state is well described. However, their impact on lipid metabolism remains relatively poorly understood in human models. We have previously shown in adipose and skeletal muscle that GCs decrease lipogenesis in the absence of insulin consistent with their role to mobilize fuel in the fasting state (Gathercole et al. 2007;Morgan et al. 2013). In the fed state, however, GCs and insulin act synergistically to drive lipid accumulation. Studies performed in rodent hepatocytes have demonstrated this relationship (Amatruda et al. 1983) and we have now shown this in primary cultures of human hepatocytes.

In our *in vitro* model, the ability of GCs to enhance the ability of insulin to drive lipogenesis was associated with increased activation of the insulin signalling cascade as demonstrated by increased phosphorylation of PKB/akt, similar to our published observations in human adipose tissue (Gathercole et al. 2007;Hazlehurst et al. 2013). Although augmentation of insulin action by GCs has been observed in rodent hepatocytes (Amatruda, Danahy, & Chang

1983), these *in vitro* data may not be reflective of more complex *in vivo* physiology. Clinical studies that have administered GCs have shown evidence of increased hepatic insulin resistance in most cases (Petersons et al. 2013) (Figure 7-1).

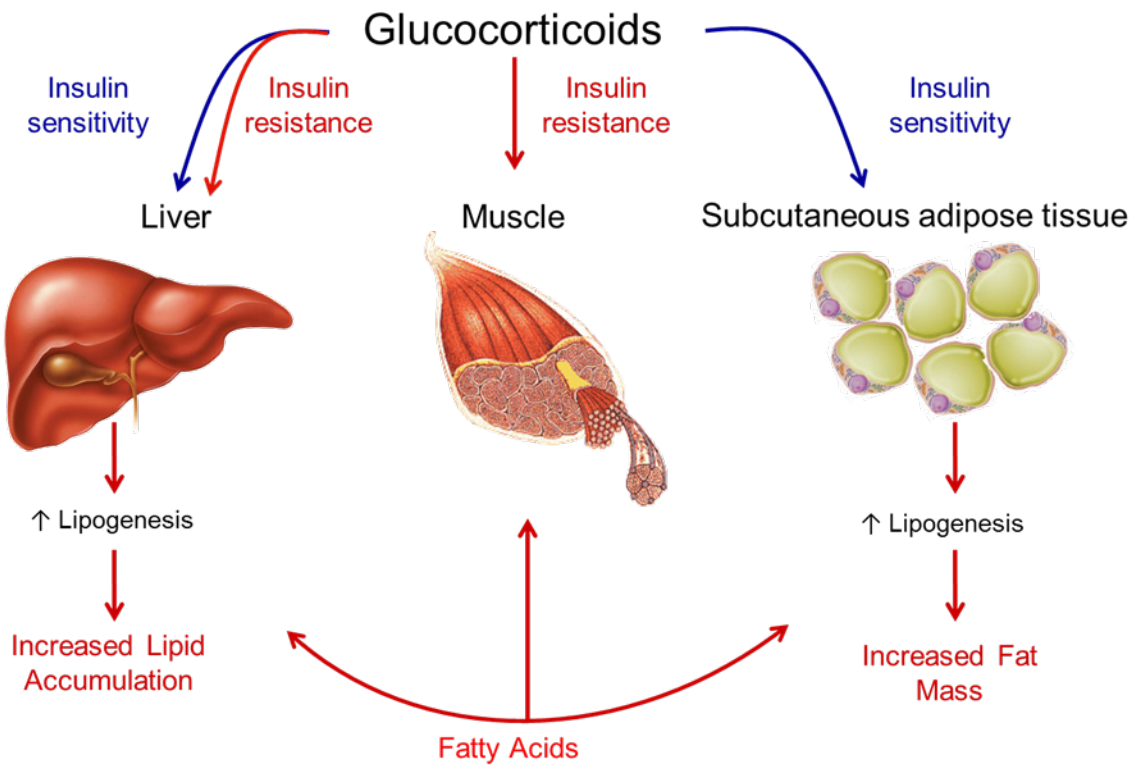

Figure 7-1 Tissue specific GC action to regulate lipid metabolism and insulin action. GCs induce insulin resistance in skeletal muscle and insulin sensitivity in adipose tissue. We have described insulin sensitisation by GCs in human hepatocytes and this may lead to increased lipid accumulation (as in adipose tissue) in the fed state. This may represent an important mechanism in the development of the Cushing's phenotype and its associated adverse metabolic features.

Low testosterone concentrations are associated with increased hepatic steatosis in men (Kim et al. 2012;Volzke et al. 2010) but women with polycystic ovarian syndrome (PCOS) are reported to be at an increased risk of developing NAFLD (Jones et al. 2012;Markou et al. 2010). We have shown that androgens are able to increase lipid accumulation within C3A

cells and in primary cultures of human hepatocytes from female, but not male donors. The observed sexually dimorphic effects in primary cultures may suggest the different mechanisms behind androgens and lipid metabolism in females compared to men.

As data from male primary cultures did not confirm the C3As data, this highlights the important of endorsing *in vitro* observations in additional models including human primary cultures. Data from male primary cultures might suggest that androgens have less impact on NAFLD phenotype when compared to GCs. This is in agreement with *in vivo* data from our group showing that liver gene expression profile in 5αR1 knockout mice overlap with those induced by GCs rather than androgens (Dowman et al. 2013). Others have recently demonstrated impaired hepatic metabolic clearance of corticosterone in 5αR1 knockout mice but persistence of the effect of finasteride in gonadectomised rats and therefore suggested that GC excess is likely to be the mechanism underpinning the observed hepatic steatosis in this model (Livingstone et al. 2015).

There is now an emerging role for the 5αR isoforms in the regulation of metabolic phenotype. The ability of testosterone to regulate lipid metabolism does not appear to be dependent upon the presence of SRD5A2. The C3A cell line does not express SRD5A2, and yet both Testosterone and DHT were able to stimulate lipogenesis to a similar extent. Our experiments therefore focused on the role of SRD5A2 to regulate the effects of GCs upon liver metabolism.

In rodent modelsSRD5A1 deletion increases lipid accumulation and promotes fibrosis, the precise mechanisms that underpin this are not clear (Dowman et al. 2013;Livingstone et al. 2015). Nonselective 5αR inhibition with dutasteride was associated with peripheral insulin resistance. This may reflect a specific role for SRD5A1 in skeletal muscle, however, pre and

post intervention assessments of hepatic lipid content were not performed. Therefore, the precise impact upon liver fat accumulation could not be determined (Upreti et al. 2014). In a recently published clinical study, dutasteride (but not finasteride) treatment increased hepatic insulin resistance and the rate of hepatic *de novo* lipogenesis. Therefore, the observed increase in hepatic lipid accumulation might be due to either 5αR1, or dual 5αR1 and 2, inhibition (Hazlehurst et al. 2016).

The role of SRD5A2 in clearing cortisol is well stablished through the examination of urinary steroid metabolite profiles in patients with proven SRD5A2 mutations (Peterson et al. 1985). Detailed metabolic studies in patients with mutations SRD5A2, have not been performed. In our study, we demonstrated that 5αR2 transfected liver cells were able to overcome and recover the inhibitory action of cortisol upon lipogenesis. This was in agreement with the published data suggesting; increasing 5αR activity is associated with an adverse metabolic phenotype (Tomlinson et al. 2008;Tsilchorozidou et al. 2003). This may reflect a compensatory mechanism to clear active GCs, in particular from the liver in an attempt to protect it from lipid accumulation. With more severe liver disease, 5αR activity decreases and this may increase GC exposure and may serve and a local anti-inflammatory measure to try to limit the progression of non-alcoholic steatohepatitis, fibrosis and scarring (Ahmed et al. 2012).

In addition, we have shown that 5αR inhibitors (both finasteride and dutasteride) augment the effect of cortisol on decreasing lipogenesis. Previously, we described that cortisol and insulin act synergistically to increase lipid accumulation and therefore we suggest that 5αR inhibitors enhance cortisol action to act synergistically with insulin (probably in the fed, postprandial state) to drive lipid accumulation. This also seems to be endorsed from findings in the rodent

5αR1 knockout mice who develop increased lipid accumulation (Dowman et.al 2013) (Figure 7-2).

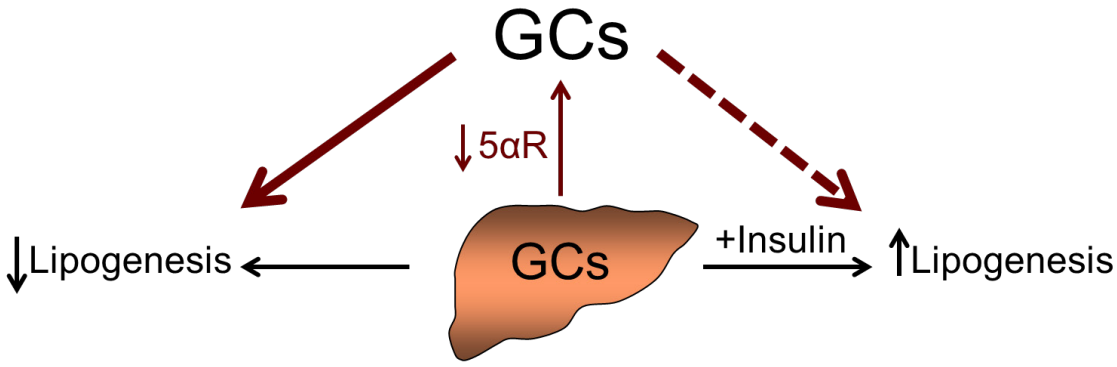

Figure 7-2 GCs acting in isolation decrease lipogenesis but enhance insulin-stimulated lipogenesis. We discovered that 5αR overexpression ameliorates the effects of cortisol upon lipid metabolism but chemical inhibition of 5αR augments the actions of cortisol. This may suggests that in presence of insulin, 5αR inhibitors enhance cortisol action to act synergistically with insulin to drive lipid accumulation. This finding has potentially significant implications for patients taking finasteride and dutasteride.

We identified 9 patients with low levels of 5α-reduced metabolites, based on urinary GC/MS analysis, which we hypothesised to be as a result of altered 5αRs activity. Therefore, we sequenced SRD5A1 and 2 in these patients but did not find any polymorphisms explaining the abnormal steroid profile. However, the expanded polymorphism and mutation data base of SRD5A genes has enhanced our understanding of the regulation of 5αR1 expression, in particular the different splicing variants.

In conclusion, we have demonstrated the potent actions of androgens and GCs to regulate lipid metabolism in human hepatocytes *in vitro* and shown that pre-receptor regulation through that expression and activity of SRD5A2 is able to modify their action. This has important implications not only in terms of predisposing individuals to the development of hepatic steatosis, but also to the large numbers of patients prescribed 5αR inhibitors. While

the role of these compounds in the treatment of prostate-related disease is stablished, the long-term metabolic consequences of these medications have not been assessed.

Chapter 8 Future studies

Comparing our *in vitro* model with translational clinical studies, we observed fundamental differences in response of insulin sensitivity to GC treatment between primary hepatocytes *in vitro* and in human liver physiology *in vivo*. Within the research group we have shown no increase in hepatic insulin sensitivity in healthy volunteers treated with GCs in a clinical study (Hazlehurst et al. 2013). However, our *in vitro* data had suggested that GCs enhance insulin sensitivity in primary hepatocytes. Possible explanations for this difference might include the organ/cell isolation system or the fact that *in vitro* single treatments are being tested (rather than trying to replicate the complex hormonal environment that is seen *in vivo*).Access to human model systems to translate laboratory-based findings is therefore crucially important.

In our laboratory-based studies, cells were treated with GCs for 24h and it is possible that prolonged administration of GCs might have differing effects. These incubations were not performed, but would provide additional valuable data. Importantly, this may then more closely mimic patients with variety range of inflammatory conditions such as rheumatoid arthritis and asthma whom receive prolong synthetic GC treatment (Wei et al. 2004).

In addition, in order to fully understand the dynamic impact of GC upon lipid homeostasis further functional assays such as β-oxidation should be performed on hepatocytes. To perform this assay, cells can be incubated with a tritiated fatty acid tracer and the amount of tritiated water, released during oxidation measured (specific activity measured using scintillation counting).

In chapter 5, we have shown that 5αR inhibitors decrease cortisol clearance and we have hypothesised that they might enhance cortisol action. It is possible therefore that enhanced cortisol availability could then act synergistically with insulin to drive lipid accumulation. Additional experiments would therefore include co-incubation of cells treated with 5αR

inhibitors with both cortisol and insulin. We would anticipate that 5αR inhibitors would significantly enhance the synergistic actions of cortisol combined with insulin.

For complete characterisation of 5αRs, further *in vivo* studies including overexpression in rodents and inhibition of 5αRs in humans are warranted. Future experiments would include liver specific overexpression of 5αR isoforms in rodent models. These transgenic models are then would be given dietary or GC treatments in order to see if 5αRs can reverse the effect of GC and ameliorate their hepatic lipid profile. These rodent studies could be extended into the clinical setting through translational studies. The clinical effect of 5αR inhibitors on hepatic lipid metabolism and insulin sensitivity could be assessed in healthy volunteers taking glucocorticoids alone or taking glucocorticoids in addition to 5αR inhibitors. As local GC availability increases (as a consequence of 5αRs inhibition), we might expect to see a worsening of metabolic hepatic phenotype. We would predict that individuals taking both GCs and 5αR inhibitors, the phenotype would be worsen in comparison to those taking GCs alone.

Additional future studies could look at long-term consequences of finasteride and dutatseride prescriptions. These drugs are widely prescribed and it is possible that these drugs may have an adverse impact upon liver fat accumulation and this may translate to an adverse clinical outcome. Currently there are no published data that examined the long-term cardiovascular outcome in patients taking these drugs.

In order to try to identify the cause of the abnormal urinary ratios, studied in chapter 6, experiments investigating the regulation of short and long 5αR1 isoforms could be undertaken. These different splicing variants may have different activities and therefore to test this hypothesis, short and long SRD5A1 constructs could be generated. These constructs

would then be expressed in cells and their enzymatic activity in the presence of GCs/androgen measured.

Whilst it is known that GCs and androgens are involved in the development of NAFLD, they may also have a role in regulating the inflammatory component of the disease. Therefore, in future studies we will also investigate the impact of GCs and androgens on inflammation and inflammatory pathways in both our animal and *in vitro* models.

Conference proceedings

Oral presentations:

Nasiri M, Nikolaou N, Bujalska IJ, Hughes BA, Taylor AE, Stewart PM, Gathercole LL, Tomlinson JW '5α-reductase is a regulator of glucocorticoid action and metabolic phenotype in human liver'- Annual Meeting of the American Endocrine Society, Chicago, USA, 2014.

Nasiri M, Nikolaou N, Bujalska IJ, Hughes BA, Taylor AE, Stewart PM, Gathercole LL, Tomlinson JW '5α-reductase is a regulator of glucocorticoid action and metabolic phenotype in human liver'- Annual Meeting of the British Endocrine Society, Liverpool, UK, 2014.

Nasiri M, Gathercole LL, Tomlinson JW 'Glucocorticoid Regulation of Metabolic Function in Human Liver'- Young Active Research in Endocrinology, Stockholm, 2011.

Poster presentation:

Nasiri M, Bujalska IJ, Stewart PM, Gathercole LL, Tomlinson JW 'Glucocorticoids Enhance Insulin Sensitivity in Human Hepatocytes'- Annual Meeting of the American Endocrine Society, San Francisco, USA, 2013.

Nasiri M, Bujalska IJ, Stewart PM, Gathercole LL, Tomlinson JW 'Glucocorticoids Enhance Insulin Sensitivity in Human Hepatocytes '- Annual Meeting of the British Endocrine Society, Harrogate, UK, 2013.

Nasiri M, Bujalska IJ, Hughes BA, Taylor AE, Stewart PM, Gathercole LL, Tomlinson JW 'Regulation of *de novo* lipogenesis in human liver by 5α-reductase'- Annual Meeting of the American Endocrine Society, Houston, USA, 2012, (presidential award).

Nasiri M, Bujalska IJ, Hughes BA, Taylor AE, Stewart PM, Gathercole LL, Tomlinson JW 'Regulation of *de novo* lipogenesis in human liver by 5α-reductase'- Annual Meeting of the British Endocrine Society, Harrogate, UK, 2012.

Nasiri M, Bujalska IJ, Gathercole LL, Hauton D, Stewart PM, Tomlinson JW 'Cortisol Decreases Lipogenesis in Human Hepatocytes'- Annual Meeting of the British Endocrine Society, Birmingham, UK, 2011.

.

Appendix

PLATEABLE CRYOPRESERVED MALE HUMAN HEPATOCYTES

PRODUCT NUMBER: M00995-P

Lot Number: QOQ **Storage Conditions:** below -150ºC (vapour phase of liquid nitrogen freezer)

Test Results:

Specification	Result
>70% post-thaw viability by trypan blue exclusion	92 %
≥ 5 million viable cells	6.27 million viable cells
≥ 2 PC/VC ratio after 48 hours with 25 µM rifampin	6.09
CYP3A4: basal rate of formation of 6β-hydroxytestosterone at day 5	1.06 pmol/10^6 cells/min
≥ 2 PC/VC ratio after 48 hours with 50 µM omeprazole	13.1
CYP1A2: basal rate of formation of acetaminophen at day 5	0.500 pmol/10^6 cells/min
PC/VC ratio after 48 hours with 1 mM phenobarbital	4.23
CYP2B6: basal rate of formation of hydroxybuproprion at day 5	0.113 pmol/10^6 cells/min
≥ 0.1 OD MTT value at day 5	0.226 OD
≥70% confluent monolayer at day 5	84 %

Lot Characterization Results:

Assay	Result	
ECOD: total rate of formation of 7-HC and metabolites	78.0	pmol/10^6 cells/min
UGT/ST:		
rate of formation of 7-hydroxycoumarin glucuronide	390	pmol/10^6 cells/min
rate of formation of 7-hydroxycoumarin sulfate	71.8	pmol/10^6 cells/min
CYP1A2: rate of formation of acetaminophen	78.5	pmol/10^6 cells/min
CYP2A6: total rate of formation of 7-HC and metabolites	20.5	pmol/10^6 cells/min
CYP2C9: rate of formation of 4′-methylhydroxytolbutamide	33.2	pmol/10^6 cells/min
CYP2C19: rate of formation of 4′-hydroxymephenytoin	1.82	pmol/10^6 cells/min
CYP2D6: rate of formation of dextrorphan	48.1	pmol/10^6 cells/min
CYP2E1: rate of formation of 6-hydroxychlorzoxazone	28.1	pmol/10^6 cells/min
CYP3A4: rate of formation of 6β-hydroxytestosterone	25.0	pmol/10^6 cells/min

[2] **genotyping data will be provided on the Celsis website as the data are made available**

Donor Demographics, as reported to Celsis | In Vitro Technologies:

Age: 66 Race: C Cause of death: CVA Height: 67" Weight: 84 Kg

Social history: ETOH: 2 drinks/day, Tobacco: 1ppd x 50yrs, no drug use

Medical history: HTN x less than 5 yrs, adenocarcinoma in lung discovered after death

Confluence – Day 5

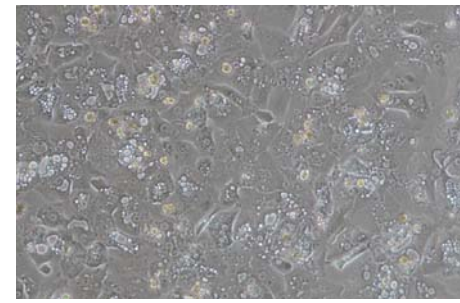

Serology:

EBV	Not reported	Hepatitis B	Negative
RPR	Negative	Hepatitis C	Negative
CMV	Negative	HIV	Negative

Carolyn Watt

Caution: This product was prepared from fresh human tissue. Treat all products containing human-derived materials as potentially infectious, as no known test methods can offer assurance that products derived from human tissues will not transmit infectious agents.

These products are for research use only. Do not use in animals or humans. These products have not been approved for any diagnostic or clinical procedures.

1450 South Rolling Road Baltimore, MD 21227 Toll Free 888.488.3232 Fax 410.455.1245 www.celsis.com/ivt

PLATEABLE CRYOPRESERVED MALE HUMAN HEPATOCYTES

PRODUCT NUMBER: M00995-P

Lot Number: OHO

Storage Conditions: below -150ºC (vapour phase of liquid nitrogen freezer)

Test Results:

Specification	Result
>70% post-thaw viability by trypan blue exclusion	86 %
≥ 5 million viable cells	6.69 million viable cells
≥ 2 PC/VC ratio after 48 hours with 25 µM rifampin	4.25
≥ 2 PC/VC ratio after 48 hours with 50 µM omeprazole	21.6
PC/VC ratio after 48 hours with 1 mM phenobarbital	6.45
≥ 0.1 OD MTT value at day 5	0.337 OD
≥70% confluent monolayer at day 5	98 %

Lot Characterization Results:

Assay	Result	
ECOD: total rate of formation of 7-HC and metabolites	172	pmol/10^6 cells/min
UGT/ST:		
rate of formation of 7-hydroxycoumarin glucuronide	427	pmol/10^6 cells/min
rate of formation of 7-hydroxycoumarin sulfate	20.4	pmol/10^6 cells/min
CYP1A2: rate of formation of acetaminophen	49.2	pmol/10^6 cells/min
CYP2A6: total rate of formation of 7-HC and metabolites	143	pmol/10^6 cells/min
CYP2C9: rate of formation of 4′-methylhydroxytolbutamide	95.4	pmol/10^6 cells/min
CYP2C19: rate of formation of 4′-hydroxymephenytoin	85.2	pmol/10^6 cells/min
CYP2D6: rate of formation of dextrorphan	27.7	pmol/10^6 cells/min
CYP2E1: rate of formation of 6-hydroxychlorzoxazone	24.3	pmol/10^6 cells/min
CYP3A4: rate of formation of 6β-hydroxytestosterone	170	pmol/10^6 cells/min

[2] **genotyping data will be provided on the Celsis website as the data are made available**

Donor Demographics, as reported to Celsis | In Vitro Technologies:

Age: 28 Race: C Cause of death: Head Trauma; 2nd to GSW Height: 173cm Weight: 85 Kg

Social history:

No ETOH or Tobacco; smoked marijuana

Medical history:

No medical issues/problems in provided history

Serology:

EBV	Positive
CMV	Positive
RPR	Negative
Hepatitis B	Negative
Hepatitis C	Negative
HIV	Negative

Confluence – Day 5

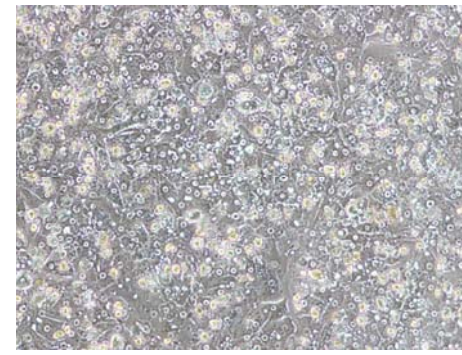

Carolyn Watt

Caution: This product was prepared from fresh human tissue. Treat all products containing human-derived materials as potentially infectious, as no known test methods can offer assurance that products derived from human tissues will not transmit infectious agents.

These products are for research use only. Do not use in animals or humans. These products have not been approved for any diagnostic or clinical procedures.

1450 South Rolling Road Baltimore, MD 21227 Toll Free 888.488.3232 Fax 410.455.1245 www.celsis.com/ivt

PLATEABLE CRYOPRESERVED MALE HUMAN HEPATOCYTES

PRODUCT NUMBER: M00995-P

Lot Number: CPQ **Storage Conditions:** below -150ºC (vapour phase of liquid nitrogen freezer)

Test Results:

Specification	Result
>70% post-thaw viability by trypan blue exclusion	93 %
≥ 5 million viable cells	11.4 million viable cells
≥ 2 PC/VC ratio after 48 hours with 25 µM rifampin	13.1
≥ 2 PC/VC ratio after 48 hours with 50 µM omeprazole	18.1
PC/VC ratio after 48 hours with 1 mM phenobarbital	4.00
≥ 0.1 OD MTT value at day 5	0.242 OD
≥70% confluent monolayer at day 5	93 %

Lot Characterization Results:

Assay	Result	
ECOD: total rate of formation of 7-HC and metabolites	78.0	pmol/10^6 cells/min
UGT/ST:		
rate of formation of 7-hydroxycoumarin glucuronide	440	pmol/10^6 cells/min
rate of formation of 7-hydroxycoumarin sulfate	41.0	pmol/10^6 cells/min
CYP1A2: rate of formation of acetaminophen	18.0	pmol/10^6 cells/min
CYP2A6: total rate of formation of 7-HC and metabolites	105	pmol/10^6 cells/min
CYP2C9: rate of formation of 4′-methylhydroxytolbutamide	36.4	pmol/10^6 cells/min
CYP2C19: rate of formation of 4′-hydroxymephenytoin	17.8	pmol/10^6 cells/min
CYP2D6: rate of formation of dextrorphan	32.1	pmol/10^6 cells/min
CYP2E1: rate of formation of 6-hydroxychlorzoxazone	49.9	pmol/10^6 cells/min
CYP3A4: rate of formation of 6β-hydroxytestosterone	95.2	pmol/10^6 cells/min

[2] **genotyping data will be provided on the Celsis website as the data are made available**

Donor Demographics, as reported to Celsis | In Vitro Technologies:

Age: 31 Race: C Cause of death: Head Trauma; 2nd to MVA Height: 73" Weight: 196lb

Social history:

No alcohol use; Tobacco: 1-1.5 ppd x 15yrs, chewed tobacco; Drugs: Smokes crack, cocaine and marijuana

Medical history:

No medical history, no meds.

Serology:

EBV	Not Reported
CMV	Negative
RPR	Positive
Hepatitis B	Negative
Hepatitis C	Negative
HIV	Negative

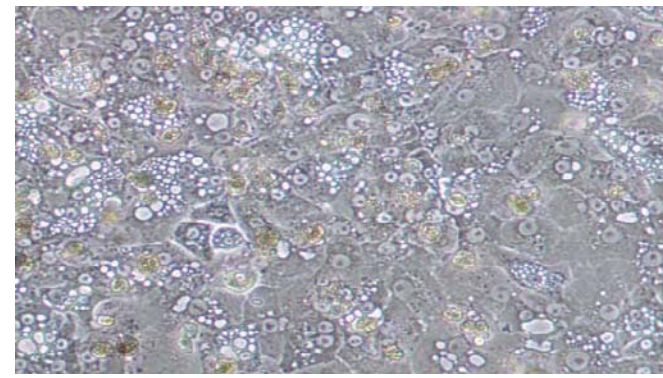

Carolyn Watt

Caution: This product was prepared from fresh human tissue. Treat all products containing human-derived materials as potentially infectious, as no known test methods can offer assurance that products derived from human tissues will not transmit infectious agents.

These products are for research use only. Do not use in animals or humans. These products have not been approved for any diagnostic or clinical procedures.

1450 South Rolling Road Baltimore, MD 21227 Toll Free 888.488.3232 Fax 410.455.1245 www.celsis.com/ivt

PLATEABLE CRYOPRESERVED MALE HUMAN HEPATOCYTES

PRODUCT NUMBER: M00995-P

Lot Number: YOW

Storage Conditions: below -150ºC (vapour phase of liquid nitrogen freezer)

Test Results:

Specification	Result
>70% post-thaw viability by trypan blue exclusion	92 %
≥ 5 million viable cells	7.41 million viable cells
≥ 2 PC/VC ratio after 48 hours with 25 µM rifampin	10.2
≥ 2 PC/VC ratio after 48 hours with 50 µM omeprazole	15.8
PC/VC ratio after 48 hours with 1 mM phenobarbital	11.3
≥ 0.1 OD MTT value at day 5	0.171 OD
≥70% confluent monolayer at day 5	87 %

Lot Characterization Results:

Assay	Result	
ECOD: total rate of formation of 7-HC and metabolites	82.3	pmol/10^6 cells/min
UGT/ST:		
rate of formation of 7-hydroxycoumarin glucuronide	448	pmol/10^6 cells/min
rate of formation of 7-hydroxycoumarin sulfate	47.4	pmol/10^6 cells/min
CYP1A2: rate of formation of acetaminophen	12.5	pmol/10^6 cells/min
CYP2A6: total rate of formation of 7-HC and metabolites	19.9	pmol/10^6 cells/min
CYP2C9: rate of formation of 4′-methylhydroxytolbutamide	20.4	pmol/10^6 cells/min
CYP2C19: rate of formation of 4′-hydroxymephenytoin	BQL	pmol/10^6 cells/min
CYP2D6: rate of formation of dextrorphan	14.7	pmol/10^6 cells/min
CYP2E1: rate of formation of 6-hydroxychlorzoxazone	36.2	pmol/10^6 cells/min
CYP3A4: rate of formation of 6β-hydroxytestosterone	3.56	pmol/10^6 cells/min

[2] **genotyping data will be provided on the Celsis website as the data are made available**

Donor Demographics, as reported to Celsis | In Vitro Technologies:

Age: 78 Race: C Cause of death: Stroke Height: 72" Weight: 76 Kg

Social history:

ETOH: 3 cans of beer/wk; Tobacco: 1ppd x 15yrs - quit 40yrs ago

Medical history:

Lupus, OA. No meds.

Serology:

EBV	Not reported
CMV	Positive
RPR	Negative
Hepatitis B	Negative
Hepatitis C	Negative
HIV	Negative

Confluence – Day 5

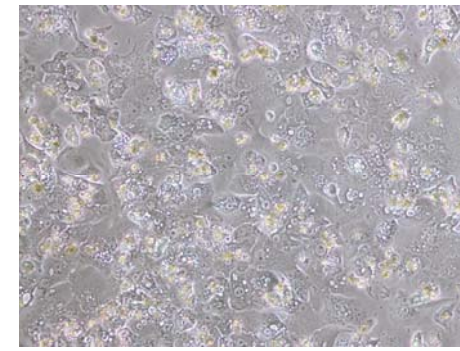

Carolyn Watt

Caution: This product was prepared from fresh human tissue. Treat all products containing human-derived materials as potentially infectious, as no known test methods can offer assurance that products derived from human tissues will not transmit infectious agents.

These products are for research use only. Do not use in animals or humans. These products have not been approved for any diagnostic or clinical procedures.

1450 South Rolling Road Baltimore, MD 21227 Toll Free 888.488.3232 Fax 410.455.1245 www.celsis.com/ivt

PLATEABLE CRYOPRESERVED FEMALE HUMAN HEPATOCYTES
PRODUCT NUMBER: F00995-P

Lot Number: TLQ **Storage Conditions:** below -150ºC (vapour phase of liquid nitrogen freezer)

Test Results:

Specification	Result
>70% post-thaw viability by trypan blue exclusion	80 %
≥ 5 million viable cells	6.39 million viable cells
≥ 2 PC/VC ratio after 48 hours with 25 µM rifampin	3.83
≥ 2 PC/VC ratio after 48 hours with 50 µM omeprazole	9.62
PC/VC ratio after 48 hours with 1 mM phenobarbital	2.00
≥ 0.1 OD MTT value at day 5	0.290 OD
≥70% confluent monolayer at day 5	93 %

Lot Characterization Results:

Assay	Result	
ECOD: total rate of formation of 7-HC and metabolites	183	pmol/10^6 cells/min
UGT/ST:		
rate of formation of 7-hydroxycoumarin glucuronide	448	pmol/10^6 cells/min
rate of formation of 7-hydroxycoumarin sulfate	42.9	pmol/10^6 cells/min
CYP1A2: rate of formation of acetaminophen	33.1	pmol/10^6 cells/min
CYP2A6: total rate of formation of 7-HC and metabolites	119	pmol/10^6 cells/min
CYP2C9: rate of formation of 4′-methylhydroxytolbutamide	59.6	pmol/10^6 cells/min
CYP2C19: rate of formation of 4′-hydroxymephenytoin	68.9	pmol/10^6 cells/min
CYP2D6: rate of formation of dextrorphan	30.5	pmol/10^6 cells/min
CYP2E1: rate of formation of 6-hydroxychlorzoxazone	19.5	pmol/10^6 cells/min
CYP3A4: rate of formation of 6β-hydroxytestosterone	99.1	pmol/10^6 cells/min

[2] **genotyping data will be provided on the Celsis website as the data are made available**

Donor Demographics, as reported to Celsis | In Vitro Technologies:

Age: 52 Race: C Cause of death: Anoxia; 2nd to Cardiac Arrest Height: 5'2" Weight: 48.2Kg

Social history:

No ETOH; Tobacco: 2ppd x 35yrs, Marijuana daily

Medical history:

COPD

Serology:

EBV	Positive
RPR	Negative
CMV	Positive
Hepatitis B	Negative
Hepatitis C	Negative
HIV	Negative

Confluence – Day 5

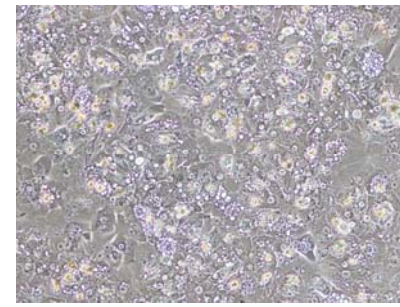

Carolyn Watt

Caution: This product was prepared from fresh human tissue. Treat all products containing human-derived materials as potentially infectious, as no known test methods can offer assurance that products derived from human tissues will not transmit infectious agents.

These products are for research use only. Do not use in animals or humans. These products have not been approved for any diagnostic or clinical procedures.

1450 South Rolling Road Baltimore, MD 21227 Toll Free 888.488.3232 Fax 410.455.1245 www.celsis.com/ivt

PLATEABLE CRYOPRESERVED FEMALE HUMAN HEPATOCYTES

PRODUCT NUMBER: F00995-P

Lot Number: GNA **Storage Conditions:** below -150ºC (vapour phase of liquid nitrogen freezer)

Test Results:

Specification	Result
>70% post-thaw viability by trypan blue exclusion	83 %
≥ 5 million viable cells	7.26 million viable cells
≥ 2 PC/VC ratio after 48 hours with 25 µM rifampin	4.24
CYP3A4: basal rate of formation of 6β-hydroxytestosterone at day 5	26.4 pmol/10^6 cells/min
≥ 2 PC/VC ratio after 48 hours with 50 µM omeprazole	18.7
CYP1A2: basal rate of formation of acetaminophen at day 5	1.53 pmol/10^6 cells/min
PC/VC ratio after 48 hours with 1 mM phenobarbital	3.89
CYP2B6: basal rate of formation of hydroxybuproprion at day 5	0.908 pmol/10^6 cells/min
≥ 0.1 OD MTT value at day 5	0.241 OD
≥70% confluent monolayer at day 5	85 %

Lot Characterization Results:

Assay	Result	
ECOD: total rate of formation of 7-HC and metabolites	173	pmol/10^6 cells/min
UGT/ST:		
rate of formation of 7-hydroxycoumarin glucuronide	473	pmol/10^6 cells/min
rate of formation of 7-hydroxycoumarin sulfate	99.9	pmol/10^6 cells/min
CYP1A2: rate of formation of acetaminophen	71.5	pmol/10^6 cells/min
CYP2A6: total rate of formation of 7-HC and metabolites	131	pmol/10^6 cells/min
CYP2C9: rate of formation of 4′-methylhydroxytolbutamide	36.8	pmol/10^6 cells/min
CYP2C19: rate of formation of 4′-hydroxymephenytoin	27.4	pmol/10^6 cells/min
CYP2D6: rate of formation of dextrorphan	19.9	pmol/10^6 cells/min
CYP2E1: rate of formation of 6-hydroxychlorzoxazone	16.9	pmol/10^6 cells/min
CYP3A4: rate of formation of 6β-hydroxytestosterone	62.0	pmol/10^6 cells/min

[2] **genotyping data will be provided on the Celsis website as the data are made available**

Donor Demographics, as reported to Celsis | In Vitro Technologies:

Age: 71 Race: C Cause of death: CVA Height: 66" Weight: 49 Kg

Social history: ETOH: Wine daily x 50yrs, Tobacco: 2ppd x 56yrs, Drugs: Heroine (IVDA), Marijuana, and Cocaine in 1960's/70's

Medical history: Sepsis 1 month ago, aneurysm 5 years ago, HTN for 15 years non compliant, seizures, COPD for 20 years, circulatory problems, bilateral forearm rash, blocked vessels to lower legs, colitis for 40 years, benign laryngeal polyp, lower back pain for 5 years, DM. Medication: Dilantin, HTN

Confluence – Day 5

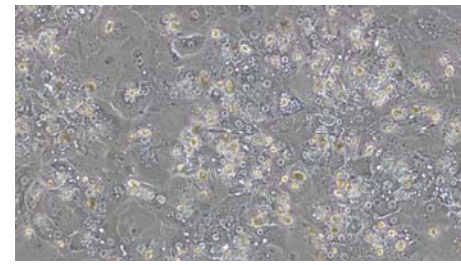

Serology:

EBV	Not reported	Hepatitis B	Negative
RPR	Negative	Hepatitis C	Negative
CMV	Positive	HIV	Negative

Carolyn Watt

Caution: This product was prepared from fresh human tissue. Treat all products containing human-derived materials as potentially infectious, as no known test methods can offer assurance that products derived from human tissues will not transmit infectious agents.

These products are for research use only. Do not use in animals or humans. These products have not been approved for any diagnostic or clinical procedures.

1450 South Rolling Road Baltimore, MD 21227 Toll Free 888.488.3232 Fax 410.455.1245 www.celsis.com/ivt

PLATEABLE CRYOPRESERVED FEMALE HUMAN HEPATOCYTES
PRODUCT NUMBER: F00995-P

Lot Number: IPH

Storage Conditions: below -150°C (vapour phase of liquid nitrogen freezer)

Test Results:

Specification	Result
>70% post-thaw viability by trypan blue exclusion	83 %
≥ 5 million viable cells	8.10 million viable cells
≥ 2 PC/VC ratio after 48 hours with 25 µM rifampin	5.21
≥ 2 PC/VC ratio after 48 hours with 50 µM omeprazole	6.20
PC/VC ratio after 48 hours with 1 mM phenobarbital	9.17
≥ 0.1 OD MTT value at day 5	0.284 OD
≥70% confluent monolayer at day 5	85 %

Lot Characterization Results:

Assay	Result	
ECOD: total rate of formation of 7-HC and metabolites	59.7	pmol/10^6 cells/min
UGT/ST:		
rate of formation of 7-hydroxycoumarin glucuronide	401	pmol/10^6 cells/min
rate of formation of 7-hydroxycoumarin sulfate	18.6	pmol/10^6 cells/min
CYP1A2: rate of formation of acetaminophen	5.80	pmol/10^6 cells/min
CYP2A6: total rate of formation of 7-HC and metabolites	64.0	pmol/10^6 cells/min
CYP2C9: rate of formation of 4′-methylhydroxytolbutamide	56.3	pmol/10^6 cells/min
CYP2C19: rate of formation of 4′-hydroxymephenytoin	1.99	pmol/10^6 cells/min
CYP2D6: rate of formation of dextrorphan	56.4	pmol/10^6 cells/min
CYP2E1: rate of formation of 6-hydroxychlorzoxazone	26.3	pmol/10^6 cells/min
CYP3A4: rate of formation of 6β-hydroxytestosterone	69.6	pmol/10^6 cells/min

genotyping data will be provided on the Celsis website as the data are made available

Donor Demographics, as reported to Celsis | In Vitro Technologies:

Age: 52 Race: C Cause of death: Anoxia; 2nd to CVA Height: 59" Weight: 65 Kg

Social history:

No ETOH, tobacco or drug use.

Medical history:

Cardiac arrest, anemia, lice, malnutrition, uterine leiomyoma (non cancerous cyst)

Serology:

EBV	Not reported
RPR	Negative
CMV	Negative
Hepatitis B	Negative
Hepatitis C	Negative
HIV	Negative

Carolyn P. Watt

Caution: This product was prepared from fresh human tissue. Treat all products containing human-derived materials as potentially infectious, as no known test methods can offer assurance that products derived from human tissues will not transmit infectious agents.

These products are for research use only. Do not use in animals or humans. These products have not been approved for any diagnostic or clinical procedures.

1450 South Rolling Road Baltimore, MD 21227 Toll Free 888.488.3232 Fax 410.455.1245 www.celsis.com/ivt

PLATEABLE CRYOPRESERVED FEMALE HUMAN HEPATOCYTES
PRODUCT NUMBER: F00995-P

Lot Number: RSF

Storage Conditions: below -150°C (vapour phase of liquid nitrogen freezer)

Test Results:

Specification	Result
>70% post-thaw viability by trypan blue exclusion	86 %
≥ 5 million viable cells	12.1 million viable cells
≥ 2 PC/VC ratio after 48 hours with 25 µM rifampin	15.8
≥ 2 PC/VC ratio after 48 hours with 50 µM omeprazole	17.1
PC/VC ratio after 48 hours with 1 mM phenobarbital	7.68
≥ 0.1 OD MTT value at day 5	0.309 OD
≥70% confluent monolayer at day 5	88 %

Lot Characterization Results:

Assay	Result	
ECOD: total rate of formation of 7-HC and metabolites	78.3	pmol/10^6 cells/min
UGT/ST:		
rate of formation of 7-hydroxycoumarin glucuronide	481	pmol/10^6 cells/min
rate of formation of 7-hydroxycoumarin sulfate	46.3	pmol/10^6 cells/min
CYP1A2: rate of formation of acetaminophen	2.37	pmol/10^6 cells/min
CYP2A6: total rate of formation of 7-HC and metabolites	20.4	pmol/10^6 cells/min
CYP2C9: rate of formation of 4'-methylhydroxytolbutamide	41.3	pmol/10^6 cells/min
CYP2C19: rate of formation of 4'-hydroxymephenytoin	0.50	pmol/10^6 cells/min
CYP2D6: rate of formation of dextrorphan	4.55	pmol/10^6 cells/min
CYP2E1: rate of formation of 6-hydroxychlorzoxazone	16.9	pmol/10^6 cells/min
CYP3A4: rate of formation of 6β-hydroxytestosterone	16.4	pmol/10^6 cells/min

genotyping data will be provided on the Celsis website as the data are made available

Donor Demographics, as reported to Celsis | In Vitro Technologies:

Age: 52 Race: C Cause of death: Respiratory failure/ Anoxia Height: 65" Weight: 181lb

Social history:

ETOH: 2-3 glasses whisky x 20 yrs
Tobacco: 2ppd-quit for 20 years restarted x 8 months

Drugs: marijuana>20 years

Medical history:

Hysterectomy for fibroids

Serology:

EBV	Positive
RPR	Negative
CMV	Positive
Hepatitis B	Negative
Hepatitis C	Negative
HIV	Negative

Carolyn P. Watt

Caution: This product was prepared from fresh human tissue. Treat all products containing human-derived materials as potentially infectious, as no known test methods can offer assurance that products derived from human tissues will not transmit infectious agents.

These products are for research use only. Do not use in animals or humans. These products have not been approved for any diagnostic or clinical procedures.

1450 South Rolling Road Baltimore, MD 21227 Toll Free 888.488.3232 Fax 410.455.1245 www.celsis.com/ivt

References

Aguirre, V., Uchida, T., Yenush, L., Davis, R., & White, M.F. 2000. The c-Jun NH(2)-terminal kinase promotes insulin resistance during association with insulin receptor substrate-1 and phosphorylation of Ser(307). *J.Biol.Chem.*, 275, (12) 9047-9054 available from: PM:10722755

Ahmed, A., Rabbitt, E., Brady, T., Brown, C., Guest, P., Bujalska, I.J., Doig, C., Newsome, P.N., Hubscher, S., Elias, E., Adams, D.H., Tomlinson, J.W., & Stewart, P.M. 2012. A switch in hepatic cortisol metabolism across the spectrum of non alcoholic fatty liver disease. *PLoS.One.*, 7, (2) e29531 available from: PM:22363403

Alberti, K.G., Zimmet, P., & Shaw, J. 2006. Metabolic syndrome--a new world-wide definition. A Consensus Statement from the International Diabetes Federation. *Diabet.Med.*, 23, (5) 469-480 available from: PM:16681555

Alberts, P., Engblom, L., Edling, N., Forsgren, M., Klingstrom, G., Larsson, C., Ronquist-Nii, Y., Ohman, B., & Abrahmsen, L. 2002. Selective inhibition of 11 beta-hydroxysteroid dehydrogenase type 1 decreases blood glucose concentrations in hyperglycaemic mice. *Diabetologia*, 45, (11) 1528-1532 available from: ISI:000179792900008

Alberts, P., Nilsson, C., Selen, G., Engblom, L.O.M., Edling, N.H.M., Norling, S., Klingstrom, G., Larsson, C., Forsgren, M., Ashkzari, M., Nilsson, C.E., Fiedler, M., Bergqvist, E., Ohman, B., Bjorkstrand, E., & Abrahmsen, L.B. 2003. Selective inhibition of 11 beta-hydroxysteroid dehydrogenase type 1 improves hepatic insulin sensitivity in hyperglycemic mice strains. *Endocrinology*, 144, (11) 4755-4762 available from: ISI:000186178300016

Alessi, D.R., James, S.R., Downes, C.P., Holmes, A.B., Gaffney, P.R., Reese, C.B., & Cohen, P. 1997. Characterization of a 3-phosphoinositide-dependent protein kinase which phosphorylates and activates protein kinase Balpha. *Curr.Biol.*, 7, (4) 261-269 available from: PM:9094314

Alkhouri, N., Dixon, L.J., & Feldstein, A.E.2009. Lipotoxicity in Nonalcoholic Fatty Liver Disease: Not All Lipids Are Created Equal. *Expert Rev Gastroenterol Hepatol.* 3(4):445-51 available from PM:19673631

Altomonte, J., Richter, A., Harbaran, S., Suriawinata, J., Nakae, J., Thung, S.N., Meseck, M., Accili, D., & Dong, H. 2003. Inhibition of Foxo1 function is associated with improved fasting glycemia in diabetic mice. *Am.J.Physiol Endocrinol.Metab*, 285, (4) E718-E728 available from: PM:12783775

Amatruda, J.M., Danahy, S.A., & Chang, C.L. 1983. The effects of glucocorticoids on insulin-stimulated lipogenesis in primary cultures of rat hepatocytes. *Biochem.J.*, 212, (1) 135-141 available from: PM:6347191

Anai, M., Funaki, M., Ogihara, T., Terasaki, J., Inukai, K., Katagiri, H., Fukushima, Y., Yazaki, Y., Kikuchi, M., Oka, Y., & Asano, T. 1998. Altered expression levels and impaired steps in the pathway to phosphatidylinositol 3-kinase activation via insulin

receptor substrates 1 and 2 in Zucker fatty rats. *Diabetes*, 47, (1) 13-23 available from: PM:9421369

Andersen, A.S., Kjeldsen, T., Wiberg, F.C., Vissing, H., Schaffer, L., Rasmussen, J.S., De, M.P., & Moller, N.P. 1992. Identification of determinants that confer ligand specificity on the insulin receptor. *J.Biol.Chem.*, 267, (19) 13681-13686 available from: PM:1320025

Andersson, S., Berman, D.M., Jenkins, E.P., & Russell, D.W. 1991. Deletion of steroid 5 alpha-reductase 2 gene in male pseudohermaphroditism. *Nature*, 354, (6349) 159-161 available from: PM:1944596

Andersson, S. & Russell, D.W. 1990. Structural and biochemical properties of cloned and expressed human and rat steroid 5 alpha-reductases. *Proc.Natl.Acad.Sci.U.S.A*, 87, (10) 3640-3644 available from: PM:2339109

Andrews, R.C., Rooyackers, O., & Walker, B.R. 2003. Effects of the 11 beta-hydroxysteroid dehydrogenase inhibitor carbenoxolone on insulin sensitivity in men with type 2 diabetes. *J.Clin.Endocrinol.Metab*, 88, (1) 285-291 available from: PM:12519867

Anstee, Q.M., Targher, G., & Day, C.P. 2013. Progression of NAFLD to diabetes mellitus, cardiovascular disease or cirrhosis. *Nat.Rev.Gastroenterol.Hepatol.*, 10, (6) 330-344 available from: PM:23507799

Araki, E., Lipes, M.A., Patti, M.E., Bruning, J.C., Haag, B., III, Johnson, R.S., & Kahn, C.R. 1994. Alternative pathway of insulin signalling in mice with targeted disruption of the IRS-1 gene. *Nature*, 372, (6502) 186-190 available from: PM:7526222

Arlt, W., Biehl, M., Taylor, A.E., Hahner, S., Libe, R., Hughes, B.A., Schneider, P., Smith, D.J., Stiekema, H., Krone, N., Porfiri, E., Opocher, G., Bertherat, J., Mantero, F., Allolio, B., Terzolo, M., Nightingale, P., Shackleton, C.H., Bertagna, X., Fassnacht, M., & Stewart, P.M. 2011. Urine steroid metabolomics as a biomarker tool for detecting malignancy in adrenal tumors. *J.Clin.Endocrinol.Metab*, 96, (12) 3775-3784 available from: PM:21917861

Arlt, W. & Stewart, P.M. 2005. Adrenal corticosteroid biosynthesis, metabolism, and action. *Endocrinol.Metab Clin.North Am.*, 34, (2) 293-313, viii available from: PM:15850843

Audet-Walsh, E., Bellemare, J., Nadeau, G., Lacombe, L., Fradet, Y., Fradet, V., Huang, S.P., Bao, B.Y., Douville, P., Girard, H., Guillemette, C., & Levesque, E. 2011. SRD5A polymorphisms and biochemical failure after radical prostatectomy. *Eur.Urol.*, 60, (6) 1226-1234 available from: PM:21715084

Azzout-Marniche, D., Becard, D., Guichard, C., Foretz, M., Ferre, P., & Foufelle, F. 2000. Insulin effects on sterol regulatory-element-binding protein-1c (SREBP-1c) transcriptional activity in rat hepatocytes. *Biochem.J.*, 350 Pt 2, 389-393 available from: PM:10947952 Ballotti, R., Le Marchand-Brustel, Y., Gammeltoft, S., & Van, O.E. 1989.

Insulin receptor: tyrosine kinase activity and insulin action. *Reprod.Nutr.Dev.*, 29, (6) 653-661 available from: PM:2534271

Barf, T., Vallgarda, J., Emond, R., Haggstrom, C., Kurz, G., Nygren, A., Larwood, V., Mosialou, E., Axelsson, K., Olsson, R., Engblom, L., Edling, N., Ronquist-Nii, Y., Ohman, B., Alberts, P., & Abrahmsen, L. 2002. Arylsulfonamidothiazoles as a new class of potential antidiabetic drugs. Discovery of potent and selective inhibitors of the 11 beta-hydroxysteroid dehydrogenase type 1. *Journal of Medicinal Chemistry*, 45, (18) 3813-3815 available from: ISI:000177657600001

Barrows, B.R., & Parks, E.J. 2006. Contributions of different fatty acid sources to very low-density lipoprotein-triacylglycerol in the fasted and fed states. *J Clin Endocrinol Metab.,* 91(4):1446-52 available from PM:16449340

Barrows, B.R., Timlin, M.T., & Parks, E.J. 2005. Spillover of dietary fatty acids and use of serum nonesterified fatty acids for the synthesis of VLDL-triacylglycerol under two different feeding regimens. *Diabetes*, 54, (9) 2668-2673 available from: PM:16123356

Barsh, G.S., Farooqi, I.S., & O'Rahilly, S. 2000. Genetics of body-weight regulation. *Nature*, 404, (6778) 644-651 available from: PM:10766251

Baxter, J.D. & Forsham, P.H. 1972. Tissue effects of glucocorticoids. *Am.J.Med.*, 53, (5) 573-589 available from: PM:4342884

Beato, M. 1989. Gene-Regulation by Steroid-Hormones. *Cell*, 56, (3) 335-344 available from: ISI:A1989T189500004

Beato, M., Truss, M., & Chavez, S. 1996. Control of transcription by steroid hormones. *Basis for Cancer Management*, 784, 93-123 available from: ISI:A1996BF66W00009

Becker, K.L., Bilezikian, J.P, Bremner, W.J. & Hung, W. (2001). Principles and practice of endocrinology and metabolism, 3 edition.

Benten, W.P., Lieberherr, M., Stamm, O., Wrehlke, C., Guo, Z., & Wunderlich, F. 1999. Testosterone signaling through internalizable surface receptors in androgen receptor-free macrophages. *Mol.Biol.Cell*, 10, (10) 3113-3123 available from: PM:10512854

Bergsten, P., Grapengiesser, E., Gylfe, E., Tengholm, A., & Hellman, B. 1994. Synchronous oscillations of cytoplasmic Ca2+ and insulin release in glucose-stimulated pancreatic islets. *J.Biol.Chem.*, 269, (12) 8749-8753 available from: PM:8132606

Berk, P.D. 2008. Regulatable fatty acid transport mechanisms are central to the pathophysiology of obesity, fatty liver, and metabolic syndrome. *Hepatology*, 48, (5) 1362-1376 available from: PM:18972439

Berthiaume, M., Laplante, M., Festuccia, W., Gelinas, Y., Poulin, S., Lalonde, J., Joanisse, D.R., Thieringer, R., & Deshaies, Y. 2007. Depot-specific modulation of rat intraabdominal adipose tissue lipid metabolism by pharmacological inhibition of 11beta-

hydroxysteroid dehydrogenase type 1. *Endocrinology*, 148, (5) 2391-2397 available from: PM:17272400

Bisgaard, H.C., Santoni-Rugiu, E., Nagy, P., & Thorgeirsson, S.S. 1998. Modulation of the plasminogen activator/plasmin system in rat liver regenerating by recruitment of oval cells. *Lab Invest*, 78, (3) 237-246 available from: PM:9520937

Bocharov, A.V., Huang, W., Vishniakova, T.G., Zaitseva, E.V., Frolova, E.G., Rampal, P., & Bertolotti, R. 1995. Glucocorticoids upregulate high-affinity, high-density lipoprotein binding sites in rat hepatocytes. *Metabolism*, 44, (6) 730-738 available from: PM:7783657

Boden, G., Jadali, F., White, J., Liang, Y., Mozzoli, M., Chen, X., Coleman, E., & Smith, C. 1991. Effects of fat on insulin-stimulated carbohydrate metabolism in normal men. *J.Clin.Invest*, 88, (3) 960-966 available from: PM:1885781

Bonen, A., Chabowski, A., Luiken, J.J., & Glatz, J.F. 2007. Is membrane transport of FFA mediated by lipid, protein, or both? Mechanisms and regulation of protein-mediated cellular fatty acid uptake: molecular, biochemical, and physiological evidence. *Physiology.(Bethesda.)*, 22, 15-29 available from: PM:17342856

Boron, W.F. & Boulpaep, E.L. (2009).Medical physiology, 2 edition, Saunders Elsevier.

Bouzakri, K., Karlsson, H.K., Vestergaard, H., Madsbad, S., Christiansen, E., & Zierath, J.R. 2006. IRS-1 serine phosphorylation and insulin resistance in skeletal muscle from pancreas transplant recipients. *Diabetes*, 55, (3) 785-791 available from: PM:16505244

Breckenridge, W.C., Little, J.A., Alaupovic, P., Wang, C.S., Kuksis, A., Kakis, G., Lindgren, F., & Gardiner, G. 1982. Lipoprotein abnormalities associated with a familial deficiency of hepatic lipase. *Atherosclerosis*, 45, (2) 161-179 available from: PM:6961921

Brien, T.G. 1981. Human corticosteroid binding globulin. *Clinical Endocrinology*., 14 193–212 available from PM:7021007

Brinkmann, A.O., Blok, L.J., De Ruiter, P.E., Doesburg, P., Steketee, K., Berrevoets, C.A., & Trapman, J. 1999. Mechanisms of androgen receptor activation and function. *J.Steroid Biochem.Mol.Biol.*, 69, (1-6) 307-313 available from: PM:10419007

Browning, J.D., Szczepaniak, L.S., Dobbins, R., Nuremberg, P., Horton, J.D., Cohen, J.C., Grundy, & S.M., Hobbs, H.H. 2004. Prevalence of hepatic steatosis in an urban population in the United States: impact of ethnicity.*Hepatology*, 40(6):1387-95 available from PM:15565570

Buckingham, J.C. 2006. Glucocorticoids: exemplars of multi-tasking. *Br.J.Pharmacol.*, 147 Suppl 1, S258-S268 available from: PM:16402112

Bujalska, I.J., Gathercole, L.L., Tomlinson, J.W., Darimont, C., Ermolieff, J., Fanjul, A.N., Rejto, P.A., & Stewart, P.M. 2008. A novel selective 11 beta-hydroxysteroid

dehydrogenase type 1 inhibitor prevents human adipogenesis. *Journal of Endocrinology*, 197, (2) 297-307 available from: ISI:000255980600011

Buque, X., Cano, A., Miquilena-Colina, M.E., Garcia-Monzon, C., Ochoa, B., & Aspichueta, P. 2012. High insulin levels are required for FAT/CD36 plasma membrane translocation and enhanced fatty acid uptake in obese Zucker rat hepatocytes. *Am.J.Physiol Endocrinol.Metab*, 303, (4) E504-E514 available from: PM:22693206

Cai, D., Dhe-Paganon, S., Melendez, P.A., Lee, J., & Shoelson, S.E. 2003. Two new substrates in insulin signaling, IRS5/DOK4 and IRS6/DOK5. *J.Biol.Chem.*, 278, (28) 25323-25330 available from: PM:12730241

Can, S., Zhu, Y.S., Cai, L.Q., Ling, Q., Katz, M.D., Akgun, S., Shackleton, C.H.L., & Imperato-McGinley, J. 1998. The identification of 5 alpha-reductase-2 and 17 beta-hydroxysteroid dehydrogenase-3 gene defects in male pseudohermaphrodites from a turkish kindred. *Journal of Clinical Endocrinology & Metabolism*, 83, (2) 560-569 available from: ISI:000071823900045

Cantagrel, V., Lefeber, D.J., Ng, B.G., Guan, Z., Silhavy, J.L., Bielas, S.L., Lehle, L., Hombauer, H., Adamowicz, M., Swiezewska, E., de Brouwer, A.P., Blumel, P., Sykut-Cegielska, J., Houliston, S., Swistun, D., Ali, B.R., Dobyns, W.B., Babovic-Vuksanovic, D., van Bokhoven, H., Wevers, R.A., Raetz, C.R., Freeze, H.H., Morava, E., Al Gazali, L., & Gleeson, J.G. 2010. SRD5A3 is required for converting polyprenol to dolichol and is mutated in a congenital glycosylation disorder. *Cell*, 142, (2) 203-217 available from: PM:20637498

Caro, J.F. & Amatruda, J.M. 1982. Glucocorticoid-induced insulin resistance: the importance of postbinding events in the regulation of insulin binding, action, and degradation in freshly isolated and primary cultures of rat hepatocytes. *J.Clin.Invest*, 69, (4) 866-875 available from: PM:7042756

Carr, B.R. & Simpson, E.R. 1984. Cholesterol synthesis by human fetal hepatocytes: effects of hormones. *J.Clin.Endocrinol.Metab*, 58, (6) 1111-1116 available from: PM:6725509

Chalasani, N., Wilson, L., Kleiner, D.E., Cummings, O.W., Brunt, E.M., & Unalp, A. 2008. Relationship of steatosis grade and zonal location to histological features of steatohepatitis in adult patients with non-alcoholic fatty liver disease. *J.Hepatol.*, 48, (5) 829-834 available from: PM:18321606

Chalasani, N., Younossi, Z., Lavine, J.E., Diehl, A.M., Brunt, E.M., Cusi, K., Charlton, M., & Sanyal, A.J. 2012. The diagnosis and management of non-alcoholic fatty liver disease: Practice guideline by the American Association for the Study of Liver Diseases, American College of Gastroenterology, and the American Gastroenterological Association. *Am.J.Gastroenterol.*, 107, (6) 811-826 available from: PM:22641309

Chan, A.O., But, B.W., Lau, G.T., Lam, A.L., Ng, K.L., Lam, Y.Y., Lee, C.Y., & Shek, C.C. 2009. Diagnosis of 5alpha-reductase 2 deficiency: a local experience. *Hong.Kong.Med.J.*, 15, (2) 130-135 available from: PM:19342739

Chazenbalk, G., Singh, P., Irge, D., Shah, A., Abbott, D.H., & Dumesic, D.A. 2013. Androgens inhibit adipogenesis during human adipose stem cell commitment to preadipocyte formation. *Steroids*, 78, (9) 920-926 available from: PM:23707571

Chen, H., Zhang, Z.W., Guo, Y., Wang, Y., Liu, Y., Luo, N., & Zhu, Y. 2012. The proliferative role of insulin and the mechanism underlying this action in human breast cancer cell line MCF-7. *J.BUON.*, 17, (4) 658-662 available from: PM:23335521

Cheon, C.K. 2011. Practical approach to steroid 5alpha-reductase type 2 deficiency. *European Journal of Pediatrics*, 170, (1) 1-8 available from: ISI:000286339900001

Chen, H.C., Smith, S.J., Ladha, Z., Jensen, D.R., Ferreira, L.D., Pulawa, L.K., McGuire, J.G., Pitas, R.E., Eckel, R.H., & Farese, R.V. Jr. 2002. Increased insulin and leptin sensitivity in mice lacking acyl CoA:diacylglycerol acyltransferase 1. *J Clin Invest,*. 109(8):1049-55 available from: PM:11956242

Chiang, D.J., Pritchard, M.T., & Nagy, L.E. 2011. Obesity, diabetes mellitus, and liver fibrosis. *Am.J.Physiol Gastrointest.Liver Physiol*, 300, (5) G697-G702 available from: PM:21350183

Choi, C.S., Savage, D.B., Kulkarni, A., Yu, X.X., Liu, Z.X., Morino, K., Kim, S., Distefano, A., Samuel, V.T., Neschen, S., Zhang, D., Wang, A., Zhang, X.M., Kahn, M., Cline, G.W.,Pandey, S.K., Geisler, J.G., Bhanot, S., Monia, B.P., & Shulman, G.I. 2007. Suppression of diacylglycerol acyltransferase-2 (DGAT2), but not DGAT1, with antisense oligonucleotides reverses diet-induced hepatic steatosis and insulin resistance. *J Biol Chem.*, 282(31):22678-88 available from: PM:17526931

Chung, W.M., Chang, W.C., Chen, L., Lin, T.Y., Chen, L.C., Hung, Y.C., & Ma, W.L. 2014. Ligand-independent androgen receptors promote ovarian teratocarcinoma cell growth by stimulating self-renewal of cancer stem/progenitor cells. *Stem Cell Res.*, 13, (1) 24-35 available from: PM:24793306

Clark, B.J., Ranganathan, V., & Combs, R. 2000. Post-translational regulation of steroidogenic acute regulatory protein by cAMP-dependent protein kinase A. *Endocr.Res.*, 26, (4) 681-689 available from: PM:11196444

Clark, B.J., Soo, S.C., Caron, K.M., Ikeda, Y., Parker, K.L., & Stocco, D.M. 1995. Hormonal and developmental regulation of the steroidogenic acute regulatory protein. *Mol.Endocrinol.*, 9, (10) 1346-1355 available from: PM:8544843

Coffey, D.S. 1993. Prostate cancer. An overview of an increasing dilemma. *Cancer*, 71, (3 Suppl) 880-886 available from: PM:8428342

Cole, T.J., Blendy, J.A., Monaghan, A.P., Krieglstein, K., Schmid, W., Aguzzi, A., Fantuzzi, G., Hummler, E., Unsicker, K., & Schutz, G. 1995. Targeted Disruption of the Glucocorticoid Receptor Gene Blocks Adrenergic Chromaffin Cell-Development and Severely Retards Lung Maturation. *Genes & Development*, 9, (13) 1608-1621 available from: ISI:A1995RK42200005

Cox, R.A., & García-Palmieri, M.R. 1990. Clinical Methods: The History, Physical, and Laboratory Examinations. 3rd edition. Chapter 31. available from PM: 21250192

Creager, M.A., Luscher, T.F., Cosentino, F., & Beckman, J.A. 2003. Diabetes and vascular disease: pathophysiology, clinical consequences, and medical therapy: Part I. *Circulation*, 108, (12) 1527-1532 available from: PM:14504252

Crowley, R.K., Hughes, B., Gray, J., McCarthy, T., Hughes, S., Shackleton, C.H., Crabtree, N., Nightingale, P., Stewart, P.M., & Tomlinson, J.W. 2014. Longitudinal changes in glucocorticoid metabolism are associated with later development of adverse metabolic phenotype. *Eur.J.Endocrinol.*, 171, (4) 433-442 available from: PM:24986533

D'Souza, A.M., Beaudry, J.L., Szigiato, A.A., Trumble, S.J., Snook, L.A., Bonen, A., Giacca, A., & Riddell, M.C. 2012. Consumption of a high-fat diet rapidly exacerbates the development of fatty liver disease that occurs with chronically elevated glucocorticoids. *Am.J.Physiol Gastrointest.Liver Physiol*, 302, (8) G850-G863 available from: PM:22268100

Dalen, K.T., Dahl, T., Holter, E., Arntsen, B., Londos, C., Sztalryd, C., & Nebb, H.I. 2007. LSDP5 is a PAT protein specifically expressed in fatty acid oxidizing tissues. *Biochim.Biophys.Acta*, 1771, (2) 210-227 available from: PM:17234449

Debuyser, A., Drews, G., & Henquin, J.C. 1991. Adrenaline inhibition of insulin release: role of the repolarization of the B cell membrane. *Pflugers Arch.*, 419, (2) 131-137 available from: PM:1961683

DeFronzo, R.A., Jacot, E., Jequier, E., Maeder, E., Wahren, J., & Felber, J.P. 1981. The effect of insulin on the disposal of intravenous glucose. Results from indirect calorimetry and hepatic and femoral venous catheterization. *Diabetes*, 30, (12) 1000-1007 available from: PM:7030826

Dich, J., Bro, B., Grunnet, N., Jensen, F., & Kondrup, J. 1983. Accumulation of triacylglycerol in cultured rat hepatocytes is increased by ethanol and by insulin and dexamethasone. *Biochem.J.*, 212, (3) 617-623 available from: PM:6349622

Dimitriadis, G., Leighton, B., Parry-Billings, M., Sasson, S., Young, M., Krause, U., Bevan, S., Piva, T., Wegener, G., & Newsholme, E.A. 1997. Effects of glucocorticoid excess on the sensitivity of glucose transport and metabolism to insulin in rat skeletal muscle. *Biochem.J.*, 321 (Pt 3), 707-712 available from: PM:9032457

Dina, C., Meyre, D., Gallina, S., Durand, E., Korner, A., Jacobson, P., Carlsson, L.M., Kiess, W., Vatin, V., Lecoeur, C., Delplanque, J., Vaillant, E., Pattou, F., Ruiz, J., Weill, J., Levy-Marchal, C., Horber, F., Potoczna, N., Hercberg, S., Le, S.C., Bougneres, P., Kovacs, P., Marre, M., Balkau, B., Cauchi, S., Chevre, J.C., & Froguel, P. 2007. Variation in FTO contributes to childhood obesity and severe adult obesity. *Nat.Genet.*, 39, (6) 724-726 available from: PM:17496892

Divertie, G.D., Jensen, M.D., & Miles, J.M. 1991. Stimulation of lipolysis in humans by physiological hypercortisolemia. *Diabetes*, 40, (10) 1228-1232 available from: PM:1936585

Djurhuus, C.B., Gravholt, C.H., Nielsen, S., Mengel, A., Christiansen, J.S., Schmitz, O.E., & Moller, N. 2002. Effects of cortisol on lipolysis and regional interstitial glycerol levels in humans. *Am.J.Physiol Endocrinol.Metab*, 283, (1) E172-E177 available from: PM:12067858

Dolinsky, V.W., Douglas, D.N., Lehner, R., & Vance, D.E. 2004. Regulation of the enzymes of hepatic microsomal triacylglycerol lipolysis and re-esterification by the glucocorticoid dexamethasone. *Biochem.J.*, 378, (Pt 3) 967-974 available from: PM:14662008

Donnelly, K.L., Smith, C.I., Schwarzenberg, S.J., Jessurun, J., Boldt, M.D., & Parks, E.J. 2005. Sources of fatty acids stored in liver and secreted via lipoproteins in patients with nonalcoholic fatty liver disease. *J.Clin.Invest*, 115, (5) 1343-1351 available from: PM:15864352

Dowman, J.K., Armstrong, M.J., Tomlinson, J.W., & Newsome, P.N. 2011. Current therapeutic strategies in non-alcoholic fatty liver disease. *Diabetes Obes.Metab*, 13, (8) 692-702 available from: PM:21449949

Dowman, J.K., Hopkins, L.J., Reynolds, G.M., Armstrong, M.J., Nasiri, M., Nikolaou, N., van Houten, E.L., Visser, J.A., Morgan, S.A., Lavery, G.G., Oprescu, A., Hubscher, S.G., Newsome, P.N., & Tomlinson, J.W. 2013. Loss of 5alpha-reductase type 1 accelerates the development of hepatic steatosis but protects against hepatocellular carcinoma in male mice. *Endocrinology*, 154, (12) 4536-4547 available from: PM:24080367

Dowman, J.K., Hopkins, L.J., Reynolds, G.M., Nikolaou, N., Armstrong, M.J., Shaw, J.C., Houlihan, D.D., Lalor, P.F., Tomlinson, J.W., Hubscher, S.G., & Newsome, P.N. 2014. Development of Hepatocellular Carcinoma in a Murine Model of Nonalcoholic Steatohepatitis Induced by Use of a High-Fat/Fructose Diet and Sedentary Lifestyle. *Am.J.Pathol.* available from: PM:24650559

Dowman, J.K., Tomlinson, J.W., & Newsome, P.N. 2010. Pathogenesis of non-alcoholic fatty liver disease. *QJM.*, 103, (2) 71-83 available from: PM:19914930

Downward, J. 1998. Mechanisms and consequences of activation of protein kinase B/Akt. *Curr.Opin.Cell Biol.*, 10, (2) 262-267 available from: PM:9561851

Droste, S.K., de Groote, L., Atkinson, H.C., Lightman, S.L., Reul, J.M., & Linthorst, A.C. 2008. Corticosterone levels in the brain show a distinct ultradian rhythm but a delayed response to forced swim stress. Endocrinology., 149:3244–3253 available from PM:18356272

Drouin, J., Sun, Y.L., Chamberland, M., Gauthier, Y., De Lean, A., Nemer, M., & Schmidt, T.J. 1993. Novel glucocorticoid receptor complex with DNA element of the hormone-repressed POMC gene. *EMBO J.*, 12, (1) 145-156 available from: PM:8428574

Duncan, A.W., Dorrell, C., & Grompe, M. 2009. Stem cells and liver regeneration. *Gastroenterology*, 137, (2) 466-481 available from: PM:19470389

Dutta, A.K. 2015. Adiponutrin (PNPLA3) in liver fibrogenesis: Is unaltered HepG2 cell line a better model system compared to murine models? *Med Hypotheses,* 85(6):736-9 available from PM:26519102

Edgerton, D.S., Jacobson, P.B., Opgenorth, T.J., Zinker, B., Beno, D., von, G.T., Ohman, L., Scott, M., Neal, D., & Cherrington, A.D. 2006. Selective antagonism of the hepatic glucocorticoid receptor reduces hepatic glucose production. *Metabolism*, 55, (9) 1255-1262 available from: PM:16919547

Edwards, C.R., Stewart, P.M., Burt, D., Brett, L., McIntyre, M.A., Sutanto, W.S., de Kloet, E.R., & Monder, C. 1988. Localisation of 11 beta-hydroxysteroid dehydrogenase--tissue specific protector of the mineralocorticoid receptor. *Lancet*, 2, (8618) 986-989 available from: PM:2902493

Ekstedt, M., Franzen, L.E., Mathiesen, U.L., Thorelius, L., Holmqvist, M., Bodemar, G., & Kechagias, S. 2006. Long-term follow-up of patients with NAFLD and elevated liver enzymes. *Hepatology*, 44, (4) 865-873 available from: PM:17006923

Ekstedt, M., Hagstrom, H., Nasr, P., Fredrikson, M., Stal, P., Kechagias, S., & Hultcrantz, R. 2015. Fibrosis stage is the strongest predictor for disease-specific mortality in NAFLD after up to 33 years of follow-up. *Hepatology*, 61, (5) 1547-1554 available from: PM:25125077

Ellis, J.A., Panagiotopoulos, S., Akdeniz, A., Jerums, G., & Harrap, S.B. 2005. Androgenic correlates of genetic variation in the gene encoding 5alpha-reductase type 1. *J.Hum.Genet.*, 50, (10) 534-537 available from: PM:16155734

Esposito, D.L., Li, Y., Cama, A., & Quon, M.J. 2001. Tyr(612) and Tyr(632) in human insulin receptor substrate-1 are important for full activation of insulin-stimulated phosphatidylinositol 3-kinase activity and translocation of GLUT4 in adipose cells. *Endocrinology*, 142, (7) 2833-2840 available from: PM:11416002

Eyre, L.J., Rabbitt, E.H., Bland, R., Hughes, S.V., Cooper, M.S., Sheppard, M.C., Stewart, P.M., & Hewison, M. 2001. Expression of 11 beta-hydroxysteroid dehydrogenase in rat osteoblastic cells: pre-receptor regulation of glucocorticoid responses in bone. *J.Cell Biochem.*, 81, (3) 453-462 available from: PM:11255228

Faucher, F., Cantin, L., Van, L., Labrie, F., & Breton, R. 2008. Crystal Structures of Human Delta 4-3-Ketosteroid 5 beta-Reductase (AKR1D1) Reveal the Presence of an Alternative Binding Site Responsible for Substrate Inhibition. *Biochemistry*, 47, (51) 13537-13546 available from: ISI:000261768100010

Feldstein, A.E. 2010. Novel insights into the pathophysiology of nonalcoholic fatty liver disease. *Semin.Liver Dis.*, 30, (4) 391-401 available from: PM:20960378

Field, A.E., Coakley, E.H., Must, A., Spadano, J.L., Laird, N., Dietz, W.H., Rimm, E., & Colditz, G.A. 2001. Impact of overweight on the risk of developing common chronic diseases during a 10-year period. *Arch.Intern.Med.*, 161, (13) 1581-1586 available from: PM:11434789

Folch, J., Lees, M., Sloane Stanley, G.H. 1957. A simple method for the isolation and purification of total lipides from animal tissues. *J Biol Chem.*, 226(1):497-509 available from PM: 13428781

Franzese, A., Vajro, P., Argenziano, A., Puzziello, A., Iannucci, M.P., Saviano, M.C., Brunetti, F., & Rubino, A. 1997. Liver involvement in obese children - Ultrasonography and liver enzyme levels at diagnosis and during follow-up in an Italian population. *Digestive Diseases and Sciences*, 42, (7) 1428-1432 available from: ISI:A1997XN21600016

Fraser, R., Ingram, M.C., Anderson, N.H., Morrison, C., Davies, E., & Connell, J.M.C. 1999. Cortisol effects on body mass, blood pressure, and cholesterol in the general population. *Hypertension*, 33, (6) 1364-1368 available from: ISI:000080954700009

Frederiksen, D.W. & Wilson, J.D. 1971. Partial characterization of the nuclear reduced nicotinamide adenine dinucleotide phosphate: delta 4-3-ketosteroid 5 alpha-oxidoreductase of rat prostate. *J.Biol.Chem.*, 246, (8) 2584-2593 available from: PM:4396507

Galliard, T. 1971. The enzymic deacylation of phospholipids and galactolipids in plants. Purification and properties of a lipolytic acyl-hydrolase from potato tubers. *Biochem.J.*, 121, (3) 379-390 available from: PM:5154523

Gann, P.H., Hennekens, C.H., Ma, J., Longcope, C., & Stampfer, M.J. 1996. Prospective study of sex hormone levels and risk of prostate cancer. *J.Natl.Cancer Inst.*, 88, (16) 1118-1126 available from: PM:8757191

Gathercole, L.L., Bujalska, I.J., Stewart, P.M., & Tomlinson, J.W. 2007. Glucocorticoid modulation of insulin signaling in human subcutaneous adipose tissue. *J.Clin.Endocrinol.Metab*, 92, (11) 4332-4339 available from: PM:17711920

Gathercole, L.L., Chapman, M., Larner, D.P., Klusonova, P., Penning, T.M., Odermatt, A., Lavery, G.G. & Tomlinson, J.W. 2015. Female 5β-reductase knockout mice are protected from diet induced obesity, insulin resistance, and glucose intolerance. *endocrine Abstracts*.

Gathercole, L.L., Morgan, S.A., Bujalska, I.J., Stewart, P.M., & Tomlinson, J.W. 2011a. Short- and long-term glucocorticoid treatment enhances insulin signalling in human subcutaneous adipose tissue. *Nutr.Diabetes*, 1, e3 available from: PM:23154295

Gathercole, L.L., Morgan, S.A., Bujalska, I.J., Hauton, D., Stewart, P.M., & Tomlinson, J.W. 2011b. Regulation of lipogenesis by glucocorticoids and insulin in human adipose tissue. *PLoS.One.*, 6, (10) e26223 available from: PM:22022575

Giguere, V., Hollenberg, S.M., Rosenfeld, M.G., & Evans, R.M. 1986. Functional Domains of the Human Glucocorticoid Receptor. *Cell*, 46, (5) 645-652 available from: ISI:A1986D837600002

Giorgetti, S., Ballotti, R., Kowalski-Chauvel, A., Tartare, S., & Van, O.E. 1993. The insulin and insulin-like growth factor-I receptor substrate IRS-1 associates with and activates phosphatidylinositol 3-kinase in vitro. *J.Biol.Chem.*, 268, (10) 7358-7364 available from: PM:8385105

Giraudi, P.J., Becerra, V.J., Marin, V., Chavez-Tapia, N.C., Tiribelli, C., & Rosso, N. 2015. The importance of the interaction between hepatocyte and hepatic stellate cells in fibrogenesis induced by fatty accumulation. *Exp Mol Pathol.*, 98(1):85-92 available from PM:25533546

Giudetti, A.M. & Gnoni, G.V. 1998. Short-term effect of dexamethasone on fatty acid and cholesterol synthesis in isolated rat hepatocytes. *Biochem.Mol.Biol.Int.*, 44, (3) 515-521 available from: PM:9556212

Gomez-Lechon, M.J., Lopez, P., Donato, T., Montoya, A., Larrauri, A., Gimenez, P., Trullenque, R., Fabra, R., & Castell, J.V. 1990. Culture of human hepatocytes from small surgical liver biopsies. Biochemical characterization and comparison with in vivo. *In Vitro Cell Dev.Biol.*, 26, (1) 67-74 available from: PM:2155194

Goodyear, L.J., Giorgino, F., Sherman, L.A., Carey, J., Smith, R.J., & Dohm, G.L. 1995. Insulin receptor phosphorylation, insulin receptor substrate-1 phosphorylation, and phosphatidylinositol 3-kinase activity are decreased in intact skeletal muscle strips from obese subjects. *J.Clin.Invest*, 95, (5) 2195-2204 available from: PM:7537758

Guillaume-Gentil, C., Assimacopoulos-Jeannet, F., & Jeanrenaud, B. 1993. Involvement of non-esterified fatty acid oxidation in glucocorticoid-induced peripheral insulin resistance in vivo in rats. *Diabetologia*, 36, (10) 899-906 available from: PM:8243867

Guzman, M. & Castro, J. 1989. Zonation of fatty acid metabolism in rat liver. *Biochem.J.*, 264, (1) 107-113 available from: PM:2574974

Haider, A., Gooren, L.J., Padungtod, P., & Saad, F. 2010. Improvement of the metabolic syndrome and of non-alcoholic liver steatosis upon treatment of hypogonadal elderly men with parenteral testosterone undecanoate. *Exp.Clin.Endocrinol.Diabetes*, 118, (3) 167-171 available from: PM:19472103

Haller, J., Mikics, E., & Makara, G.B. 2008. The effects of non-genomic glucocorticoid mechanisms on bodily functions and the central neural system. A critical evaluation of findings. *Front Neuroendocrinol.*, 29, (2) 273-291 available from: PM:18054070

Hanada, M., Feng, J., & Hemmings, B.A. 2004. Structure, regulation and function of PKB/AKT--a major therapeutic target. *Biochim.Biophys.Acta*, 1697, (1-2) 3-16 available from: PM:15023346

Hardie, D.G. 1992. Regulation of fatty acid and cholesterol metabolism by the AMP-activated protein kinase. *Biochim.Biophys.Acta*, 1123, (3) 231-238 available from: PM:1536860

Harvey, R. A. & Champe, P. C. (2005). Biochemistry.3 edition.Lippincott Williams & Wilkins.

Hassan-Smith, Z.K., Morgan, S.A., Sherlock, M., Hughes, B., Taylor, A.E., Lavery, G.G., Tomlinson, J.W., & Stewart, P.M. 2015. Gender-Specific Differences in Skeletal Muscle 11beta-HSD1 Expression Across Healthy Aging. *J.Clin.Endocrinol.Metab*, 100, (7) 2673-2681 available from: PM:25989394

Haystead, T.A., Campbell, D.G., & Hardie, D.G. 1988. Analysis of sites phosphorylated on acetyl-CoA carboxylase in response to insulin in isolated adipocytes. Comparison with sites phosphorylated by casein kinase-2 and the calmodulin-dependent multiprotein kinase. *Eur.J.Biochem.*, 175, (2) 347-354 available from: PM:2900140

Hazlehurst, J.M., Gathercole, L.L., Nasiri, M., Armstrong, M.J., Borrows, S., Yu, J., Wagenmakers, A.J., Stewart, P.M., & Tomlinson, J.W. 2013. Glucocorticoids fail to cause insulin resistance in human subcutaneous adipose tissue in vivo. *J.Clin.Endocrinol.Metab*, 98, (4) 1631-1640 available from: PM:23426618

Hazlehurst, J.M., Oprescu, A.I., Nikolaou, N., Di Guida, R., Grinbergs, A.E., Davies, N.P., Flintham, R.B., Armstrong, M.J., Taylor, A.E., Hughes, B.A., Yu, J., Hodson, L., Dunn, W.B., Tomlinson, J.W. 2016. Dual-5α-Reductase Inhibition Promotes Hepatic Lipid Accumulation in Man. *J Clin Endocrinol Metab*. 101(1):103-13 available from PM:26574953

He, S., McPhaul, C., Li, J.Z., Garuti, R., Kinch, L., Grishin, N.V., Cohen, J.C., & Hobbs, H.H. 2010. A sequence variation (I148M) in PNPLA3 associated with nonalcoholic fatty liver disease disrupts triglyceride hydrolysis. *J.Biol.Chem.*, 285, (9) 6706-6715 available from: PM:20034933

Hegele, R.A., Little, J.A., Vezina, C., Maguire, G.F., Tu, L., Wolever, T.S., Jenkins, D.J., & Connelly, P.W. 1993. Hepatic lipase deficiency. Clinical, biochemical, and molecular genetic characteristics. *Arterioscler.Thromb.*, 13, (5) 720-728 available from: PM:8485124

Herbert, A., Gerry, N.P., McQueen, M.B., Heid, I.M., Pfeufer, A., Illig, T., Wichmann, H.E., Meitinger, T., Hunter, D., Hu, F.B., Colditz, G., Hinney, A., Hebebrand, J., Koberwitz, K., Zhu, X., Cooper, R., Ardlie, K., Lyon, H., Hirschhorn, J.N., Laird, N.M., Lenburg, M.E., Lange, C., & Christman, M.F. 2006. A common genetic variant is associated with adult and childhood obesity. *Science*, 312, (5771) 279-283 available from: PM:16614226

Hofland, J., Delhanty, P.J., Steenbergen, J., Hofland, L.J., van Koetsveld, P.M., van Nederveen, F.H., de Herder, W.W., Feelders, R.A., & de Jong, F.H. 2012. Melanocortin 2 receptor-associated protein (MRAP) and MRAP2 in human adrenocortical tissues: regulation of expression and association with ACTH responsiveness. *J.Clin.Endocrinol.Metab*, 97, (5) E747-E754 available from: PM:22419722

Hollenberg, S.M., Weinberger, C., Ong, E.S., Cerelli, G., Oro, A., Lebo, R., Thompson, E.B., Rosenfeld, M.G., & Evans, R.M. 1985. Primary structure and expression of a functional human glucocorticoid receptor cDNA. *Nature*, 318, (6047) 635-641 available from: PM:2867473

Hoyos, C.M., Yee, B.J., Phillips, C.L., Machan, E.A., Grunstein, R.R., & Liu, P.Y. 2012. Body compositional and cardiometabolic effects of testosterone therapy in obese men with severe obstructive sleep apnoea: a randomised placebo-controlled trial. *Eur.J.Endocrinol.*, 167, (4) 531-541 available from: PM:22848006

Huang, G., Bhasin, S., Tang, E.R., Aakil, A., Anderson, S.W., Jara, H., Davda, M., Travison, T.G., & Basaria, S. 2013. Effect of testosterone administration on liver fat in older men with mobility limitation: results from a randomized controlled trial. *J.Gerontol.A Biol.Sci.Med.Sci.*, 68, (8) 954-959 available from: PM:23292288

Hubel, J.M., Schmidt, S.A., Mason, R.A., Haenle, M.M., Oeztuerk, S., Koenig, W., Boehm, B.O., Kratzer, W., Graeter, T., & Flechtner-Mors, M. 2015. Influence of plasma cortisol and other laboratory parameters on nonalcoholic Fatty liver disease. *Horm.Metab Res.*, 47, (7) 479-484 available from: PM:25295415

Hurt, R.T., Kulisek, C., Buchanan, L.A., & McClave, S.A. 2010. The obesity epidemic: challenges, health initiatives, and implications for gastroenterologists. *Gastroenterol.Hepatol.(N.Y.)*, 6, (12) 780-792 available from: PM:21301632

Jaffe, J.M., Malkowicz, S.B., Walker, A.H., MacBride, S., Peschel, R., Tomaszewski, J., Van, A.K., Wein, A.J., & Rebbeck, T.R. 2000. Association of SRD5A2 genotype and pathological characteristics of prostate tumors. *Cancer Res.*, 60, (6) 1626-1630 available from: PM:10749132

Jakubowski, A., Ambrose, C., Parr, M., Lincecum, J.M., Wang, M.Z., Zheng, T.S., Browning, B., Michaelson, J.S., Baetscher, M., Wang, B., Bissell, D.M., & Burkly, L.C. 2005a. TWEAK induces liver progenitor cell proliferation. *J.Clin.Invest*, 115, (9) 2330-2340 available from: PM:16110324

Janne, O.A., Palvimo, J.J., Kallio, P., & Mehto, M. 1993. Androgen receptor and mechanism of androgen action. *Ann.Med.*, 25, (1) 83-89 available from: PM:8435194

Jantzen, H.M., Strahle, U., Gloss, B., Stewart, F., Schmid, W., Boshart, M., Miksicek, R., & Schutz, G. 1987. Cooperativity of Glucocorticoid Response Elements Located Far Upstream of the Tyrosine Aminotransferase Gene. *Cell*, 49, (1) 29-38 available from: ISI:A1987G882600005

Johnson, T.M., Mann, W.R., Dragland, C.J., Anderson, R.C., Nemecek, G.M., & Bell, P.A. 1995. Over-expression and characterization of active recombinant rat liver carnitine palmitoyltransferase II using baculovirus. *Biochem.J.*, 309 (Pt 2), 689-693 available from: PM:7626037

Jones, H., Sprung, V.S., Pugh, C.J., Daousi, C., Irwin, A., Aziz, N., Adams, V.L., Thomas, E.L., Bell, J.D., Kemp, G.J., & Cuthbertson, D.J. 2012. Polycystic ovary syndrome with hyperandrogenism is characterized by an increased risk of hepatic steatosis compared to nonhyperandrogenic PCOS phenotypes and healthy controls, independent of obesity and insulin resistance. *J.Clin.Endocrinol.Metab*, 97, (10) 3709-3716 available from: PM:22837189

Jou, J., Choi, S.S., & Diehl, A.M. 2008. Mechanisms of Disease Progression in Nonalcoholic Fatty Liver Disease. *Seminars in Liver Disease*, 28, (4) 370-379 available from: ISI:000260779800005

Jungermann, K. & Katz, N. 1982. Functional hepatocellular heterogeneity. *Hepatology*, 2, (3) 385-395 available from: PM:7042508

Kahn, S.E. 2003. The relative contributions of insulin resistance and beta-cell dysfunction to the pathophysiology of Type 2 diabetes. *Diabetologia*, 46, (1) 3-19 available from: PM:12637977

Kahrizi, K., Hu, C.H., Garshasbi, M., Abedini, S.S., Ghadami, S., Kariminejad, R., Ullmann, R., Chen, W., Ropers, H.H., Kuss, A.W., Najmabadi, H., & Tzschach, A. 2011. Next generation sequencing in a family with autosomal recessive Kahrizi syndrome (OMIM 612713) reveals a homozygous frameshift mutation in SRD5A3. *Eur.J.Hum.Genet.*, 19, (1) 115-117 available from: PM:20700148

Kalra, M., Mayes, J., Assefa, S., Kaul, A.K., & Kaul, R. 2008. Role of sex steroid receptors in pathobiology of hepatocellular carcinoma. *World J.Gastroenterol.*, 14, (39) 5945-5961 available from: PM:18932272

Kasina, S. & Macoska, J.A. 2012. The CXCL12/CXCR4 axis promotes ligand-independent activation of the androgen receptor. *Mol.Cell Endocrinol.*, 351, (2) 249-263 available from: PM:22245379

Kawano, Y., & Cohen, D. 2013. Mechanisms of hepatic triglyceride accumulation in non-alcoholic fatty liver disease. *Journal of Gastroenterology* 48(4):434-41 available from PM: 23397118

Kelly, D.M. & Jones, T.H. 2013. Testosterone: a metabolic hormone in health and disease. *J.Endocrinol.*, 217, (3) R25-R45 available from: PM:23378050

Kelly, D.M., Nettleship, J.E., Akhtar, S., Muraleedharan, V., Sellers, D.J., Brooke, J.C., McLaren, D.S., Channer, K.S., & Jones, T.H. 2014. Testosterone suppresses the expression of regulatory enzymes of fatty acid synthesis and protects against hepatic

steatosis in cholesterol-fed androgen deficient mice. *Life Sci.*, 109, (2) 95-103 available from: PM:24953607

Kerouz, N.J., Horsch, D., Pons, S., & Kahn, C.R. 1997a. Differential regulation of insulin receptor substrates-1 and -2 (IRS-1 and IRS-2) and phosphatidylinositol 3-kinase isoforms in liver and muscle of the obese diabetic (ob/ob) mouse. *J.Clin.Invest*, 100, (12) 3164-3172 available from: PM:9399964

Kido, Y., Burks, D.J., Withers, D., Bruning, J.C., Kahn, C.R., White, M.F., & Accili, D. 2000. Tissue-specific insulin resistance in mice with mutations in the insulin receptor, IRS-1, and IRS-2. *J.Clin.Invest*, 105, (2) 199-205 available from: PM:10642598

Kim, C.H. & Cho, Y.S. 2010. Selection and optimization of MCF-7 cell line for screening selective inhibitors of 11 beta-hydroxysteroid dehydrogenase 2. *Cell Biochemistry and Function*, 28, (6) 440-447 available from: ISI:000281539100002

Kim, J.B., Sarraf, P., Wright, M., Yao, K.M., Mueller, E., Solanes, G., Lowell, B.B., & Spiegelman, B.M. 1998. Nutritional and insulin regulation of fatty acid synthetase and leptin gene expression through ADD1/SREBP1. *J.Clin.Invest*, 101, (1) 1-9 available from: PM:9421459

Kim, S., Kwon, H., Park, J.H., Cho, B., Kim, D., Oh, S.W., Lee, C.M., & Choi, H.C. 2012. A low level of serum total testosterone is independently associated with nonalcoholic fatty liver disease. *BMC.Gastroenterol.*, 12, 69 available from: PM:22691278

Kitamura, T., Kitamura, Y., Kuroda, S., Hino, Y., Ando, M., Kotani, K., Konishi, H., Matsuzaki, H., Kikkawa, U., Ogawa, W., & Kasuga, M. 1999. Insulin-induced phosphorylation and activation of cyclic nucleotide phosphodiesterase 3B by the serine-threonine kinase Akt. *Mol.Cell Biol.*, 19, (9) 6286-6296 available from: PM:10454575

Klein, H.H., Ullmann, S., Drenckhan, M., Grimmsmann, T., Unthan-Fechner, K., & Probst, I. 2002. Differential modulation of insulin actions by dexamethasone: studies in primary cultures of adult rat hepatocytes. *J.Hepatol.*, 37, (4) 432-440 available from: PM:12217595

Konopelska, S., Kienitz, T., Hughes, B., Pirlich, M., Bauditz, J., Lochs, H., Strasburger, C.J., Stewart, P.M., & Quinkler, M. 2009a. Hepatic 11beta-HSD1 mRNA expression in fatty liver and nonalcoholic steatohepatitis. *Clin.Endocrinol.(Oxf)*, 70, (4) 554-560 available from: PM:18665910

Kosaki, A. & Webster, N.J. 1993. Effect of dexamethasone on the alternative splicing of the insulin receptor mRNA and insulin action in HepG2 hepatoma cells. *J.Biol.Chem.*, 268, (29) 21990-21996 available from: PM:8408055

Kotronen, A., Seppanen-Laakso, T., Westerbacka, J., Kiviluoto, T., Arola, J., Ruskeepaa, A.-L., Oresic, M., & Yki-Jarvinen, H. (2009a). Hepatic stearoyl-CoA desaturase (SCD)-1 activity and diacylglycerol but not ceramide concentrations are

increased in the nonalcoholic human fatty liver. *Diabetes,* 58(1):203-8 available from PM:18952834

Kotronen, A., Velagapudi, V. R., Yetukuri, L., Westerbacka, J., Bergholm, R., Ekroos, K., Makkonen, J., Taskinen, M. R., Oresic, M., & Yki-Jarvinen , H. (2009b). Serum saturated fatty acids containing triacylglycerols are better markers of insulin resistance than total serum triacylglycerol concentrations. *Diabetologia,* 52(4):684-90 available from PM:19214471

Krapp, A., Ahle, S., Kersting, S., Hua, Y., Kneser, K., Nielsen, M., Gliemann, J., & Beisiegel, U. 1996. Hepatic lipase mediates the uptake of chylomicrons and beta-VLDL into cells via the LDL receptor-related protein (LRP). *J.Lipid Res.*, 37, (5) 926-936 available from: PM:8725146

Krone, N., Hughes, B.A., Lavery, G.G., Stewart, P.M., Arlt, W., & Shackleton, C.H. 2010. Gas chromatography/mass spectrometry (GC/MS) remains a pre-eminent discovery tool in clinical steroid investigations even in the era of fast liquid chromatography tandem mass spectrometry (LC/MS/MS). *J.Steroid Biochem.Mol.Biol.*, 121, (3-5) 496-504 available from: PM:20417277

Kubota, N., Tobe, K., Terauchi, Y., Eto, K., Yamauchi, T., Suzuki, R., Tsubamoto, Y., Komeda, K., Nakano, R., Miki, H., Satoh, S., Sekihara, H., Sciacchitano, S., Lesniak, M., Aizawa, S., Nagai, R., Kimura, S., Akanuma, Y., Taylor, S.I., & Kadowaki, T. 2000. Disruption of insulin receptor substrate 2 causes type 2 diabetes because of liver insulin resistance and lack of compensatory beta-cell hyperplasia. *Diabetes*, 49, (11) 1880-1889 available from: PM:11078455

Labrie, F., Sugimoto, Y., Luu-The, V., Simard, J., Lachance, Y., Bachvarov, D., Leblanc, G., Durocher, F., & Paquet, N. 1992. Structure of human type II 5 alpha-reductase gene. *Endocrinology*, 131, (3) 1571-1573 available from: PM:1505484

Larance, M., Ramm, G., Stockli, J., van Dam, E.M., Winata, S., Wasinger, V., Simpson, F., Graham, M., Junutula, J.R., Guilhaus, M., & James, D.E. 2005. Characterization of the role of the Rab GTPase-activating protein AS160 in insulin-regulated GLUT4 trafficking. *J.Biol.Chem.*, 280, (45) 37803-37813 available from: PM:16154996

Larsen, P.R., Kronenberg, H. M., Melmed, S. & Polonsky, K.S. (2003). Williams textbook of endocrinology, 10 edition.

Larsson, H. & Ahren, B. 1996. Short-term dexamethasone treatment increases plasma leptin independently of changes in insulin sensitivity in healthy women. *J.Clin.Endocrinol.Metab*, 81, (12) 4428-4432 available from: PM:8954054

Lavery, G.G., Walker, E.A., Draper, N., Jeyasuria, P., Marcos, J., Shackleton, C.H.L., Parker, K.L., White, P.C., & Stewart, P.M. 2006. Hexose-6-phosphate dehydrogenase knock-out mice lack 11 beta-hydroxysteroid dehydrogenase type 1-mediated

glucocorticoid generation. *Journal of Biological Chemistry*, 281, (10) 6546-6551 available from: ISI:000236030800050

Lemke, U., Krones-Herzig, A., Berriel, D.M., Narvekar, P., Ziegler, A., Vegiopoulos, A., Cato, A.C., Bohl, S., Klingmuller, U., Screaton, R.A., Muller-Decker, K., Kersten, S., & Herzig, S. 2008a. The glucocorticoid receptor controls hepatic dyslipidemia through Hes1. *Cell Metab*, 8, (3) 212-223 available from: PM:18762022

Lemonde, H.A., Custard, E.J., Bouquet, J., Duran, M., Overmars, H., Scambler, P.J., & Clayton, P.T. 2003. Mutations in SRD5B1 (AKR1D1), the gene encoding delta(4)-3-oxosteroid 5beta-reductase, in hepatitis and liver failure in infancy. *Gut*, 52, (10) 1494-1499 available from: PM:12970144

Li, Z.Z., Berk, M., McIntyre, T.M., & Feldstein, A.E. 2009. Hepatic lipid partitioning and liver damage in nonalcoholic fatty liver disease: role of stearoyl-CoA desaturase. *J Biol Chem.*, 284(9):5637-44 available from PM:19119140

Lim, J.S., Mietus-Snyder, M., Valente, A., Schwarz, J.M., & Lustig, R.H. 2010. The role of fructose in the pathogenesis of NAFLD and the metabolic syndrome. *Nat.Rev.Gastroenterol.Hepatol.*, 7, (5) 251-264 available from: PM:20368739

Lin, H.Y., Yu, I.C., Wang, R.S., Chen, Y.T., Liu, N.C., Altuwaijri, S., Hsu, C.L., Ma, W.L., Jokinen, J., Sparks, J.D., Yeh, S., & Chang, C. 2008. Increased hepatic steatosis and insulin resistance in mice lacking hepatic androgen receptor. *Hepatology*, 47, (6) 1924-1935 available from: PM:18449947

Liu, Y.J., Shieh, P.C., Lee, J.C., Chen, F.A., Lee, C.H., Kuo, S.C., Ho, C.T., Kuo, D.H., Huang, L.J., & Way, T.D. 2014. Hypolipidemic activity of Taraxacum mongolicum associated with the activation of AMP-activated protein kinase in human HepG2 cells. *Food Funct.*, 5, (8) 1755-1762 available from: PM:24903219

Livingstone, D.E., Barat, P., Di Rollo, E.M., Rees, G.A., Weldin, B.A., Rog-Zielinska, E.A., MacFarlane, D.P., Walker, B.R., & Andrew, R. 2015. 5alpha-reductase type 1 deficiency or inhibition predisposes to insulin resistance, hepatic steatosis, and liver fibrosis in rodents. *Diabetes*, 64, (2) 447-458 available from: PM:25239636

Livingstone, D.E., Di Rollo, E.M., Yang, C., Codrington, L.E., Mathews, J.A., Kara, M., Hughes, K.A., Kenyon, C.J., Walker, B.R., & Andrew, R. 2014. Relative adrenal insufficiency in mice deficient in 5alpha-reductase 1. *J.Endocrinol.*, 222, (2) 257-266 available from: PM:24872577

Livingstone, D.E.W., Grassick, S.L., Currie, G.L., Walker, B.R., & Andrew, R. 2009. Dysregulation of glucocorticoid metabolism in murine obesity: comparable effects of leptin resistance and deficiency. *Journal of Endocrinology*, 201, (2) 211-218 available from: ISI:000272629100004

Lonergan, P.E. & Tindall, D.J. 2011. Androgen receptor signaling in prostate cancer development and progression. *J.Carcinog.*, 10, 20 available from: PM:21886458

Lopez, A.D., Mathers, C.D., Ezzati, M., Jamison, D.T., & Murray, C.J. 2006. Global and regional burden of disease and risk factors, 2001: systematic analysis of population health data. *Lancet*, 367, (9524) 1747-1757 available from: PM:16731270

Losel, R.M., Falkenstein, E., Feuring, M., Schultz, A., Tillmann, H.C., Rossol-Haseroth, K., & Wehling, M. 2003. Nongenomic steroid action: controversies, questions, and answers. *Physiol Rev.*, 83, (3) 965-1016 available from: PM:12843413

Lou-Bonafonte, J.M., Arnal, C., & Osada, J. 2011. New genes involved in hepatic steatosis. *Curr.Opin.Lipidol.*, 22, (3) 159-164 available from: PM:21494144

Luiken, J.J., Arumugam, Y., Bell, R.C., Calles-Escandon, J., Tandon, N.N., Glatz, J.F., & Bonen, A. 2002. Changes in fatty acid transport and transporters are related to the severity of insulin deficiency. *Am.J.Physiol Endocrinol.Metab*, 283, (3) E612-E621 available from: PM:12169456

Maimoun, L., Philibert, P., Cammas, B., Audran, F., Bouchard, P., Fenichel, P., Cartigny, M., Pienkowski, C., Polak, M., Skordis, N., Mazen, I., Ocal, G., Berberoglu, M., Reynaud, R., Baumann, C., Cabrol, S., Simon, D., Kayemba-Kay's, K., De, K.M., Kurtz, F., Leheup, B., Heinrichs, C., Tenoutasse, S., Van, V.G., Gruters, A., Eunice, M., Ammini, A.C., Hafez, M., Hochberg, Z., Einaudi, S., Al, M.H., Nunez, C.J., Servant, N., Lumbroso, S., Paris, F., & Sultan, C. 2011. Phenotypical, biological, and molecular heterogeneity of 5alpha-reductase deficiency: an extensive international experience of 55 patients. *J.Clin.Endocrinol.Metab*, 96, (2) 296-307 available from: PM:21147889

Makridakis, N., Ross, R.K., Pike, M.C., Chang, L., Stanczyk, F.Z., Kolonel, L.N., Shi, C.Y., Yu, M.C., Henderson, B.E., & Reichardt, J.K. 1997. A prevalent missense substitution that modulates activity of prostatic steroid 5alpha-reductase. *Cancer Res.*, 57, (6) 1020-1022 available from: PM:9067262

Makridakis, N.M., Ross, R.K., Pike, M.C., Crocitto, L.E., Kolonel, L.N., Pearce, C.L., Henderson, B.E., & Reichardt, J.K. 1999. Association of mis-sense substitution in SRD5A2 gene with prostate cancer in African-American and Hispanic men in Los Angeles, USA. *Lancet*, 354, (9183) 975-978 available from: PM:10501358

Mangiapane, E.H. & Brindley, D.N. 1986. Effects of dexamethasone and insulin on the synthesis of triacylglycerols and phosphatidylcholine and the secretion of very-low-density lipoproteins and lysophosphatidylcholine by monolayer cultures of rat hepatocytes. *Biochem.J.*, 233, (1) 151-160 available from: PM:3513755

Mao, J., DeMayo, F.J., Li, H., Abu-Elheiga, L., Gu, Z., Shaikenov, T.E., Kordari, P., Chirala, S.S., Heird, W.C., & Wakil, S.J. 2006. Liver-specific deletion of acetyl-CoA carboxylase 1 reduces hepatic triglyceride accumulation without affecting glucose homeostasis. *Proc.Natl.Acad.Sci.U.S.A*, 103, (22) 8552-8557 available from: PM:16717184

Makridaskis, N.M., Ross, R.K., Pike, M.C., Crocitto, L.E., Kolonel, L.N., Pearce., C.L., Henderson, B.E., Reichardt, J.K. 1999. Association of mis-sense substitution in SRD5A2

gene with prostate cancer in African-American and Hispanic men in Los Angeles, USA. *Lancet*, 354(9183):975-8 available from PM:10501358

Markou, A., Androulakis, I.I., Mourmouris, C., Tsikkini, A., Samara, C., Sougioultzis, S., Piaditis, G., & Kaltsas, G. 2010. Hepatic steatosis in young lean insulin resistant women with polycystic ovary syndrome. *Fertil.Steril.*, 93, (4) 1220-1226 available from: PM:19171337

Marques-Vidal, P., Azema, C., Collet, X., Vieu, C., Chap, H., & Perret, B. 1994. Hepatic lipase promotes the uptake of HDL esterified cholesterol by the perfused rat liver: a study using reconstituted HDL particles of defined phospholipid composition. *J.Lipid Res.*, 35, (3) 373-384 available from: PM:8014574

Maslak, E., Zabielski, P., Kochan, K., Kus, K., Jasztal, A., Sitek, B., Proniewski, B., Wojcik, T., Gula, K., Kij, A., Walczak, M., Baranska, M., Chabowski, A., Holland, R.J., Saavedra, J.E., Keefer, L.K., & Chlopicki, S. 2015. The liver-selective NO donor, V-PYRRO/NO, protects against liver steatosis and improves postprandial glucose tolerance in mice fed high fat diet. *Biochem.Pharmacol.*, 93, (3) 389-400 available from: PM:25534988

Matsumoto, M., Pocai, A., Rossetti, L., Depinho, R.A., & Accili, D. 2007. Impaired regulation of hepatic glucose production in mice lacking the forkhead transcription factor Foxo1 in liver. *Cell Metab*, 6, (3) 208-216 available from: PM:17767907

McInnes, K.J., Smith, L.B., Hunger, N.I., Saunders, P.T., Andrew, R., & Walker, B.R.2012a. Deletion of the androgen receptor in adipose tissue in male mice elevates retinol binding protein 4 and reveals independent effects on visceral fat mass and on glucose homeostasis. *Diabetes,* 61(5):1072-81 available from PM:22415878

McInnes, K.J., Brown, K.A., Hunger, N.I., & Simpson, E.R. 2012b. Regulation of LKB1 expression by sex hormones in adipocytes. *Int J Obes (Lond).,* 36(7):982-5 available from PM:21876548

Mehrani, H. & Storey, K.B. 1993. Control of glycogenolysis and effects of exercise on phosphorylase kinase and cAMP-dependent protein kinase in rainbow trout organs. *Biochem.Cell Biol.*, 71, (11-12) 501-506 available from: PM:8192887

Meikle, A.W., Bishop, D.T., Stringham, J.D., & West, D.W. 1986. Quantitating genetic and nongenetic factors that determine plasma sex steroid variation in normal male twins. *Metabolism*, 35, (12) 1090-1095 available from: PM:3097456

Mendoza-Figueroa, T., Hernandez, A., De Lourdes, L.M., & Kuri-Harcuch, W. 1988. Intracytoplasmic triglyceride accumulation produced by dexamethasone in adult rat hepatocytes cultivated on 3T3 cells. *Toxicology*, 52, (3) 273-286 available from: PM:3188039

Miller, W.L. 2007. Steroidogenic acute regulatory protein (StAR), a novel mitochondrial cholesterol transporter. *Biochim.Biophys.Acta*, 1771, (6) 663-676 available from: PM:17433772

Mononen, N., Ikonen, T., Syrjakoski, K., Matikainen, M., Schleutker, J., Tammela, T.L., Koivisto, P.A., & Kallioniemi, O.P. 2001. A missense substitution A49T in the steroid 5-alpha-reductase gene (SRD5A2) is not associated with prostate cancer in Finland. *Br.J.Cancer*, 84, (10) 1344-1347 available from: PM:11355945

Moon, J.S., Jin, W.J., Kwak, J.H., Kim, H.J., Yun, M.J., Kim, J.W., Park, S.W., & Kim, K.S. 2011. Androgen stimulates glycolysis for *de novo* lipid synthesis by increasing the activities of hexokinase 2 and 6-phosphofructo-2-kinase/fructose-2,6-bisphosphatase 2 in prostate cancer cells. *Biochem.J.*, 433, (1) 225-233 available from: PM:20958264

Morgan, S.A., Gathercole, L.L., Simonet, C., Hassan-Smith, Z.K., Bujalska, I., Guest, P., Abrahams, L., Smith, D.M., Stewart, P.M., Lavery, G.G., & Tomlinson, J.W. 2013. Regulation of lipid metabolism by glucocorticoids and 11beta-HSD1 in skeletal muscle. *Endocrinology*, 154, (7) 2374-2384 available from: PM:23633532

Morgan, S.A., McCabe, E.L., Gathercole, L.L., Hassan-Smith, Z.K., Larner, D.P., Bujalska, I.J., Stewart, P.M., Tomlinson, J.W., & Lavery, G.G. 2014. 11beta-HSD1 is the major regulator of the tissue-specific effects of circulating glucocorticoid excess. *Proc.Natl.Acad.Sci.U.S.A*, 111, (24) E2482-E2491 available from: PM:24889609

Morgan, S.A. & Tomlinson, J.W. 2010. 11beta-hydroxysteroid dehydrogenase type 1 inhibitors for the treatment of type 2 diabetes. *Expert.Opin.Investig.Drugs*, 19, (9) 1067-1076 available from: PM:20707593

Moverare-Skrtic, S., Venken, K., Andersson, N., Lindberg, M.K., Svensson, J., Swanson, C., Vanderschueren, D., Oscarsson, J., Gustafsson, J.A., & Ohlsson, C. 2006. Dihydrotestosterone treatment results in obesity and altered lipid metabolism in orchidectomized mice. *Obesity.(Silver.Spring)*, 14, (4) 662-672 available from: PM:16741268

Mueller, K.M., Themanns, M., Friedbichler, K., Kornfeld, J.W., Esterbauer, H., Tuckermann, J.P., & Moriggl, R. 2012. Hepatic growth hormone and glucocorticoid receptor signaling in body growth, steatosis and metabolic liver cancer development. *Mol.Cell Endocrinol.*, 361, (1-2) 1-11 available from: PM:22564914

Murata, Y., Ogawa, Y., Saibara, T., Nishioka, A., Fujiwara, Y., Fukumoto, M., Inomata, T., Enzan, H., Onishi, S., Yoshida, S. 2000. Unrecognized hepatic steatosis and non-alcoholic steatohepatitis in adjuvant tamoxifen for breast cancer patients. *Oncol Rep.*, 7(6):1299-304 available from PM:11032933

Murthy, M.S. & Pande, S.V. 1984. Mechanism of carnitine acylcarnitine translocase-catalyzed import of acylcarnitines into mitochondria. *J.Biol.Chem.*, 259, (14) 9082-9089 available from: PM:6430896

Muthusamy, T., Murugesan, P., & Balasubramanian, K. 2009. Sex steroids deficiency impairs glucose transporter 4 expression and its translocation through defective Akt phosphorylation in target tissues of adult male rat. *Metabolism*, 58, (11) 1581-1592 available from: PM:19615701

Muthusamy, T., Murugesan, P., Srinivasan, C., & Balasubramanian, K. 2011. Sex steroids influence glucose oxidation through modulation of insulin receptor expression and IRS-1 serine phosphorylation in target tissues of adult male rat. *Mol.Cell Biochem.*, 352, (1-2) 35-45 available from: PM:21301931

Nagle, C.A., Klett, E.L., & Coleman, R.A. 2009. Hepatic triacylglycerol accumulation and insulin resistance. *J.Lipid Res.*, 50 Suppl, S74-S79 available from: PM:18997164

Nixon, M., Upreti, R., & Andrew, R. 2012. 5alpha-Reduced glucocorticoids: a story of natural selection. *J.Endocrinol.*, 212, (2) 111-127 available from: PM:21903862

Normington, K. & Russell, D.W. 1992. Tissue distribution and kinetic characteristics of rat steroid 5 alpha-reductase isozymes. Evidence for distinct physiological functions. *J.Biol.Chem.*, 267, (27) 19548-19554 available from: PM:1527072

Norrheim, L., Sorensen, H., Gautvik, K., Bremer, J., & Spydevold, O. 1990. Synergistic actions of tetradecylthioacetic acid (TTA) and dexamethasone on induction of the peroxisomal beta-oxidation and on growth inhibition of Morris hepatoma cells. Both effects are counteracted by insulin. *Biochim.Biophys.Acta*, 1051, (3) 319-323 available from: PM:1968766

Nugent, C. & Younossi, Z.M. 2007. Evaluation and management of obesity-related nonalcoholic fatty liver disease. *Nature Clinical Practice Gastroenterology & Hepatology*, 4, (8) 432-441 available from: ISI:000248412200009

Oakley, R.H., Jewell, C.M., Yudt, M.R., Bofetiado, D.M., & Cidlowski, J.A. 1999. The dominant negative activity of the human glucocorticoid receptor beta isoform. Specificity and mechanisms of action. *J.Biol.Chem.*, 274, (39) 27857-27866 available from: PM:10488132

Ogden, C.L., Yanovski, S.Z., Carroll, M.D., & Flegal, K.M. 2007. The epidemiology of obesity. *Gastroenterology*, 132, (6) 2087-2102 available from: PM:17498505

Okaya, A., Kitanaka, J., Kitanaka, N., Satake, M., Kim, Y., Terada, K., Sugiyama, T., Takemura, M., Fujimoto, J., Terada, N., Miyajima, A., & Tsujimura, T. 2005. Oncostatin M inhibits proliferation of rat oval cells, OC15-5, inducing differentiation into hepatocytes. *Am.J.Pathol.*, 166, (3) 709-719 available from: PM:15743783

Olefsky, J.M., Johnson, J., Liu, F., Jen, P., & Reaven, G.M. 1975. The effects of acute and chronic dexamethasone administration on insulin binding to isolated rat hepatocytes and adipocytes. *Metabolism*, 24, (4) 517-527 available from: PM:1117842

Omori, N., Evarts, R.P., Omori, M., Hu, Z., Marsden, E.R., & Thorgeirsson, S.S. 1996. Expression of leukemia inhibitory factor and its receptor during liver regeneration in the adult rat. *Lab Invest*, 75, (1) 15-24 available from: PM:8683936

Overman, R.A., Yeh, J.Y., & Deal, C.L. 2013. Prevalence of oral glucocorticoid usage in the United States: a general population perspective. *Arthritis Care Res.(Hoboken.)*, 65, (2) 294-298 available from: PM:22807233

Palermo, M., Shackleton, C.H., Mantero, F., & Stewart, P.M. 1996. Urinary free cortisone and the assessment of 11 beta-hydroxysteroid dehydrogenase activity in man. *Clin.Endocrinol.(Oxf)*, 45, (5) 605-611 available from: PM:8977758

Park, K., Li, Q., Rask-Madsen, C., Mima, A., Mizutani, K., Winnay, J., Maeda, Y., D'Aquino, K., White, M.F., Feener, E.P., & King, G.L. 2013. Serine phosphorylation sites on IRS2 activated by angiotensin II and protein kinase C to induce selective insulin resistance in endothelial cells. *Mol.Cell Biol.*, 33, (16) 3227-3241 available from: PM:23775122

Parthasarathy, C., Renuka, V.N., & Balasubramanian, K. 2009. Sex steroids enhance insulin receptors and glucose oxidation in Chang liver cells. *Clin.Chim.Acta*, 399, (1-2) 49-53 available from: PM:18834871

Parvez, M.K., Purcell, R.H., & Emerson, S.U. 2011. Hepatitis E virus ORF2 protein over-expressed by baculovirus in hepatoma cells, efficiently encapsidates and transmits the viral RNA to naive cells. *Virology Journal*, 8, available from: ISI:000289951400001

Pascale, A., Pais, R., & Ratziu, V. 2010. An overview of nonalcoholic steatohepatitis: past, present and future directions. *J.Gastrointestin.Liver Dis.*, 19, (4) 415-423 available from: PM:21188334

Patti, M.E., Sun, X.J., Bruening, J.C., Araki, E., Lipes, M.A., White, M.F., & Kahn, C.R. 1995. 4PS/insulin receptor substrate (IRS)-2 is the alternative substrate of the insulin receptor in IRS-1-deficient mice. *J.Biol.Chem.*, 270, (42) 24670-24673 available from: PM:7559579

Pearce, C.L., Makridakis, N.M., Ross, R.K., Pike, M.C., Kolonel, L.N., Henderson, B.E., & Reichardt, J.K. 2002. Steroid 5-alpha reductase type II V89L substitution is not associated with risk of prostate cancer in a multiethnic population study. *Cancer Epidemiol.Biomarkers Prev.*, 11, (4) 417-418 available from: PM:11927504

Peterson, R.E., Imperato-McGinley, J., Gautier, T., & Shackleton, C. 1985. Urinary steroid metabolites in subjects with male pseudohermaphroditism due to 5 alpha-reductase deficiency. *Clin.Endocrinol.(Oxf)*, 23, (1) 43-53 available from: PM:4028464

Petersons, C.J., Mangelsdorf, B.L., Jenkins, A.B., Poljak, A., Smith, M.D., Greenfield, J.R., Thompson, C.H., & Burt, M.G. 2013. Effects of low-dose prednisolone on hepatic and peripheral insulin sensitivity, insulin secretion, and abdominal adiposity in patients with inflammatory rheumatologic disease. *Diabetes Care*, 36, (9) 2822-2829 available from: PM:23670996

Piao, Y.F., Li, J.T., & Shi, Y. 2003. Relationship between genetic polymorphism of cytochrome P450IIE1 and fatty liver. *World J.Gastroenterol.*, 9, (11) 2612-2615 available from: PM:14606109

Platt, D.E., Ghassibe-Sabbagh, M., Youhanna, S., Hager, J., Cazier, J.B., Kamatani, Y., Salloum, A.K., Haber, M., Romanos, J., Doueihy, B., Mouzaya, F., Kibbani, S., Sbeite, H., Deeb, M.E., Chammas, E., El Bayeh, H., Khazen, G., Gauguier, D., Zalloua, P.A., Abchee, A.B. 2015. Circulating lipid levels and risk of coronary artery disease in a large group of patients undergoing coronaryangiography. *J Thromb Thrombolysis.* 39(1):15-22 available from PM:24788070

Postic, C. & Girard, J. 2008. Contribution of *de novo* fatty acid synthesis to hepatic steatosis and insulin resistance: lessons from genetically engineered mice. *Journal of Clinical Investigation*, 118, (3) 829-838 available from: ISI:000253646400005

Pramfalk, C., Pavlides, M., Banerjee, R., McNeil, C.A., Neubauer, S., Karpe, F., Hodson, L. 2015. Sex-Specific Differences in Hepatic Fat Oxidation and Synthesis May Explain the Higher Propensity for NAFLD in Men. *J Clin Endocrinol Metab.*, 100(12):4425-33 available from PM:26414963

Pratt, W.B. & Toft, D.O. 1997. Steroid receptor interactions with heat shock protein and immunophilin chaperones. *Endocr.Rev.*, 18, (3) 306-360 available from: PM:9183567

Previs, S.F., Withers, D.J., Ren, J.M., White, M.F., & Shulman, G.I. 2000. Contrasting effects of IRS-1 versus IRS-2 gene disruption on carbohydrate and lipid metabolism in vivo. *J.Biol.Chem.*, 275, (50) 38990-38994 available from: PM:10995761

Purdy, R.H., Morrow, A.L., Blinn, J.R., & Paul, S.M. 1990. Synthesis, metabolism, and pharmacological activity of 3 alpha-hydroxy steroids which potentiate GABA-receptor-mediated chloride ion uptake in rat cerebral cortical synaptoneurosomes. *J.Med.Chem.*, 33, (6) 1572-1581 available from: PM:2160534

Qu, S., Altomonte, J., Perdomo, G., He, J., Fan, Y., Kamagate, A., Meseck, M., & Dong, H.H. 2006. Aberrant Forkhead box O1 function is associated with impaired hepatic metabolism. *Endocrinology*, 147, (12) 5641-5652 available from: PM:16997836

Raddatz, D. & Ramadori, G. 2007. Carbohydrate metabolism and the liver: actual aspects from physiology and disease. *Z.Gastroenterol.*, 45, (1) 51-62 available from: PM:17236121

Ramm, G., Larance, M., Guilhaus, M., & James, D.E. 2006. A role for 14-3-3 in insulin-stimulated GLUT4 translocation through its interaction with the RabGAP AS160. *J.Biol.Chem.*, 281, (39) 29174-29180 available from: PM:16880201

Rang, H.P., Dale M., Ritter J.M. (1999). Pharmacology. Churchill Livingston.

Rappaport, A.M. 1980. Hepatic blood flow: morphologic aspects and physiologic regulation. *Int.Rev.Physiol*, 21, 1-63 available from: PM:6993392

Rasmussen, H., Zawalich, K.C., Ganesan, S., Calle, R., & Zawalich, W.S. 1990. Physiology and pathophysiology of insulin secretion. *Diabetes Care*, 13, (6) 655-666 available from: PM:2192849

Rautou, P.E., Mansouri, A., Lebrec, D., Durand, F., Valla, D., & Moreau, R. 2010. Autophagy in liver diseases. *J.Hepatol.*, 53, (6) 1123-1134 available from: PM:20810185

Reid, B.N., Ables, G.P., Otlivanchik, O.A., Schoiswohl, G., Zechner, R., Blaner, W.S., Goldberg, I.J., Schwabe, R.F., Chua, S.C., Jr., & Huang, L.S. 2008. Hepatic overexpression of hormone-sensitive lipase and adipose triglyceride lipase promotes fatty acid oxidation, stimulates direct release of free fatty acids, and ameliorates steatosis. *J.Biol.Chem.*, 283, (19) 13087-13099 available from: PM:18337240

Renehan, A.G., Tyson, M., Egger, M., Heller, R.F., & Zwahlen, M. 2008. Body-mass index and incidence of cancer: a systematic review and meta-analysis of prospective observational studies. *Lancet*, 371, (9612) 569-578 available from: PM:18280327

Repa, J.J., Liang, G., Ou, J., Bashmakov, Y., Lobaccaro, J.M., Shimomura, I., Shan, B., Brown, M.S., Goldstein, J.L., & Mangelsdorf, D.J. 2000. Regulation of mouse sterol regulatory element-binding protein-1c gene (SREBP-1c) by oxysterol receptors, LXRalpha and LXRbeta. *Genes Dev.*, 14, (22) 2819-2830 available from: PM:11090130

Rieder, J.M., Nisbet, A.A., Wuerstle, M.C., Tran, V.Q., Kwon, E.O., & Chien, G.W. 2010. Differences in left and right laparoscopic adrenalectomy. *JSLS.*, 14, (3) 369-373 available from: PM:21333190

Rivers, C., Levy, A., Hancock, J., Lightman, S., & Norman, M. 1999. Insertion of an amino acid in the DNA-binding domain of the glucocorticoid receptor as a result of alternative splicing. *J.Clin.Endocrinol.Metab*, 84, (11) 4283-4286 available from: PM:10566686

Rockall, A.G., Sohaib, S.A., Evans, D., Kaltsas, G., Isidori, A.M., Monson, J.P., Besser, G.M., Grossman, A.B., & Reznek, R.H. 2003. Hepatic steatosis in Cushing's syndrome: a radiological assessment using computed tomography. *Eur.J.Endocrinol.*, 149, (6) 543-548 available from: PM:14640995

Romeo, S., Kozlitina, J., Xing, C., Pertsemlidis, A., Cox, D., Pennacchio, L.A., Boerwinkle, E., Cohen, J.C., & Hobbs, H.H. 2008. Genetic variation in PNPLA3 confers susceptibility to nonalcoholic fatty liver disease. *Nat.Genet.*, 40, (12) 1461-1465 available from: PM:18820647

Rommerts, F.F.G.2004. Testosterone: an overview of biosynthesis, transport, metabolism and non-genomic actions. In Testosterone: Actions, Deficiency, Substitution. Nieschlag, E. and Behre, H.M., editors. Cambridge University, UK.

Ross, R.K., Bernstein, L., Lobo, R.A., Shimizu, H., Stanczyk, F.Z., Pike, M.C., & Henderson, B.E. 1992. 5-alpha-reductase activity and risk of prostate cancer among Japanese and US white and black males. *Lancet*, 339, (8798) 887-889 available from: PM:1348296

Ruderman, N.B., Saha, A.K., & Kraegen, E.W. 2003. Minireview: Malonyl CoA, AMP-activated protein kinase, and adiposity. *Endocrinology*, 144, (12) 5166-5171 available from: ISI:000186771800006

Ruderman, N.B., Saha, A.K., Vavvas, D., & Witters, L.A. 1999. Malonyl-CoA, fuel sensing, and insulin resistance. *Am.J.Physiol*, 276, (1 Pt 1) E1-E18 available from: PM:9886945

Russell, D.W. & Wilson, J.D. 1994. Steroid 5 alpha-reductase: two genes/two enzymes. *Annu.Rev.Biochem.*, 63, 25-61 available from: PM:7979239

Ruzzin, J., Wagman, A.S., & Jensen, J. 2005. Glucocorticoid-induced insulin resistance in skeletal muscles: defects in insulin signalling and the effects of a selective glycogen synthase kinase-3 inhibitor. *Diabetologia*, 48, (10) 2119-2130 available from: PM:16078016

Saad, M.J.A., Folli, F., & Kahn, C.R. 1995. Insulin and Dexamethasone Regulate Insulin-Receptors, Insulin-Receptor Substrate-1, and Phosphatidylinositol 3-Kinase in Fao Hepatoma-Cells. *Endocrinology*, 136, (4) 1579-1588 available from: ISI:A1995QP11700037

Sakoda, H., Ogihara, T., Anai, M., Funaki, M., Inukai, K., Katagiri, H., Fukushima, Y., Onishi, Y., Ono, H., Fujishiro, M., Kikuchi, M., Oka, Y., & Asano, T. 2000. Dexamethasone-induced insulin resistance in 3T3-L1 adipocytes is due to inhibition of glucose transport rather than insulin signal transduction. *Diabetes*, 49, (10) 1700-1708 available from: PM:11016454

Sanan, D.A., Fan, J., Bensadoun, A., & Taylor, J.M. 1997. Hepatic lipase is abundant on both hepatocyte and endothelial cell surfaces in the liver. *J.Lipid Res.*, 38, (5) 1002-1013 available from: PM:9186917

SANGER, F. 1960. Chemistry of insulin. *Br.Med.Bull.*, 16, 183-188 available from: PM:13746240

Sandberg, A.A., & Slaunwhite, W.R. Jr. 1959. Transcortin: a corticosteroid-binding protein of plasma. II. Levels in various conditions and the effects of estrogens. *J Clin Invest.* 38(8):1290-7 available from PM:13673085

Sanders, F.W., & Griffin, J.L. 2016. *De novo* lipogenesis in the liver in health and disease: more than just a shunting yard for glucose. *Biol Rev Camb Philos Soc*., 91(2):452-68 available from PM:25740151

Sano, H., Kane, S., Sano, E., Miinea, C.P., Asara, J.M., Lane, W.S., Garner, C.W., & Lienhard, G.E. 2003. Insulin-stimulated phosphorylation of a Rab GTPase-activating protein regulates GLUT4 translocation. *J.Biol.Chem.*, 278, (17) 14599-14602 available from: PM:12637568

Sarbassov, D.D., Guertin, D.A., Ali, S.M., & Sabatini, D.M. 2005. Phosphorylation and regulation of Akt/PKB by the rictor-mTOR complex. *Science*, 307, (5712) 1098-1101 available from: PM:15718470

Sarwar, N., Danesh, J., Eiriksdottir, G., Sigurdsson, G., Wareham, N., Bingham, S., Boekholdt, S.M., Khaw, K.T., & Gudnason, V. 2007. Triglycerides and the risk of coronary heart disease: 10,158 incident cases among 262,525 participants in 29 Western prospective studies. *Circulation* 115: 450–458 available from PM:17190864

Savage, D.B. & Semple, R.K. 2010. Recent insights into fatty liver, metabolic dyslipidaemia and their links to insulin resistance. *Curr.Opin.Lipidol.*, 21, (4) 329-336 available from: PM:20581678

Scarborough, P., Bhatnagar, P., Wickramasinghe, K.K., Allender, S., Foster, C., & Rayner, M. 2011. The economic burden of ill health due to diet, physical inactivity, smoking, alcohol and obesity in the UK: an update to 2006-07 NHS costs. *J.Public Health (Oxf)* available from: PM:21562029

Schwartz, J.I., Tanaka, W.K., Wang, D.Z., Ebel, D.L., Geissler, L.A., Dallob, A., Hafkin, B., & Gertz, B.J. 1997. MK-386, an inhibitor of 5alpha-reductase type 1, reduces dihydrotestosterone concentrations in serum and sebum without affecting dihydrotestosterone concentrations in semen. *J.Clin.Endocrinol.Metab*, 82, (5) 1373-1377 available from: PM:9141518

Schwartz, J.I., Van, H.A., De Schepper, P.J., De, L., I, Lasseter, K.C., Shamblen, E.C., Winchell, G.A., Constanzer, M.L., Chavez, C.M., Wang, D.Z., Ebel, D.L., Justice, S.J., & Gertz, B.J. 1996. Effect of MK-386, a novel inhibitor of type 1 5 alpha-reductase, alone and in combination with finasteride, on serum dihydrotestosterone concentrations in men. *J.Clin.Endocrinol.Metab*, 81, (8) 2942-2947 available from: PM:8768856

Senmaru, T., Fukui, M., Okada, H., Mineoka, Y., Yamazaki, M., Tsujikawa, M., Hasegawa, G., Kitawaki, J., Obayashi, H., & Nakamura, N. 2013. Testosterone deficiency induces markedly decreased serum triglycerides, increased small dense LDL, and hepatic steatosis mediated by dysregulation of lipid assembly and secretion in mice fed a high-fat diet. *Metabolism*, 62, (6) 851-860 available from: PM:23332447

Setlur, S.R., Chen, C.X., Hossain, R.R., Ha, J.S., Van Doren, V.E., Stenzel, B., Steiner, E., Oldridge, D., Kitabayashi, N., Banerjee, S., Chen, J.Y., Schafer, G., Horninger, W., Lee, C., Rubin, M.A., Klocker, H., & Demichelis, F. 2010. Genetic variation of genes involved in dihydrotestosterone metabolism and the risk of prostate cancer. *Cancer Epidemiol.Biomarkers Prev.*, 19, (1) 229-239 available from: PM:20056642

Shen, L.X., Basilion, J.P., & Stanton, V.P. Jr. 1999. Single-nucleotide polymorphisms can cause different structural folds of mRNA. *Proc Natl Acad Sci U S A.,* 6;96(14):7871-6 available from PM:10393914

Sherwood, R.I., Chen, T.Y., & Melton, D.A. 2009. Transcriptional dynamics of endodermal organ formation. *Dev.Dyn.*, 238, (1) 29-42 available from: PM:19097184

Shibli-Rahhal, A., Van, B.M., & Schlechte, J.A. 2006. Cushing's syndrome. *Clin.Dermatol.*, 24, (4) 260-265 available from: PM:16828407

Silbernagel, G., Kovarova, M., Cegan, A., Machann, J., Schick, F., Lehmann, R., Häring, H.U., Stefan, N., Schleicher, E., Fritsche, A., & Peter, A. 2012. High hepatic SCD1 activity is associated with low liver fat content in healthy subjects under a lipogenic diet. *J Clin Endocrinol Metab.,* 97(12):E2288-92 available from PM: 23015656

Silverstein, R.L. & Febbraio, M. 2009. CD36, a scavenger receptor involved in immunity, metabolism, angiogenesis, and behavior. *Sci.Signal.*, 2, (72) re3 available from: PM:19471024

Silverthorn, D.U. (1997). Human physiology; an integrated approach. Benjamin Cummings.

Singh, R., Artaza, J.N., Taylor, W.E., Braga, M., Yuan, X., Gonzalez-Cadavid, N.F., & Bhasin, S. 2006. Testosterone inhibits adipogenic differentiation in 3T3-L1 cells: nuclear translocation of androgen receptor complex with beta-catenin and T-cell factor 4 may bypass canonical Wnt signaling to down-regulate adipogenic transcription factors. *Endocrinology*, 147, (1) 141-154 available from: PM:16210377

Smith, P.A., Rorsman, P., & Ashcroft, F.M. 1989. Modulation of dihydropyridine-sensitive Ca2+ channels by glucose metabolism in mouse pancreatic beta-cells. *Nature*, 342, (6249) 550-553 available from: PM:2479839

Smith, S.J., Cases, S., Jensen, D.R., Chen, H.C., Sande, E., Tow, B., Sanan, D.A., Raber, J., Eckel, R.H., & Farese, R.V. Jr. 2000. Obesity resistance and multiple mechanisms of triglyceride synthesis in mice lacking Dgat. *Nat Genet.,* 25(1):87-90 available from PM:10802663

Spiga, F., Walker, J.J., Terry, J.R., & Lightman, S.L. 2014. HPA axis-rhythms. *Compr Physiol.,* 4(3):1273-98 available from PM:24944037

Sprecher, H., Luthria, D.L., Mohammed, B.S., & Baykousheva, S.P. 1995. Reevaluation of the pathways for the biosynthesis of polyunsaturated fatty acids. *J.Lipid Res.*, 36, (12) 2471-2477 available from: PM:8847474

Stahn, C. & Buttgereit, F. 2008. Genomic and nongenomic effects of glucocorticoids. *Nat.Clin.Pract.Rheumatol.*, 4, (10) 525-533 available from: PM:18762788

Stephens, L., Anderson, K., Stokoe, D., Erdjument-Bromage, H., Painter, G.F., Holmes, A.B., Gaffney, P.R., Reese, C.B., McCormick, F., Tempst, P., Coadwell, J., & Hawkins, P.T. 1998. Protein kinase B kinases that mediate phosphatidylinositol 3,4,5-trisphosphate-dependent activation of protein kinase B. *Science*, 279, (5351) 710-714 available from: PM:9445477

Stevens and Lowe 2005). Stevens, A. & Lowe, J.S. (2005). 3 edition. Human histology. Elsevier Mosby.

Stewart, P.M., Krozowski, Z.S., Gupta, A., Milford, D.V., Howie, A.J., Sheppard, M.C., & Whorwood, C.B. 1996. Hypertension in the syndrome of apparent mineralocorticoid excess due to mutation of the 11 beta-hydroxysteroid dehydrogenase type 2 gene. *Lancet*, 347, (8994) 88-91 available from: PM:8538347

Sun, X.J., Goldberg, J.L., Qiao, L.Y., & Mitchell, J.J. 1999. Insulin-induced insulin receptor substrate-1 degradation is mediated by the proteasome degradation pathway. *Diabetes*, 48, (7) 1359-1364 available from: PM:10389839

Sutherland, C., Leighton, I.A., & Cohen, P. 1993a. Inactivation of glycogen synthase kinase-3 beta by phosphorylation: new kinase connections in insulin and growth-factor signalling. *Biochem.J.*, 296 (Pt 1), 15-19 available from: PM:8250835

Swinnen, J.V., Esquenet, M., Goossens, K., Heyns, W., & Verhoeven, G. 1997. Androgens stimulate fatty acid synthase in the human prostate cancer cell line LNCaP. *Cancer Res.*, 57, (6) 1086-1090 available from: PM:9067276

Swinnen, J.V.1., Brusselmans, K., Verhoeven, G. 2006. Increased lipogenesis in cancer cells: new players, novel targets. 2006. Increased lipogenesis in cancer cells: new players, novel targets. *Curr Opin Clin Nutr Metab Care.* 9(4):358-65 available from PM:16778563

Swinnen, J.V., Ulrix, W., Heyns, W., & Verhoeven, G. 1997. Coordinate regulation of lipogenic gene expression by androgens: evidence for a cascade mechanism involving sterol regulatory element binding proteins. *Proc Natl Acad Sci U S A*., 94(24):12975-80 available from PM:9371785

Takaishi, K., Duplomb, L., Wang, M.Y., Li, J., & Unger, R.H. 2004. Hepatic insig-1 or -2 overexpression reduces lipogenesis in obese Zucker diabetic fatty rats and in fasted/refed normal rats. *Proc.Natl.Acad.Sci.U.S.A*, 101, (18) 7106-7111 available from: PM:15096598

Tang, Z.Q., Wu, T., Cui, S.W., Zhu, X.H., Yin, T., Wang, C.F., Zhu, J.Y., & Wu, A.J. 2013. Stimulation of insulin secretion by large-dose oral arginine administration in healthy adults. *Exp.Ther.Med.*, 6, (1) 248-252 available from: PM:23935755

Targher, G., Bertolini, L., Rodella, S., Zoppini, G., Zenari, L., & Falezza, G. 2006. Associations between liver histology and cortisol secretion in subjects with nonalcoholic fatty liver disease. *Clin.Endocrinol.(Oxf)*, 64, (3) 337-341 available from: PM:16487446

Targher, G., Bertolini, L., Zoppini, G., Zenari, L., & Falezza, G. 2005. Relationship of non-alcoholic hepatic steatosis to cortisol secretion in diet-controlled Type 2 diabetic patients. *Diabet.Med.*, 22, (9) 1146-1150 available from: PM:16108840

Taskinen, M.R., Nikkila, E.A., Pelkonen, R., & Sane, T. 1983. Plasma lipoproteins, lipolytic enzymes, and very low density lipoprotein triglyceride turnover in Cushing's syndrome. *J.Clin.Endocrinol.Metab*, 57, (3) 619-626 available from: PM:6348067

Taves, M.D., Gomez-Sanchez, C.E., & Soma, K.K. 2011. Extra-adrenal glucocorticoids and mineralocorticoids: evidence for local synthesis, regulation, and function. *American*

Journal of Physiology-Endocrinology and Metabolism, 301, (1) E11-E24 available from: ISI:000292085900002

Tetri, L.H., Basaranoglu, M., Brunt, E.M., Yerian, L.M., & Neuschwander-Tetri, B.A. 2008. Severe NAFLD with hepatic necroinflammatory changes in mice fed trans fats and a high-fructose corn syrup equivalent. _Am.J.Physiol Gastrointest.Liver Physiol_, 295, (5) G987-G995 available from: PM:18772365

Thiboutot, D., Jabara, S., McAllister, J.M., Sivarajah, A., Gilliland, K., Cong, Z., & Clawson, G. 2003. Human skin is a steroidogenic tissue: steroidogenic enzymes and cofactors are expressed in epidermis, normal sebocytes, and an immortalized sebocyte cell line (SEB-1). _J.Invest Dermatol._, 120, (6) 905-914 available from: PM:12787114

Tiwari, S. & Siddiqi, S.A. 2012. Intracellular trafficking and secretion of VLDL. _Arterioscler.Thromb.Vasc.Biol._, 32, (5) 1079-1086 available from: PM:22517366

Tominaga, K., Kurata, J.H., Chen, Y.K., Fujimoto, E., Miyagawa, S., Abe, I., & Kusano, Y. 1995. Prevalence of Fatty Liver in Japanese Children and Relationship to Obesity - An Epidemiologic Ultrasonographic Survey. _Digestive Diseases and Sciences_, 40, (9) 2002-2009 available from: ISI:A1995RX56300025

Tomlinson, J.J., Boudreau, A., Wu, D., Abdou, S.H., Carrigan, A., Gagnon, A., Mears, A.J., Sorisky, A., Atlas, E., & Hache, R.J. 2010. Insulin sensitization of human preadipocytes through glucocorticoid hormone induction of forkhead transcription factors. _Mol.Endocrinol._, 24, (1) 104-113 available from: PM:19887648

Tomlinson, J.W., Finney, J., Gay, C., Hughes, B.A., Hughes, S.V., & Stewart, P.M. 2008. Impaired glucose tolerance and insulin resistance are associated with increased adipose 11beta-hydroxysteroid dehydrogenase type 1 expression and elevated hepatic 5alpha-reductase activity. _Diabetes_, 57, (10) 2652-2660 available from: PM:18633104

Tomlinson, J.W., Walker, E.A., Bujalska, I.J., Draper, N., Lavery, G.G., Cooper, M.S., Hewison, M., & Stewart, P.M. 2004. 11beta-hydroxysteroid dehydrogenase type 1: a tissue-specific regulator of glucocorticoid response. _Endocr.Rev._, 25, (5) 831-866 available from: PM:15466942

Tortora, G.T. & Derrickson, B.H. (2011).Principles of anatomy and physiology. 13 edition.

Trauner, M., Arrese, M., & Wagner, M. 2010. Fatty liver and lipotoxicity. _Biochimica et Biophysica Acta-Molecular and Cell Biology of Lipids_, 1801, (3) 299-310 available from: ISI:000275563300014

Truss, M., & Beato, M. 1993. Steroid hormone receptors: interaction with deoxyribonucleic acid and transcription factors. _Endocr Rev._, 14(4):459-79 available from PM: 8223341

Tsilchorozidou, T., Honour, J.W., & Conway, G.S. 2003. Altered cortisol metabolism in polycystic ovary syndrome: insulin enhances 5alpha-reduction but not the elevated

adrenal steroid production rates. *J.Clin.Endocrinol.Metab*, 88, (12) 5907-5913 available from: PM:14671189

Uemura, M., Tamura, K., Chung, S., Honma, S., Okuyama, A., Nakamura, Y., & Nakagawa, H. 2008. Novel 5 alpha-steroid reductase (SRD5A3, type-3) is overexpressed in hormone-refractory prostate cancer. *Cancer Sci.*, 99, (1) 81-86 available from: PM:17986282

Upreti, R., Hughes, K.A., Livingstone, D.E., Gray, C.D., Minns, F.C., Macfarlane, D.P., Marshall, I., Stewart, L.H., Walker, B.R., & Andrew, R. 2014. 5alpha-reductase type 1 modulates insulin sensitivity in men. *J.Clin.Endocrinol.Metab*, 99, (8) E1397-E1406 available from: PM:24823464

Van Staa, T.P., Abenhaim, L., Cooper, C., Zhang, B., & Leufkens, H.G.M. 2000. The use of a large pharmacoepidemiological database to study exposure to oral corticosteroids and risk of fractures: Validation of study population and results. *Pharmacoepidemiology and Drug Safety*, 9, (5) 359-366 available from: ISI:000090096600001

Vermeulen, A. & Verdonck, L. 1968. Studies on the binding of testosterone to human plasma. *Steroids*, 11, (5) 609-635 available from: PM:4172115

Volzke, H., Aumann, N., Krebs, A., Nauck, M., Steveling, A., Lerch, M.M., Rosskopf, D., & Wallaschofski, H. 2010. Hepatic steatosis is associated with low serum testosterone and high serum DHEAS levels in men. *Int.J.Androl*, 33, (1) 45-53 available from: PM:19226405

Walker, B.R., Connacher, A.A., Lindsay, R.M., Webb, D.J., & Edwards, C.R. 1995. Carbenoxolone increases hepatic insulin sensitivity in man: a novel role for 11-oxosteroid reductase in enhancing glucocorticoid receptor activation. *J.Clin.Endocrinol.Metab*, 80, (11) 3155-3159 available from: PM:7593419

Wang, C., Jackson, G., Jones, T.H., Matsumoto, A.M., Nehra, A., Perelman, M.A., Swerdloff, R.S., Traish, A., Zitzmann, M., & Cunningham, G. 2011. Low testosterone associated with obesity and the metabolic syndrome contributes to sexual dysfunction and cardiovascular disease risk in men with type 2 diabetes. *Diabetes Care*, 34, (7) 1669-1675 available from: PM:21709300

Wang, C.N., McLeod, R.S., Yao, Z., & Brindley, D.N. 1995. Effects of dexamethasone on the synthesis, degradation, and secretion of apolipoprotein B in cultured rat hepatocytes. *Arterioscler.Thromb.Vasc.Biol.*, 15, (9) 1481-1491 available from: PM:7670964

Wang, H.J., Zhang, H., Zhang, J., Wang, Y., & Ma, J. 2010. [Association of abnormal lipid metabolism with INSIG2 gene variant in overweight and obese children]. *Zhonghua Liu Xing.Bing.Xue.Za Zhi.*, 31, (6) 650-654 available from: PM:21163096

Wang, J.C., Gray, N.E., Kuo, T., & Harris, C.A. 2012a. Regulation of triglyceride metabolism by glucocorticoid receptor. *Cell Biosci.*, 2, (1) 19 available from: PM:22640645

Wang, Y.X., Voy, B.J., Urs, S., Kim, S., Soltani-Bejnood, M., Quigley, N., Heo, Y.R., Standridge, M., Andersen, B., Dhar, M., Joshi, R., Wortman, P., Taylor, J.W., Chun, J., Leuze, M., Claycombe, K., Saxton, A.M., & Moustaid-Moussa, N. 2004. The human fatty acid synthase gene and *de novo* lipogenesis are coordinately regulated in human adipose tissue. *Journal of Nutrition*, 134, (5) 1032-1038 available from: ISI:000221423000007

Wardle, J., Carnell, S., Haworth, C.M., Farooqi, I.S., O'Rahilly, S., & Plomin, R. 2008. Obesity associated genetic variation in FTO is associated with diminished satiety. *J.Clin.Endocrinol.Metab*, 93, (9) 3640-3643 available from: PM:18583465

Wei, L., MacDonald, T.M., & Walker, B.R. 2004. Taking glucocorticoids by prescription is associated with subsequent cardiovascular disease. *Annals of Internal Medicine*, 141, (10) 764-770 available from: ISI:000225206900003

Welsh, G.I. & Proud, C.G. 1993. Glycogen synthase kinase-3 is rapidly inactivated in response to insulin and phosphorylates eukaryotic initiation factor eIF-2B. *Biochem.J.*, 294 (Pt 3), 625-629 available from: PM:8397507

White, D.L., Liu, Y., Garcia, J., El-Serag, H.B., Jiao, L., Tsavachidis, S., Franco, L.M., Lee, J.S., Tavakoli-Tabasi, S., Moore, D., Goldman, R., Kuzniarek, J., Ramsey, D.J., Kanwal, F., & Marcelli, M. 2014. Sex hormone pathway gene polymorphisms are associated with risk of advanced hepatitis C-related liver disease in males. *Int.J.Mol.Epidemiol.Genet.*, 5, (3) 164-176 available from: PM:25379136

Widmer, J., Fassihi, K.S., Schlichter, S.C., Wheeler, K.S., Crute, B.E., King, N., Nutile-McMenemy, N., Noll, W.W., Daniel, S., Ha, J., Kim, K.H., & Witters, L.A. 1996. Identification of a second human acetyl-CoA carboxylase gene. *Biochem.J.*, 316 (Pt 3), 915-922 available from: PM:8670171

Wiegman, C.H., Bandsma, R.H., Ouwens, M., van der Sluijs, F.H., Havinga, R., Boer, T., Reijngoud, D.J., Romijn, J.A., & Kuipers, F. 2003. Hepatic VLDL production in ob/ob mice is not stimulated by massive *de novo* lipogenesis but is less sensitive to the suppressive effects of insulin. *Diabetes*, 52, (5) 1081-1089 available from: PM:12716736

Witters, L.A. & Kemp, B.E. 1992. Insulin activation of acetyl-CoA carboxylase accompanied by inhibition of the 5'-AMP-activated protein kinase. *J.Biol.Chem.*, 267, (5) 2864-2867 available from: PM:1346611

Xu, C., He, J., Jiang, H., Zu, L., Zhai, W., Pu, S., & Xu, G. 2009. Direct effect of glucocorticoids on lipolysis in adipocytes. *Mol.Endocrinol.*, 23, (8) 1161-1170 available from: PM:19443609

Yakirevich, E., Morris, D.J., Tavares, R., Meitner, P.A., Lechpammer, M., Noble, L., de Rodriguez, A.F., Gomez-Sanchez, C.E., Wang, L.J., Sabo, E., DeLellis, R.A., & Resnick, M.B. 2008. Mineralocorticoid receptor and 11 beta-hydroxysteroid dehydrogenase type II expression in renal cell neoplasms. *American Journal of Surgical Pathology*, 32A, (6) 874-883 available from: ISI:000256553000009

Yamana, K., Labrie, F., & Luu-The, V. 2010. Human type 3 5alpha-reductase is expressed in peripheral tissues at higher levels than types 1 and 2 and its activity is potently inhibited by finasteride and dutasteride. *Horm.Mol.Biol.Clin.Investig.*, 2, (3) 293-299 available from: PM:25961201

Yang, J., Chi, Y., Burkhardt, B.R., Guan, Y., & Wolf, B.A. 2010a. Leucine metabolism in regulation of insulin secretion from pancreatic beta cells. *Nutr.Rev.*, 68, (5) 270-279 available from: PM:20500788

Yang, L., Li, P., Fu, S., Calay, E.S., & Hotamisligil, G.S. 2010b. Defective hepatic autophagy in obesity promotes ER stress and causes insulin resistance. *Cell Metab*, 11, (6) 467-478 available from: PM:20519119

Young, B. & Heath. J.W. (2000).Wheater's Functional Histology: A Text and Colour Atlas. 4 edition. Churchill Livingston.

Yu, C., Chen, Y., Cline, G.W., Zhang, D., Zong, H., Wang, Y., Bergeron, R., Kim, J.K., Cushman, S.W., Cooney, G.J., Atcheson, B., White, M.F., Kraegen, E.W., & Shulman, G.I. 2002. Mechanism by which fatty acids inhibit insulin activation of insulin receptor substrate-1 (IRS-1)-associated phosphatidylinositol 3-kinase activity in muscle. *J.Biol.Chem.*, 277, (52) 50230-50236 available from: PM:12006582

Yu, J., Zhang, Y., McIlroy, J., Rordorf-Nikolic, T., Orr, G.A., & Backer, J.M. 1998. Regulation of the p85/p110 phosphatidylinositol 3'-kinase: stabilization and inhibition of the p110alpha catalytic subunit by the p85 regulatory subunit. *Mol.Cell Biol.*, 18, (3) 1379-1387 available from: PM:9488453

Zammit, V.A. 1999. The malonyl-CoA-long-chain acyl-CoA axis in the maintenance of mammalian cell function. *Biochem.J.*, 343 Pt 3, 505-515 available from: PM:10527927

Zarkovic, M., Beleslin, B., Ciric, J., Penezic, Z., Stojkovic, M., Trbojevic, B., Drezgic, M., & Savic, S. 2008. Glucocorticoid effect on insulin sensitivity: a time frame. *J.Endocrinol.Invest*, 31, (3) 238-242 available from: PM:18401206

Zhang, H., Liu, Y., Wang, L., Li, Z., Zhang, H., Wu, J., Rahman, N., Guo, Y., Li, D., Li, N., Huhtaniemi, I., Tsang, S.Y., Gao, G.F., Li, X.2013.Differential effects of estrogen/androgen on the prevention of nonalcoholic fatty liver disease in the male rat. *J Lipid Res.*,54(2):345-57 available from PM:23175777

Zhang, W., Patil, S., Chauhan, B., Guo, S., Powell, D.R., Le, J., Klotsas, A., Matika, R., Xiao, X., Franks, R., Heidenreich, K.A., Sajan, M.P., Farese, R.V., Stolz, D.B., Tso, P., Koo, S.H., Montminy, M., & Unterman, T.G. 2006. FoxO1 regulates multiple metabolic pathways in the liver: effects on gluconeogenic, glycolytic, and lipogenic gene expression. *J.Biol.Chem.*, 281, (15) 10105-10117 available from: PM:16492665

Zhao, L.F., Iwasaki, Y., Zhe, W., Nishiyama, M., Taguchi, T., Tsugita, M., Kambayashi, M., Hashimoto, K., & Terada, Y. 2010. Hormonal Regulation of Acetyl-CoA Carboxylase Isoenzyme Gene Transcription. *Endocrine Journal*, 57, (4) 317-324 available from: ISI:000277443500006

Zhu, Y.S. & Sun, G.H. 2005. 5alpha-Reductase Isozymes in the Prostate. *J.Med.Sci.*, 25, (1) 1-12 available from: PM:18483578

Zimmer, V. & Lammert, F. 2011. Genetics and epigenetics in the fibrogenic evolution of chronic liver diseases. *Best.Pract.Res.Clin.Gastroenterol.*, 25, (2) 269-280 available from: PM:21497744

Zoppini, G., Targher, G., Venturi, C., Zamboni, C., & Muggeo, M. 2004. Relationship of nonalcoholic hepatic steatosis to overnight low-dose dexamethasone suppression test in obese individuals. *Clin.Endocrinol.(Oxf)*, 61, (6) 711-715 available from: PM:15579185

Zorn, A.M. 2008. Liver development. available from: PM:20614624

Publications

5α-reductase type 2 regulates glucocorticoid action and metabolic phenotype in human hepatocytes

Maryam Nasiri[1], Nikolaos Nikolaou[2,3], Silvia Parajes[1] Nils P Krone[1], George Valsamakis[3], George Mastorakos[3], Beverly Hughes[1], Angela Taylor[1], Iwona J Bujalska[1], Laura L Gathercole[2], and Jeremy W Tomlinson[2]

Centre for Endocrinology, Diabetes and Metabolism, Institute of Biomedical Research, School of Clinical and Experimental Medicine, University of Birmingham, Edgbaston, Birmingham, UK. B15 2TT; 2. Oxford Centre for Diabetes, Endocrinology & Metabolism, NIHR Oxford Biomedical Research Centre, University of Oxford, Churchill Hospital, Headington, Oxford, UK. OX3 7LJ; 3. Endocrine Unit, second Department of Obstetrics and Gynecology and Pathology Department, Aretaieion University Hospital, Athens Medical School, Athens, Greece

Glucocorticoids and androgens have both been implicated in the pathogenesis of non-alcoholic fatty liver disease (NAFLD); androgen deficiency in males, androgen excess in females and glucocorticoid excess in both sexes are associated with NAFLD. Glucocorticoid and androgen action are regulated at a pre-receptor level by the enzyme 5α-reductase type 2 (SRD5A2) that inactivates glucocorticoids to their dihydrometabolites and converts testosterone to dihydrotestosterone (DHT). We have therefore explored the role of androgens and glucocorticoids and their metabolism by SRD5A2 upon lipid homeostasis in human hepatocytes.

In both primary human hepatocytes and human hepatoma cell lines, glucocorticoids decreased *de novo* lipogenesis in a dose-dependent manner. Whilst androgen treatment (testosterone and DHT) increased lipogenesis in cell lines and in primary cultures of human hepatocytes from female donors, it was without effect in primary hepatocyte cultures from men. SRD5A2 over-expression *reduced* the effects of cortisol to suppress lipogenesis and this effect was lost following transfection with an inactive mutant construct. Conversely, pharmacological inhibition using the 5α-reductase inhibitors finasteride and dutasteride, augmented cortisol action.

We have demonstrated that manipulation of *5α-reductase type 2 activity can regulate lipogenesis in human hepatocytes in vitro*. This may have significant clinical implications for those patients prescribed 5α-reductase inhibitors, in particular augmenting the actions of glucocorticoids to modulate hepatic lipid flux.

The global epidemic of obesity and type 2 diabetes is tightly linked to the increasing prevalence of nonalcoholic fatty liver disease (NAFLD) which contributes significantly to increased morbidity and mortality (1). The potent role of glucocorticoids (GC) to modulate metabolic phenotype is exemplified in patients with GC excess, Cushing's syndrome, and many of these patients develop NAFLD (2). However, in most patients with metabolic disease and NAFLD, circulating GC levels are not elevated (3). At a tissue-specific level, notably within the liver, GCs are cleared by a series of enzymes including the A-ring reductases (5α-reductase type 1 (SRD5A1) and 2 (SRD5A2) and 5β-reductase). 5α-reductase exists as 2 isoforms (SRD5A1 and 2), both have 5 exons and 4 introns, but share less than 50% homology and both isoforms are expressed in human liver (4); SRD5A1 alone is expressed

Abbreviations:

ISSN Print 0013-7227 ISSN Online 1945-7170
Printed in U.S.A.

Received February 13, 2015. Accepted May 11, 2015.

in mouse liver. SRD5A2 is believed to be the major isoform in clearing cortisol in human studies (5), however, there is an emerging role for SRD5A1 in the pathogenesis of metabolic disease. We, and others, have shown that in a rodent model, genetic ablation of SRD5A1 increase lipid accumulation in the liver and the severity of NAFLD (6, 7).

The role of androgens in the pathogenesis of metabolic disease remains controversial. There is evidence documenting an association between hypogonadism and NAFLD (8, 9) with some evidence for improvement following androgen treatment (10, 11). SRD5A2 has an established role in the conversion of testosterone to dihydrotestosterone (DHT) and genetic mutations lead to 46XY DSD (Disorder of Sex Development). *While DHT is a more potent activator of the androgen receptor (AR), testosterone binds and activates the AR*. We have shown that increased *global 5α*-reductase activity is associated with impaired glucose tolerance and may be a future predictor of metabolic disease (12, 13). The lack of SRD5A2 expression in the mouse liver (contrasting with human liver) has limited the interpretation of data from SRD5A2 knock out mice (7) and has highlighted the importance of the use of human models. The translational importance of this not only relates to enhancing our understanding of the pathogenesis of NAFLD, but also to the widespread use of SRD5A2 inhibitors including the selective, SRD5A2 inhibitor, Finasteride, and the nonselective (SRD5A1 and 2) inhibitor, Dutasteride.

Lipid accumulation within hepatocytes is the first step in the development of NAFLD, and in some individuals can progress through inflammation (NASH), to fibrosis and eventual cirrhosis. There are multiple mechanisms that contribute to lipid accumulation in vivo including re-esterification of free fatty acids (FFA) delivered principally from intra-abdominal tissue depots, de novo synthesis of triacylglycerol from acetyl CoA (de novo lipogenesis, DNL) as well as limitation of β-oxidation and lipid export and secretion. While FFA delivery is believed to be the most important process in the development of NAFLD, the contribution of DNL increases significantly in patients with NAFLD (14). The rate-limiting step in DNL is the carboxylation of acetyl CoA to malonyl-CoA by acetyl CoA carboxylase (ACC) which is subsequently converted by a multistep reaction to palmitate by fatty acid synthase (FAS). There are two isoforms of ACC (ACC1 and ACC2); in lipogenic tissues ACC1 predominates and is the key regulatory step of fatty acid synthesis. ACC2 is localized to the mitochondrial membrane, and its role is to limit β-oxidation through malonyl-CoA mediated inhibition of carnitine palmitoyl transferase I (CPT I).

Although it is not possible to replicate all the processes that contribute to the development of NAFLD using in vitro systems, using established cellular models, we have tested the hypothesis that SRD5A2 represents an important regulator of the metabolic actions of androgens and GCs to modulate lipid homeostasis within human hepatocytes.

Materials and Methods

C3A and primary human hepatocyte culture

The C3A human hepatocyte cell line was purchased from LGC Standards (ATCC - CRL-10 741, Middlesex, UK), and cultured in Eagle's Minimum Essential Medium (EMEM) containing 10% fetal calf serum and glutamine/penicillin/streptococcus. Cells were seeded in 24-well plates and at 70%–80% confluence were incubated with control media with or without hormonal treatments. The precise conditions for individual experiments is detailed in the results section. All reagents were supplied by Sigma-Aldrich (Dorset, UK) unless otherwise stated.

Primary human hepatocytes were purchased from Celsis In Vitro Technologies (Baltimore, Maryland, US). *All donors were healthy, nondiabetic, none consumed alcohol above recommended limits (female < 14 U/wk, male < 21 U/wk), none were taking regular medications and all had negative viral hepatitis serology (male: n = 4, age 54 ± 14years, BMI 28.4 ± 3.3 kg/m^2; female: n = 4, age 56 ± 4.7years, BMI 23.98 ± 3.1 kg/m^2).* Cells were cultured overnight in Williams' Medium E without any supplements before being treated with GCs or androgens. For insulin signaling studies, media was spiked with insulin 15-minutes prior to cell harvest as described above. Lipogenesis was measured by the uptake of 1-[14C]-acetate into the lipid component (see below)

RNA extraction and Reverse Transcription

Total RNA was extracted from tissue and cells using the Tri-Reagent system. RNA integrity was assessed by electrophoresis on 1% agarose gel. Concentration was determined spectrophotometrically at OD_{260}. In a 50 μl volume, 500ng of total RNA was incubated with 250uM random hexamers, 500uM dNTPs, 20U RNase inhibitor, 63U Multiscribe reverse transcriptase, 5.5 mM MgCl and 1 x reaction buffer. The reverse transcription reaction was carried out at 25°C for 10min, 48°C for 30min and then the reaction was terminated by heating to 95°C for 5min.

Real-Time PCR

mRNA levels were determined using an ABI 7500 sequence detection system (Perkin-Elmer Applied Biosystems, Warrington, UK). Reactions were performed in 10μl volumes on 96-well plates in reaction buffer containing 2 x TaqMan Universal PCR Master mix (Applied Biosystems, Foster City, CA, USA). All primers and probes were supplied by applied biosystems 'assay on demand' (Applied Biosystems) and reactions normalized against the house keeping gene 18S rRNA, provided as a preoptimized control probe. All target genes were labeled with FAM and the housekeeping gene with VIC. The reaction conditions were as follows: 95°C for 10-minutes, then 40 cycles of 95°C for 15-seconds and 60°C for 1min.

Data were obtained as ct values (ct=cycle number at which logarithmic PCR plots cross a calculated threshold line) and used

to determine Δct values (Δct = (ct of the target gene) – (ct of the housekeeping gene). Data were expressed as arbitrary units using the following transformation [expression = $1000_*(2^{-\Delta ct})$ arbitrary units (AU)].

Protein extraction and Immunoblotting

Total protein was extracted from cells using RIPA buffer (50 mM Tris pH 7.4, 1% NP40, 0.25% sodium deoxycholate, 150 mM NaCl, 1 mM EDTA, 1 mM PMSF and protease inhibitor cocktail (Roche, Lewes, UK) dissolved in 10 mL of distilled water) and freeze thawing. Protein concentrations were measured using a commercially available assay (Bio-Rad Laboratories Inc., Hercules, CA). 15 μg of protein was resolved on a 12.5% SDS PAGE gel and transferred onto nitrocellulose membrane, Hybond ECL (GE Healthcare, Chalfont St Giles, UK). Primary (PKB/akt, Biosource, Nivelles, Belgium and anti phosphoPKB/akt (serine 473), R&D Systems, Abingdon, UK) and secondary antibodies (Dako, Glostrop, UK) used at a dilution of 1/1000. Membranes were reprobed for β-Actin. Primary and secondary antibodies were used at a dilution of 1/5000 (Abcam plc, Cambridge, UK). For antibody characteristics see Supplemental Table 1. Bands were quantified with Genesnap by Syngene (Cambridge, UK) and expressed relative to β-actin to normalize for gel loading.

De novo lipogenesis (DNL)

DNL was measured by the uptake of 1-[^{14}C] -acetate into the lipid component of hepatocytes *as has been described previously (15)*. Cells were cultured in a 24-well plate, washed 3 times with serum free media and then incubated with 500μl of serum free media *with 4.44kBq/L* 1-[^{14}C]-acetic acid with cold sodium acetate to a final concentration of 10 μM acetate and treated with or without insulin (0.5ng/ml). The cells were incubated at 37°C for 6-hours. After incubation activity was terminated by washing the cells 3 times with cold PBS and scraping into 250μl of PBS. The lipid fraction was recovered in Folch solvent, the solvent was evaporated and the radioactivity retained in the cellular lipid was determined by scintillation counting and expressed as disintegrations per minute (dpm)/well. *To account for variability between experimental replicates, data are presented as percentage change from control.*

β-oxidation

Rates of β-oxidation were measured by the conversion of [^3H]-*palmitate to* ^3H_2O. Cells were cultured in a 24-well plates and were washed 3 times with serum free media. Cells were then incubated with 300μl of low glucose serum free media with *4.44kBq/L* [^3H]-*palmitic acid* with cold palmitate to a final concentration of 10 μM. The cells were incubated at 37°C for 24hours. After incubation medium was recovered and precipitated with an equal volume of 10% tricholoroacetic acid. The aqueous component of the supernatants was extracted with 2:1 choloform methanol solution. Radioactivity was determined by scintillation counting, expressed as disintegrations per minute (dpm)/well *and finally calculated as percentage change from control.*

Transfection studies

The Androgen receptor (AR) and SRD5A2 cDNAs were cloned into the pcDNA3.1 vector (Invitrogen, Paisley, UK) and transiently transfected into C3A cells. Prior to transfection, cells were seeded into a 24-well plate. Cells were ~60%-70% confluent in order to obtain the most efficient transfection results. Transfection mixture comprised 1.5 μg of DNA diluted in 50 μL of OptiMEM serum free media (Invitrogen, UK) and 2 μL of Lipofectamine 2000 (Invitrogen, Paisley, UK) diluted in 50 μL of Optimem serum free media. 100 μL of transfection mixture was added drop-wise to each well. The plates were rocked gently and left for incubation at 37°C. Transfection duration was 48h and its efficiency was determined by applying a plasmid containing the Green Fluorescent Protein (GFP) gene. Changes in AR and SRD5A2 mRNA expression level were confirmed by real-time PCR.

Site directed mutagenesis

The R246Q mutant was inserted by site directed mutagenesis into the SDR5A2 cDNA using the Quikchange II site-directed mutagenesis kit (Agilent Technologies UK Limited, Cheshire, UK) as per the manufactures guidance. In a 50μl reaction the following components were added: 5μl of 10× reaction buffer, forward and reverse primers (125ng) 10ng of double-strand DNA template, 1μl of dNTP mix, 3μl of QuikSolution and ddH_2O to a final volume of 50μl. Using a thermal cycler (Biometra, Göttingen, Germany) samples were incubated at 95°C for 1min and then cycled 18 times at 95°C for 50 seconds, 53.4 to 60°C for 50 seconds, and 68°C for 60 seconds. Samples were then incubated for 68°C for 7min. 1μl of DpnI was added to PCR reaction, vortexed and incubated for 1 hour at 37°C. 1ml of ethanol (100%) was then added to each tube and incubated for 1hour at –80°C. The mixture was centrifuged at 16 000 XG for 20 minutes at 4°C and the supernatant aspirated. The DNA pellet was washed with 75% ethanol, centrifuged, aspirated, air dried for 10 minutes, resuspended in 10μl of RNase free water. Finally, the DNA vector containing the R246Q mutation was transformed to XL10-Gold ultracompetent cells.

Gas and Liquid chromatography/Mass spectrometry (GC/MS and LC/MS)

Cortisol was extracted from cell media after addition of the internal standard cortisol-d4. Briefly, transfected cells were incubated with 200 nM of cortisol for 24h. 1ml of media was collected, extracted by SPE and the samples were derivatized overnight to form methyloxime-trimethylsilylethers (MO-TMS). The final derivative was dissolved in 55ul cyclohexane, which was transferred to an autosampler vial for GC/MS analysis. An Agilent 5973 instrument (www.agilent.com) was used in a selected ion monitoring mode.

5α-reductase activity was measured using LC/MS. Briefly, cells were incubated with *100 nM* Testosterone for 30min. Media was removed and transferred into glass tubes. 5ml dichloromethane was added to each tube, vortexed for 30 seconds and then centrifuged for 10 minutes at 1600 rpm. The aqueous phase was removed and the steroid-containing organic solvent phase evaporated in air to dryness. The steroid extract was analyzed using LC/MSMS (Xevo TQ mass spectrometer combined with an acquity uPLC system) with an electro-spray ionisation source in positive ion mode. Steroid hormones were eluted from a BEH C_{18} 2.1 × 50 mm 1.7 μm column using a methanol/water gradient system, solvent A was water 0.1% formic acid, and B was methanol 0.1% formic acid. The flow rate was 0.6 mL/min and

starting conditions were 45% B increasing linearly to 75% B over 5 minutes. Steroid hormones were positively identified by comparison of retention times and mass transitions to steroid standards.

Statistical analysis

Data are presented as mean ± standard error. Where data were normally distributed, t-tests (paired or unpaired where appropriate) were used to compare single treatments to control. If normality tests failed, nonparametric tests were used. ANOVA was used to compare multiple doses and / or treatments. Statistical analysis on real-time PCR data was performed on mean Δct values and not fold changes. All analysis was performed using the GraphPad Prism 6.0 software package (GraphPad Software, Inc. La Jolla, CA)

Results

Regulation of lipogenesis human hepatocytes by androgens

Fatty acid synthase (FASN), ACC1, ACC2 and CPT1 mRNA expression increased after treatment with testosterone in a dose-dependent manner (*Figure 1a-d*) in C3A human hepatoma cells. Observations were similar following DHT treatment (*Figure 1a-d)*. Absolute changes in mRNA expression levels are presented in Supplemental Table 2. Lipogenic gene expression changes were mirrored by functional assays of 1-[^{14}C]-acetate incorporation into lipid; both testosterone and DHT increased lipogenesis Lipogenic gene expression changes were mirrored by functional assays of 1-[^{14}C]-acetate incorporation into lipid; both testosterone and DHT increased lipogenesis (*ctrl 100% vs. T (50 nM, 24h) 124.9 ± 6.2%, DHT (10 nM, 24h) 128.1 ± 4.7%)*. AR overexpression was confirmed by real-time PCR (ctrl 0.02 ± 0.003 vs. AR 30.04 ± 0.018AU, $P < .05$). Even in the absence of testosterone or DHT, AR overexpression alone caused a significant increases in 1-[^{14}C]-acetate incorporation into lipid (*ctrl vector only 100% vs. AR 202.7 ± 10.8%, P < .05). Treatment with both testosterone and DHT did not further enhance lipid accumulation (ctrl 202.7 ± 10.8% vs. T (50 nM, 24h) 209.6 ± 16.5%, DHT (10 nM, 24h) 224.6 ± 8.6%) (Figure 1e)*. In addition, AR overexpression increased lipid metabolism gene expression compared to cells transfected with vector alone (FASN: ctrl 13.9 ± 2.0 vs. AR 66.8 ± 6.2, ACC1: ctrl 1.0 ± 0.3 vs. AR 3.5 ± 0.3, ACC2: ctrl 0.5 ± 0.1 vs. AR 1.0 ± 0.1, CPT1: ctrl 1.8 ± 0.3 vs. AR 4.3 ± 0.2, $P < .05$).

Studies were also performed in primary cultures of human hepatocytes from both male and female donors. Both testosterone and DHT were without effect in cultures from male patients, however, in samples from female donors, testosterone *increased lipogenesis (139.6 ± 17.6% (Testosterone, 5 nM, 24h) vs. 100% (control), P < .05). Interestingly, DHT decreased lipogenesis in hepatocytes from female donors only (Figure 1f)*.

Regulation of lipid flux in human hepatocytes by glucocorticoids and insulin

GC receptor, IRS1/2, Insulin receptor and AKT1/2 were all expressed in primary cultures of human hepatocytes *from male donors*. Incubation with cortisol alone or in combination with insulin did not alter gene expression levels (Supplemental Table 3). Cortisol decreased 1-[^{14}C]-acetate incorporation into lipid in a dose-dependent manner (Figure 2a). Insulin increased lipogenesis in primary cultures of human hepatocytes (123.6 ± 10.7% (insulin, 5 nM, 24h) vs. 100% (control), $P < .05$) (*Figure 2b*). Interestingly, coincubation with increasing doses of cortisol increased the ability of insulin to simulate lipogenesis suggesting that insulin and glucocorticoids may work synergistically to promote lipid storage in human hepatocytes (43.9 ± 12.7% [250 nM], 66.13 ± 9.8% [1000 nM] vs. control (23.61 ± 10.7%), $P < .05$) (*Figure 2c*).

Cortisol treatment did not alter total PKB/akt levels. However, insulin-stimulated phosphorylation of PKB/akt at serine 473 increased following cortisol pretreatment in a dose dependant manner (1.23-fold [100 nM], 1.68-fold [250 nM], 2.44-fold [1000 nM] vs. control n = 4 $P < .05$) (*Figure 2d and e*).

Cortisol treatment did not alter rates of β-oxidation of free fatty acid uptake in C3A cells (data not shown)

SRD5A2 regulates lipogenesis in human hepatocytes

The effects of testosterone were similar to that of DHT upon lipogenesis in our hepatocyte models and we therefore postulated that SRD5A2 may have a more important role to regulate GC exposure in this context.

SRD5A2 overexpression was confirmed using real-time PCR (Figure 3a). Functional activity was assessed through increased DHT generation following incubation with T (Figure 3b) and clearance of cortisol (Figure 3c) as measured by LC/MSMS and GC/MS respectively. The mutant SRD5A2 construct, R246Q, was without activity. Conversion of testosterone to DHT was similar to that observed in the vector only transfection control (Figure 3b).

As observed previously, cortisol decreased lipogenesis in a dose dependent manner in C3A cells transfected with vector construct alone and in the absence of cortisol, SRD5A2 overexpression had no effect. However, in the presence of cortisol, SRD5A2 restored lipogenesis to levels observed in untreated controls (eg, 61.9 ± 7.6%[cortisol] vs. 103.8 ± 8.8% [SRD5A2+cortisol], $P < .05$, control =

100%) (Figure 4a). Complementary experiments using the R246Q SRD5A2 construct that is devoid of functional activity did not alter cortisol-mediated suppression of DNL (Figure 4b). To further endorse these findings, experiments were undertaken using pharmacological inhibitors of 5α-reductase isoforms in primary cultures of human hepatocytes. Consistent with our transfection studies, both finasteride (selective SRD5A2 inhibitor) and

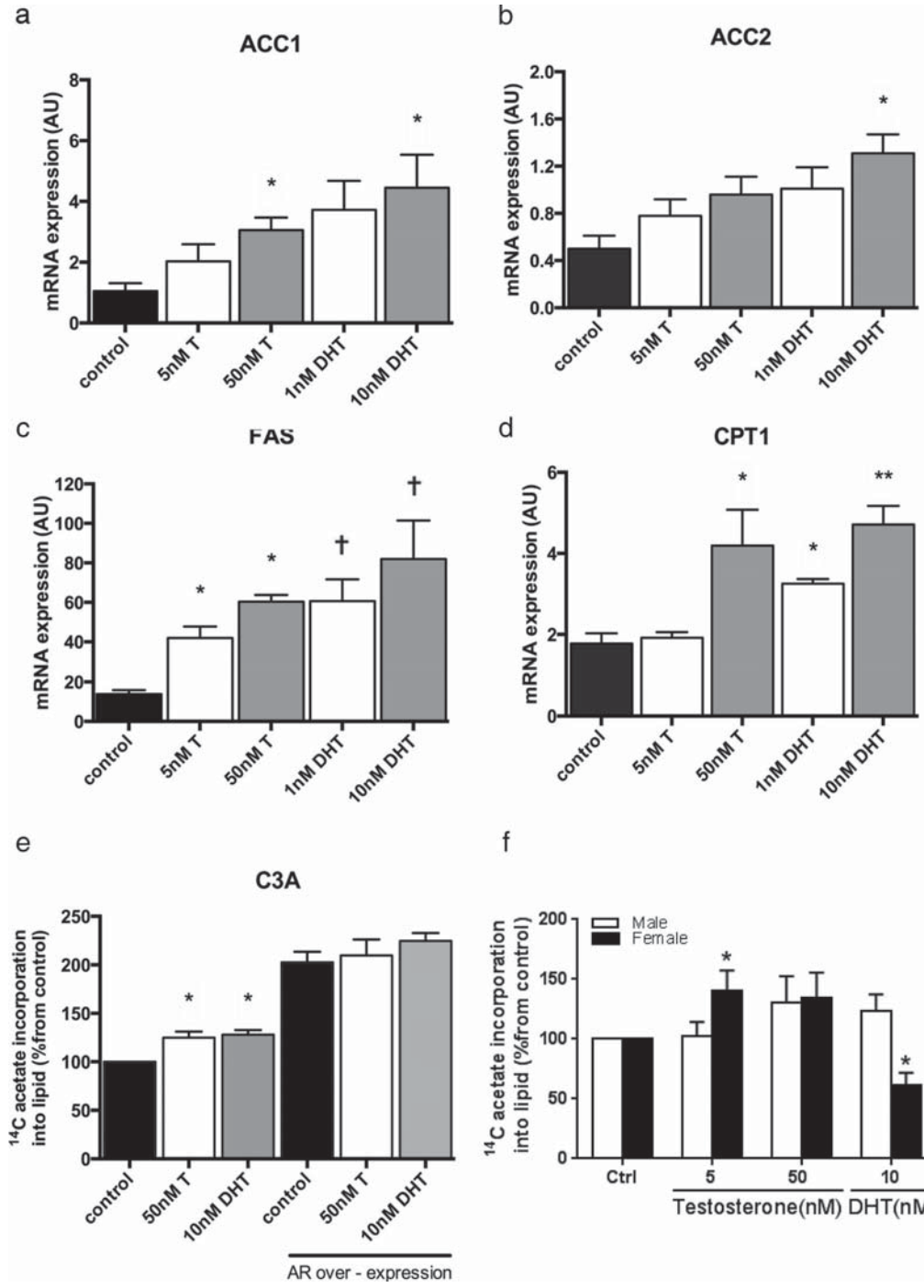

Figure 1. Testosterone [To] and dihydrotestosterone [DHT] cause a dose-dependent increase in lipogenic genes as well as increasing carnitine palmitoyl trasferase 1 [CPT1], the rate-limiting step in mitochondrial β-oxidation, in human C3A cells (a-d). Changes in lipogenic gene expression are paralleled by function increases in 1-[^{14}C]-acetate incorporation into lipid (e). Androgen receptor (AR) overexpression alone, and in the presence of T or DHT increases functional lipogenesis (e). In primary cultures of human hepatocytes, T, but not DHT increases 1-[^{14}C]-acetate incorporation into lipid in female patients (black bars), but have no effect in samples from male patients (white bars) (f). Data presented are mean$\pm$SE of n = 3–5 experiments performed in triplicate, *$P < .05$.

dutasteride (nonselective SRD5A1 and 2 inhibitor) augmented the action of cortisol to suppress DNL (eg, 88.3 ± 5.3 vs. 76.9 ± 5.2%, cortisol vs. cortisol + finasteride, $P = .05$) (Figure 4c).

Discussion

In this study, we have shown that androgens are able to increase lipid accumulation within human hepatocytes. Cross-sectional *clinical studies* have shown that low testosterone *concentrations* are associated with increased hepatic steatosis in men (8, 9) and are consistent with findings in rodent models suggesting that DHT treatment can decrease hepatic lipid accumulation (16). *In contrast, women with polycystic ovarian syndrome (PCOS), a condition characterized by androgen excess as well as insulin resistance, are at an increased risk of developing NAFLD although the precise contribution of each of these processes (insulin resistance and androgen excess) to the development of NALFD remains unclear (17, 18).*

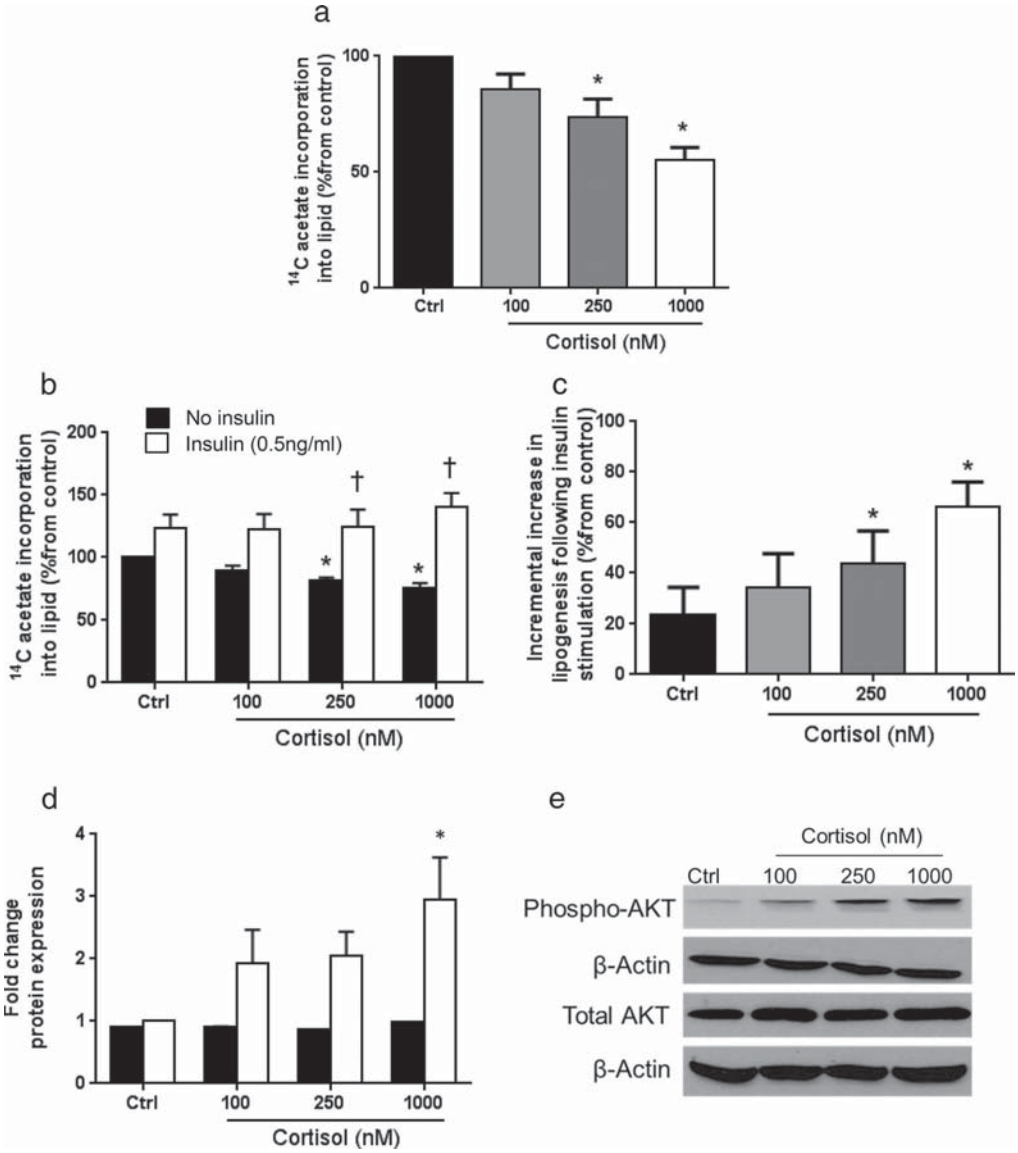

Figure 2. a. Cortisol decreases 1-[^{14}C]-acetate incorporation into lipid in *primary human hepatocytes from male donors*. b. While cortisol (*black bars) decreases lipogenesis, under hyperinsulinemic conditions (white bars), cortisol increases acetate incorporation into lipid. c. Cortisol treatment increases the ability of insulin to stimulate lipogenesis in a dose-dependent manner. d. Pretreatment of primary human hepatocytes from male donors with cortisol increases insulin-stimulated phosphorylation of AKT at residue ser473. The formal quantification of Western blot densitometry relative to β-actin (n = 4 experiments) is presented (total AKT (black bars) and pAKT ser473 (white bars)). e. Representative Western blot*. Data presented are mean±SE, $*P < .05$.

Although in vitro cell models are not able to replicate all the processes that contribute to the development of NAFLD in vivo, in C3A cells, testosterone *and DHT* increased lipid accumulation, but interestingly, in primary cultures, we observed sexually dimorphic effects. In cells derived from male donors, androgen treatment failed to have a

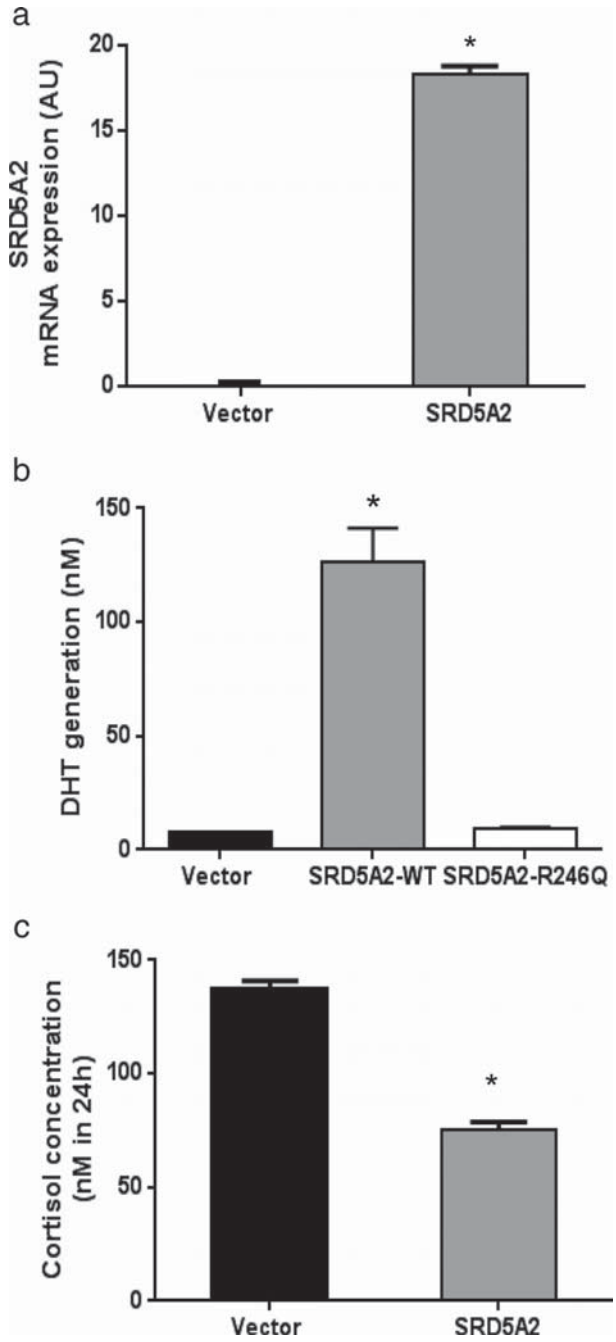

Figure 3. Increased 5α-reductase type 2 expression following transfection into C3A cells (a). Transfection of wild-type 5α-reductase type 2 (in contrast to the mutant R246Q construct) is associated with increased dihydrotestosterone [DHT] generation from Testosterone [To] (b) as well as clearance of cortisol (c). Data presented are mean±SE of n = 3 experiments performed in triplicate, $*P < .05$

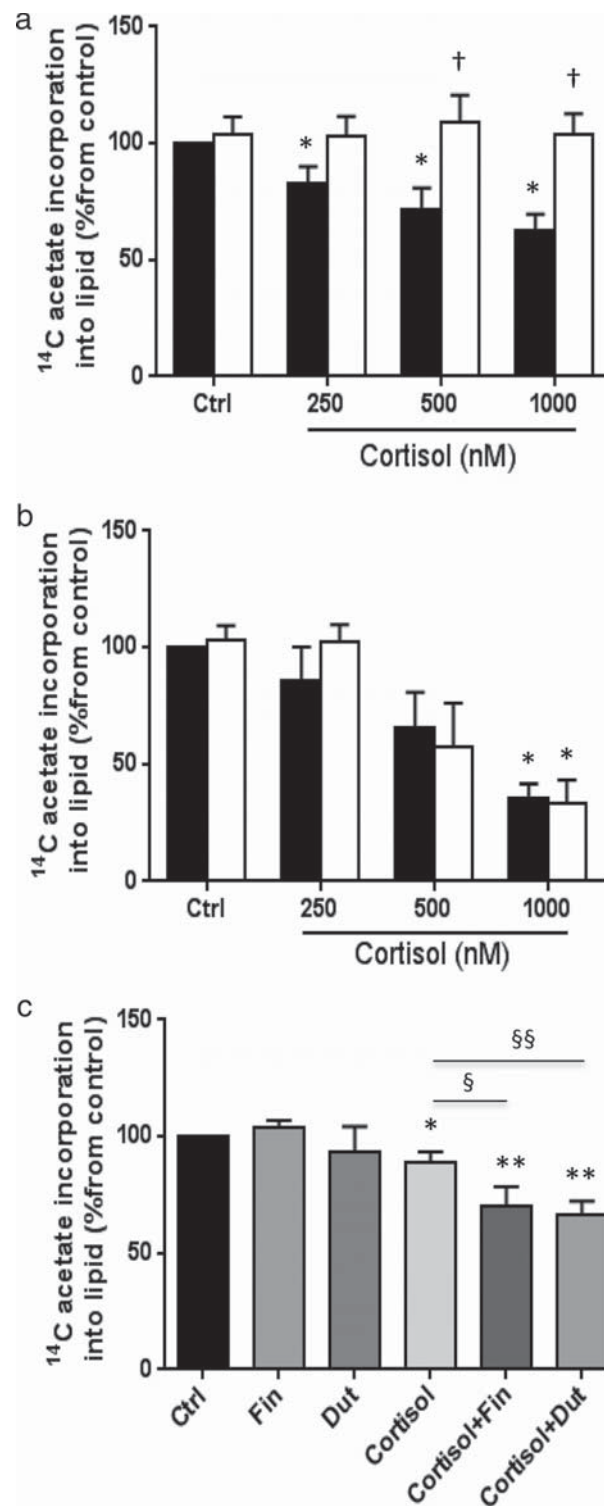

Figure 4. In C3A cells, the decrease in lipogenesis associated with increasing doses of cortisol (black bars, vector only transfection) was abolished in cells transfected with wild-type 5α-reductase type 2 (white bars) (a). Transfection of mutant R246Q 5α-reductase type 2 was without effect (vector only black bars, R246Q white bars) (b). In primary cultures of human hepatocytes, pharmacological inhibition of 5α-reductase type 2 with either the selective (Finasteride) or nonselective inhibitor (Dutasteride), augments the action of cortisol to

significant impact upon lipogenesis, however in female samples, 5 nM testosterone increased DNL. *It is interesting to note that DHT did not alter lipogenesis in hepatocytes from male donors, but decreased lipogenesis in female hepatocytes. The mechanisms underpinning this observation and the physiological relevance (the concentrations of DHT used far exceed those seen in the female circulation) are not clear. The discrepancy between the effects of androgens on C3A cells and in primary cultures may reflect origin of C3A cells from human hepatoma (and the well described impact of androgens upon their pathogenesis (19)) and serves to emphasize the important of endorsing in vitro observations in additional models including human primary cultures.*

Enhancing androgen action through androgen receptor overexpression increased DNL providing further evidence as to the potent ability of this pathway to regulate lipid accumulation. Interestingly, we observed no additional effects of providing additional AR ligand, perhaps suggesting maximal stimulation with receptor overexpression alone. Furthermore, AR over expression alone in the absence of ligand was able to increase lipogenesis. While, it is possible that this may reflect existing intracellular androgen availability, ligand-independent activation of the AR remains plausible. This has been identified as a potential mechanism that might be crucial in regulating cell growth in the context of malignancy (20) notably in prostate cancer (21) although the precise mechanisms that underpin ligand-independent AR activation remain unclear. Importantly, not all actions of androgens upon the liver may be mediated by classical AR signaling. AR-independent regulation of lipogenesis in the liver has been observed in testicular feminized mice that lack a functional androgen receptor, with a reduction in lipogenesis following testosterone treatment (22).

The impact of GCs to regulate carbohydrate metabolism in particular gluconeogenesis in the fasting state is well described. However, their impact on lipid metabolism remains relatively poorly understood in human models. We have previously shown in adipose and skeletal muscle that GCs decrease lipogenesis in the absence of insulin consistent with their role to mobilize fuel in the fasting state (23, 24). In the fed state, however, GCs and insulin act synergistically to drive lipid accumulation. Studies performed in rodent hepatocytes have demonstrated this relationship (25) and we have now shown this in primary cultures of human hepatocytes. In our in vitro model, the ability of GCs to enhance the ability of insulin to drive lipogenesis was associated with increased activation of the insulin signaling cascade as demonstrated by increased phosphorylation of PKB/akt, similar to our published observations in human adipose tissue (26, 27). Although augmentation of insulin action by GCs has been observed in rodent hepatocytes (25), these in vitro data may not be reflective of more complex in vivo physiology. Clinical studies that have administered GCs have shown evidence of increased hepatic insulin resistance in most cases (28).

There is now an emerging role for the 5α-reductase isoforms in the regulation of metabolic phenotype. The ability of testosterone to regulate lipid metabolism does not appear to be dependent upon the presence of SRD5A2. The C3A cell line does not express SRD5A2, and yet both Testosterone and DHT were able to stimulate lipogenesis to a similar extent. Our experiments therefore focused on the role of SRD5A2 to regulate the effects of GCs upon liver metabolism. While genetic ablation of SRD5A1 in rodent models increases lipid accumulation and fibrosis, the precise mechanisms that underpin this are not clear (6, 7). In a recently published clinical study, nonselective 5α-reductase inhibition with Dutasteride was associated with peripheral insulin resistance and it has been suggested that this may reflect a specific role for SRD5A1 in skeletal muscle (29). The precise impact upon liver fat accumulation could not be determined as pre and post intervention assessment of hepatic lipid content was not performed.

The role of SRD5A2 in clearing cortisol is well established through the examination of urinary steroid metabolite profiles in patients with proven SRD5A2 mutations (5). Detailed metabolic studies in patients with mutations SRD5A2, have not been performed. Increasing 5α-reductase activity is associated with an adverse metabolic phenotype (12, 30). This may reflect a compensatory mechanism to clear active GCs, in particular from the liver in an attempt to protect it from lipid accumulation. With more severe disease activity decreases and this may increase GC exposure and may serve and a local anti-inflammatory measure to try to limit the progression of nonalcoholic steatohepatitis, fibrosis and scarring (31).

In conclusion, we have demonstrated the potent actions of androgens and GCs to regulate lipid metabolism in human hepatocytes in vitro and shown that prereceptor regulation through that expression and activity of SRD5A2 is able to modify their action. This has important implications not only in terms of predisposing individuals to the development of hepatic steatosis, but also to the large numbers of patients prescribed 5α-reductase inhibitors. While the role of these compounds in the treatment of prostate-related disease is established, the long-term met-

Legend to Figure 4 Continued. . .
suppress lipogenesis. Data presented are mean±SE of n = 3–5 experiments performed in triplicate, *$P < .05$, **$P < .01$ *vs.* control and § $P < .05$, §§ $P < .01$ vs. cortisol)

abolic consequences of these medications have not been assessed.

Acknowledgments

This work was supported by the Medical Research Council (Senior Clinical Fellowship to JWT Ref. G0802765) and through the NIHR Oxford Biomedical Research Centre.

Address all correspondence and requests for reprints to: Jeremy W Tomlinson PhD FRCP, Oxford Centre for Diabetes, Endocrinology & Metabolism University of Oxford, Churchill Hospital, Headington, Oxford, OX3 7LJ, Tel 0.44 (0)1865 857 359, E-Mail. jeremy.tomlinson@ocdem.ox.ac.uk.

This work was supported by .

Disclosure: The authors have nothing to disclose

References

1. **Ekstedt M, Hagstrom H, Nasr P, Fredrikson M, Stal P, Kechagias S, Hultcrantz R. Fibrosis stage is the strongest predictor for disease-specific mortality in NAFLD after up to 33 years of follow-up.** *Hepatology*. 2014. doi: 10.1002/hep.27368. [Epub ahead of print]
2. **Rockall AG, Sohaib SA, Evans D, Kaltsas G, Isidori AM, Monson JP, Besser GM, Grossman AB, Reznek RH.** Computed tomography assessment of fat distribution in male and female patients with Cushing's syndrome. *European journal of endocrinology*. 2003;149(6):561–567.
3. **Fraser R, Ingram MC, Anderson NH, Morrison C, Davies E, Connell JM.** Cortisol effects on body mass, blood pressure, and cholesterol in the general population. *Hypertension*. 1999;33(6):1364–1368.
4. **Russell DW, Wilson JD.** Steroid 5α-reductase: two genes/two enzymes. *AnnuRevBiochem*. 1994;63:25–61.
5. **Peterson RE, Imperato-McGinley J, Gautier T, Shackleton C.** Urinary steroid metabolites in subjects with male pseudohermaphroditism due to 5α-reductase deficiency. *Clinical endocrinology*. 1985;23(1):43–53.
6. **Livingstone DE, Barat P, Di Rollo EM, Rees GA, Weldin BA, Rog-Zielinska EA, MacFarlane DP, Walker BR, Andrew R.** 5α-reductase type 1 deficiency or inhibition predisposes to insulin resistance, hepatic steatosis and liver fibrosis in rodents. *Diabetes*. 2015;64(2):447–58.
7. **Dowman JK, Hopkins LJ, Reynolds GM, Armstrong MJ, Nasiri M, Nikolaou N, van Houten EL, Visser JA, Morgan SA, Lavery GG, Oprescu A, Hubscher SG, Newsome PN, Tomlinson JW.** Loss of 5α-reductase type 1 accelerates the development of hepatic steatosis but protects against hepatocellular carcinoma in male mice. *Endocrinology*. 2013;154(12):4536–4547.
8. **Kim S, Kwon H, Park JH, Cho B, Kim D, OH SW, Lee CM, Choi HC.** A low level of serum total testosterone is independently associated with nonalcoholic fatty liver disease. *BMC gastroenterology*. 2012;12:69.
9. **Volzke H, Aumann N, Krebs A, Nauck M, Steveling A, Lerch MM, Rosskopf D, Wallaschofski H.** Hepatic steatosis is associated with low serum testosterone and high serum DHEAS levels in men. *International journal of andrology*. 2010;33(1):45–53.
10. **Haider A, Gooren LJ, Padungtod P, Saad F.** Improvement of the metabolic syndrome and of non-alcoholic liver steatosis upon treatment of hypogonadal elderly men with parenteral testosterone undecanoate. *Experimental and clinical endocrinology, diabetes*. 2010;118(3):167–171.
11. **Hoyos CM, Yee BJ, Phillips CL, Machan EA, Grunstein RR, Liu PY.** Body compositional and cardiometabolic effects of testosterone therapy in obese men with severe obstructive sleep apnoea: a randomised placebo-controlled trial. *European journal of endocrinology*. 2012;167(4):531–541.
12. **Tomlinson JW, Finney J, Gay C, Hughes BA, Hughes SV, Stewart PM.** Impaired glucose tolerance and insulin resistance are associated with increased adipose 11β-hydroxysteroid dehydrogenase type 1 expression and elevated hepatic 5α-reductase activity. *Diabetes*. 2008;57(10):2652–60.
13. **Crowley RK, Hughes B, Gray J, McCarthy T, Hughes S, Shackleton CH, Crabtree N, Nightingale P, Stewart PM, Tomlinson JW.** Longitudinal changes in glucocorticoid metabolism are associated with later development of adverse metabolic phenotype. *European journal of endocrinology*. 2014;171(4):433–442.
14. **Donnelly KL, Smith CI, Schwarzenberg SJ, Jessurun J, Boldt MD, Parks EJ.** Sources of fatty acids stored in liver and secreted via lipoproteins in patients with nonalcoholic fatty liver disease. *The Journal of clinical investigation*. 2005;115(5):1343–1351.
15. **Jamdar SC.** Glycerolipid biosynthesis in rat adipose tissue. Influence of adipose-cell size and site of adipose tissue on triacylglycerol formation in lean and obese rats. *Biochem J*. 1978;170(1):153–160.
16. **Zhang H, Liu Y, Wang L, Li Z, Zhang H, Wu J, Rahman N, Guo Y, Li D, Li N, Huhtaniemi I, Tsang SY, Gao GF, Li X.** Differential effects of estrogen/androgen on the prevention of nonalcoholic fatty liver disease in the male rat. *Journal of lipid research*. 2013;54(2):345–357.
17. **Markou A, Androulakis, II, Mourmouris C, Tsikkini A, Samara C, Sougioultzis S, Piaditis G, Kaltsas G.** Hepatic steatosis in young lean insulin resistant women with polycystic ovary syndrome. *Fertility and sterility*. 2010;93(4):1220–1226.
18. **Jones H, Sprung VS, Pugh CJ, Daousi C, Irwin A, Aziz N, Adams VL, Thomas EL, Bell JD, Kemp GJ, Cuthbertson DJ.** Polycystic ovary syndrome with hyperandrogenism is characterized by an increased risk of hepatic steatosis compared to nonhyperandrogenic PCOS phenotypes and healthy controls, independent of obesity and insulin resistance. *The Journal of clinical endocrinology and metabolism*. 2012;97(10):3709–3716.
19. **Kalra M, Mayes J, Assefa S, Kaul AK, Kaul R.** Role of sex steroid receptors in pathobiology of hepatocellular carcinoma. *World journal of gastroenterology*. 2008;14(39):5945–5961.
20. **Chung WM, Chang WC, Chen L, Lin TY, Chen LC, Hung YC, Ma WL.** Ligand-independent androgen receptors promote ovarian teratocarcinoma cell growth by stimulating self-renewal of cancer stem/progenitor cells. *Stem cell research*. 2014;13(1):24–35.
21. **Kasina S, Macoska JA.** The CXCL12/CXCR4 axis promotes ligand-independent activation of the androgen receptor. *Molecular and cellular endocrinology*. 2012;351(2):249–263.
22. **Kelly DM, Nettleship JE, Akhtar S, Muraleedharan V, Sellers DJ, Brooke JC, McLaren DS, Channer KS, Jones TH.** Testosterone suppresses the expression of regulatory enzymes of fatty acid synthesis and protects against hepatic steatosis in cholesterol-fed androgen deficient mice. *Life sciences*. 2014;109(2):95–103.
23. **Gathercole LL, Morgan SA, Bujalska IJ, Hauton D, Stewart PM, Tomlinson JW.** Regulation of lipogenesis by glucocorticoids and insulin in human adipose tissue. *PloS one*. 2011;6(10):e26223.
24. **Morgan SA, Gathercole LL, Simonet C, Hassan-Smith ZK, Bujalska I, Guest P, Abrahams L, Smith DM, Stewart PM, Lavery GG, Tomlinson JW.** Regulation of lipid metabolism by glucocorticoids and 11β-HSD1 in skeletal muscle. *Endocrinology*. 2013;154(7):2374–2384.
25. **Amatruda JM, Danahy SA, Chang CL.** The effects of glucocorticoids on insulin-stimulated lipogenesis in primary cultures of rat hepatocytes. *Biochem J*. 1983;212(1):135–141.
26. **Gathercole LL, Bujalska IJ, Stewart PM, Tomlinson JW.** Glucocor-

ticoid modulation of insulin signaling in human subcutaneous adipose tissue. *The Journal of clinical endocrinology and metabolism*. 2007;92(11):4332–4339.

27. **Hazlehurst JM, Gathercole LL, Nasiri M, Armstrong MJ, Borrows S, Yu J, Wagenmakers AJ, Stewart PM, Tomlinson JW.** Glucocorticoids fail to cause insulin resistance in human subcutaneous adipose tissue in vivo. *The Journal of clinical endocrinology and metabolism*. 2013;98(4):1631–1640.
28. **Petersons CJ, Mangelsdorf BL, Jenkins AB, Poljak A, Smith MD, Greenfield JR, Thompson CH, Burt MG.** Effects of low-dose prednisolone on hepatic and peripheral insulin sensitivity, insulin secretion, and abdominal adiposity in patients with inflammatory rheumatologic disease. *Diabetes care*. 2013;36(9):2822–2829.
29. **Upreti R, Hughes KA, Livingstone DE, Gray CD, Minns FC, Macfarlane DP, Marshall I, Stewart LH, Walker BR, Andrew R.** 5alpha-reductase type 1 modulates insulin sensitivity in men. *The Journal of clinical endocrinology and metabolism*. 2014;99(8):E1397–1406.
30. **Tsilchorozidou T, Honour JW, Conway GS.** Altered cortisol metabolism in polycystic ovary syndrome: insulin enhances 5alpha-reduction but not the elevated adrenal steroid production rates. *The Journal of clinical endocrinology and metabolism*. 2003;88(12):5907–5913.
31. **Ahmed A, Rabbitt E, Brady T, Brown C, Guest P, Bujalska IJ, Doig C, Newsome PN, Hubscher S, Elias E, Adams DH, Tomlinson JW, Stewart PM.** A switch in hepatic cortisol metabolism across the spectrum of non alcoholic fatty liver disease. *PloS one*. 2012;7(2):e29531.